Soil Moisture Prediction:

Bridging Event and Continuous Runoff Modelling

2006

Promotor: Prof. dr. ir. L. Stroosnijder
Hoogleraar Erosie en Bodem & Waterconservering

Co-promotor: dr. ir. E.E. van Loon
Universitair docent bij het Instituut voor Biodiversiteit en Ecosystemen, Universiteit van Amsterdam

Promotiecommissie:
Prof. dr. P. Kabat (Wageningen Universiteit)
Prof. dr. V.G. Jetten (ITC en Utrecht Universiteit)
Prof. dr. J. Feyen (Katholieke Universiteit Leuven)
Dr. Ir. J.C. van Dam (Wageningen Universiteit)

Dit onderzoek is uitgevoerd binnen de C.T. de Wit onderzoekschool PE & RC

Soil Moisture Prediction:

Bridging Event and Continuous Runoff Modelling

Vahedberdi Sheikh

Proefschrift
ter verkrijging van de graad van doctor
op gezag van de rector magnificus
van Wageningen Universiteit
Prof. dr. M.J. Kropff
in het openbaar te verdedigen
op dinsdag 28 november 2006
des namiddags te 16.00 uur in de Aula

Vahedberdi Sheikh (2006)

Soil Moisture Prediction: Bridging Event and Continuous Runoff Modelling

Thesis Wageningen-UR -with ref. -with summaries in English, Dutch, and Farsi.

ISBN: 90-8504-533-9

Keywords: soil moisture monitoring, soil moisture modelling, sensitivity analysis, event-based models, continuous models, South Limburg.

Acknowledgement

I would like to express my profound gratitude and praises to the Almighty Allah for all good graces and mercies he granted me in my life and career. I am also grateful of the Ministry of Science, Research, and Technology (MSRT) of Iran for granting me a fulltime scholarship to follow my PhD study in abroad. The work presented in this thesis was made possible with the support and contribution of many individuals whom I like to sincerely acknowledge.

First and foremost, I respectfully render my regards and gratitude to my promotor, Prof. Leo Stroosnijder. I heartedly appreciate his brilliant thoughts and inspiring guidance which kept my on the right way to the planned destination of PhD promotion. Leo, you gave all due attention to my work despite the limited time you had due to being the promotor or supervisor of many other PhD students. Thank you for every thing.

My very special thanks go to my co-promotor, Dr. Emiel van Loon for his help, intellectual ideas, and valuable guidance. Soon after starting of my PhD study, he moved to the Universiteit van Amsterdam. His enthusiastic ideas and prompt solutions to my technical questions convinced me to continue getting benefited by his creativity and supervision. Emiel, if you had stayed in Wageningen I would have learned from you much more useful scientific qualities than what I have already acquired.

I sincerely acknowledge Dr. Wim Spaan, who was the first person in the Erosion, Soil & Water Conservation group with who I communicated. He arranged all preliminary and logistic affairs before and after my arrival to the Netherlands. Wim, I enjoyed very much your hospitality and readiness to help me at settling down in Wageningen and setting up my field work in south Limburg.

I would also like to express my sincere gratitude to Piet Peters, the highly valuable technician of the ESWC group. He assisted me in the tough tasks of equipment installation and maintenance, data collection, and laboratory tests. My special thanks go to Paul Peter, an M.Sc student who helped me with fieldwork and data collection at the beginning of my field campaigns. The hospitality and generosity of Paul and his parents who are living nearby the study site, made the difficult task of field visits as comfortable as possible. I never forget the coffee drinks with the homemade Limburgse special cakes at their house.

I sincerely thank Prof. Victor Jetten from ITC, Dr. Rudi Hessel , Dr. Saskia Visser and Dr. Jos van Dam from Wageningen UR for their valuable support, time, advice, and comments. The farmers of the Catsop catchment are sincerely acknowledged for their permission to conduct my field works on their properties. I would also like to acknowledge the Roer & Overmaas Waterboard in south Limburg, especially Ruben IJpelaar and Peter Hulst for providing the discharge data and basic information about the catsop catchment.

I enjoyed the friendly atmosphere of the ESWC group. I experienced very pleasant times during school trips (Schoolreis) and drinks and dinners organized by the group. My special thanks go to Dirk Meindertsma, Jolanda Hendriks, and Tony Sijm who were always ready to translate so many letters and forms which I was receiving in Dutch language and to handle all the bureaucratic administration affairs which I was facing. I enjoyed very much working in a real internationalized group with many colleagues and friends from different parts of the world: Europe, Africa, India, China, and Latin America. I learned so many useful qualities during our conversations and discussions. Therefore I would like to state thanks Jan de Graaff, Geert Sterk, Olga Vigiak, Consuelo Romero, Kidanu, Karim, Aklilu, Semere, Helena, Jakolien, Michel, Luuk, Aad, Monique, Biamah, Kumar, Sameer, Robert, Elisee, …

I would like to take the opportunity to express my gratitude to all the members of the Iranian student community here in Wageningen. However we were far away from our parents, relatives, and our lovely country (Iran), but our occasional gatherings and your emotional support prevented me and my family to get homesick. Thanks all. My special thanks go to Majid Vazifedoust, Ali Talebi, and Kaka Shahedi. We shared pleasant moments during our daily coffee and tea times talking and discussing about work, as well as personal matters.

As always it is impossible to list by name all the individuals whose support benefited this study. Therefore, I apologize if your name has not been mentioned here; your contribution was highly valued.

I wish to express my deepest appreciation to my parents and other family members. Although most of my life I was living far from them but their continuous emotional and financial support and encouraging words helped me to accomplish all my academic studies successfully.

Finally, I am extremely grateful of my wife Amangol and my sons Javad, Ehsan, and Danial. I am quite sure that it would not be possible to accomplish my academic duties, particularly my PhD, without benefiting their patience, tolerance, good willing, and emotional support. My dears I know that it is impossible to compensate by words what you suffered and whatever you lost in lieu of my academic achievements, but I would like to say THANK YOU for every thing.

I dedicate this thesis to:
my wife, Amangol
my sons, Javad, Ehsan, and Danial

This PhD thesis was financially supported by the Ministry of Science, Research, and Technology of I.R. of Iran.

Table of contents

Chapter 1	General introduction	1
Chapter 2	Study area	7
Chapter 3	Data collection and methods	23
Chapter 4	Sensitivity of catchment discharge to initial soil moisture	47
Chapter 5	Understanding the relation between topography, land use and soil moisture in a small rural catchment in the Dutch loess area	71
Chapter 6	Adequacy of a 1-D unsaturated zone model (SWAP) to describe the soil moisture dynamics from point to catchment scale	93
Chapter 7	A simple buddy model to predict soil moisture: bridging the gap between event and continuous runoff modelling	123
Chapter 8	Synthesis	153
References		166
Summary		181
Samenvatting		185
خلاصه		189
Curriculum Vitae		193
PE&RC PhD Education Statement Form		194

Chapter 1

Introduction

1 Introduction

1.1 The importance of soil moisture

Although soil moisture constitutes an insignificant part of the global water budget, it controls nearly all the hydrological processes occurring at or near the land surface. It regulates the partitioning of precipitation into runoff and groundwater storage. Soil moisture also regulates the partitioning of available energy at the earth's surface into sensible and latent heat exchange with the atmosphere (Silberstein et al., 1999). Consequently it influences evapotranspiration rate and the success of agriculture. Therefore, soil moisture is often described as the water in the root zone that can interact with the atmosphere through evapotranspiration and precipitation (Houser et al., 1998).

The root zone moisture content is widely used as a key variable in many environmental studies, in relation to hydrology, meteorology, climate change and agriculture, for example (Walker, 1999). An accurate monitoring of soil moisture content in space and time can contribute significantly in water resources management, flood forecasting, drought forecasting, erosion studies and prediction of global climate change.

1.2 Problem definition

Unlike discharge or climate variables, the root zone soil moisture is not monitored regularly – in spite of its importance. The lack of regular monitoring of soil moisture is basically a measurement problem. It is very difficult to observe soil moisture at a fine spatial and temporal resolution, while covering the whole study area of interest. We are still constrained by technology, either to making detailed observations (at the appropriate resolution) at a few points with in situ measurements, or to collecting regional observations (at too coarse a resolution) over the entire study area with remote sensing.

On the other hand, as a result of heterogeneity of soil properties, topography, land cover, evapotranspiration and precipitation, the soil moisture content is highly variable in three-dimensional space and time (Engman, 1991; Wood et al., 1992). The high variation of soil moisture limits the usefulness of both observation methods. For instance, while in situ measurements can provide fairly accurate estimates of soil moisture at point scale, it is difficult to extrapolate these values to other points and areas. Several studies have indicated that the correlation length of soil moisture is so low that it is practically impossible for in situ measurements to accurately describe its spatial distribution (Huisman et al., 2001). Moreover, in situ measurements are usually accompanied by considerable uncertainties (Evett et al., 2002). Later in this chapter the advantages and disadvantages of some widely used in situ measurement tools will be discussed in detail.

Remote sensing data potentially give spatial patterns of moisture content for a limited and variable depth (between 2 and 20 cm, but mostly 5 cm deep) of the soil profile (Walker, 1999; Western and Blöschl, 1999; Heathman et al., 2003). Furthermore, remote sensing gives average values of soil moisture over footprints that are usually much larger than the observed correlation length of soil moisture. Also, the interpretation of the remotely sensed data is often difficult, due to confounding impacts of vegetation cover, soil characteristics and surface roughness (Western and Blöschl, 1999; Heathman et al., 2003; Western et al., 2004). However, the most limiting characteristic of the remote sensing data is that the snapshots of a specific location are too infrequent to cover all the temporal changes of the surface soil moisture variations.

The difficulties associated with continuously monitoring the spatial distribution of the root zone soil moisture content by means of the currently available methods, plus the need to have spatially distributed soil moisture information for coupled land–atmosphere models and event-based hydrology and soil erosion models have led to statistical or hydrological models being used to obtain the spatially distributed soil moisture data. Yet these models produce uncertain estimates of soil moisture values due to their underlying assumptions, boundary conditions, and conceptual simplifications.

1.3 Objectives and scope of study

Surface layer moisture content is a state variable that is either simulated or required as input in many hydrological models (Hawley et al., 1983). Its estimation is the central focus of many continuous unsaturated zone models, but it is critical to input accurate initial soil moisture content into event-based hydrology and soil erosion models. Therefore soil moisture can be used as a link between continuous and event-based hydrological models.

In the research described in this thesis, the LImburg Soil Erosion Model (LISEM) was used as the event-based model for scrutiny. LISEM is a physically based hydrological and soil erosion model developed as a tool for planning and conservation purposes in the hilly loess area in South Limburg, the Netherlands (De Roo et al., 1995; De Roo et al., 1996a; De Roo and Jetten, 1999; Jetten et al., 1999; Jetten, 2002; Hessel, 2002). It simulates the hydrology and sediment transport during and immediately after a single rainfall event in a drainage basin. The model simulates both the effects of current land use and of introducing soil conservation measures.

LISEM is a spatially distributed model. At the start of a simulation it requires spatially distributed input values: initial soil moisture content, for example. These data are usually obtained from field sampling. It is especially difficult to obtain observations just prior to a rainfall event and at a high spatial density. That is the problem that the research described in this thesis addresses. The research objectives, formulated as questions, were based on this problem. They are:

1. How sensitive is the discharge or overland flow predicted by the LISEM model to initial soil moisture content at different depths of root zone profile?

2. What is the relationship between the soil moisture content of the root zone, topography, land use and land management practices in a small-scale catchment?

3. How adequate is a one-dimensional unsaturated zone model for describing the soil moisture dynamics at catchment scale?

4. How can the requirement for large amounts of data at the beginning of each new event be avoided by using a buddy model that links events? (The buddy model in question is a module developed to predict soil moisture content by using meteorological data and key soil parameters at a coarser time scale than the LISEM time scale.)

5. How can qualitative observations in the form of visible and near infrared imagery be used to reduce parameter uncertainty and therewith also the reliability of LISEM's predictions?

The fieldwork area selected for answering the five research questions was the Catsop catchment, a small agricultural catchment in South Limburg. All observation tools in hand were implemented in this catchment. Monitoring and field surveys were conducted from November 2003 to August 2005.

1.4 Study outline

The eco-physical characteristics of the study area are described in Chapter 2. Data collection and methodologies are given in Chapter 3. In this study, various models with different levels of complexity were used. The application of each model is discussed in separate chapters of this thesis.

In Chapter 4 the sensitivity of discharge predicted by an event-based model to soil moisture changes at different depths of the root zone soil profile is studied by applying the physically based LISEM model to two rainfall events in the study area. The sensitivity of predicted discharge to the application of two different infiltration sub-modules within the LISEM model is compared.

Chapter 5 discusses the application of statistical methods to analyse the soil moisture distribution. A multiple linear regression model is applied to explore the relationship between the soil moisture content at different soil depths and the topography, land use, and land management practices.

In Chapter 6 the adequacy of a one-dimensional unsaturated zone model, SWAP, to predict soil moisture content at different depths of the root zone soil profile is tested. Physically-based one-dimensional soil water models such as SWAP have proven capability to retrieve soil moisture content at a given point, especially on flat surfaces or fields with a gentle slope where lateral water movement is negligible. In order to decrease the complexity of lumped and distributed hydrological models for hillslope and catchment scales, the infiltration and soil water redistribution is usually assumed to be vertical only. In this chapter, the quality of SWAP predictions is evaluated when the scale of simulation is increased from point to catchment level.

In Chapter 7 a simple spatial buddy model is developed in order to predict the spatially distributed daily soil moisture values. The model is developed in a freely available GIS and programming environment, PCRaster.

Finally, Chapter 8 synthesizes the findings of this research and provides some recommendations for future studies.

Chapter 2

Study area

2 Study area

2.1 Introduction

The study area is a small catchment, called Catsop, which is situated in the hilly loess region of South Limburg, the Netherlands (50º 95´N, 5º 78´E; Figure 2.1).

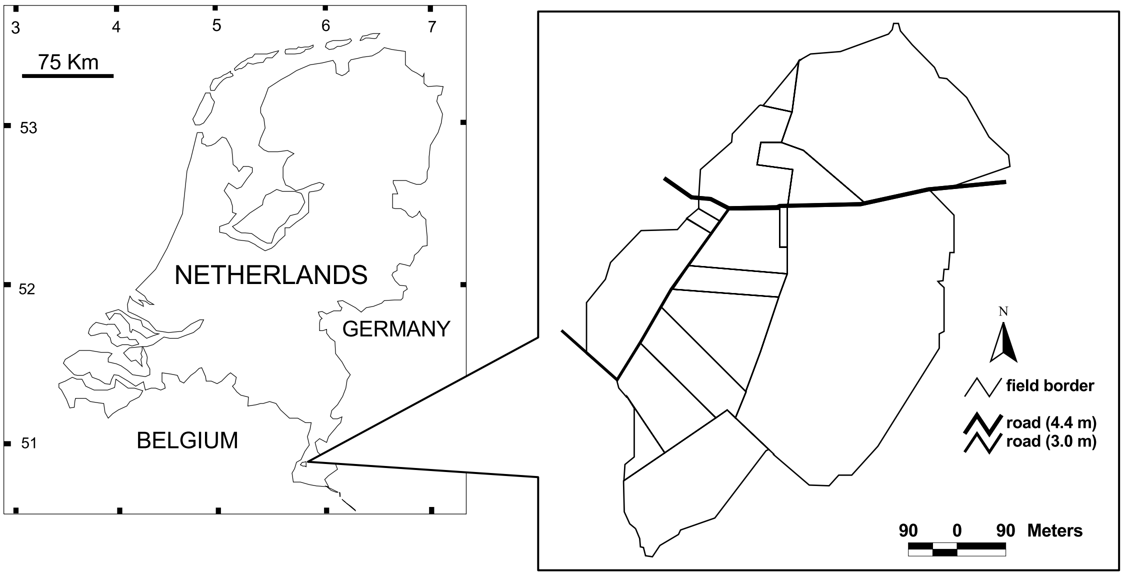

Figure 2.1. Location of the Catsop study catchment, S-Limburg, The Netherlands.

It has an area of 0.42 km^2, and the dominant land use is agriculture. This catchment is typical of the loess area in Limburg, which has soil erosion problems that occasionally cause flooding of private and public land. The main cause of the problems is the reduced infiltration rate following changes in land use and intensification of agriculture. Figure 2.1 shows the geographical position of the Catsop catchment in the Netherlands. In the following sections the physical environment dominating on the catchment is described.

2.2 Climate

The climate of the study area is temperate humid, with a long-term (1970–2000) mean annual precipitation of 740 mm (KNMI). Table 2.1 summarises the 30-year averages of climate data from the Beek (the nearest airport) weather station (less than 2 km to the south of the study area). Precipitation occurs mainly as rainfall and is evenly distributed over the year. Figure 2.2 shows the monthly distribution of precipitation, precipitation duration and mean daily temperature at this weather station. The winter and summer rainfall patterns differ: the summer events are shorter and more intensive, while the winter events are on average longer and less intensive.

Table 2.1. Average (1970–2000) climate data for Beek airport, The Netherlands.

Variables	J	F	M	A	M	J	J	A	S	O	N	D
Precipitation (mm)	60.5	50.7	60.5	46	63.8	73.9	67.1	58.1	60.4	62.8	66	70.2
Ppt duration (h)	68.6	58.5	66.1	48	45.8	51	37.4	31.8	43.2	51.2	66.2	75
Mean temp. (^oC)	2.6	2.9	5.9	8.4	13	15.6	17.7	17.6	14.3	10.3	5.9	3.8
Rel. humidity (%)	88	85	81	76	74	76	76	76	82	85	88	89
Wind speed (m s^{-1})	5.3	4.8	4.9	4.3	4	3.8	3.7	3.5	3.9	4.2	4.8	5.2
Solar radiation (kJ cm^{-2})	7.8	13.9	55.4	39.4	52.6	51.9	53.4	47.3	30.9	19.6	9.5	5.8

On average, 30 percent of days are not accompanied by any precipitation. About 35 percent of days receive 1 mm or more precipitation. The precipitation exceeds 10 mm per day on only slightly more than 5 percent of days. These major rainfall events are almost equally distributed over each month. Whereas the first 4 months of a year receive one major rainfall event per month, other months have two days with more than 10 mm precipitation per day. The mean annual relative humidity is above 80 percent. The extreme of mean daily temperature varies from -15 ^oC to 29 ^oC. Based on the 30 years of data, the coldest month is January (mean daily temperature 2.6 ^oC) and the hottest is July (mean daily temperature 17.7 ^oC): see Table 2.1. The mean daily wind speed is 4.3 $m.s^{-1}$ and the wind blows dominantly from the south-west.

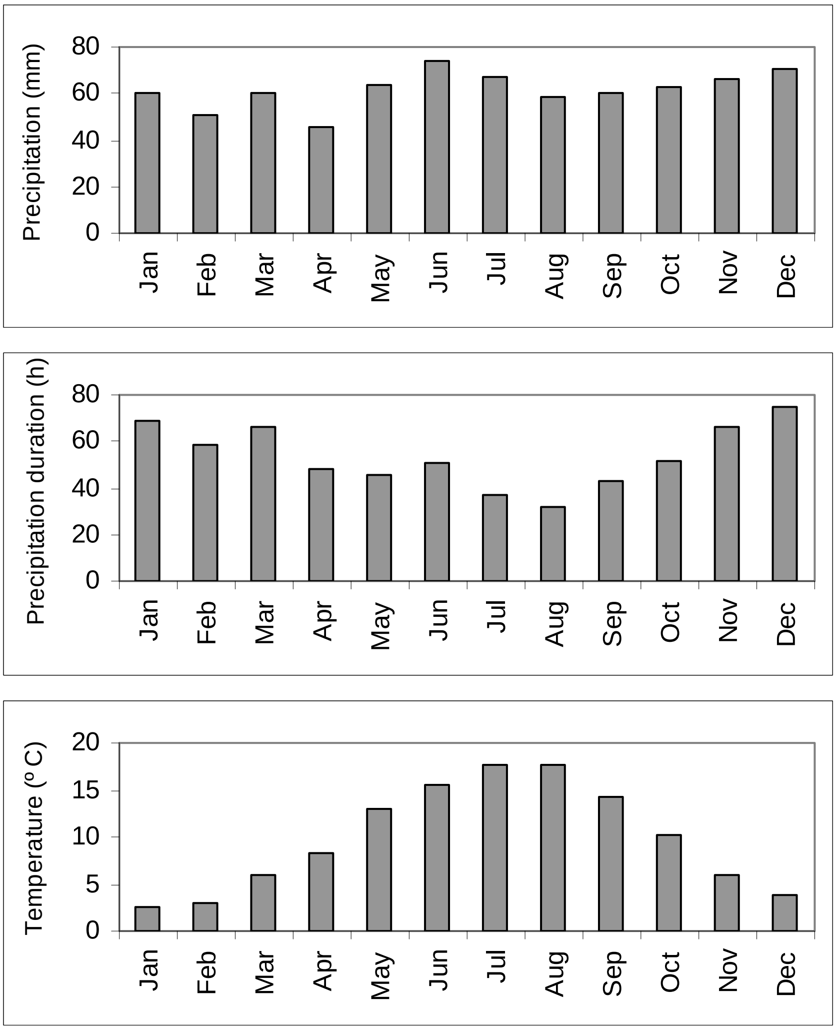

Figure 2.2. Averaged (1970–2000) climate data from Beek airport, the Netherlands.

2.3 Relief

The topographical characteristics of the South Limburg district distinguish it from other districts in the Netherlands. As the Netherlands is mostly flat lowlands, the undulating hills with moderate to steep slopes in South Limburg make an impressive landscape to Dutch tourists. The area is a popular Dutch holiday destination. The highest point (321 m.a.s.l) in the Netherlands is located in this district.

In contrast to most of the Netherlands, there are no ditches and the water table is not shallow. In the flat areas of the Netherlands, the drainage ditches are linear features running parallel to field borders. In sloping areas of South Limburg the *graften* constitute the distinctive artificial linear features (Figure 2.3). *Graften* are man-made scarps across the slopes, running parallel to contours. They will be referred to later in this chapter.

Figure 2.3 Example of a graft in the Catsop catchment, South Limburg, The Netherlands.

The pronounced relief of plateaux, slopes, dry valleys and small river valleys was formed in the early Pleistocene. Later, windborne loess was deposited, smoothing but not obliterating the relief (De Bakker, 1979). The hollow ways running from the plateaux to the valleys provide drainage routes for the surface runoff from rainfall events. The only available drainage channel in the catchment also runs alongside the main metalled road in the catchment linking the small village of Catsop on the downstream side of the catchment to the town of Beek on the upstream side of the catchment. This road divides the study area into two hill slopes: one to the north and the other to the south.

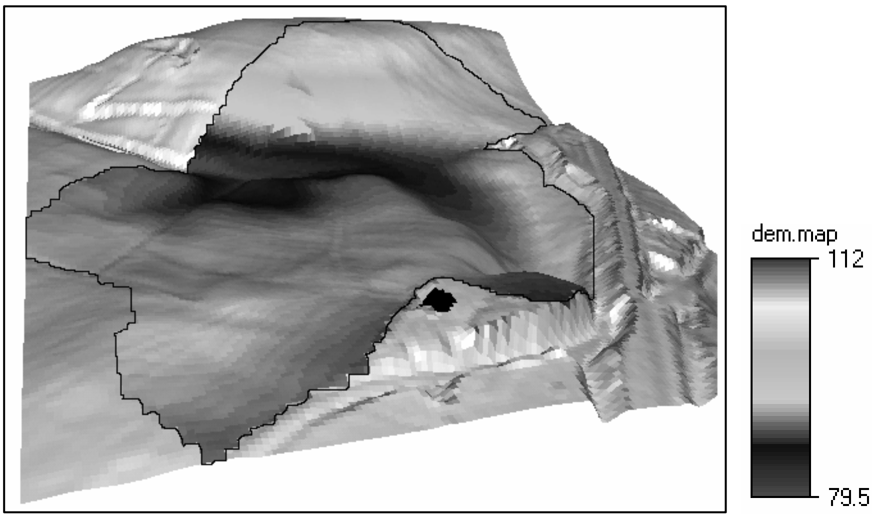

Figure 2.4. Digital Elevation Model of the Catsop catchment. Elevation ranges from 79 to 112 m.a.s.l. (*Source: Derived from DTM; DTM was provided by Waterboard Roer & Overmaas*)

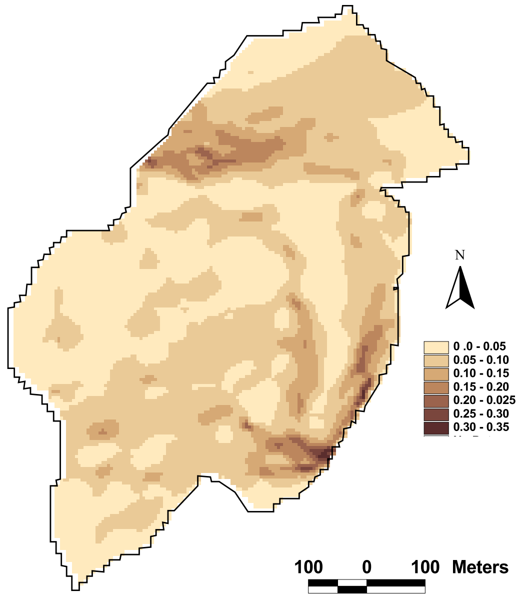

Figure 2.5. Slope map of the Catsop catchment. (Source*: DTM; DTM was provided by Waterboard Roer & Overmaas*)

Figure 2.4 presents the Digital Terrain Model (DTM) of the study area. The elevation within the catchment varies between 79 and 112 m.a.s.l. Like the district in which it lies, the terrain is undulating, with gently to moderately sloping topography. Figure 2.5 displays the slope map of the area. About 86 % of the slopes have a gradient of around 10 % or less; 3.5 % of the slopes are steeper than 15 %. The catchment has a dominant flow direction to the west, towards the river Meuse.

2.4 Geology and soils

The soils of the catchment have been formed on aeolian deposits (Ice-age period 0.01–0.2 Ma) and are typical of the scattered loess areas in northwestern Europe. In the Netherlands, this parent material is found only in South Limburg province. This Dutch loess region is the most northern extremity of the West European loess belt. Therefore its clay content is less than 20 % (De Bakker, 1979). In geological terms, these aeolian deposits are the upper part of Pleistocene sediments deposited in the late Weichsel ice age over the Tertiary sand deposits and Quaternary deposits of the "West Meuse" river.

Using the FAO classification, the soils of the Catsop catchment can be classified into three types: *Luvisols, eroded Luvisols,* and *Colluvial soils.* In Dutch soil nomenclature the luvisols and eroded luvisols are called *Radebrikgronden* and *Bergbrikgronden*, respectively. Table 2.2 compares the proportion of these soils in the loess district of the Netherlands and in the Catsop catchment. The proportion of the eroded luvisols in the study area is about 65 percent above the average for the whole district. This implies that the process of soil erosion in the study area has been considerable.

Table 2.2. Areal cover (in %) of soils in the loess district of S-Limburg, the Netherlands and in the Catsop catchment.

	area (%)	
Soil type	**Loess district**	**Catsop**
luvisols (ABC)	37	8
eroded luvisols (BC)	30	40
eroded luvisols (C)	10	25
colluvial soils	22	27

Figure 2.6 shows the spatial distribution of soils in the catchment. The eroded luvisols have a higher clay content than the luvisols and colluvial soils (De Roo, 1993). The non-eroded luvisols are present on plateaux; the colluvials have accumulated in dry valleys.

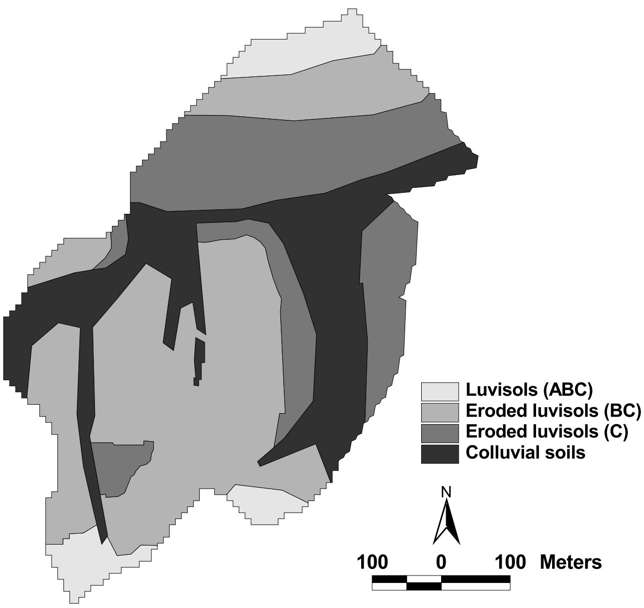

Figure 2.6. Soil map of the study area, according to FAO classification. (*Source: De Roo, 1993*)

Loess is a medium-textured wind-blown material, dominantly brownish in colour, and with progressive soil formation there is deep calcification and a textural B horizon is formed. In accordance to the USDA soil taxonomy procedure (Soil Survey Staff, 2003) three representative soil profiles can be distinguished in the study area: see Figure 2.7. The Dutch loess deposits are rarely thicker than 10 metres and over half are thinner than 5 metres. Thick deposits in this area are calcareous below approximately 2.5 metres depth (De Bakker, 1979). The upper layers of soils in this area are all loess-derived silty loams with a clay content of about 5 %, a silt content of about 70 %, and a sand content of about 25 %. They have high fertility, good productivity and are mainly used for agriculture.

The weak aggregate stability of loess soils favours soil sealing and crusting, thus reducing infiltration rates (Stroosnijder and Hoogmoed, 1984). Groeneveld and Daniels (1985) carried out laboratory rainfall simulation experiments on loess soil samples from two catchments in South Limburg near Catsop and Hulsberg. During lab studies, they observed crust formation when infiltration capacities were 2–4 times less than the saturated conductivity of the soils. The Catsop samples had infiltration capacities of 0.3–5.3 mm h^{-1}. These measured values of infiltration capacity are low enough to produce surface runoff even during normal rain storms. Groeneveld and Daniels concluded that a soil cover of vegetation or crops or the presence of easily decomposable plant remains increases the aggregate stability by enhancing the activity of soil fauna and the effects of plant roots, thereby improving infiltration capacity.

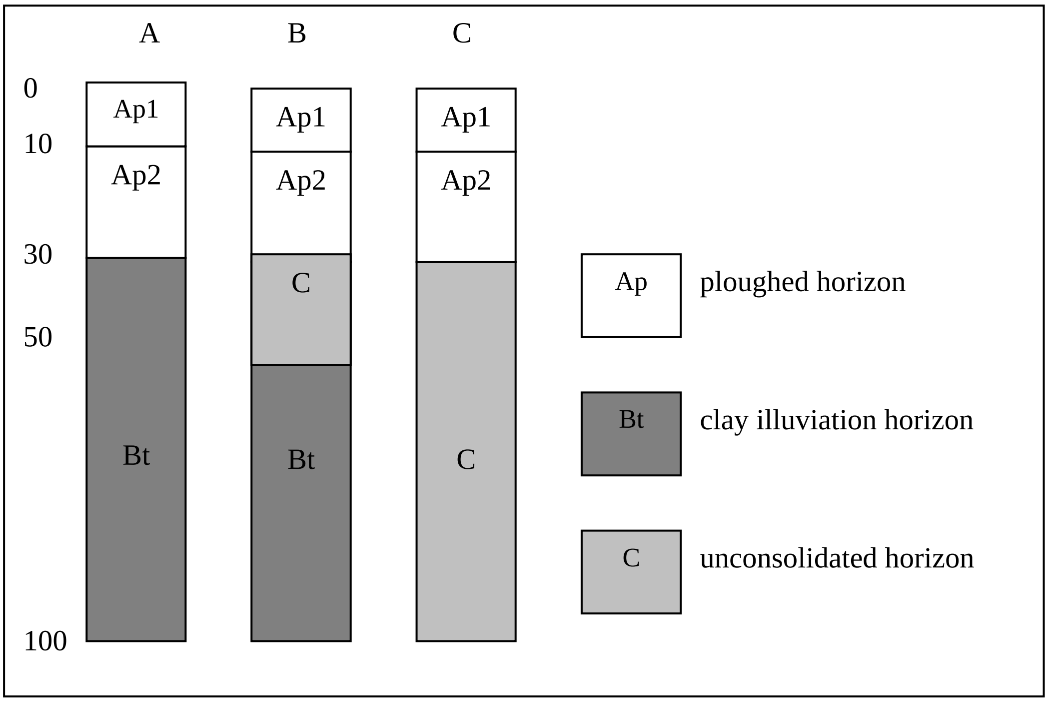

Figure 2.7. Representative soil profiles of the study area. A: fine-silty, mixed, mesic, Typic Hapludalf. B: fine-silty, mixed, mesic, Typic Udorthent (fine-silty (loess) colluvial deposit less than 100 cm thick over fine-silty material (loess)). C: fine-silty, mixed, mesic, Typic Udorthent (fine-silty (loess) colluvial deposit).

Figure 2.8 presents a typical non-eroded soil profile for loess soils in South Limburg. As shown in this figure, within 15–35 cm depth there is a compacted soil layer. Our penetrologger survey (see also Chapter 3) also supported the presence of a hardpan within the top 50 cm of the soil profile.

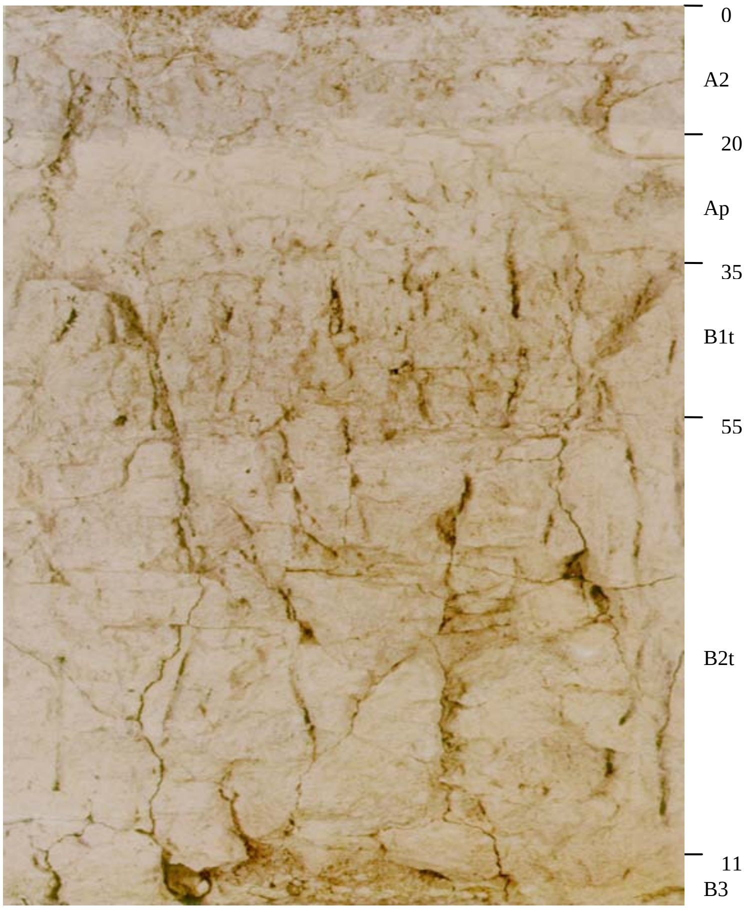

Figure 2.8. A typical loess soil profile from the Catsop study area, The Netherlands. (*Source: De Bakker, 1979*).

2.5 Vegetation and land use

Land use in the Catsop catchment is dominated by agriculture. Within this small catchment, four main land use types can be distinguished: *Arable (80 %), Orchard (8 %), Grassland (12 %), and Infrastructure (1 %).* Arable land is cultivated mainly with winter wheat, spring barley, sugar beet, potato, and yellow mustard. Yellow mustard is a second crop, functioning as a green cover to prevent the generation of surface runoff and soil erosion. It is sown at the end of the summer, after the cereals have been harvested. It is a fast-growing crop, which can completely cover the soil surface within three weeks of sowing. After being killed by the first winter frost, it lodges. Even after dying it covers about 40 percent of the soil surface (Figure 2.9), therefore helping to protect the soil surface during wet seasons. If the yellow mustard grows tall, some farmers chop it and spread it over the soil as mulch.

The grasslands are utilised in two ways. Some fields are grazed by cows from April to October (less than 5 cows per ha) while others are harvested mechanically. Table 2.3 shows the land use data for the catchment during the last twenty years. In the last five years, the area under orchards has grown from zero to about 8 percent. On the other hand, the area of grassland has shrunk. Figure 2.10 presents land use maps of the Catsop catchment during the 2004 and 2005 experiments.

Figure 2.9. Yellow mustard after first winter frost.

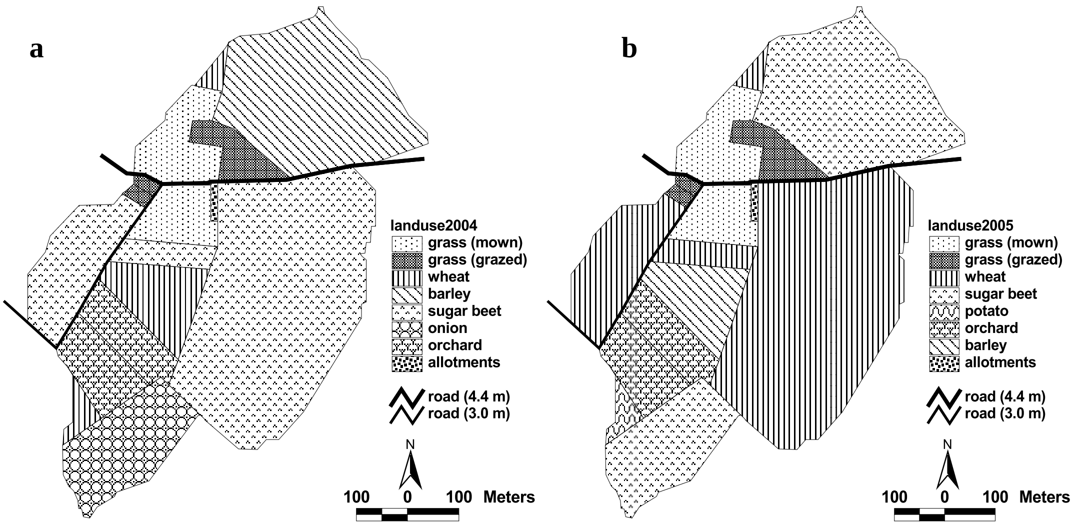

Figure 2.10. Land use map of the study area. (a) 2004 and (b) 2005. (*Source: field survey*)

Table 2.3. Land use in the Catsop catchment (as % of total area). (*Source: De Roo, 1993 (the first 5 columns) and field survey (the last 3 columns)*).

Land use	1987	1988	1989	1990	1991	2003	2004	2005
Woodland	0.4	0.4	0.4	0.4	0.4	-	-	-
Grassland	15.1	15.1	19.2	19.2	19.2	11.8	11.8	11.8
Infrastructure	0.7	0.7	0.7	0.7	0.8	0.8	0.8	0.8
Wheat	41.8	12.6	34.1	41.8	12.6	18.4	6.7	44.0
Barley	4.1	-	-	7.7	7.3	-	19.9	5.7
Maize	1.0	4.1	-	-	1.5	-	-	-
Sugar beet	13.0	28.5	42.6	3.7	24.8	5.7	44.0	28.5
Potato	19.3	37.1	1.5	26.0	33.0	34.2	-	1.0
Field beans	4.1	1.0	-	-	-	-	-	-
Allotments	0.5	0.5	0.5	0.5	0.5	0.3	0.3	0.3
Orchard	-	-	-	-	-	8.0	8.0	8.0
Carrot	-	-	-	-	-	19.9	-	-
Cabbage	-	-	-	-	-	1.0	-	-
Onion	-	-	-	-	-	-	8.6	-

Figure 2.10 indicates that over half of the catchment area consists of two big fields in the west. The southern field covers over one third of the catchment area. Both fields are arable. During field surveys it was observed that most of the soil erosion and runoff originated from these two fields, especially from the southern one. Therefore the crop type and management practice on this field highly influence the catchment response. From the number of major runoff events in the catchment (Table 2.4) it can be seen that during 2005 the number of runoff events decreased remarkably. This is attributable to the crop grown in the largest field in the catchment: winter wheat, planted in October 2005. In 2005 the area (%) under row crops, which induce more surface runoff and soil erosion than broadcast-sown crops, was much greater than 2004. Excluding the biggest field, the area under row crops was 9.4 in 2004 and 28.5 percent in 2005.

The only runoff events during the first nine months of 2005 occurred in the first two months of the year, when the winter wheat cover was negligible. The reason there were fewer major runoff events during these two months by comparison with the previous year is that the main rill on the biggest field changed direction, flowing towards a field of grass before it reached the main channel, instead of entering the main channel directly as it had done the previous year. Figure 2.11 shows the upstream parts of this rill in January 2005.

Like most of the steep areas in South Limburg, there were some *graften* (lynchets) on steep slopes of the catchment (Figure 2.3). However, at present the remnants of these anti-erosion features only survive in small patches in northern parts of the catchment.

Figure 2.11. Formation of rills.

The increase in field size and disappearance of lynchets started with the modernisation and intensification of agriculture, especially after 1945 (De Roo, 1993). The process accelerated in the early 1960s in South Limburg, when land consolidation schemes were implemented (De Gier, 2004). Diemont and Van de Westeringh (1978) reported that between 1910 and 1950 the total length of lynchets in South Limburg decreased from 200 km to 120 km (a 40 % decrease). Saris (1984) reported a further 30 % decrease since 1950. Thus, within about 70 years 70 % of the lynchets disappeared. Moreover, De Roo (1993) noted that lynchets are still being removed by farmers very gradually, a small part during every tillage operation. The removal of lynchets increases the pressure of fauna (e.g. mice, moles, rabbits) on the remaining lynchets. Due to this concentration of animals and insufficient maintenance, the remaining lynchets become unstable and vulnerable to gully formation (De Roo, 1993).

Figure 2.12. Land subsidence, which might lead to gully formation, near the top of a lynchet in the Catsop catchment in 2004.

Figure 2.12 shows the possible beginnings of gully formation on a lynchet in the Catsop catchment in 2004.

2.6 Hydrology

Table 2.4 shows the hydrological data for major events during the study period from January 2004 to August 2005. There were more frequent runoff events during 2004, probably related to the land use pattern in 2004. It will be recalled that much of the catchment area was under row crops that year.

Table 2.4. Major hydrological events for the Catsop catchment between January 2004 and August 2005. (*Source: KNMI (rainfall)and Waterboard Roer & Overmaas (discharge)*)

Date	Rainfall (mm)	Rain duration (min)	Discharge (m^3)	Peak discharge (m^3/s)
12-01-2004	15.72	453.0	406.68	0.049
13-01-2004	11.43	342.8	390.25	0.038
19-01-2004	16.50	1371.2	157.55	0.018
02-02-2004	11.86	279.4	164.18	0.024
07-04-2004	22.69	711.6	174.17	0.031
17-07-2004	12.02	85.2	89.50	0.040
18-08-2004	27.26	195.0	474.50	0.162
11-09-2004	10.57	131.4	136.35	0.054
05-10-2004	7.43	175.8	43.68	0.019
05-10-2004	8.61	327.2	112.71	0.016
18-11-2004	30.40	1433.6	671.05	0.107
19-11-2004	11.80	180.3	234.09	0.024
17-12-2004	19.74	592.8	431.15	0.088
25-12-2004	7.25	151.4	242.28	0.051
20-01-2005	12.49	300.2	808.47	0.230
12-02-2005	14.50	743.8	113.18	0.025

De Roo (1993) has reported that during major storms in the catchment, 3–30 % of the total rainfall reaches the catchment outlet. A small buffer basin has since been constructed here, as part of the provincial government’s policy to control soil erosion and prevent the flooding of property. The stimulus for the construction of this retention basin was the off-site damage from the runoff and sediment from the catchment to Catsop village (Figure 2.13) and main railway connecting Maastricht to other parts of the country in 1989. Water and sediment from flash floods accumulate in the basin; the water discharges gradually, but the sediment load settles out and is dredged out of the basin regularly.

Figure 2.13. Flooding in Catsop village in 1989; the floodwater originated from the study area. (*Source: LISEM homepage (http://www.geog.uu.nl/lisem/)*)

Chapter 3

Data collection and methods

3 Data collection and methods

3.1 Introduction

Data were collected to obtain values for two purposes: for the input parameters of the various models used in this study, and for several state variables used for the evaluation of these models. Some parameters were obtained from a number of point sampling sites (referred to as "spatially distributed"); others gave the integrated behaviour of the catchment as a whole. Table 3.1 gives an overview of all methods used and described in this chapter. All the methods and equipment applied during this study are described below. Though some novel techniques tested were rejected because of their poor performance, they are nevertheless briefly described, together with the reasons for their failure.

Table 3.1 Overview of methods used to collect model parameters and state variables (to be used in model evaluation) in a spatially distributed or integrated way and giving the chapter section where they are discussed.

Model parameters	**Spatially distributed**	**Chapter section**	**Integrated**	**Chapter section**
Climate	Rain gauges	3.2	Beek weather station	3.2
Soil properties: surface layer	Soil texture Saturated hydraulic conductivity	3.3 3.3		
Soil properties: root zone	Penetrometer resistance	3.4		
Hydrology: surface	Runoff Evaporation	3.5 3.5		
Land use	Surveys Explorer	3.6 3.6		
State variables	**Spatially distributed**		**Integrated**	
Soil moisture: surface layer	Theta probe E-sense	3.7.1 3.7.1		
Soil moisture: root zone	Trime depth probe	3.7.2		
Hydrology: integrated			Discharge	3.8

Data collection began in November 2003 with the installation of TRIME access tubes. Other experimental devices were gradually added in the field during the measurement period. Figure 3.1 shows the locations of field measurements within the study area.

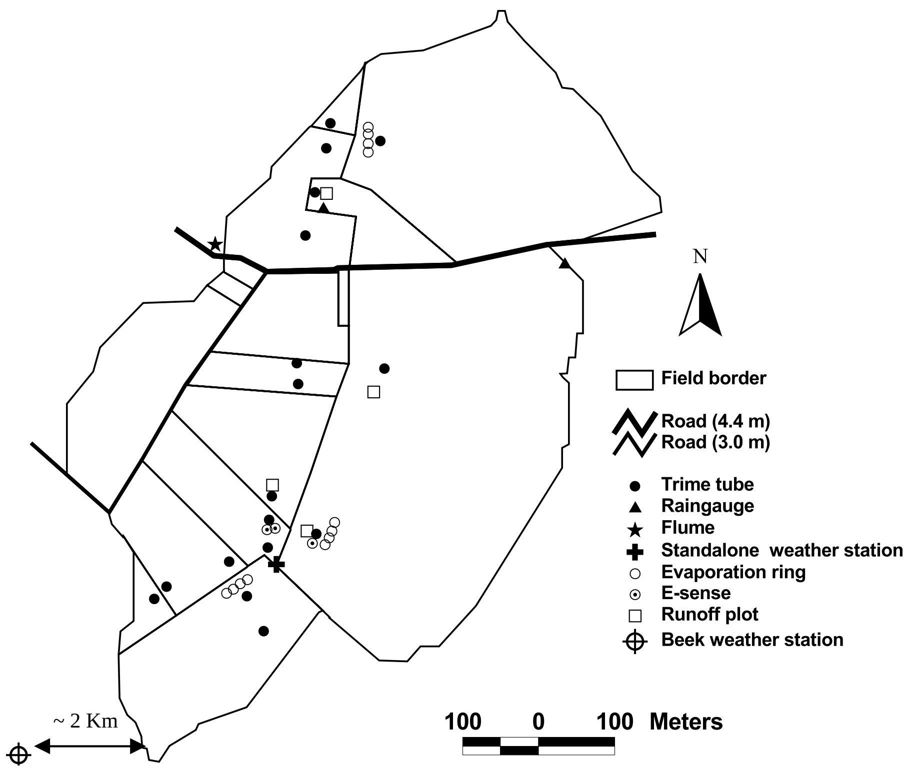

Figure 3.1. Location of measurements and tools in the Catsop catchment, S-Limburg, The Netherlands.

3.2 Meteorological data

At the start of 2004, two tipping bucket rain gauges and one small standalone weather station (SPECTRUM) were installed in the catchment. However, only the meteorological data from the Beek weather station (50º 55´N, 5º 47´E) were used in this research, because the standalone weather station stopped working after a few weeks and as well as being inconsistent, the data from the tipping buckets were logged at a time interval that was too large for the simulation of storm events. The time interval of the tipping bucket rain gauges was 60 minutes in the first year (2004). In the second year it was changed to 10 minutes. Fortunately, the available contemporary data measured by these gauges agreed well with the data from the Beek station, which is less than 2 km from the study area.

The potential evapotranspiration rate was calculated with the Penman–Monteith equation using daily meteorological data from the Beek station.

3.3 Soil properties: surface layer

Soil texture

Soil texture was analysed with a laser granolometry technique. Only the surface layer (0–6 cm) was analysed. In December 2003 twelve samples were randomly taken from the study area and then analysed at the Laboratory of Soil Science and Geology of Wageningen University and Research centre. There was no significant difference in the particle size distribution of the samples. The clay content of the samples was 5.40 % ± 0.27 %, the silt content was 67.69 % ± 0.87 %, and sand content was 24.55 % ± 0.80 %. The results deviate slightly from those reported in earlier studies of the area. For instance Stolte et al. (1996) reported a clay content of 14.5 % ± 2.5 % and a silt content of 76.6 % ± 2.6 % for the surface soil layer (0–8 cm). The disparity might be associated with the method of texture analysis.

Saturated hydraulic conductivity

The saturated hydraulic conductivity is an important parameter in hydrological modelling. In this study the saturated hydraulic conductivity was determined using a steady state constant head method (Stolte, 1997) based on Darcy’s law. Figure 3.2 shows the set-up used for this measurement.

Figure 3.2. Laboratory set-up for measuring the saturated hydraulic conductivity.

As will be mentioned in section 3.5, 12 rings had been installed in the catchment on 7 April 2004, to measure soil evaporation. They were left in situ after the measurements had been completed. Three months later they were removed and taken to the laboratory of the Erosion and Soil and Water Conservation Group of Wageningen University, in order to measure the saturated hydraulic conductivity. The rings had been left undisturbed in the field for such a long time that they provided excellent samples for the measurement of hydraulic conductivity. The samples were saturated before the measurements began. A layer of water 2 cm deep was maintained on top of the samples and the volume of water that percolated through the sample was measured over time. The saturated conductivity was calculated as follows (Stolte, 1997):

$$K_s = \frac{Vl}{(At)(l+d)}$$

Where K_s is saturated hydraulic conductivity (cm d^{-1}), V is outflow volume (cm^3), A is the surface area of the soil sample (cm^2), l is the height of soil column (cm), d is the depth of water on top of the soil sample (cm) and t is time (d). The results are presented in Table 3.2.

Table 3.2. Measured saturated hydraulic conductivity (cm d^{-1}) of loess topsoil in S-Limburg, The Netherlands.

	Sample					
Field	**1**	**2**	**3**	**4**	**mean**	**SD***
Winter wheat	25.92	23.52	30.00	--	26.4	3.28
Sugar beet 1	29.52	120.96	109.44	153.1	103.25	52.52
Sugar beet 2	5.04	12.24	5.04	19.68	10.50	7.00

* Standard deviation

As shown in Table 3.2, the standard deviation (SD) of the measured saturated hydraulic conductivities in each field is not very large. However, there is a large disparity between the values of saturated conductivity for two different fields of sugar beet. Presumably, this difference is related to the management practices applied in the fields. In the field with higher conductivity (Sugar beet 1) a green manure crop (yellow mustard) had been sown after the cereal harvest in August 2003. In November 2004 the green cover had been mown, chopped into small pieces and spread over the land. In April 2005 the field had shallowly been ploughed and sown with sugar beet. The concentration of organic matter in the topsoil might have improved the infiltration capacity of the soil. The other field (Sugar beet 2) had been ploughed conventionally.

3.4 Soil properties: root zone

Penetrometer resistance

While augering to install TRIME access tubes it was noticed that at most of the auguring locations there was a compacted layer at a depth of between 15 and 50 cm in the soil profile. Despite the presence of deep loess soils in the catchment, the main cause of the surface runoff in the area is saturated runoff generation (De Roo et al., 1996). On 20 August 2004, therefore a penetrometer survey was conducted within the study area. As its name implies, a penetrometer is used to determine the resistance to penetration of the soil. It is a useful tool for detecting compacted soil layers. In this study an electronic penetrometer (Penetrologger) with a built-in data logger was used. The penetrologger consists of a force sensor, the logger, a probing rod, a cone and an ultrasonic depth measurement system. Using the device, the resistance of each layer of soil profile up to 80 cm depth can be measured continuously. The resistance to penetration is measured in kilo Pascal (kPa) or Newton.

Generally speaking a compacted sublayer produced because of leaching or ploughing practice within the first metre of the soil profile, shows higher resistance to penetration. The presence of a compacted layer reduces the conductivity of the soil profile for water.

The penetrometer survey showed that the presence of the compacted layer depends on land use and land management practices. Figure 3.3 displays the penetrographs for some locations in the catchment with their specific land use type or land management practice. As shown in the figure, resistance was measured at two locations in each field. Each series in the graphs is the average of three reiterations at each location. In orchards there was a significant difference between tree rows and the grassed strips used as paths (Orchard*). In grass strips the resistance was high near the surface and it had a constant value for the deeper layers. But in tree rows (Orchard) the resistance was low for the first 20 cm and then increased gradually until 40 cm depth. In grasslands (Gr.d (located in downslope) and Gr.u (located in upslope)) the resistance increases gradually from the land surface down to 60 cm. However on pastures (Gr.g) the pattern is similar to that of the grassed paths in orchards (Orchard*). On pastures, a shallow compacted layer is created by the trampling of cattle.

Like the observations during augering, the penetrometer survey also revealed the presence of a compacted layer within the first 50 cm of the soil profile.

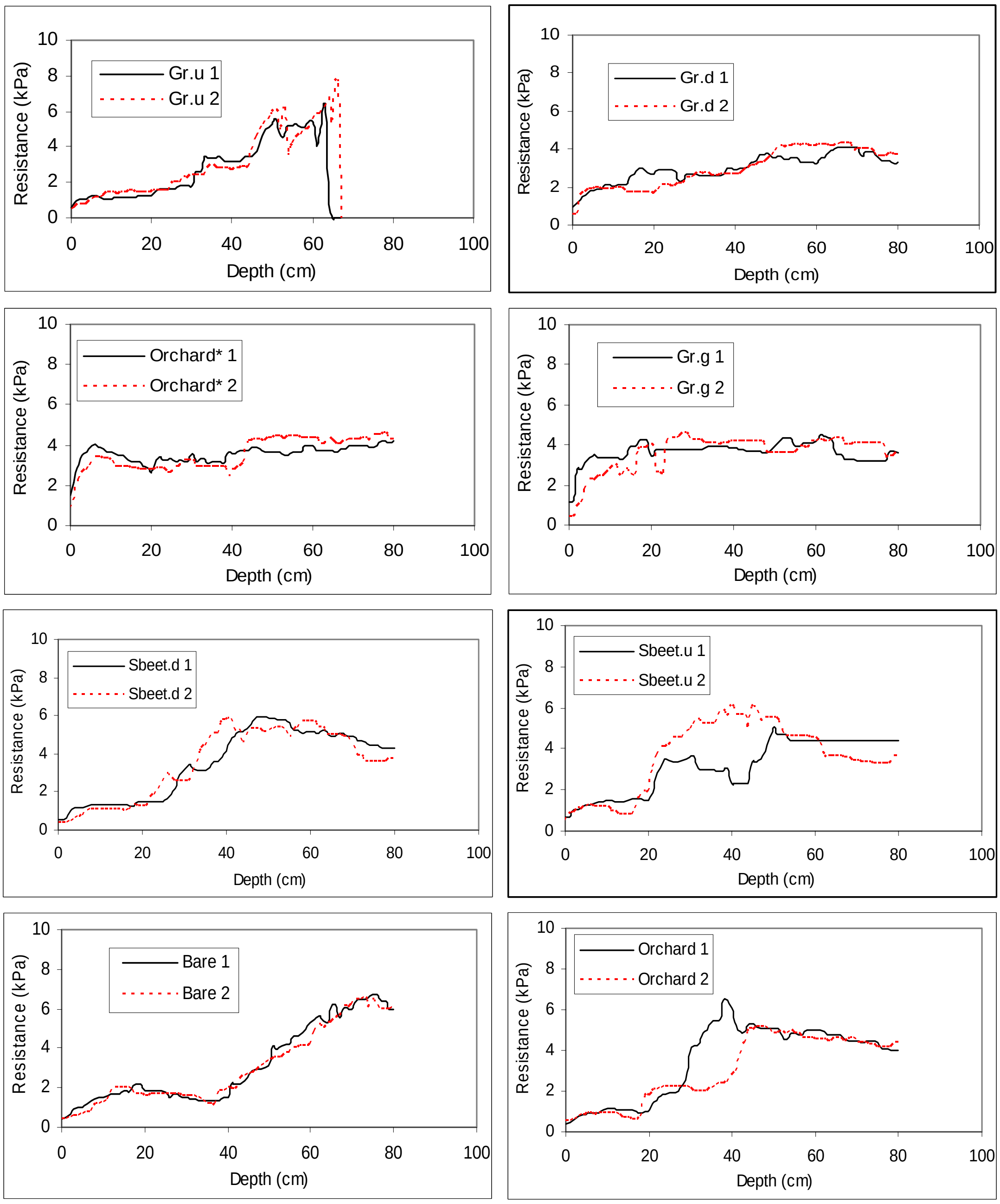

Figure 3.3. Penetrographs of the different land uses in the Catsop catchment.

3.5 Hydrology: at the soil surface

Surface runoff measurements

Surface runoff was measured at two scales. For the small scale, small runoff plots about 1.1 m^2 in area were used (Figure 3.4).

Figure 3.4. A small plot used to measure surface runoff.

The discharge from two runoff plots was measured automatically with pressure transducers in the buckets that collected the runoff from the plots. Contrary to expectations, the surface runoff from the two runoff plots was very high and therefore the buckets overflowed between field visits. Both of the plots were in the biggest field, in which a small gully forms every year after tillage. These two plots produced runoff during most of the rainfall events during winter, though the number of observed runoff events at the outlet of the catchment was far fewer. This suggests that runoff generated in some upstream areas during small to medium rainfall events never reaches the outlet: instead it re-infiltrates in downstream areas before reaching the main channel. This phenomenon was observed at several locations within the catchment during field visits. Some small rills in upstream areas peter out when they reach locally flat areas, field borders, or when they enter another field with a dense crop. This implies that data measured at the outlet are not sufficient for validating a distributed hydrological and erosion model such as LISEM.

Soil evaporation measurement

Evapotranspiration constitutes a major component of the water balance in the root zone soil profile. It consists of two parts: evaporation from the soil surface and transpiration by plants.

In many agroclimatological and water balance studies they are considered as a single variable, while in other situations, the eparation of evaporation and transpiration will give a better understanding of the relevant processes under consideration (Stroosnijder, 1987). The evapotranspiration (ET) rate from a cropped surface can be measured directly by the mass transfer or the energy balance method. It can also be derived from meteorological and crop data by means of the Penman–Monteith equation, or determined from field measurements within large-scale weighing lysimeters.

The most common method used to separate evaporation from the soil surface (E) from transpiration by plants (T) in soil water balance investigations is to measure or estimate both ET and E. T is then obtained by subtraction (Stroosnijder, 1987). In principle, evaporation from the soil surface can be estimated by mechanistic models or by empirical models. In mechanistic models based on Darcy's law, the soil water flux in both the liquid and vapour phases is calculated by multiplying the gradient of the water pressure head by the corresponding hydraulic conductivity. However, such mechanistic models require input data that are not readily available. Therefore, in practice, empirical parametric evaporation models are used. These models require their parameters to be calibrated for the local climate, soil, cultivation and drainage situation. In parametric models, evaporation from the soil is usually considered in three stages (Black et al., 1969; Ritchie, 1972; Boesten & Stroosnijder, 1986; Hillel, 1998). During the first stage, evaporation occurs at a potential rate (E_{pot}); during the second stage, evaporation decreases rapidly in proportion to E_{pot}. During stage three, no evaporation occurs. Micro-lysimeters have proved to be useful, cheap and simple tools for measuring evaporation from bare soil. They are undeniably important in the calibration of empirical and semi-empirical evaporation models. The type of micro-lysimeter used to measure soil evaporation in this study is described in detail below.

The evaporation measurements were carried out on 12 days during spring 2005. It was assumed that the spring is the appropriate time for such measurements, since good quality data on evaporation in the field can be obtained at the beginning of a drying period following saturation or near-saturation conditions. In winter, the entire soil profile in the root zone gradually becomes saturated and remains near saturation for a long period. In spring it starts to dry out. Thus, a medium-size rainfall event at the beginning of spring followed by a dry period of a few days would provide ideal conditions for monitoring the evaporation rate in the field.

According to the local weather forecast, some showers were expected on 7, 8 and 9 April 2005. It was therefore decided to start the experiment on 7 April by installing 12 evaporation rings in three fields (4 rings per field). The evaporation rings were small PVC rings with 75 mm inner diameter and 20 cm height. One end of the rings was sharpened, to facilitate insertion into the soil. The rings were removed from the soil carefully, by twisting them; once removed, a piece of cloth was put over the base. After being weighed with a digital kitchen scales of approximately 1 g accuracy, they were replaced in the soil. The undisturbed soil samples in the rings were weighed twice or three times per day. Despite the local weather forecast, no rain fell, neither was the atmospheric drying sufficient to produce a measurable change in soil moisture content during the monitoring days. Until 15 April the weather was settled: cloudy, mild (about 9 °C), foggy in the mornings, and with some drizzle (less than 1 mm per day). There was no perceptible change in the weight of the rings over time. Therefore it was decided to suspend the measurements, leave the rings in situ and monitor the weather of the region from the office.

Some showers, totalling about 10 mm, fell on 19 April and in the morning of 20 April 2005. Thus a second round of measurements started on 20 April. This time, the measurements were carried out three times per a day at 9–10 h, 12–13 h, and 15–16 h hours. At the start of the measurements the soils were saturated for at least the first 20 cm. Fortunately the weather on subsequent days was also conducive for the measurements. The measurements on the first day showed a rapid decrease of soil moisture content. As expected (Boesten and Stroosnijder, 1986; Stroosnijder, 1987), on subsequent days the rate of decrease slowed down, ceasing after three days (Figure 3.5).

The experiment was stopped after the last repetition at 15–16 h on the fourth day. It is worth mentioning that the evaporation measurement was in concomitant with the intensive field monitoring plan to observe soil moisture changes in space and time at detailed resolution for two weeks: one week in spring and the other in summer. It was planned to observe soil moisture with a combination of the gravimetric, Theta surface probe, TRIME depth probe, E-sense, and visible and near infrared photography methods. The main aim of this plan was to test the applicability of the latter two methods for monitoring soil moisture content. However, as both these methods failed to function properly (see sections 3.6 and 3.7.1), intensive field monitoring for the summer period was cancelled.

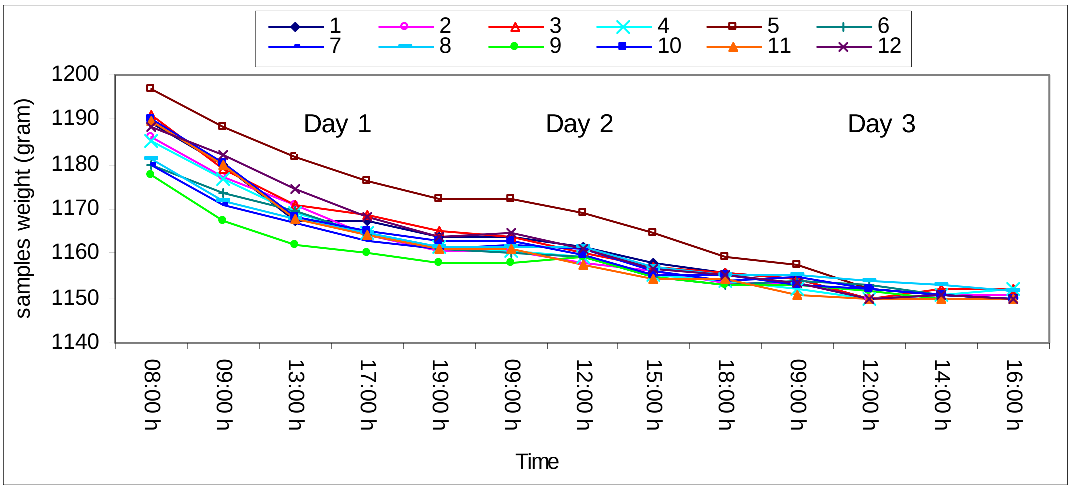

Figure 3.5. Decrease of soil moisture content in evaporation rings, April 2005 for loess soil in the Catsop catchment, S-Limburg, The Netherlands.

3.6 Land use

Field surveys

Field surveys were done in order to prepare a land use map of the study area. A hand- held GPS with horizontal accuracy of 5 metres was used to define the field borders. The geographical position of reference points such as field corners, road junctions, etc. were also determined with this GPS. This point information was converted to a map of the fields, using PCRaster and ArcView. The catchment divide was derived from DEM with PCRaster. The map of the fields was overlain on the catchment divide map, to produce the land use map of the study area.

The Erosion Explorer

The LISEM model is one of the first examples of a spatially distributed physically- based model that is completely incorporated in a raster Geographical Information System, PCRaster (Van Deursen and Wesseling, 1992). Therefore all the input parameters and variables are entered as raster format. For a new drainage basin, the following basic maps should be made by the user.

- DEM (Digital Elevation Model, continuous)
- Land use map (classified)
- Soil map (classified)

Since the topography and distribution of soil types of an area are constant physical characteristics, the DEM and soil map are made once for a catchment. However, the land use is a dynamic characteristic of a catchment.

Most of the input variables and parameters for the LISEM model are derived from these three basic maps. In South Limburg, most of the variables are strongly related to land use (De Roo et al., 1995). LISEM requires updated input maps of antecedent soil moisture content and land use parameters for each rainfall event. The most important land use parameters are percentage of crop cover and leaf area index. Remote sensing images (radar, airplane or satellite) usually provide a reliable source for land use maps and possibly for surface layer soil moisture content at catchment scale and higher. But the use of radar and of airplanes is very costly, especially for repeated snapshots. Satellite images are cheaper, but the resolution of widely used satellite images is too coarse (particularly the thermal bands which are used for moisture prediction) for application to a small catchment such as Catsop. Moreover, the fixed temporal resolution of these images restricts their suitability for use in event-based models that require an image just a few days before an event.

Another possible option to acquire repeated snapshots at a proper temporal and spatial resolution is to use small, radio-controlled airplanes. Therefore at the start of 2005 a remotely controlled parasail, “le drone Pixy” (Figure 3.6) was purchased to use in this research and other studies done by the Erosion and Soil and Water Conservation group of Wageningen

University and Research centre. It was intended to use this craft to take visible and near infrared photographs to monitor temporal changes in land use parameters and surface layer soil moisture content. Unfortunately, it was very soon discovered that this was not possible, because of the limitations discussed below.

Technical limitation

Due to the design of the motor, it is difficult to get the craft to fly in a straight line. Moreover imaging with infrared photography requires the camera to remain focused on a particular area for a few seconds. It is impossible to get the Pixy to hover for a few seconds.

Weather limitation

Due to its light weight (maximum 10 kg for airplane plus equipment load), it is difficult to fly the airplane at wind speeds above 4 m s^{-1}, because of the risk that it will become uncontrollable. At wind speeds above 5.5 m s^{-1} it is impossible to fly the craft (Luisman, 2005); the long-term (1970–2000) mean daily wind speed of the study area is 4.3 m s^{-1}.

Figure 3.6. Erosion Explorer

Regulation limitation

Under a regulation of the Dutch Ministry of Defence, the maximum flight height over the study area is 100 m. However, even to fly within this range, permission must be obtained from the Ministry. And as the Catsop catchment is less than 2 km from the international airport of Maastricht–Aachen, permission from the airport authorities is also necessary in order to be able to fly over the catchment. The permission must be applied for a few days before each flight, stating a definite date and time. It appeared to be impossible to get a scheduled permission plan in advance. Moreover, given the unpredictability of the weather more than one week ahead, it is difficult to fly on the basis of a predefined schedule.
In spite of the problems mentioned above, the aircraft's great potential for reconnoitring soil erosion features makes its application for soil erosion studies and validation of the erosion models promising. For instance, Figure 3.7 shows small rills of about 35 cm width and 25 cm depth developed in the study area. Due to its value as a reconnaissance tool, the craft was christened the “Erosion Explorer”.

Figure 3.7. A photo taken by the Erosion explorer on 21 April 2005. The rectangle on the photo indicates small rills developed in the filed during winter 2004 – 2005.

Recently the Erosion Explorer has been applied to create and validate a DEM created from aerial photographs taken with a Nikon Coolpix 5400 digital camera (Luisman, 2005). The main aim of that study was in line with the objective of our study, which was to improve the simulation quality of LISEM. Luisman (2005) attempted to test the capability of the Erosion Explorer to create a DEM with a precision of at least 0.3 m, which could be used to determine the random roughness and local micro depressions (the surface storage in micro depressions determines the runoff generation threshold). In the LISEM model a nonlinear relation between the depression storage and random roughness is used. Therefore LISEM requires spatially distributed random roughness data to be input by the user. Since LISEM is sensitive to random roughness (De Roo et al., 1996), accurate values for random roughness will improve the accuracy of the model's predictions.

Unfortunately, the results showed that the maximum accuracy of DEM obtainable by the Erosion Explorer is about 0.3 m. This accuracy is obtained when the Erosion Explorer flies at the optimum height of 60 m above the ground. In the current study, the random roughness data according to the reference data in the user guide of the LISEM (De Roo et al., 1995) were used.

3.7 Soil moisture measurements

It has long been recognised that reliable, robust and automated methods for the measurement of soil moisture content can be extremely useful in hydrological, environmental and agricultural applications. Over the last 50 or 60 years, this recognition has stimulated a considerable amount of ingenuity to be invested in developing such methods (Walker, 1999). Nowadays there are various soil moisture measurement tools, each applying a different technique. The most widely used techniques are: thermogravimetric; neutron scattering; Gamma ray attenuation; soil electrical conductivity; tensiometric; and soil dielectric techniques. The Soil Moisture Neutron Probe (SMNP), which was developed more than 50 years ago, has been one of the most accurate methods to date. It has served well the need for accurate measurement of soil moisture content. However, increasing regulatory burdens and the impossibility of acquiring data automatically and unattended have limited the usefulness of this device. Newer methods, especially devices operating on the basis of soil electrical conductivity properties, allow data logging and unattended measurement of soil moisture content, but with uncertain precision and accuracy (Evett et al., 2002).

Reviews on the advantages and disadvantages of the most widely used methods have been well documented in the work of Walker (1999). Various methods have been compared by Schmugge et al., (1980), Evett et al. (2002), and Walker et al. (2004). Readers are referred to these references for more information about each individual method and its accuracy. Since only the thermogravimetric and Time Domain Reflectometry (TDR) techniques were used in this research, they are briefly explained below.

The thermogravimetric method is the standard method of measuring the soil moisture content. In this method, a known volume of soil is oven-dried at 105 ^{o}C for 24 hours and the weight loss is calculated. The advantages of this method are that it is inexpensive (i.e. does not require expensive equipment) and soil moisture is calculated easily. However, it is time consuming and destructive to the sampled soil, especially for measurement in deeper layers. Hence, it cannot be used for repeated measurements at the same location. Moreover, this method is prone to large errors due to sampling, transporting and handling. Soils with organic matter may exhibit a mass loss during oven drying, due to oxidation and decomposition of the organic matter, while some clay particles will retain considerable amounts of adsorbed water. Measurement errors will be reduced by increasing the size and number of samples (Zegelin, 1996). In spite of these deficiencies, it is indispensable as a standard method for calibration and evaluation purposes (Walker et al., 2004).

In this research, the method was used to evaluate two different TDR probes (Theta surface probe and IMKO TRIME-FM depth probe) and also to determine saturated moisture content. Thin-walled stainless steel cylindrical tube samplers with a known volume of 100 cm^3 were used for this method, as according to Evett et al. (2002), the most accurate volumetric moisture contents are obtained with these cylinders.

In a TDR method, an electromagnetic wave is propagated along a wave guide embedded in a material whose dielectric constant is required. The dielectric constant is a measure of how polarisable a material is when subjected to an electric field (Zegelin, 1996). This material property is usually measured relative to that of free space, and is referred to as the relative dielectric constant.

Soil consists of air, soil particles and water. Therefore the relative dielectric constant of soil is a composite of these components. Soil moisture content can be determined from measurements of the soil dielectric constant, as a result of the large difference between the relative dielectric properties of liquid water (approximately 81) and dry soil (< 5) (Topp et al., 1980). In soil moisture probes the down and return travel time of the electromagnetic wave along the wave guide is measured. Since the dielectric constant of water is much higher than the soil particles, the travel time decreases as soil moisture content increases. In this research, three different probes that apply the TDR technique were used.

3.7.1 Soil moisture: surface layer

Theta Probe

The Theta Probe has a configuration of 3 rods (wave guides) surrounding a central rod, all of which are inserted into the soil. The difference between voltage at a crystal oscillator (enclosed in the body of the probe) and that reflected by the rods is used to determine the dielectric constant of the soil. The length and diameter of the rods are 50 and 1.5 mm, respectively. This device was connected to a simple-to-use push-button hand-held readout unit (Figure 3.8). The Theta Probe in combination with a readout unit provides a compact and fully portable volumetric moisture measurement system.

Figure 3.8. Theta probe and TRIME-FM

The Theta Probe was used for surface layer soil moisture monitoring within 0–5 cm depth. In Figure 3.9 the soil moisture content readings of the Theta Probe are compared with those determined with the gravimetric method. The probe is fairly accurate ($R^2 \approx 0.84$). This comparative study showed that the RMSE of the measurement with Theta Probe is about 2.6 cm^3 cm^{-3}. Based on the specification in the catalogue, the accuracy of this device is approximately 5 percent with standard calibration and 2 percent with a soil-specific calibration.

Since the wave guides are inserted directly into soil, the gap between the wave guide and surrounding medium is negligible, which reduces the measurement errors. Problems arise when using this device in dry and compacted soil. When the device is forced into such soil (e.g. in grasslands and untilled fields) the rods easily diverge and generate a large observation error. Since the material used for the rods is a soft metal, the bent rods can easily be straightened by hand. However if this is done several times, the rods break. Therefore this device is only suitable for tilled land and moist areas. For untilled areas with compacted or heterogeneous soils, the theta probes must have stronger rods.

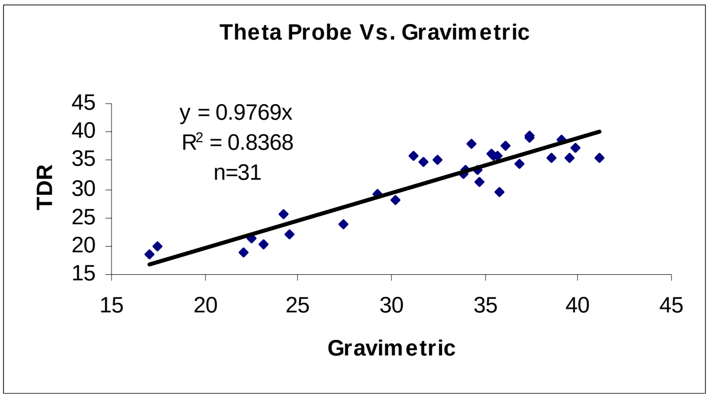

Figure 3.9. Comparison of soil moisture contents measured with the Theta Probe and gravimetric methods

E-sensors

The technology for long-distance communication continues to advance apace and is becoming affordable for most of the world's community. The labour costs of repeated field sampling and measurements for the continuous monitoring of environmental variables such as soil moisture content are prohibitively expensive, particularly in remote areas. Using automated soil moisture measurements and storing the data in a logger has already alleviated the problem of continuous monitoring. But there is no guarantee that the measurement device will continue to function properly after installation. Furthermore, loggers have a limited storage capacity. The ideal system to enable continuous monitoring of environmental variables would therefore be to have measurement devices and sensors which can be programmed and controlled remotely.

Recently, Eijkelkamp Agrisearch Equipment Company has released a system called "e-SENSE" which meets this need. In the e-SENSE system, which can be accessed via the internet, intelligent sensors are installed in the field and connected to a modem. The measured data from the sensors are read and sent as SMS code messages to the internet database (www.longcat.nl) Moreover e-SENSE enables two-way communication between a measuring unit in the field and a central computer system. The data are transmitted from the sensors to the central database. The central computer system allows the sensors to be remotely controlled: users can alter the settings of the sensors in the field from their office. This is an important advantage, as the user can adjust the measurement interval to take account of the rate of change of a dynamic variable such as unsaturated zone soil moisture content. For instance, the soil moisture content in the unsaturated zone changes rapidly during and just after rainfall events, but changes slowly in the interval between such events. The e-SENSE system can also be used in an early warning system for flooding.

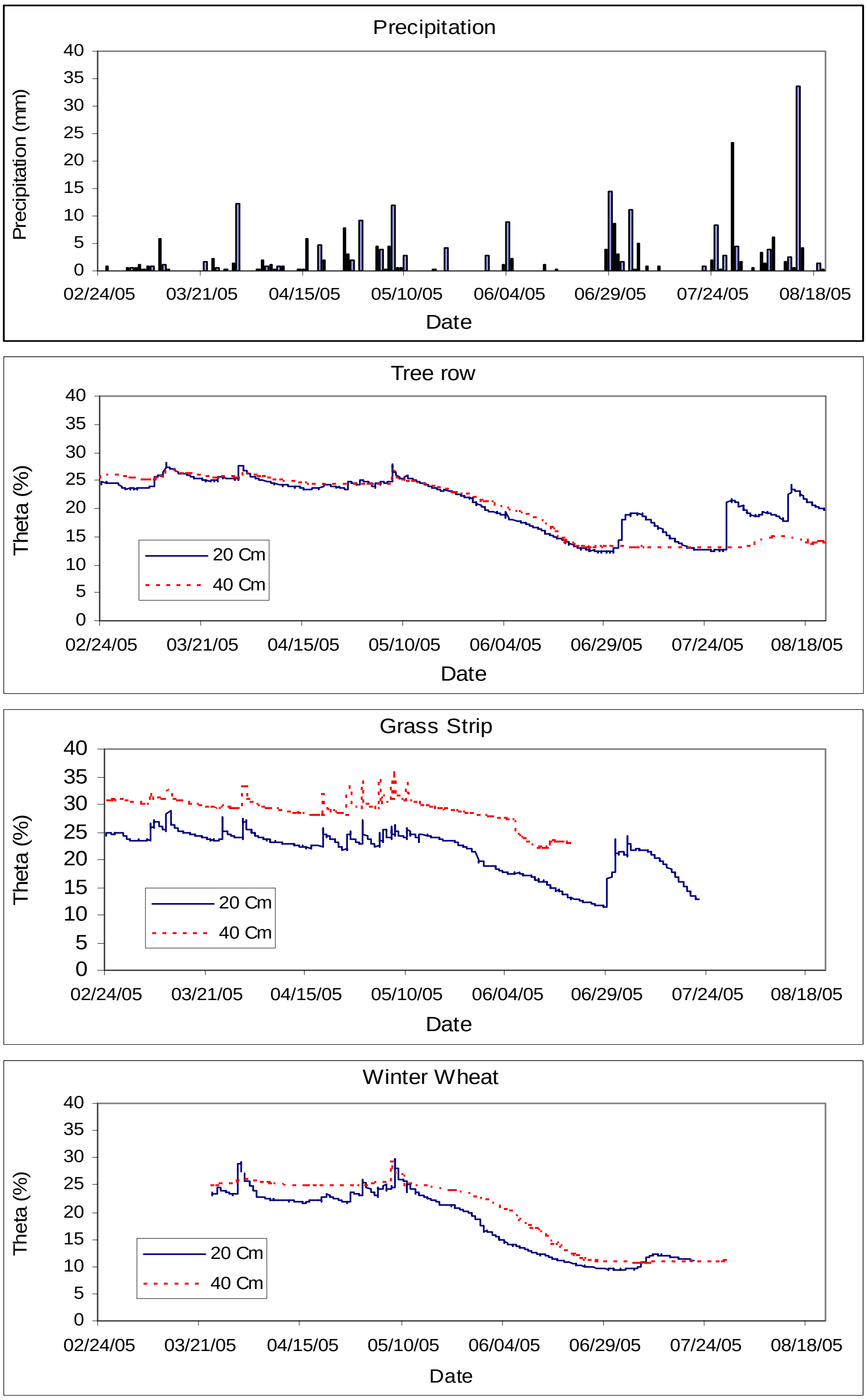

Figure 3.10. Time series of precipitation (data from the Beek station) and soil moisture content (measured with E-sense sensors) at three locations differing in crop cover.

Since the main aim of this study was to link an event-based simulation model (LISEM) with a continuous daily based buddy model, it was assumed that e-SENSE would be an appropriate system for obtaining a soil moisture data set with different time intervals. Therefore six soil moisture sensors compatible with this system and that apply TDR technique were purchased in 2004. Since the part of the root zone profile that varies most is the first top few centimetres, the sensors were installed at 10 cm depth at six points in the catchment. Unfortunately, monitoring of the recorded data at the internet database during the first weeks after installation proved that the sensors were not functioning properly. Therefore all sensors were returned to the Eijkelkamp Company, for repair. In 2005, six new sensors were installed at three locations. This time, two sensors were installed at each location: one at a depth of 20 cm and the other at 40 cm. Although one of the sensors developed a small problem and stopped functioning after four months' recording, the other sensors provided reliable values.

Figure 3.10 shows the time series of moisture content recorded by these sensors. The sensors at 20 cm show a rapid response to rainfall, but those at 40 cm depth show more gradual changes. Though only one metre apart, the sensors in Tree rows and Grass strips reacted differently to precipitation. It is assumed that this difference is related to differences in the amount of interception. Trees usually intercept a considerable proportion of the precipitation, particularly for small rainfall events.

3.7.2 Soil moisture: root zone

TDR depth probe to be used in access tubes

The TRIME probe used in this study was the TRIME-FM (Figure 3.11) from the IMKO Company. It is a portable instrument, developed for field use. The probe consists of a cylindrical PVC body (probe), which has two aluminium plates as TDR wave guides on opposite sides, a coaxial cable (2 m), and a readout device. As the aluminium plates are 175 mm long, the probe gives depth- averaged soil moisture content for about 18 cm.

The fibreglass access tubes (with inner diameter of 44 mm) used for the TRIME probe are more expensive than the tubes used for the neutron probe. Like access tubes for the neutron probe, the TDR access tubes are installed before the measurements and can be left in the field for repeat measurements.

The measurement field penetrates the soil to a depth of up to 100 mm. The measurement sensitivity is the highest near the access tube and decreases exponentially away from the tube into the soil. Therefore in order to obtain reliable measurements, it is important for the access tube to be in close contact with the surrounding soil. A small air gap between the tube and surrounding soil produces a significant deviation in soil moisture values. The influence of such an air gap is dependent on the water content. For example, in a soil with 15 cm^3 cm^{-3} soil moisture content, an air gap of 1 mm around the whole length of the tube would result in the water content being 1–2 cm^3 cm^{-3} lower water content. At a water content of 25

$cm^3\ cm^{-3}$ the error would be 5 $cm^3\ cm^{-3}$. At a very high water content it is even possible for the error to exceed 10 $cm^3\ cm^{-3}$, yet if there were a water-filled gap under saturated moisture content, the error produced by the gap would be much smaller (IMKO Micromodultechnik GmbH, 2001). Therefore this instrument is only suitable for homogenous soils when the access tubes have been installed carefully.

In this study, the tubes were installed with the help of an experienced soil science technician. We did not use the special drilling set developed for installing the access tubes in homogeneous soils. It was assumed that the access tubes would be in close contact with the surrounding soil within a few weeks after installation, thanks to the very active soil fauna in the study area and the soil's propensity to become saturated, especially during winter. However, when the soil around some of the tubes was dug out at the end of the measurement period, it was found that these assumptions were false, especially in the fields with permanent crops (Figure 3.12).

To check the accuracy of the TRIME tube probe data and also the influence of the air gap on the measurements, the soil moisture content was measured by the TRIME tube probe just before the tubes were dug out. While the tubes were being dug out soil samples were taken around four tubes so that the moisture content could be measured with the gravimetric method. The values obtained using the two methods were then compared. The results showed that when there is an air gap, the TRIME tube probe gives lower soil moisture values. However, it gives higher values for soil moisture content when the tubes are in close contact with the surrounding soil (Table 3.3).

Figure 3.12. Air gap between TRIME access tube and surrounding soil.

Table 3.3. Comparison of values for soil moisture content obtained with the TDR and Gravimetric methods.

Land use	Layer (cm)	TDR	Mean Grav.*	Std. Grav.*
Orchard down	0 – 20	39.8	34.12	0.24
	20 – 40**	25.1	31.34	1.60
	40 – 60**	21.9	29.52	0.57
Orchard up	0 – 20	39.8	31.36	1.00
	20 – 40	41.0	31.68	2.49
	40 – 60**	27.4	32.05	0.82
Grass down	0 – 20	45.5	32.51	0.58
	20 – 40	39.7	28.36	1.52
	40 – 60	30.6	25.93	0.92
Grass (grazed)	0 – 20	44.9	33.84	2.05
	20 – 40**	27.6	31.97	1.18
	40 – 60	23.1	24.91	3.12

*. Mean and standard deviation of three samples used for gravimetric measurement

**. There was a small gap between the tube and surrounding soil.

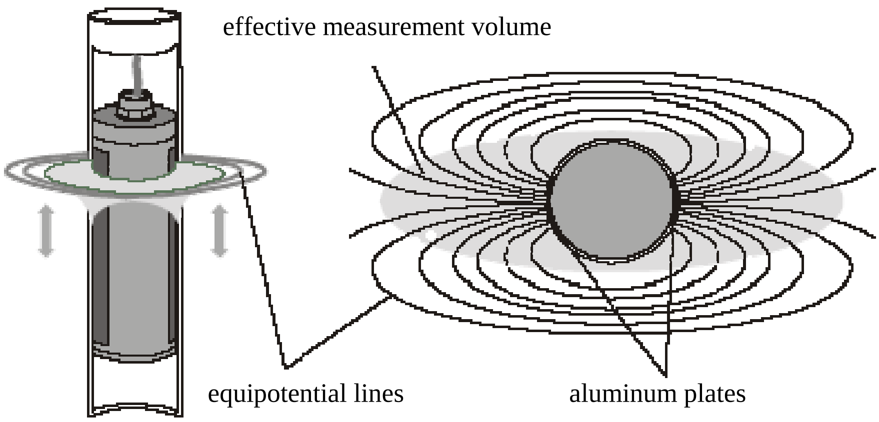

Figure 3.11 Electric field distribution of the TRIME tube probe and approximate measuring volume (source: IMKO Micromodultechnik GmbH).

As the measurement volume is elliptical, (Figure 3.11), for each depth interval the soil moisture readings should be repeated several times (e.g. three times) by each time, rotating the probe slightly. The average of the repeated readings should be regarded as the soil moisture content measured for each depth interval (TRIME-FM manual). Note that it is difficult to determine how far to rotate the tube for each repetition; also, the repetition is only random. Since it was time-consuming to repeat the measurements for all tubes and soil layers, at the start of the monitoring period it was decided to begin by repeating the measurements at 10 tubes only. Analysis of the readings from these tubes showed that the standard deviation of the repeated measurements ranged from 0.003 to 0.03 $cm^3\ cm^{-3}$. Therefore it was decided to continue the measurements by taking only one reading per depth interval each time.

3.8 Hydrology: integrated

Surface runoff was measured at two different scales. Discharge was measured at the catchment outlet using a partial flume with a capacity of 950 $l\ s^{-1}$ and a stilling well with a vertical float recorder. This station had been installed by Wageningen University in 1987 but is currently administered by the "Roer en Overmaas" water board. It has been used sporadically during the last two decades. The data series available from this station coincided with the period when research was being done in the catchment.

Prior to 1989, data were written on a drum chart. Since 1989, data have been stored in a logger. During 1987, sediment loads were also measured by automatically taking water samples during large runoff events. At the start of my research this hydrometric station was reactivated (on 27 December 2003). Data were stored at 5-minute intervals in a logger.

Figure 3.13. Surface runoff monitoring equipment used in the Catsop watershed.

The water level in the retention basin about 50 m downstream of the outlet was monitored to check the consistency of data from the flume. A pressure transducer sensor was installed in the basin (Figure 3.13). In 2004, the correspondence between flume data and water level data in the basin was good. Figure 3.14 shows typical time series of water level in the flume and retarding basin (from 1 January to 21 April 2004). In 2005 the outlet of the basin, which is controlled manually, was readjusted.

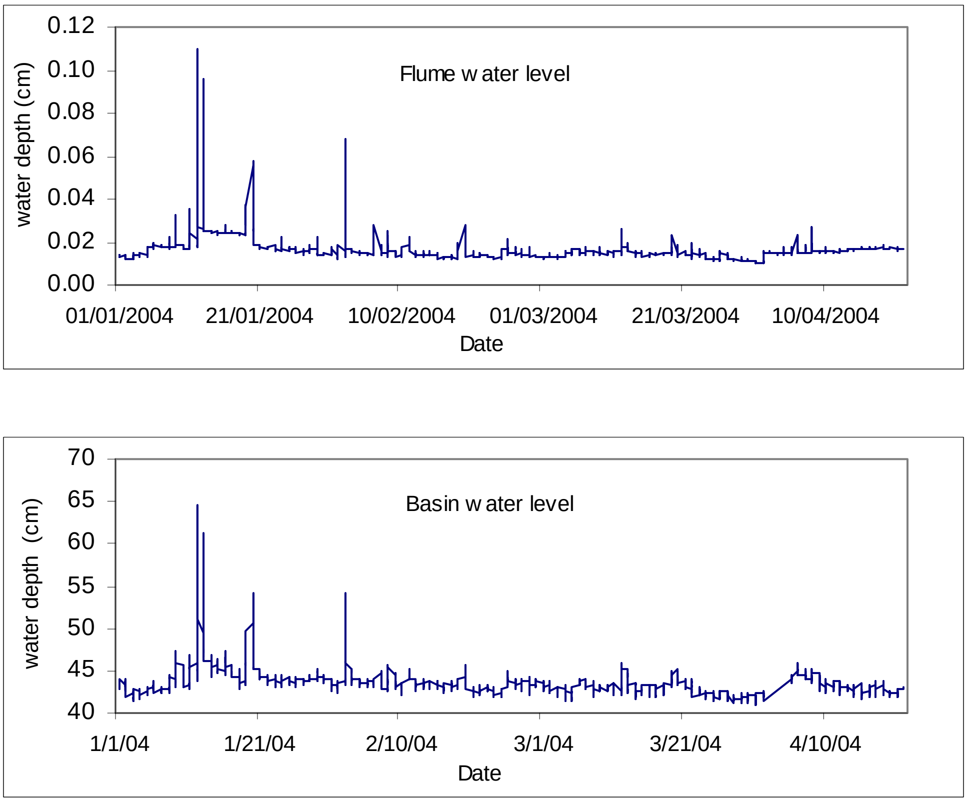

Figure 3.14. Time series of water depth at the flume and in the retention basin.

Chapter 4

Sensitivity of catchment discharge to initial soil moisture

Vahedberdi Sheikh, Emiel van Loon, Rudi Hessel, Victor Jetten
Submitted to: Hydrological Processes

4 Sensitivity of catchment discharge to initial soil moisture

Abstract
Pre-event soil moisture is generally considered as an important determinant in runoff generation. Previous investigations to this relation considered one or two relevant co-variables. When looking across these studies, however, many variables seem to be relevant. This study conducts a broad sensitivity analysis, taking into account the influence of initial soil moisture content in two soil layers, layer depths, event properties, and two infiltration models. A distributed hydrology and soil erosion model (LISEM) is used. LISEM allows selecting various infiltration models. Using the terrain data from the Catsop research catchment and two different rainfall events, the sensitivity of discharge is investigated for a range of pre-event soil moisture contents (0.05 to 0.40 cm^3 cm^{-3}) in two layers for a two-layer Green-Ampt as well as Richards infiltration model. The sensitivity of the predicted discharge to the initial condition of soil moisture appears to depend highly on all factors: infiltration model, event properties, topsoil/subsoil depth configuration and the level of initial soil moisture itself. There are interaction effects between all the factors. However, the effect of the different infiltration models is most pronounced. Discharge is less sensitive to the moisture content of both top and subsoil for the Green-Ampt model in comparison to the Richards model. Moreover, the response is much more linear for the Green-Ampt model. The Richards model shows a highly variable discharge - initial soil moisture relation with changing rainfall intensity and topsoil/subsoil depth configurations. Considering ±0.05 cm^3 cm^{-3} changes at initial soil moisture content of the surface layer Green-Ampt shows -25 to +50 percent changes in discharge depending on topsoil / subsoil depth and the initial condition of the second layer. In case of Richards it varies from -100 to more than +100 percent.

Keywords: soil moisture, infiltration, soil depth, sensitivity analysis, discharge, rainfall-runoff**,** LISEM

4.1 Introduction

Although soil moisture is a negligible part of the global water budget, it plays a central role in success of agriculture and regulates the partitioning of precipitation into surface runoff, evapotranspiration and percolation into deeper ground water storage. Soil moisture storage is considered an important parameter in both event-based and seasonal hydrological modeling (Troch et al., 1993; Akinremi et al., 1995; Famiglietti et al., 1998) as well as in modeling the interaction between the land surface and atmosphere (Acs, 1994; Chen and Hu, 2004). In an intercomparison study of different land surface models, Koster and Milly (1997) concluded that the wide disparity in model results was related to two key functional relationships of soil moisture control on evapotranspiration and soil moisture control on runoff and drainage. Therefore, to achieve a better understanding of environmental processes such as surface runoff generation, inundation, climate change, soil erosion and solute transport, their relationship with the root zone soil moisture content has to be understood.

Often, infiltration and redistribution within the unsaturated zone is modeled with the well known Richards soil moisture state – flux relationship. It is highly nonlinear and difficult to parameterize, hence it poses a considerable numerical overhead and does not always lead to more accurate predictions than other infiltration models such as Horton, Philip and Green-Ampt (Chen et al., 1994; Smith et al. 2002; Hsu et al., 2002). Among the various alternative models the Green-Ampt model is used most frequently in rainfall-runoff modeling. Regardless of model choice, any open loop prediction of root zone soil moisture is prone to error, even in cases with simple boundary conditions, appropriate calibration and detailed forcing data (e.g. van Loon and Troch, 2002; Margulis et al. 2002). On the other hand, soil moisture observations, both in-situ and remotely sensed, are also prone to errors. At the same time soil moisture exhibits a high spatio-temporal variability due to the heterogeneity in rainfall, topography, soil, and vegetation (Entekhabi and Eagleson, 1989; Wood et al., 1992; Troch et al., 1993). The combination of considerable measurement errors and spatio-temporal heterogeneity limit the possibilities for regular soil moisture monitoring in space and time. Currently there is no observation method that can provide soil moisture measurements at the right spatial and temporal resolution, especially when soil moisture information at deeper layers is required (Walker, 1999; Western and Blöschl, 1999; Heathman et al., 2003). To overcome the limitations of the dynamic models and observations several studies have applied data assimilation (Kostov and Jackson, 1993; Entekhabi et al., 1994; Hymer et al., 2000; Heathman et al., 2003) and geostatistics (Schmugge et al., 1980; Famiglietti et al., 1998; Hymer et al., 2000; Laio et al, 2001; Hupet and Vanclooster, 2002; Western et al., 2004). However, assessments of these methodologies on well-instrumented sites have lead to mixed results (Chen et al., 1996; Shao and Henderson-Sellers, 1996). For some time to come, we will have to accept a certain limit to the accuracy at which soil moisture can be described or predicted. Naturally, the question did arise how this uncertainty propagates in hydrological models. With this question in mind several studies did investigate the sensitivity of catchment discharge to the initial soil moisture content (Veihe and Quinton, 2000; Zehe et al., 2005; Merz and Plate, 1997; Bronstert and Bardossy, 1999; Hantush and Kalin, 2005). Initial soil moisture is an input requirement in most (if not all) event-based hydrological models. In order to apply or further extend these models, knowledge about the sensitivity of catchment discharge to various processes and initial conditions is essential. Most studies did concentrate only on the effects of surface layer soil moisture content and its spatial variation (Merz and Plate, 1997; Bronstert and Bardossy, 1999; Hantush and Kalin, 2005). A few studies have considered sensitivity to event properties and the initial soil moisture content jointly (Grayson et al., 1995; Merz and Plate, 1997; Hantush and Kalin, 2005). And even less information is available in the hydrologic literature on the sensitivity of catchment discharge to soil moisture content at deeper layers and variation of sensitivity for different levels of initial saturation. However, the mixed results from the aforementioned studies, suggest that all these factors may be very relevant.

In this study we try to take more factors into account than in previous investigations to analyse the effect of initial soil moisture on discharge from a small catchment. We apply a straightforward and generic approach, based on a full-factorial design to study the sensitivity of catchment discharge to initial soil moisture, which can easily be transferred to other hydrologic models and case studies.

4.2 Site description

This study uses data from a small experimental catchment named Catsop, which is situated in the hilly loess region of South Limburg in the Netherlands (50º 95´N, 5º 78´E; Figure 4.1). It is representative for the loess region in Limburg, which has problems with soil erosion and flooding. These loess soils originate from the aeolian deposits of the late-Weichsel ice age which are typical for the scattered loess areas in northwestern Europe. A weak aggregate stability of loess soils favours soil sealing and crusting, thus reducing the infiltration rate. Catsop has an area of 0.42 km^2, and is dominantly used for agriculture. Four main land use types are distinguished within the catchments: Arable (79.5 %), Orchard (7.9 %), Grassland (11.8 %), and Infrastructure (0.8 %). Arable land is mainly cultivated with cereals such as winter wheat and barley or root crops such as sugar beet and potato. During major storms in the catchment 3 – 30 % of the total rainfall reaches the catchment outlet. Elevation ranges from 79 to 112 m.a.s.l, and the terrain is undulating with a gently to moderately sloping topography. About 86% of the slopes have a gradient of less than or around 10 % and 3.5 % of the slopes are steeper than 15 % . The climate of the study area is temperate humid. Annual precipitation is about 740 mm, which is evenly distributed over the year. On average, the summer events are shorter and more intensive while the winter events are longer and less intensive.

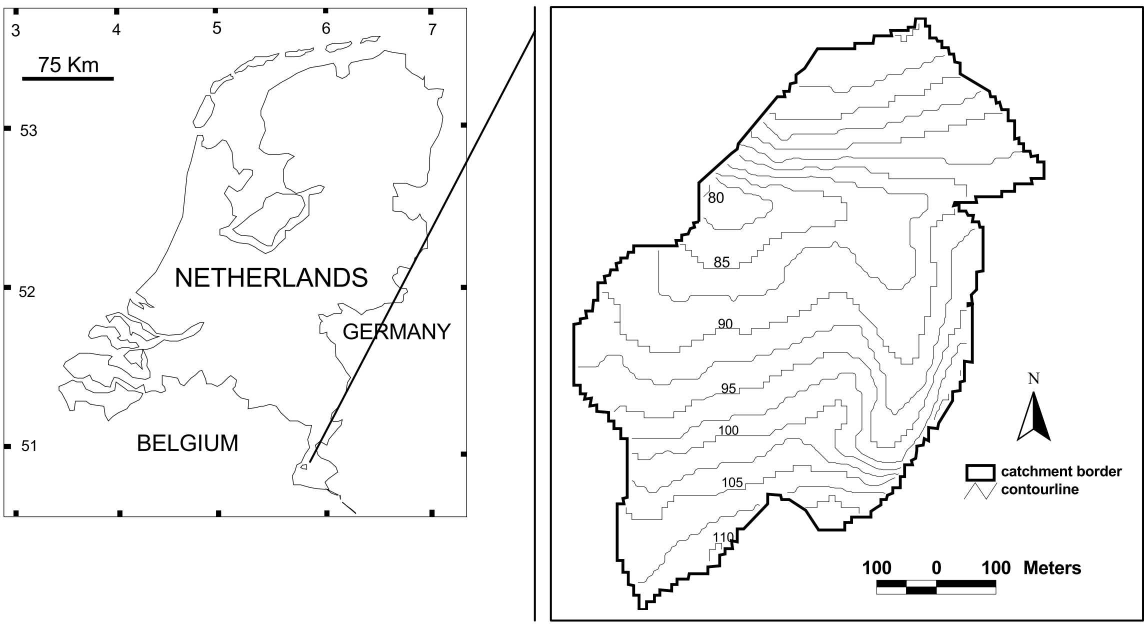

Figure 4.1. Geographical location of the study area, catchment shape and topography.

4.3 Experimental setup

4.3.1 Model selection

The Limburg Soil Erosion Model (LISEM) is a catchment scale hydrology and soil erosion model which can simulate infiltration and water redistribution. It allows describing infiltration with three different methods: Holtan-Overton, Green-Ampt, or Richards (De Roo et al., 1995). Two different configurations of the Green-Ampt model have been implemented in the LISEM, a one layer and two layer configurations. Both the Green-Ampt and Richards models require initial soil moisture content for each soil layer as initial condition. In this study the two-layer Green-Ampt (henceforth called Green-Ampt) and Richards models were used.

4.3.2 Input parameters and variables

To enable a detailed sensitivity analysis and keep the results tractable, we assumed that the whole catchment was homogeneous with regard to land use parameters and soil physical properties - an assumption that should be relaxed in a future studies (see the discussion and conclusions section). For all parameter settings, the conditions of a winter wheat crop in January were taken. At this time of the year winter wheat hardly covers the land surface and land surface is susceptible to soil erosion. Most parameter values were estimated according to the guidelines in the LISEM manual (De Roo et al., 1995). Table 4.1 represents the values of the soil physical parameters which have been used in this study. Simulations were conducted for a soil profile depth of one meter. The topsoil depth (d1) was varied between 5 and 40 cm (5, 10, 15, 20, 25, 30 and 40 cm - 7 different depths in total), the subsoil depth (d2) was adjusted such that the whole profile remained one meter. The initial soil moisture content was for each layer systematically varied from 0.05 (approximately air dry) to 0.4 cm^3 cm^{-3} (approximately saturation) volumetric soil moisture content, with steps of 0.05 cm^3 cm^{-3} (8 soil moisture values in total per layer).

4.3.3 Rainfall events

Two rainfall events with different intensity and duration were used. Both of these events are measured events in the catchment, and both generated discharge at the outlet. The first event (recorded at 12-01-2004), is used as a representative of the long and less intensive rainfall events that usually occur in the winter season. The other event (recorded at 18-08-2004), is representative for summer events (short and more intensive). Figure 4.2 shows the hyteographs of these events.

Table 4.1. Values of the soil hydraulic input parameters used in simulations.

Parameter	Green-Ampt	Richards	Value	unit
θ_{sat}	x	x	0.42	$cm^3\ cm^{-3}$
θ_{init}	x	x	0.05 – 0.42	$cm^3\ cm^{-3}$
θ_{res}		x	0.01	$cm^3\ cm^{-3}$
Ψ	x		3.19	cm
α		x	0.0067	cm^{-1}
λ		x	0.00	-
n		x	1.376	-
Ksat	x	x	3.94	cm day^{-1}
d_1	x	x	5 – 40	Cm
d_2	x	x	60 – 95	cm

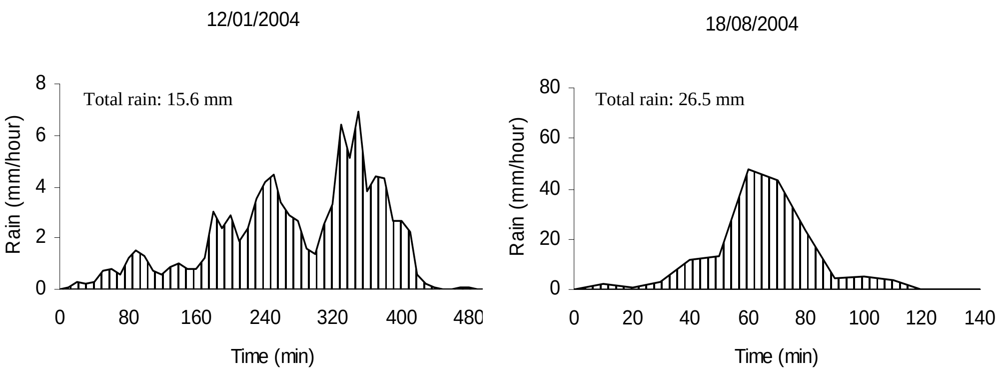

Figure 4.2. Rainfall events used in this study.

4.3.4 Sensitivity analysis

In this study we used LISEM version 2.392, which can be linked to the PEST parameter estimation environment (Doherty, 2002). The SENSAN component of PEST facilitates the sensitivity analysis process by automating the repeated simulation of the model for various input parameter sets. After a model run based on a certain parameter set, it reads the outputs of interest (in this study total discharge and peak discharge), stores these in a text file and then commences the simulation for the next parameter set. This procedure is repeated until the model is run for the last parameter set. As stated previously, the soil moisture data of two layers were systematically varied between 0.05 and 0.40 $cm^3\ cm^{-3}$ by 0.05 $cm^3\ cm^{-3}$ intervals (two times 8 categories), and also soil layer depths were varied between 5 and 40 cm (7 categories). Therefore for each event and each infiltration model the LISEM model was run 448 times (8x8x7), in total 1792 runs.

We define the sensitivity of a particular model output (O) to a parameter set (**P**) as:

$$SEN_i = \frac{O_i - O_b}{\left\| \mathbf{P}_i - \mathbf{P}_b \right\|} \tag{4.1}$$

where O_b is the model output for the base parameter set of $\mathbf{P}_b$ and O_i is the model output pertaining to a particular parameter set of $\mathbf{P}_i$. Note that the denominator of the equation is the square root of the sum of squared differences between a particular parameter set and the base parameter set (the L2 norm of a vector difference). In our study **P** is comprised of soil moisture in the two soil layers, whereby the base parameter set is chosen at 0.05 cm^3 cm^{-3} for both layers.

$$\begin{aligned} \mathbf{P}_i &= \begin{bmatrix} \theta_1 & \theta_2 \end{bmatrix}^T \\ \mathbf{P}_b &= \begin{bmatrix} 0.05 & 0.05 \end{bmatrix}^T \end{aligned} \tag{4.2}$$

Obviously SEN_i can take any unit, depending on the units of the parameters and outputs being considered. In our study, with the choice for initial volumetric soil moisture in **P,** SEN_i gets the same unit as the model output being considered (O).

4.4 Results

4.4.1 General

The results of this study are presented in Figures 4.3 – 4.9 and Tables 4.2 – 4.5. While Figures 4.3 and 4.4 show a small part of the output in detail with the hydrographs of some selected simulations, Figures 4.5 – 4.8 and Tables 4.2 – 4.5 contain nearly all results of the 1792 simulations, in a condensed form. Each figure or table shows the influence of 4 factors: infiltration model, topsoil/subsoil depth, initial soil moisture of the topsoil, and initial soil moisture of the subsoil (see e.g. Figure 4.5). The results for each event have been presented in a separate figure or table. Figures 4.5 and 4.7 show the distribution of absolute values of the outputs (total discharge and peak discharge) while Figures 4.6 and 4.8 show the distribution of sensitivities according to equation 1. Figures 4.5 – 4.8 share the same lay-out. The mean total discharge or peak discharge per combination of model, topsoil/subsoil depth, and initial soil moisture of the topsoil is shown with bold dots in the x-axis direction in each sub-plot. In other words, each dot shows the average value of total discharge or peak discharge when all factors except the sub-soil initial moisture remain constant. In addition to the mean, a box-and-whisker plot shows the distribution of absolute value (Figures 4.5 and 4.7) or sensitivity (Figures 4.6 and 4.8) for the range of initial sub-soil moisture. Figure 4.9 shows the relative sensitivity of total discharge with respect to 0.05 cm^3 cm^{-3} changes around different initial conditions of topsoil and subsoil moisture content. Tables 4.2 – 4.5 give some statistics on the sensitivities of total discharge (Tables 4.2 and 4.4) and peak discharge (Tables 4.3 and 4.5) to moisture in the topsoil for different combinations of the four aforementioned factors.

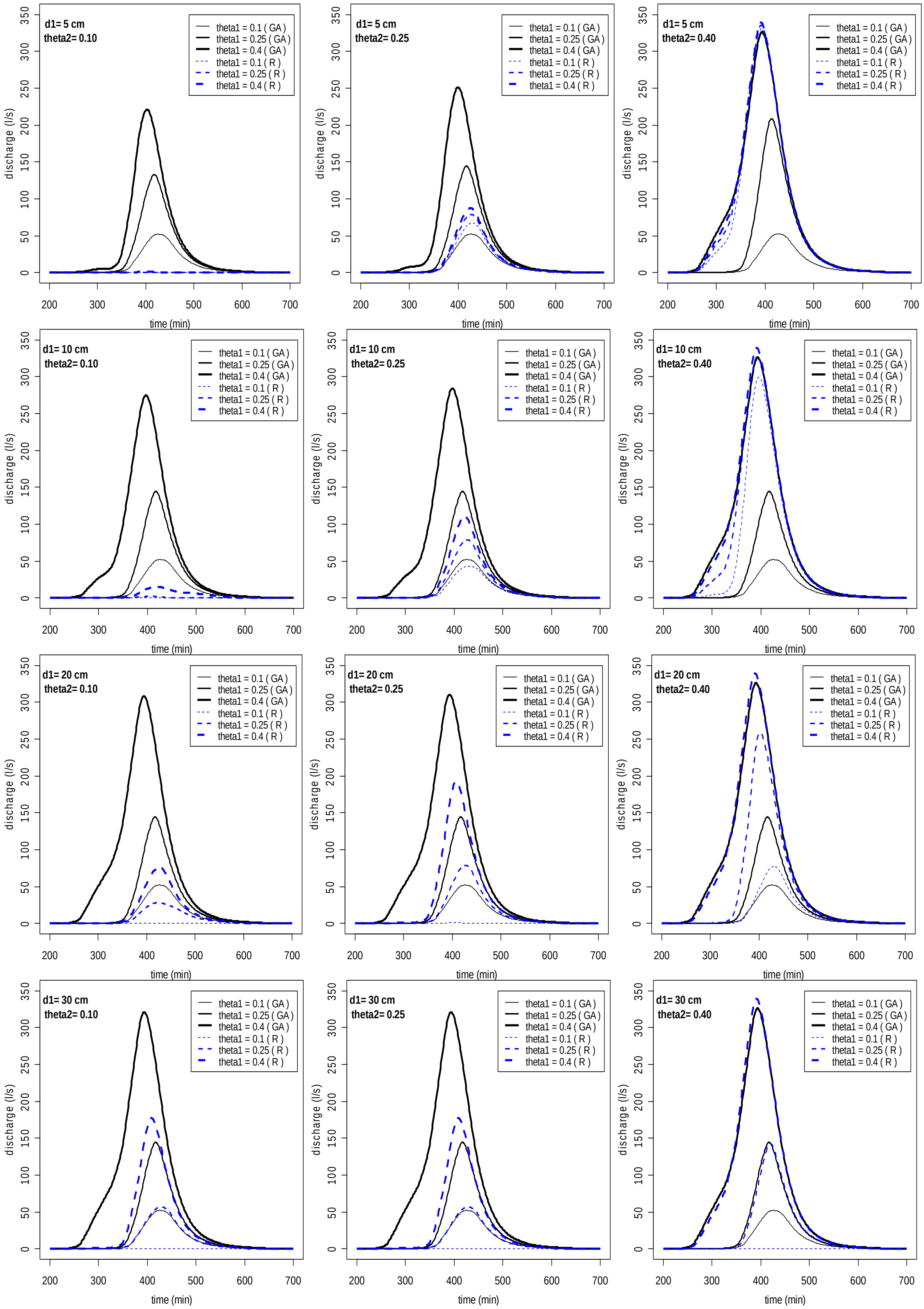

Figure 4.3. Comparison of hydrographs for the event at 12/01/2004, calculated with the Richards (R) and Green-Ampt (GA) model. *d1* is topsoil depth, *theta1* the moisture content of the topsoil, *theta2* the moisture content of the subsoil.

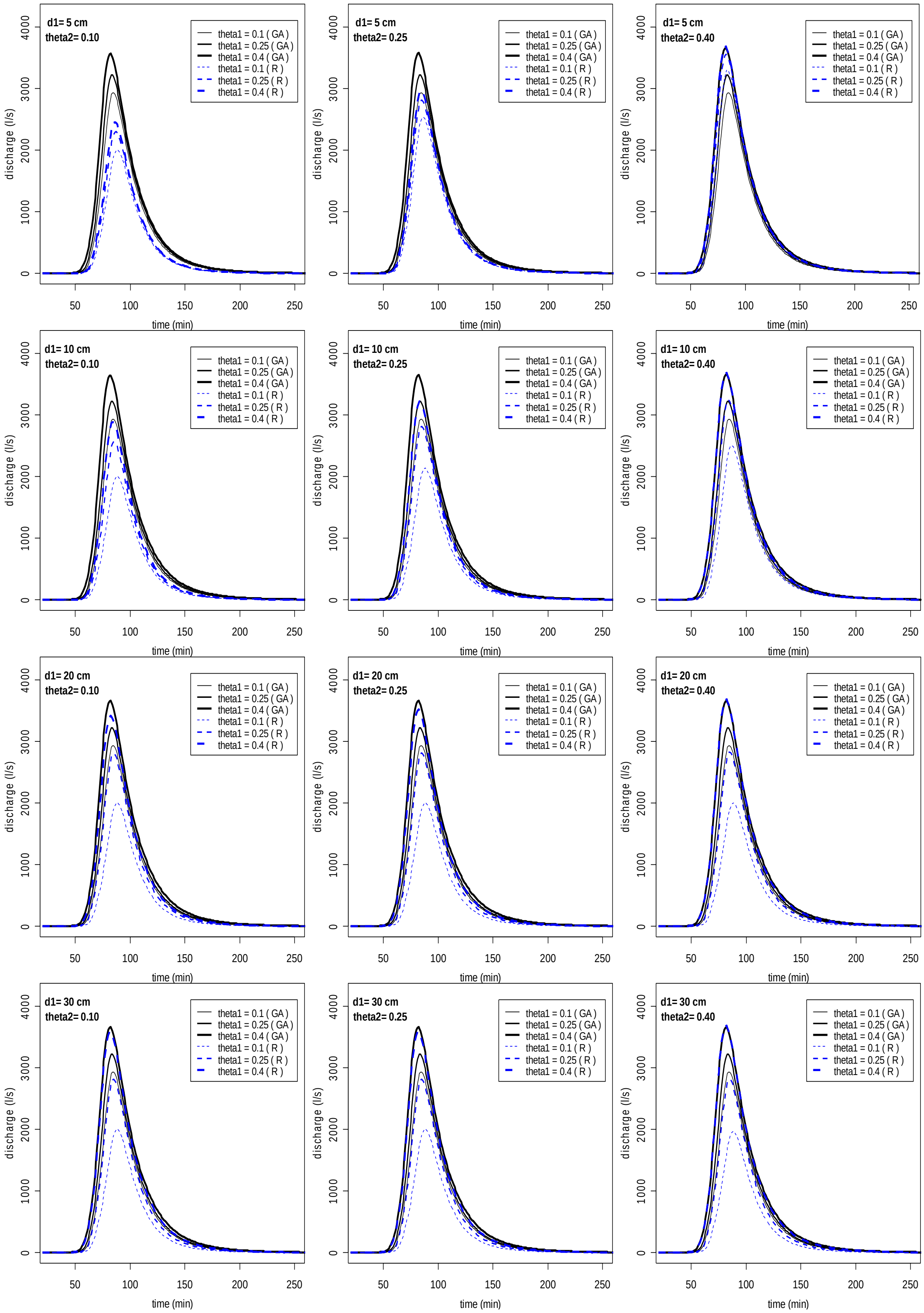

Figure 4.4. Comparison of hydrographs for the event at 18/08/2004, calculated with the Richards (R) and Green-Ampt (GA) model. *d1* is topsoil depth, *theta1* the moisture content of the topsoil, *theta2* the moisture content of the subsoil.

Three statistics have been included: mean, standard deviation (S.D.), and coefficient of variation (C.V.). In principle, Tables 4.2 – 4.5 show the same type of information as Figures 4.5 – 4.8. However, by defining the topsoil / subsoil categories differently, Tables 4.2 – 4.5 highlight a cross-section through the data which is orthogonal to that shown in Figures 4.5 – 4.8: in the tables variation in moisture of the topsoil is studied, given a fixed level of soil moisture in the subsoil; in the figures variation in moisture of the subsoil is studied, given a fixed soil moisture level in the topsoil. We could also have visualized the information in Tables 4.2 – 4.5 with another set of figures.

4.4.1 Difference between Green – Ampt and Richards models

The Green-Ampt and Richards models give quite different discharge predictions as a function of topsoil depth and the moisture content of the subsoil (Figure 4.3 and 4.4). It appears that the Green-Ampt model leads to higher total discharge and peak discharge for lower soil moisture contents of the subsoil (especially with small topsoil depths), while the Richards model leads to higher discharge values for higher soil moisture contents of the subsoil. By increasing the depth of the topsoil the difference between the models diminishes. Also with regard to sensitivity the Green-Ampt and Richards models are quite dissimilar. For instance, Figures 4.5 and 4.7 show a remarkable change in the total discharge and peak discharge for changes of soil moisture content at topsoil depths of 5 and 10 cm for Green-Ampt, while for Richards these change hardly. Contrary to the impact of the soil moisture changes in the topsoil, the Richards model shows a higher sensitivity to soil moisture changes in the subsoil, especially, for shallower topsoils. The length of boxes plus their whiskers at both sides in Figures 4.5 and 4.7, represents the range of changes in model outputs due to changes of the soil moisture content in the subsoil from 0.05 to 0.40 $cm^3\ cm^{-3}$. Considering these boxes and whiskers, the Green-Ampt model appears to be insensitive to soil moisture changes in the subsoil when the depth of the surface layer exceeds 10 cm. However the Richards model shows some sensitivity to soil moisture content in the subsoil even when the topsoil depth is 40 cm (see Figure 4.5 and Table 4.2).

Regardless of topsoil depth, by increasing the level of soil moisture saturation in the topsoil the sensitivity of the model outputs to changes in soil moisture content in the subsoil increases in both models. This finding can be easily supported by examining the length of the boxes in Figures 4.5 and 4.7. However, by increasing the level of soil moisture in the subsoil the two models produce conflicting results. For decreasing topsoil depths Green-Ampt shows higher C.V.'s and Richards gives lower C.V.'s (Table 4.2). For instance Table 4.2 shows that changing the soil moisture content of the subsoil from 10 to 40 percent alters the C.V. of total discharge from 51.8 to 70.9 percent for the Green-Ampt model with a topsoil depth of 5 cm. For the Richards model it varies from 55.6 to 3.3 percent (also 5 cm topsoil). These variations are less pronounced in case of the intensive event (Table 4.4). Moreover, the rate of variations is less for peak discharge than total discharge (Tables 4.3 and 4.5). Overseeing all results for both events, we conclude that the sensitivity for the Green-Ampt model is quite linear, whereas for the Richards model it is non-linear.

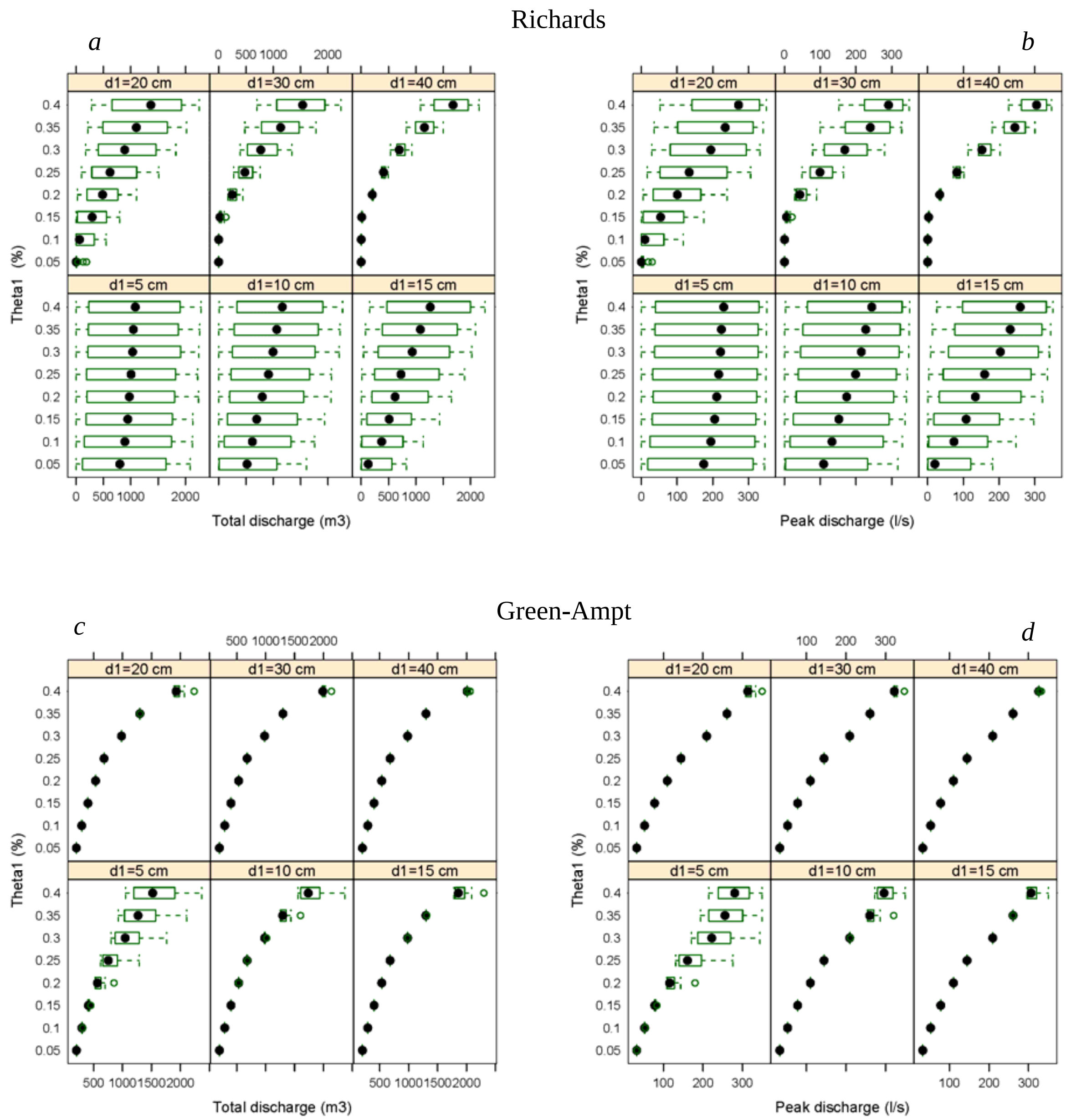

Figure 4.5. Total discharge (m^3) and peak discharge (l.s^{-1}) for the event on 12/1/2004, for different levels of soil moisture content in the topsoil (*Theta1*) and different levels of topsoil depth (*d1*). The dots show the mean total discharge (peak discharge) for the entire range of soil moisture values (0.05 - 0.40 cm^3 cm^{-3}) in the subsoil. The length of the boxes plus their whisker at both sides indicates variations in response to changes in the subsoil moisture content. The sub-plots *a* and *b* represent the results from the Richards infiltration model; *c* and *d* show the results from the Green-Ampt model.

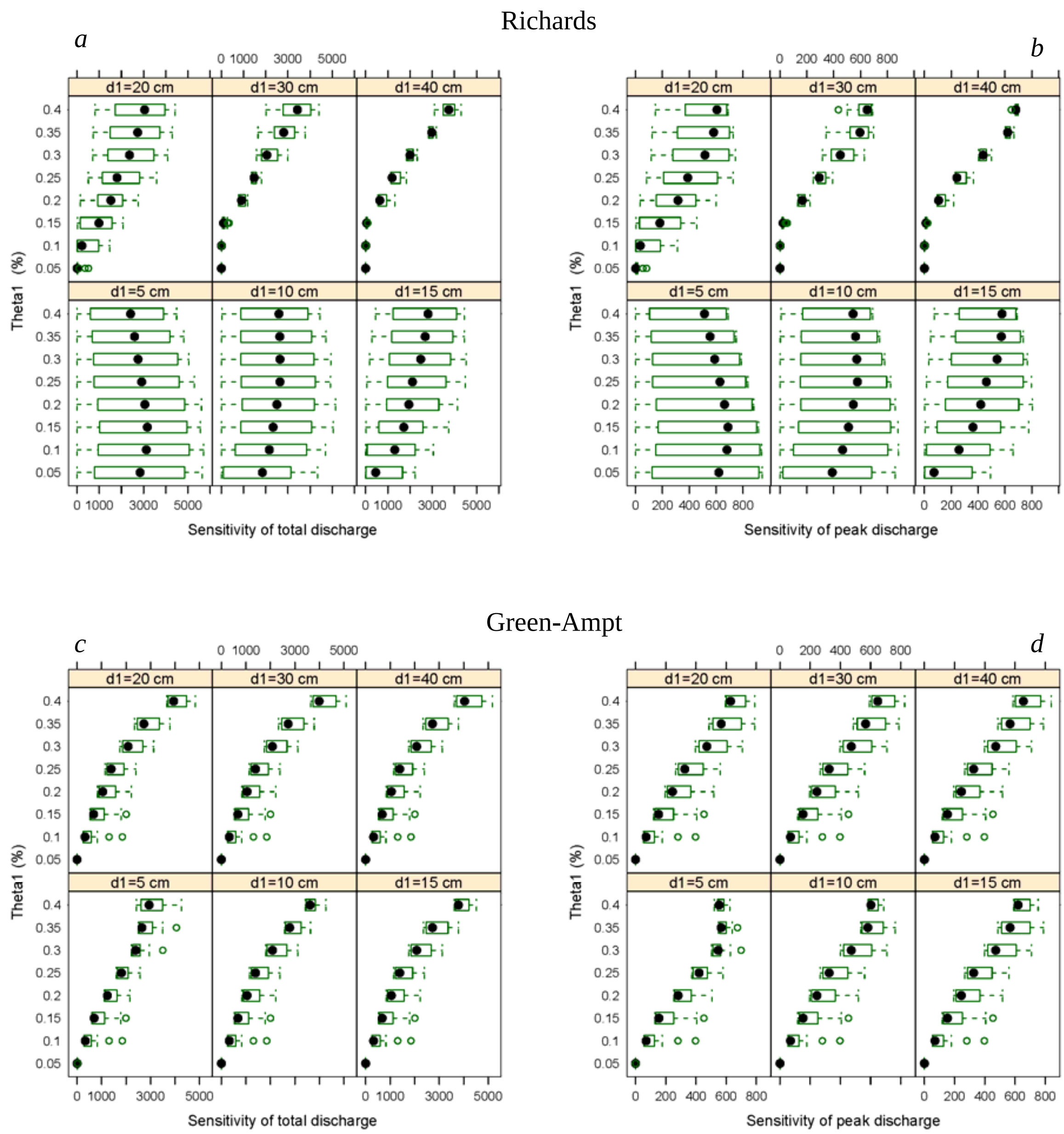

Figure 4.6. Sensitivity of total discharge (m^3) and peak discharge (l/s) calculated with equation 1 for event at 12/1/2004. For further explanation see Figure 4.5.

Table 4.2. Sensitivity of total discharge (m^3) to topsoil moisture content (12/01/04). The first column indicates the depth of the topsoil, the depth of the subsoil is automatically 100 cm - (top soil depth). The subsequent columns give the sensitivity of discharge to soil moisture changes in the topsoil only (θ_1), at different soil moisture values in the subsoil (θ_2, columns 2 – 4 and 5 – 6). The column labelled 'Mean' shows the average for all soil moisture levels (0.05, 0.10, 0.15, 0.20, 0.25, 0.30, 0.35, and 0.40 cm^3 cm^{-3}) in the subsoil.

depth		Green – Ampt				Richards			
topsoil		θ_2=10	θ_2=25	θ_2=40	Mean	θ_2=10	θ_2=25	θ_2=40	Mean
5 cm									
	Mean	613.6	676.5	951.1	701.4	1.6	383.5	1953.2	538.4
	S.D.	317.8	389.1	674.3	413.6	0.9	43.3	64.2	41.6
	C.V.	0.518	0.575	0.709	0.590	0.556	0.113	0.033	0.077
10 cm									
	Mean	740.0	750.5	812.6	757.0	21.2	362.8	1731.4	792.7
	S.D.	488.4	507.5	622.3	562.9	32.1	129.0	262.7	128.5
	C.V.	0.660	0.676	0.766	0.686	1.517	0.355	0.152	0.261
15 cm									
	Mean	772.3	775.8	801.0	778.6	79.8	334.3	1401.3	438.6
	S.D.	549.2	556.6	611.7	562.9	90.2	233.6	512.8	237.2
	C.V.	0.711	0.717	0.764	0.723	1.313	0.779	0.392	0.541
20 cm									
	Mean	785.5	787.1	800.7	788.7	144.5	352.9	1070.6	406.0
	S.D.	577.7	581.1	611.5	584.6	145.2	313.9	707.4	330.7
	C.V.	0.735	0.738	0.764	0.741	1.000	0.889	0.661	0.815
30 cm									
	Mean	796.5	796.9	800.6	797.3	293.3	412.4	731.9	426.7
	S.D.	602.1	602.9	611.4	603.9	302.4	450.8	771.9	457.7
	C.V.	0.756	0.756	0.764	0.757	1.031	1.093	1.055	1.073
40 cm									
	Mean	799.8	799.9	800.6	800.0	408.3	471.5	618.2	471.8
	S.D.	609.7	609.8	611.3	610.0	456.4	540.2	750.6	543.9
	C.V.	0.762	0.762	0.764	0.762	1.120	1.145	1.214	1.153

4.4.2 Difference between events

The two rainfall events produce model outputs that differ an order of magnitude (see the ranges on the y-axes in Figures 4.3 and 4.4). The most striking difference between the events is the divergence between the Green-Ampt and Richards models with respect to hydrograph shape for the 12-01-2004 event, while for the 18-08-2004 event the two models correspond relatively well. Apparently, due to the limited duration of the 18-08-2004 event (120 minutes), only the state of the topsoil dominates the system (see the relatively short boxes in Figure 4.8, indicating that moisture of the subsoil is unimportant), even when this layer has only a limited depth. Under these conditions, with a sharp wetting front and a homogeneous

Table 4.3. Sensitivity of peak discharge ($l.s^{-1}$) to surface layer soil moisture content (12/01/04). For a detailed explanation, see the caption of Table 4.2.

depth		Green – Ampt				Richards			
topsoil		θ_2=10	θ_2=25	θ_2=40	Mean	θ_2=10	θ_2=25	θ_2=40	Mean
5 cm									
	Mean	124.9	136.3	178.9	139.7	0.5	75.9	334.6	103.0
	S.D.	69.5	81.7	120.4	84.3	0.3	10.6	3.6	7.2
	C.V.	0.556	0.599	0.673	0.603	0.546	0.139	0.011	0.070
10 cm									
	Mean	144.3	145.7	153.5	146.5	3.9	71.7	317.6	96.7
	S.D.	92.6	94.9	107.4	96.2	5.2	29.9	22.8	22.6
	C.V.	0.642	0.651	0.699	0.656	1.321	0.417	0.072	0.234
15 cm									
	Mean	147.9	148.3	151.6	148.7	13.5	67.9	268.2	87.0
	S.D.	98.3	99.1	105.0	99.8	15.0	51.2	75.5	45.3
	C.V.	0.664	0.668	0.693	0.671	1.111	0.755	0.282	0.520
20 cm									
	Mean	149.4	149.6	151.6	149.8	26.3	73.1	205.8	80.8
	S.D.	100.9	101.3	105.0	101.8	27.6	69.1	123.5	65.8
	C.V.	0.675	0.677	0.693	0.679	1.048	0.944	0.600	0.814
30 cm									
	Mean	150.9	151.0	151.6	151.1	60.5	85.7	140.0	86.2
	S.D.	103.8	103.9	105.0	104.0	65.6	95.3	140.6	92.9
	C.V.	0.688	0.688	0.693	0.689	1.083	1.112	1.000	1.078
40 cm									
	Mean	151.5	151.5	151.5	151.5	84.1	95.7	117.5	94.9
	S.D.	104.9	104.9	105.0	104.9	95.1	109.4	135.2	108.2
	C.V.	0.692	0.692	0.692	0.692	1.131	1.143	1.151	1.141

boundary condition at the top, it is not surprising that the Green-Ampt and Richards models produce comparable results (Smith et al., 2002). The 12-01-2004 event differs not only with respect to total duration (480 minutes), but also the homogeneity of rainfall over time (see Figure 4.2). Under these conditions, the Richards model leads to much more infiltration and less runoff, especially with dry initial conditions.

These results make clear that it is difficult to consider the effect of event properties on model sensitivity in isolation; there are strong interactions between (the choice for) an infiltration model, topsoil/subsoil geometry and initial values on one side and event properties (total rainfall and event duration in this study) on the other. Moreover we cannot fully analyze the effect of event properties in this study since only two events were considered that differed with respect to total depth as well as intensity (hence the effects are collinear). Still we attempt to summarize the effect of event properties. Due to the definition of sensitivity in this study (viz. eq 1), effects due to event size are reflected in the result. However, even when taking this effect into account, there remain remarkable differences between the events. For the rainfall event of 12-01-2004 the sensitivities of the total and peak discharge vary between

0 - 5000 m^3 and 0 - 800 l.s^{-1} respectively (Figure 4.6), while for the rainfall event of 18-08-2004 the sensitivities vary between 0 - 15000 m^3 and 0 - 8000 l.s^{-1} (Figure 4.8). However, the low outflow values are much more prominent in the 0 - 5000 m^3 case than in the 0 - 15000 m^3 case. It would for instance be more reasonable to choose the total-discharge range for the intensive event from 5000 - 15000 m^3. By considering the C.V.'s these range differences are automatically weighted in a standardized way. By comparing the relevant rows in Table 4.2 and 4.4 (as well as Tables 4.3 and 4.5), it appears that the C.V. values are

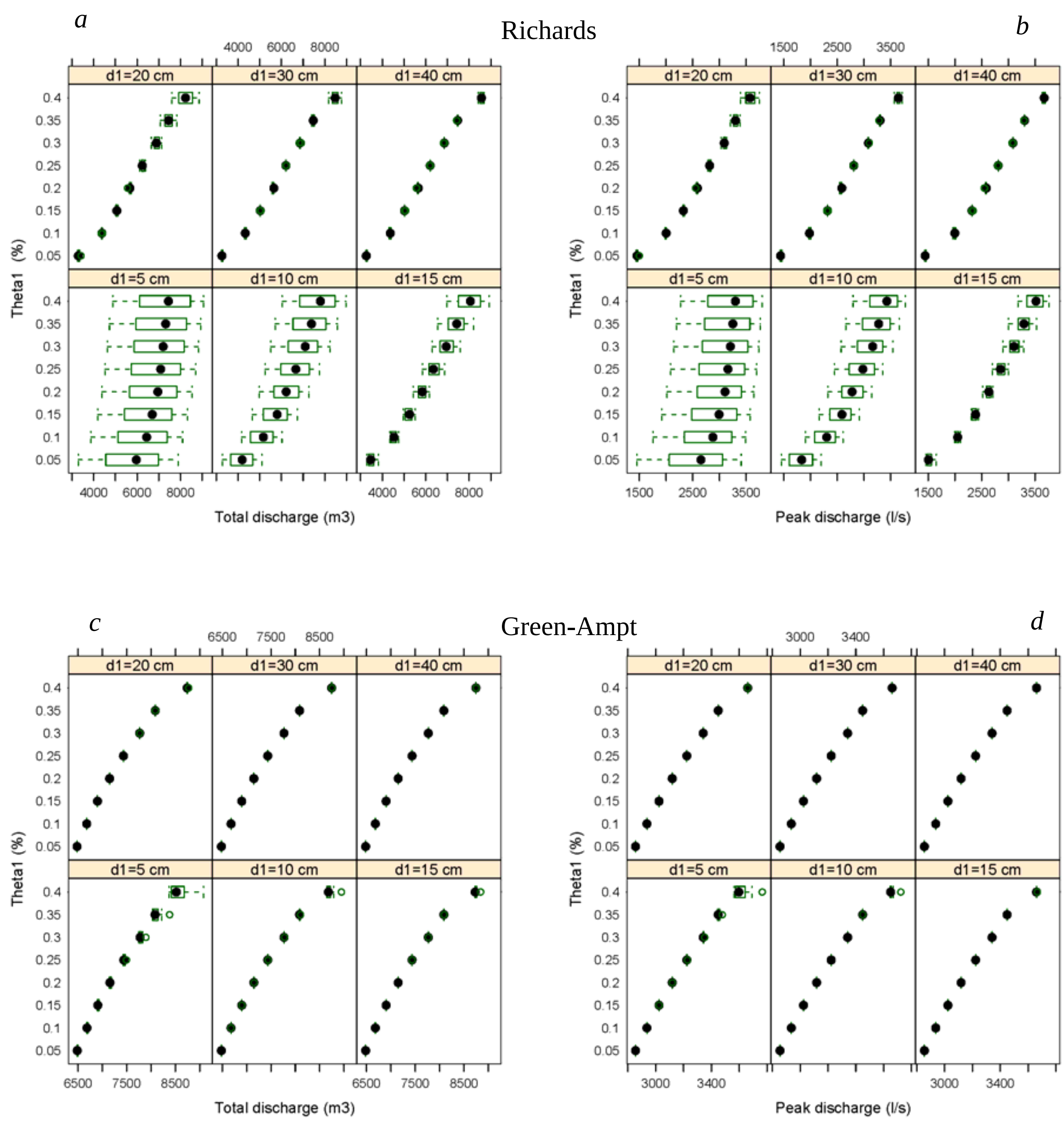

Figure 4.7. Total discharge (m^3) and peak discharge (l/s) for event at 18/8/2004. For further explanation see Figure 4.5.

much higher for the 12-01-2004 event. This leads to the conclusion that both total discharge and peak discharge are more sensitive to initial soil moisture for the smaller and less intensive event (12-01-2004). The effects are however much smaller than those due to a different infiltration model (see Section 4.1).

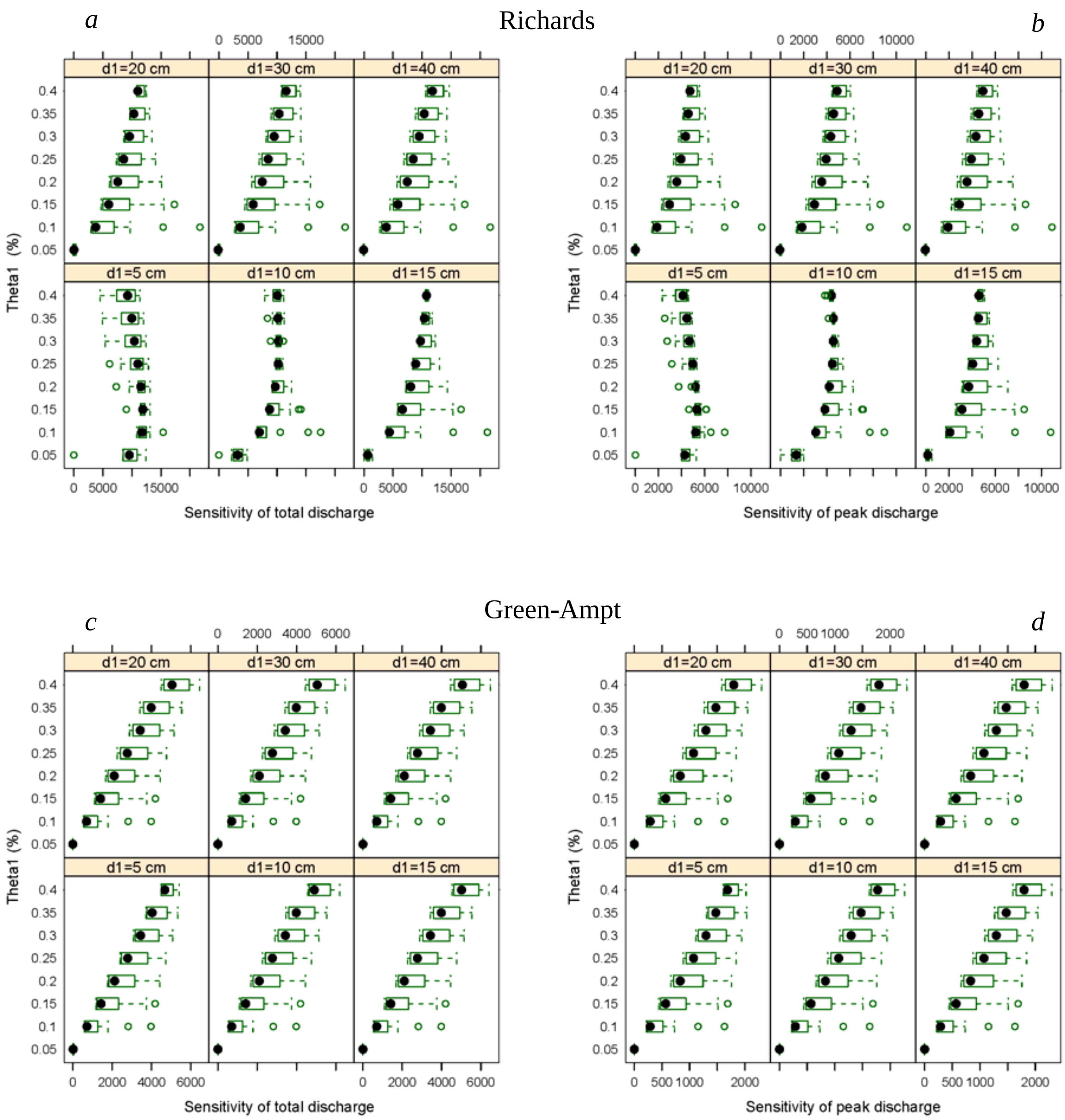

Figure 4.8. Sensitivity of total discharge (m^3) and peak discharge (l/s) calculated with equation 1 for event at 18/8/2004. For further explanation see Figure 4.5.

Table 4.4. Sensitivity of total discharge (m^3) to surface layer soil moisture content (18/08/04) . For a detailed explanation, see the caption of Table 4.2.

depth		Green – Ampt				Richards			
topsoil		θ_2=10	θ_2=25	θ_2=40	Mean	θ_2=10	θ_2=25	θ_2=40	Mean
5 cm									
	Mean	7350.4	7364.0	7433.3	7370.7	4703.7	5969.2	8014.3	5922.7
	S.D.	670.7	686.4	774.2	695.3	531.5	508.0	495.9	500.8
	C.V.	0.091	0.093	0.104	0.094	0.113	0.085	0.062	0.084
10 cm									
	Mean	7393.4	7395.0	7407.4	7396.5	5107.6	5696.8	6876.2	5798.7
	S.D.	741.1	743.9	766.1	746.4	989.5	1171.2	1357.4	1094.2
	C.V.	0.100	0.100	0.103	0.101	0.194	0.205	0.197	0.189
15 cm									
	Mean	7402.8	7403.1	7406.1	7403.5	5443.0	5666.2	6146.8	5802.0
	S.D.	785.9	759.5	765.3	760.2	1344.3	1506.9	1753.4	1429.5
	C.V.	0.102	0.102	0.103	0.103	0.247	0.266	0.285	0.246
20 cm									
	Mean	7405.1	7405.2	7405.9	7405.3	5618.1	5699.3	5886.0	5840.8
	S.D.	763.4	763.6	765.1	763.8	1540.0	1655.1	1835.9	1573.3
	C.V.	0.103	0.103	0.103	0.103	0.274	0.290	0.312	0.269
30 cm									
	Mean	7405.8	7405.8	7405.9	7405.7	5745.7	5765.8	5788.0	5898.3
	S.D.	764.8	764.8	765.1	764.9	1718.3	1762.8	1853.9	1673.7
	C.V.	0.103	0.103	0.103	0.103	0.299	0.306	0.320	0.284
40 cm									
	Mean	7405.8	7405.8	7405.9	7405.8	5777.6	5793.6	5798.6	5920.1
	S.D.	765.0	765.0	765.1	765.0	1771.2	1791.8	1838.8	1703.1
	C.V.	0.103	0.103	0.103	0.103	0.306	0.309	0.317	0.288

4.4.3 Impact of the surface layer depth

It has already been noted that topsoil depth has a high influence on the discharge as calculated by the Richards model, whereas it rarely affects discharge according to the Green-Ampt model. For instance the coefficient of variation of the total discharge, averaged of all soil moisture levels in the subsoil, varies from 59 to 76.2 percent in case of the Green-Ampt model and the 12-01-2004 event (see column 5 of Table 4.2).
For the Richards model it changes from 7.7 to 115.3 percent (see column 9 in Table 4.2). For the event of 18-08-2004 the impact of topsoil depth is less than the other event (see Table 4.4 where the C.V. of the total discharge for the average of all soil moisture levels in the subsoil ranges from 9.4 to 10.3 and 8.4 to 28.8 for Green-Ampt and Richards respectively).

Table 4.5. Sensitivity of peak discharge ($l.s^{-1}$) to surface layer soil moisture content (18/08/04). For a detailed explanation, see the caption of Table 4.2.

depth		Green – Ampt				Richards			
topsoil		θ_2=10	θ_2=25	θ_2=40	Mean	θ_2=10	θ_2=25	θ_2=40	Mean
5 cm									
	Mean	3188.3	3190.2	3202.5	3191.6	2188.8	2723.1	3480.2	2663.5
	S.D.	250.2	253.3	274.0	255.5	259.3	222.9	178.5	232.1
	C.V.	0.078	0.079	0.085	0.080	0.118	0.082	0.051	0.087
10 cm									
	Mean	3199.3	3199.4	3201.0	3199.6	2389.7	2619.5	3035.7	2610.9
	S.D.	269.5	269.8	272.8	270.2	459.2	525.7	546.2	504.4
	C.V.	0.084	0.084	0.085	0.084	0.192	0.200	0.180	0.193
15 cm									
	Mean	3200.9	3200.9	3201.0	3200.9	2543.5	2616.0	2755.8	2613.7
	S.D.	272.6	272.6	272.8	272.6	597.2	647.7	708.6	639.3
	C.V.	0.085	0.085	0.085	0.085	0.230	0.248	0.257	0.245
20 cm									
	Mean	3201.0	3201.0	3201.0	3201.0	2607.4	2629.1	2672.2	2628.2
	S.D.	272.8	272.8	272.8	272.8	659.7	692.3	728.7	686.6
	C.V.	0.085	0.085	0.085	0.085	0.255	0.263	0.273	0.261
30 cm									
	Mean	3201.0	3201.0	3201.0	3201.0	2642.6	2646.8	2644.0	2645.1
	S.D.	272.8	272.8	272.8	272.8	703.8	715.4	736.3	713.8
	C.V.	0.085	0.085	0.085	0.085	0.266	0.270	0.278	0.270
40 cm									
	Mean	3201.0	3201.0	3201.0	3201.0	2650.8	2654.1	2651.1	2651.3
	S.D.	272.8	272.8	272.8	272.8	715.4	718.2	730.7	720.1
	C.V.	0.085	0.085	0.085	0.085	0.270	0.270	0.275	0.272

Another way to look at the effect of topsoil depth is by comparing the width of the bars between different depths (d1) in Figures 4.5 – 4.8. Consider f.i. the bars for the Richards model for d1 from 5 to 20 cm. A wide bar implies that the soil moisture content of the subsoil layer does influence discharge a lot, whereas a small (or no) bar implies no influence. Apparently (considering the Richards model in Figure 4.5) the subsoil ceases to be influential when the depth of the upper soil layer exceeds 20 cm. In Figure 4.7 it can be seen that this critical depth is only 10 cm for the 18-08-2004 event. Moreover it is apparent that for the Green-Ampt model the depth of the topsoil never plays an important role.

4.4.4 Relative sensitivity of the total discharge

In Figures 4.6 and 4.7 and Tables 4.3 and 4.5, sensitivity is expressed as a change in discharge relative to a soil moisture change, with a baseline discharge for a soil moisture content of 0.05 $cm^3 cm^{-3}$. This fixed baseline value is useful with linear responses, however it appeared that for especially the Richards model the discharge response to initial soil moisture changes can be quite nonlinear (see Section 4.1). Therefore, the percentage of change in total discharge in relation to 5 percent changes in soil moisture content are also analysed locally. Three levels of soil moisture saturation (15, 25, and 35 percent), four topsoil depth (5, 10, 20, and 40 cm) and four scenarios (S1, S2, S3, and S4) are selected. In the first scenario (S1), soil moisture content of the topsoil is decreased 5 percent. In the second scenario (S2) soil moisture content of the subsoil is decreased 5 percent. In the third scenario (S3) the soil moisture content of the topsoil is increased 5 percent, and in the fourth scenario (S4) the soil -

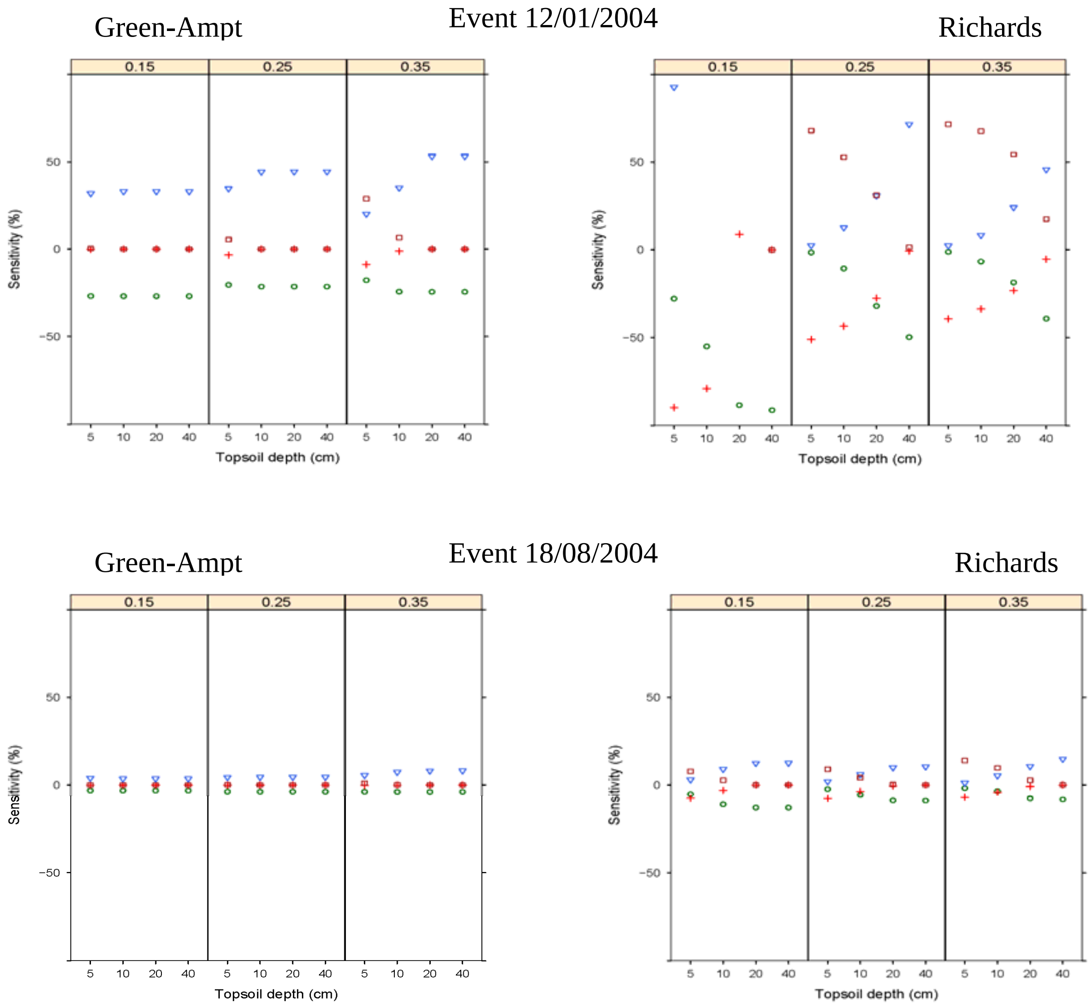

Figure 4.9. Relative sensitivity of total discharge to 0.05 cm^3 cm^{-3} changes in initial soil moisture content of the topsoil. The header of each box shows the base soil moisture content (15, 25 or 35) of the topsoil. Circles indicate scenario one (S1), plus signs (S2), triangles (S3), and squares (S4). S1: soil moisture content of the topsoil is decreased 0.05 cm^3 cm^{-3}. S2: soil moisture content of the subsoil is decreased 0.05 cm^3 cm^{-3}. S3: soil moisture content of the topsoil is increased 0.05 cm^3 cm^{-3}. S4: soil moisture content of the subsoil is increased 0.05 cm^3 cm^{-3}.

moisture content of the subsoil is increased 5 percent. The results for two events and two models are shown in Figure 4.9. The 12-01-2004 (less intensive) event is shown in top row. The sensitivity of the total discharge to 5 percent error in initial soil moisture content ranges between -25 to +50 percent for the Green-Ampt model. S1 and S3 result in higher sensitivities, hence the Green-Ampt model is more sensitive to soil moisture changes in the top layer than in the bottom layer (as concluded previously). For the lower levels of soil moisture saturation (15 and 25 percent) the impact of the topsoil depth is negligible in case of the Green-Ampt model. It should be noted that we do in fact not expect additional insights via Figure 4.9 about the response with a Green-Ampt model, since for this model the response was close to linear. The sensitivity of the total discharge varies from about -100 through more than +100 percent in case of the Richards model. The Richards shows a high sensitivity for all scenarios. Considering the soil moisture saturation level of 15 percent, the sensitivity of total discharge with S3 and S4 (more than +100 percent) are out of the assumed range of the y-axis (±100 percent). The results for the 18-08-12004 event are shown in the bottom row. Both models are relatively insensitive for any scenario.

4.5 Discussion and Conclusions

This case study clearly indicates the importance of the initial soil moisture for discharge predictions, particularly when a rainfall event is less intensive and surface runoff constitutes only a small fraction of the precipitation. Therefore, even an indicative pre-event soil moisture observation or estimation would be valuable to reduce uncertainty of catchment discharge predictions. It has also been shown that importance of the initial soil moisture content further depends on the type of system dynamics (in our study represented by the different infiltration models), forcing variables (e.g. rain intensity and duration in this study), and choice of all relevant parameters (e.g. topsoil depth in this study).

Our results are in agreement with the findings of earlier studies on this subject (Philip, 1975; Hawly et al., 1983; Coles et al., 1997; and Folly et al., 1999). Cole et al. (1997) reported a very high sensitivity of catchment runoff generation to the initial soil moisture, particularly when the ratio of surface runoff to rainfall is small. Wilkening (1981), cited by Hawley et al. (1983), performed a number of numerical analyses with a Richards model and concluded that 5 percent error in soil moisture estimation resulted in errors of 20 and 30 percent in estimating the volume of excess rainfall for 76 and 50 mm storms, respectively.

To our knowledge, the importance of considering surface soil moisture not in isolation but jointly with moisture in deeper layers and event properties has not been shown previously. Also the comparison between different infiltration models has not been made in this context.

Interestingly, several other sensitivity studies have been done for the Catsop catchment, including some studies that used LISEM (De Roo et al., 1996; and Jetten et al., 1998). These studies did show that the saturated hydraulic conductivity (Ksat) is the most influential parameter for almost all processes. Pre-event soil moisture was not included in the study by Jetten et al. (1998) and the study by De Roo et al. (1996) ranked it as one of the less important parameters (although pressure head was used in calibrating of the LISEM model in the same study). It should be noted that these studies did apply an OAT (One factor-At-a-Time) type of sensitivity analysis, which overlooks interactions and non-linear effects (Saltelli et al. 2000). In contrast with these results, the sensitivity analysis of other similar models (ANSWERS, EUROSEM, KINEROS2) indicated that initial soil moisture content is the most influential parameter for catchment discharge (De Roo, 1993; Folly et al., 1999; Hantush and Kalin, 2005). We think that sensitivity to initial soil moisture and saturated hydraulic conductivity are equally important (when considering a Richards model). This is based on the results by De Roo et al. (1996), showing that 20 percent increase in saturated hydraulic conductivity results in 50 percent change of total discharge and 60 percent change of peak discharge. The current study shows that increasing of initial soil moisture content of the topsoil (d1=20 cm) from 0.25 to 0.30 $cm^3\ m^{-3}$ (20 percent change) results in 30 and 45 percent changes in total discharge for Richards and Green-Ampt models, respectively.

We applied homogeneous parameter values over the study catchment. However, inclusion of the spatial variability of the parameters is expected to affect the results, most likely leading to increasing sensitivities. Binley et al. (1989), using a 3-D model, showed that peak discharge and runoff volume are generally increased in the presence of heterogeneity in saturated hydraulic conductivity. Also Bronstert and Bardossy (1999) reported that spatial variability of initial soil moisture content results in an increase in runoff volume and peak discharge when compared to using an average value. In this study peak discharge was in most cases less sensitive to initial soil moisture than total discharge. This is again in accordance with the findings of Bronstert and Bardossy (1999), who concluded that inclusion of stochastic spatial variability of initial soil moisture increased the peak discharge and total discharge by a factor of 3 and 5.5 respectively.

Although a sensitivity analysis is not generally conducted prior to applying a hydrologic model to new situations, the topic is receiving increasingly more attention in hydrology (see e.g. Van Griensven et al. 2006, and references therein). Presently, there are several designs to choose from and the strengths and weaknesses of each are known (Saltelli et al., 2000). The inherent problem of a sensitivity analysis with complex models (like the LISEM model studied here) is the amount of factors to evaluate. It is not so much the computational cost (that can be overcome, even when conducting more than 10^6 model runs), but much more the analysis of the complex multi-dimensional output which leads to difficulties (see also Saltelli et al. 2004 and Kleijnen, 2005). In this study we dealt with a seven-dimensional data set. Beyond this, there are no possibilities to explore data sets visually. Analysis is then limited to multiple regression (ANOVA, GLM, or GAM in case of non-linear responses; see Saltelli et al., 2004). Effectively, one is then building a meta-model to interpret model output. When such a meta-model contains more than ten significant variables (including interaction terms) it becomes very hard to interpret (Kleijnen, 2005;

Satlelli et al. 2004), and it does not serve its objective of enhancing insight anymore. However, for the particular question at hand (how catchment discharge depends on initial soil moisture and the several other relevant variables like rainfall characteristics, terrain and soil properties), these limits have clearly not been reached yet. We think it is worthwhile to increase the number of factors to be varied in a subsequent study, and analyse the response with a suitable regression model.

Chapter 5

Understanding the relation between topography, land use and soil moisture in a small rural catchment in the Dutch Loess area

Vahedberdi Sheikh, Emiel van Loon, Wim Spaan, Leo Stroosnijder
Submitted to: Hydrologic Processes

5 Understanding the relation between topography, land use and soil moisture in a small rural catchment in the Dutch Loess area

Abstract

The relationship between topography, land use, and topsoil moisture storage is investigated for a 0.42 km^2 catchment in the south of the Netherlands. This catchment has an undulating landform, heterogeneous land use and contains deep, well drained soils with a high water retention capacity. Under these conditions it is unclear whether soil moisture patterns (both laterally and vertically) arise due to topography or land use effects. For a period of 10 months, soil moisture profiles have been measured weekly at 15 locations throughout the catchment. Also meteorological variables and catchment discharge was monitored. We employ a Generalized Additive Model to find relationships between the various factors influencing soil moisture. It defines a water balance as a sum of non-linear components. The water balance is applied to our data at various spatial (catchment, response unit, hillslope and plot), and temporal (monthly, weekly and daily) scales. Each of the water balance components is parameterized as a function of topographic variables, land use variables, weather variables and antecedent soil moisture. The model framework is hierarchical: our analysis starts at the coarsest spatial and temporal resolution, the water balance components found here act as constraints when identifying models at finer resolutions. It turns out that the importance of land-use variables varies considerably with temporal resolution. At coarse resolutions land-use is unimportant, whereas at finer temporal resolutions it becomes more relevant. Land use is equally important over all spatial resolutions (response unit and finer). Topography is mostly relevant at the plot scale. The water balance terms become increasingly non-linear at finer scales. Evapotranspiration is found to depend mainly on reference evapotranspiration and crop cover. Drainage to deeper layers depends mainly on soil moisture and to a lesser extent on topography. Lateral transport is weakly dependent on topography. It appears that autoregressive components become increasingly important at finer temporal resolutions. While the model does not assume any structural relationships (it is entirely data-based), it leads to prediction errors that are similar to those obtained with a Richards based water balance model (SWAP) when applied at the same resolution. This case study shows that our hierarchical model framework provides an elegant way to summarize and structure hydrological observations at different scales. It enables the identification of dominant processes over a range of scales and also facilitates a straightforward sensitivity analysis to evaluate e.g. the importance of bio-physical factors, relative to forcing or state variables. Since the General Additive Modelling technique is well developed and our hierarchical framework is data based, the tools can easily be adopted to new case studies.

Keywords: LISEM, catchment discharge, initial soil moisture, sensitivity analysis.

5.1 Introduction

Soil moisture storage plays an important role in hydrological modeling (Troch et al., 1993; Akinremi et al., 1995) as well as in modeling the interaction between the land and atmosphere (Wood et al. 1992; Acs, 1994; Chen and Hu, 2004). Spatial heterogeneity in terrain properties and spatio-temporal variation in vegetation and weather result in highly variable soil moisture content at various scales (Entekhabi and Eagleson, 1989; Wood et al., 1992; Troch et al., 1993). Due to this variability it is, compared to e.g. discharge and ground water, relatively difficult to observe soil moisture adequately on a regular basis. Apart from detailed field experiments in relatively small areas (see Teuling et al., 2006), in-situ soil moisture observations are rare. A notable exception is the regular gravimetric observation of soil moisture in the former Soviet Union that started at a few hundred agro-meteorological stations from 1930s (Robock, et al., 2000). Most of these data plus the soil moisture data from Illinois and Iowa states in USA have been gathered in the Global Soil Moisture Data Bank (Robock, et al., 2000). In spite of this difficulty with in-situ soil moisture monitoring, it is generally acknowledged that knowledge of the (profile average) soil moisture state is important for the initialization of current generation of land-atmosphere models (Jikang and Islam, 2002). Furthermore it plays a key role in any catchment-scale hydrological modeling since it largely controls surface flow, infiltration, interflow, deep seepage, capillary rise, root water uptake, evaporation, transpiration, soil moisture storage and redistribution (Abbaspour and Schulin, 1996).

Most field to catchment scale unsaturated zone models use the Richards equation to describe the movement of water through the catchment. The applicability of this solution is however often questioned, especially when describing the system at larger spatial and temporal scales and when only limited observational data is available for model calibration (Blöschl and Sivapalan, 1995). In the domain of dynamic modeling there are hardly any studies available that evaluate other model concepts. In contrast, using static models, there are quite a number of studies to the effect of topography (Reid, 1973; Burt and Butcher, 1985; Carve and Gascuel-odux, 1997; Famiglietti et al. 1998; Western et al. 1999; Moore et al. 1988; Qiu et al., 2001; Svetlitchnyi et al., 2003; Pellenq et al., 2003) and land use (Fu et al., 2000; Hawley et al., 1983; Qiu et al., 2001; Mahe et al., 2005) on soil moisture distribution.

In this study we try to gain insight in the most important factors influencing the soil moisture dynamics in a small catchment by identifying dynamic models. The study catchment has an undulating landform, heterogeneous land use and contains deep, well drained soils with a high water retention capacity. Under these conditions it is unclear whether soil moisture patterns (both laterally and vertically) arise due to topography or land use effects. In the identification we take both topographic and land use factors into account. Our ultimate aim is to compare the structure of models at different scales, to answer the question what mechanisms are dominant at different scales. Identifying these dominant mechanisms makes it easier to build suitable conceptual models for soil moisture prediction and more efficient to collect relevant data.

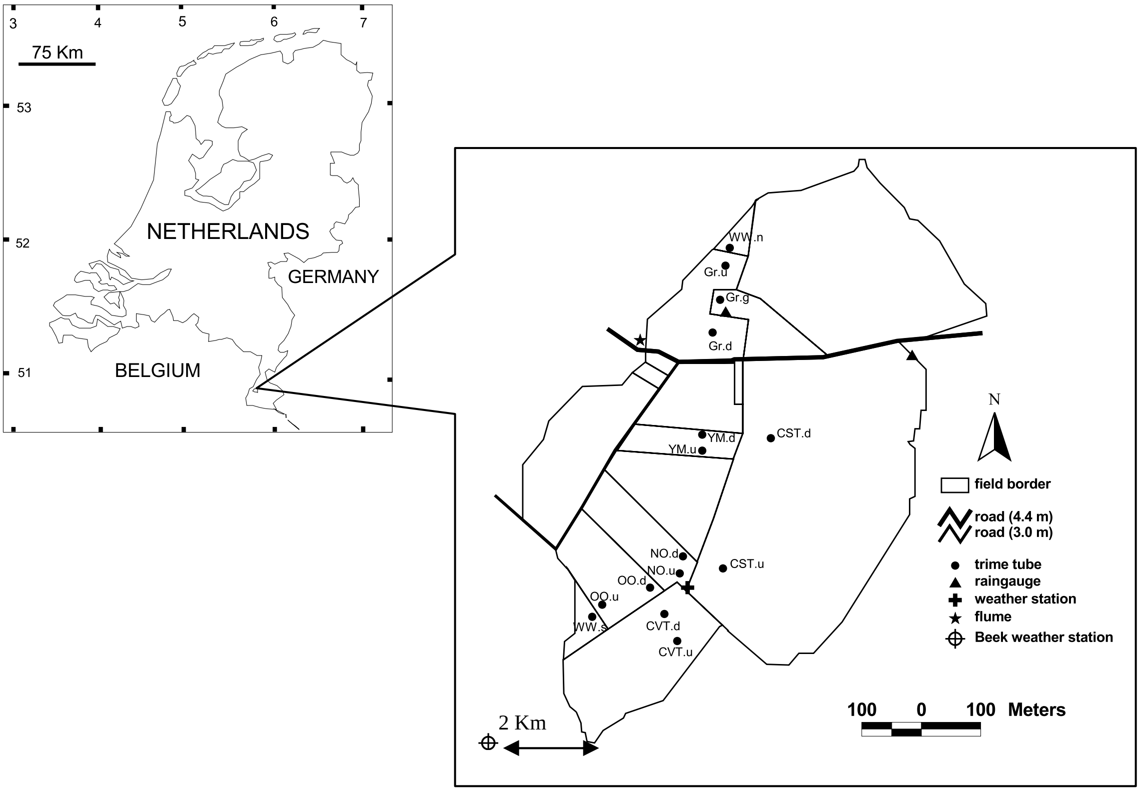

Figure 5. 1. Geographical position of study area and location of the measurements (for abbreviations, see Table 5.1). The observations at Gr.g were omitted from the analysis because this location was intermediate to Gr.u, Gr.d, but with a different management practice.

5.2 Description of the study area

The data used in this study originate from the Catsop catchment. The catchment is situated in the hilly loess region of South Limburg in the Netherlands (50º 95´N, 5º 78´E; Figure 5.1). It has an area of 0.42 km^2, and is almost entirely used for agricultural purposes. Within this small catchment four land use types were distinguished: Arable (79.5 %), Orchard (7.9 %), Grassland (11.8 %), and Infrastructure (0.8 %). Figure 5.2 presents the land use pattern of the Catsop catchment during the winter season of 2003-2004. Arable land is cultivated mainly with winter wheat, spring barley, sugar beet, potato, and yellow mustard. Yellow mustard is a second crop, functioning as an erosion prevention measure. It is planted after harvesting the cereals at the end of the summer, and later in the season chopped into small pieces and spread on land surface as green manure and protection cover. Grasslands are utilized in two ways.

Some fields are grazed by cows from April till October (less than 0.5 cows per ha) and the other fields are harvested by machinery (Figure 5.2). During the last 5 years the area of orchards increased from nil to about 8 %. The only available infrastructure within the catchment are a few tarred roads and one ditch near to the outlet which runs parallel to the main road (shown in Figure 5.1).

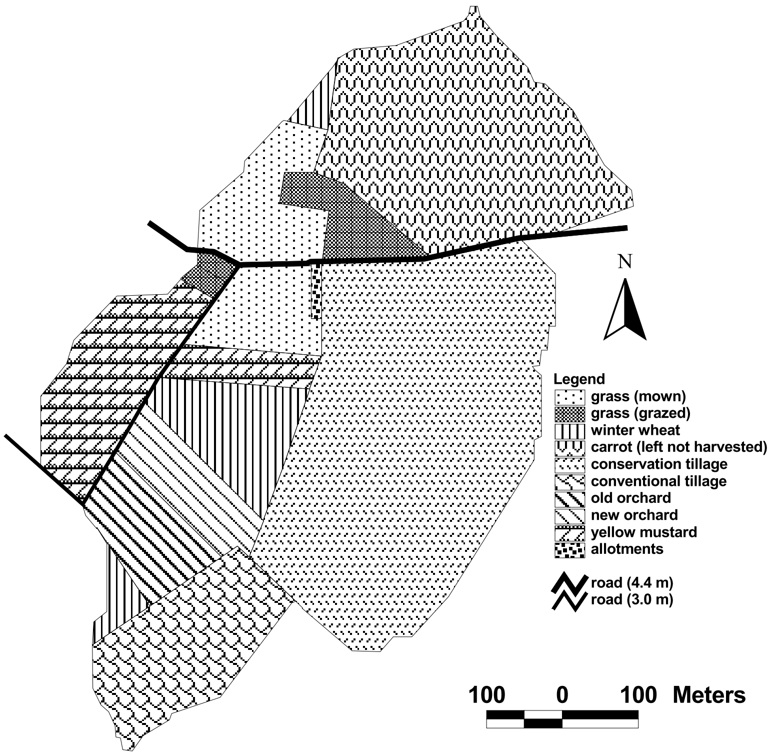

Figure 5.2. Land use in the Catsop catchment during the winter season of 2003-2004.

Table 5.1 lists some of the properties at the observation locations. The climate is temperate humid, with a mean annual precipitation of ca. 740 mm. Precipitation occurs mainly as rainfall and is evenly distributed over the whole year. However the rainfall pattern in winter and summer is different. Summer events are shorter and more intensive while winter events are on average longer and less intensive.

5.3 Data collection

Soil moisture was monitored in 15 tubes of 1 meter depth with a Time Domain Reflectometry system (*Trime-FM*) once every week for the period of November 2003 – September 2004.

Table 5.1. General information of the observation locations (see Figure 5.1 for a map).

Land use	Observation location	Nr[1]	Slope	Upslope length[2]	Upslope area[3]	Topog. index[4]	Wetness coef[5]
Grass	Gr.u	44	9.2	54.1	0.06	8.73	0.87
	Gr.d	47	14.1	78.3	0.1	8.94	0.91
Conservational tillage	CST.u	21	8.7	122.4	0.15	9.73	0.97
	CST.d	16	5.4	160.7	0.61	11.62	1.01
Conventional tillage	CVT.u	19	7.0	84.1	0.1	9.59	1.17
	CVT.d	14	4.1	60.0	0.07	9.70	1.07
Wheat	WW.n	36	3.9	5.0	0.01	7.75	0.85
	WW.s	37	4.3	147.3	0.21	10.62	0.99
Yellow mustard	YM.u	21	5.0	340.0	1.88	12.83	1.14
	YM.d	21	4.8	360.0	1.9	12.88	1.20
Old orchard	OO.u	16	5.7	78.3	0.09	9.67	0.90
	OO.d	16	7.7	162.4	0.17	10.04	1.12
New orchard	NO.u	21	6.1	70.0	0.08	9.48	1.15
	NO.d	21	7.1	224.1	0.33	10.80	1.04

[1] Number of measurement times for each observation location
[2] Distance between divide and the observation point along hillslope in m
[3] Area of upstream catchment area at the observation point in ha
[4] $\ln(a/\tan\beta)$ topographic index (Beven and Kirkby, 1979)
[5] Wetness coefficient according to Svetlitchnyi et al. (2003)

The values for the top four layers are averaged to one mean root-zone soil moisture value, which is the value that is henceforth called *soil moisture* in this study. The values for the 80-100 cm layer were excluded because of the large observation errors in this layer (see Chapter 3). The locations of these tubes and other measurement equipment are shown in Figure 5.1. The main topographic characteristics of each observation location are given in Table 5.1. For each land use type and management practice at least two tubes were installed. Two tipping bucket rain gauges and one small standalone weather station were installed as well. All observed meteorological variables did agree well with the observations at the Beek weather station (50 55'N,5 47'E), at a distance of less than 2 km from the study area. The reference evapotranspiration rate has been calculated with the Penman-Monteith equation using daily meteorological data of the Beek station. Discharge was measured at the catchment outlet using a partial flume with a capacity of 950 l/s and a stilling well with a vertical float recorder. Discharge measurements were collected at 5 minute intervals during the period November 2003 - September 2004. Although the discharge observations may be relevant to questions about (multi-scale) unsaturated zone soil moisture modelling, these data were not used in this study (see the last part of the discussion and conclusions section).

5.4 Model framework

We are identifying water balance models at different scales. In space we distinguish catchment, response unit (arable, grass or orchard), hillslope (7 units) and plot (14 units) scales; temporally, we distinguish monthly, bi-weekly and weekly scales. At each scale, for each spatio-temporal unit the water balance of the root zone is described by the following equation

$$S_{j,k} = S_{j,k-1} + EP_{j,k} + c_{ju} LI_{j,k} - LO_{j,k} - ET_{j,k} - D_{j,k} \tag{5.1}$$

where all units are in mm. $S_{j,k}$ is soil moisture at spatial unit j and time instant k, EP is effective precipitation, LI is lateral inflow (from an upslope unit), LO is lateral outflow (to a downslope unit into the river channel), ET is evapotranspiration and D is drainage out of the root zone to deeper layers. c_{ju} is a factor to correct for the surface area upslope from j (which can be different from the area of unit j) , hence $c_{ju} = area_{\text{upslope}}/area_{\text{j}}$. The LI component is only present at the plot scale. We indicate the spatial scale with the following letters: C for catchment, R for response unit, H for hillslope and P for plot; and the temporal scale is indicated with the letters M for monthly, B for bi-weakly, and W for weekly. Thus, evapotranspiration for the bi-weekly response unit scale, in the second unit and the fifth time period is indicated by $ET_{R2,B5}$.

The water balance model is hierarchical, meaning that the water balance components for spatio-temporal units at finer scale sum up to the value of the corresponding components at a coarser scale, for instance

$$ET_{R2,M1} = \frac{\sum_{u=2}^{6} area_u ET_{Hu,M1}}{area_{R1}} = \frac{\sum_{u=2}^{6}\sum_{v=1}^{4} area_u ET_{Hu,Wv}}{area_{R1}} = \frac{\sum_{u=3}^{10}\sum_{v=1}^{4} area_u ET_{Pu,Wv}}{area_{R1}} \tag{5.2}$$

This equation states that the evapotranspiration for the second response unit in the first month (first term at left) equals the total evapotranspiration of the five hillslopes inside this response unit for that month (second term). It also equals evapotranspiration summed over the hillslopes and the four weeks in this month (third term), as well as the sum over plots 3 to 10 (which are located in hillslopes two to six, and response unit two), and the four weeks in this month (fourth term). The reason for using a hierarchical model is that it constrains the water balance model at finer resolutions, so that unique solutions are always obtained. Without such constraints it is (for our data and modeling technique) not possible to obtain stable models at weekly and plot scales. Note however, that constraints are applied only to the water balance fluxes (not to soil moisture storage).

Two additional constraints are applied to the GAM models: evapotranspiration is always equal to or smaller than the reference evapotranspiration, and no more than 5 % of soil moisture can drain out of the soil profile in any time period.

We employ a Generalized Additive Model (GAM) to find relationships between the various factors influencing soil moisture. A GAM is a non-parametric model that has been described in detail in Hastie and Tibshirani (1990). Since the early nineties it has especially been applied especially in biological applications (e.g. Guisan et al. 2002). We will very briefly describe the technique here, starting with the definition of linear model as a sum of k variables with associated parameters β.

$$Y(i) = \beta_0 + \beta_1 X_1(i) + \ldots + \beta_k X_k(i) + e(i) \tag{5.3}$$

The error e is assumed to be normally distributed with mean zero. A variable X refers to any variable or composite variable that can be explicitly calculated (i.e. independent of Y), e.g. $X_3 = X_1 X_2$. Therefore the linear model can quite well describe all kinds of parametric nonlinear relations. In additive models the terms βX are replaced by (usually fairly simple) non-parametric functions of the X variables. The model in eq. 5.3 can be re-written as

$$Y(i) = \alpha + f_1(X_1(i)) + \ldots + f_k(X_k(i)) + e(i) \tag{5.4}$$

The functions $f_k(..)$ are usually assumed to be splines with a small number of knots, or the output from a loess smoother (Cleveland, 1979; Venables and Ripley, 2002). More complex functions can be used, but this may cause the model to over-fit the observed data and thus not generalize well to new data sets. Obviously, the choice of the function $f(..)$ (both type and complexity) is critical. GAMs fit within the framework of the generalized linear model (GLM), which extends the linear model to errors with a non-normal distribution but is still limited to distributions of the exponential family (such as binomial, Poisson or gamma). For an explanation of GLMs see McCullagh and Nelder (1989). Coming back to the water balance as given in eq. 5.1, in terms of a GAM it looks as follows

$$\begin{aligned}
g(S_{j,k}) &= S_{j,k-1} + EP_{j,k} + c_{ju} LI_{ju,k} - LO_{jd,k} - ET_{j,k} - D_{j,k} + e_{i,k} \\
EP_{j,k} &= f(P_k, S_{j,k-1}, T_j, L_{j,k}) \\
LI_{j,k} &= f(P_k, S_{j,k-1}, T_j, L_{j,k}, S_{ju,k-1}, T_{ju}, L_{ju,k}) \\
LO_{j,k} &= f(P_k, S_{j,k-1}, T_j, L_{j,k}, S_{jd,k-1}, T_{jd}, L_{ju,k}) \\
ET_{j,k} &= f(P_k, S_{j,k-1}, ETP_{j,k}, T_j, L_{j,k}) \\
D_{j,k} &= f(P_k, S_{j,k-1}, T_j) \\
e_i &\sim r(\mu_i)
\end{aligned} \tag{5.5}$$

The independent variable, $S_{j,k}$, may be transformed by the function g, depending on the error distribution that is chosen for r. For instance, if r is the Normal distribution, g is the identity function; and if r follows a Poisson distribution g is the natural logarithm, if r follows a Gamma function, g is the inverse function (see McCullagh and Nelder, 1989). In this study we evaluate these three distributions for *r*: Normal, Poisson and Gamma.

All the independent variables in the non-parametric functions *f(..)* are observed variables. However a list of observed variables is given for each water balance component, only two of these may be chosen at maximum. Thus *f(..)* is a non-parametric function of one or two variables. The variable *P* stands for observed precipitation which is homogeneous over the entire catchment, therefore *P* does not contain a subscript *j*. The variable *T* refers to one of the terrain variables: soil type, slope (%), upslope length (m), upslope area (ha), the ln($a/\tan\beta$) topographic index (see Figure 5.3; Beven and Kirkby, 1979), and the wetness coefficient (see Figure 5.3; Svetlitchnyi et al., 2003). The terrain variables only vary spatially. All these variables are calculated for 10 m pixels. At plot, hillslope and response unit scales the terrain variables are defined as averages of the values at the pixel scale. At the catchment scale terrain variables are not defined. The variable *L* refers to one of the land use variables: crop cover (none, sparsely, or full), and tillage (land is tilled or not tilled). The land use variables are calculated per plot. At higher aggregation levels the value of the dominant land use is taken. Land use variables are not defined at the catchment scale. The variable ETP refers to the Penman-Monteith reference evapotranspiration, calculated on the basis of the weather data. The subscript *ju* indicates a spatial unit located upslope from *j*, and *jd* a spatial unit downslope from *j*. The model as formulated by equation 5.5 is only valid for the plot scale. For the catchment, response unit and hillslope scales, *LI* is zero and *LO* is given by

$$LO_{j,k} = f(P_k, S_{j,k-1}, T_j, L_{j,k}) \tag{5.6}$$

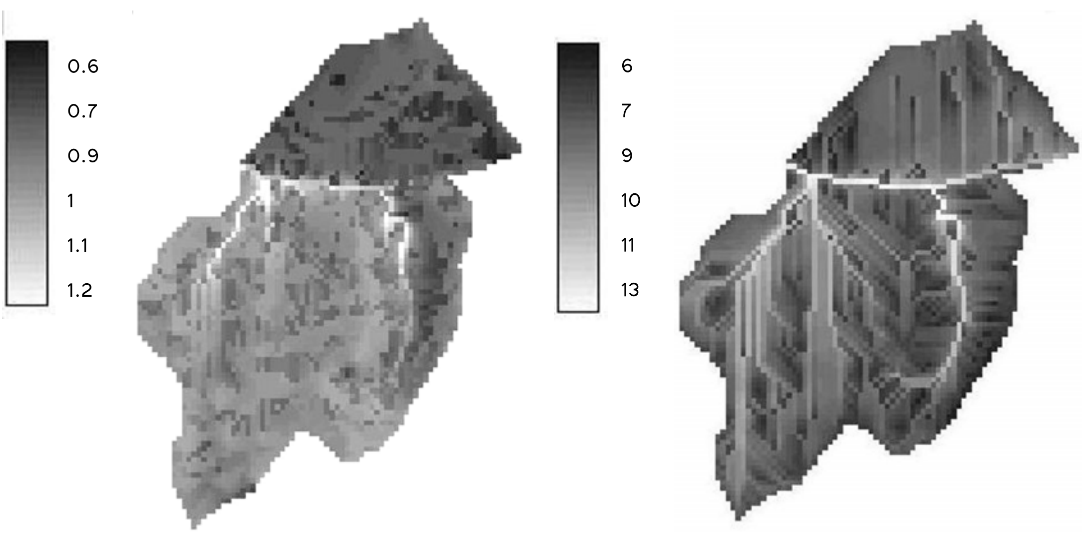

a b

Figure 5.3. a) Wetness coefficient (Svetlitchnyi et al. 2003); and b) topographic index (Beven and Kirkby, 1979) for the Catsop catchment.

Unfortunately there is no unique metric available to measure non-linearity of one or two-dimensional functions. In this study we measure the non-linearity of the water balance terms *f(..)* by fitting a linear line (or plane) through the response variables and comparing the fit through the data with this model, relative to the fit by the corresponding loess model (where fit is in both cases expressed in RMSE). Hence

$$NI = 1 - \frac{RMSE_{loess}}{RMSE_{lin}} \tag{5.7}$$

where NI is a non-linearity index, $RMSE_{lin}$ is the RMSE of the linear model and $RMSE_{loess}$ is the RMSE of the loess model for the same water balance component. A high value of NI (close to 1) indicates a highly non-linear relation, whereas a low value indicates a linear relation.

5.5 Model fitting

We fit the GAM models to our data using the R programming environment using the *gam* library (Hastie, 1991; Venables and Ripley, 2002). We apply the loess smoother with a span of 0.8 (i.e. considering 80% of the data within one window) and using a first order polynomial. The values at observation locations are assumed to be representative for the plot in which it is located; averages for plots are used for the accompanying hillslope (and so on). The aggregation scheme that was used is shown in Table 5.2. To choose the appropriate explanatory variables (only one or two per water balance component) from the list of allowed variables, we use a leave-one-out cross validation scheme. A model is fitted on all the data minus the data that applies to one spatio-temporal unit, and the value for this unit is predicted back. This is subsequently repeated while leaving out data for each spatio-temporal unit. The average error is calculated from the individual errors, using the root mean squared error (RMSE) statistic. The best-performing models are further tested by investigating all the non-parametric functions for the water balance components visually to see whether the shape can be explained qualitatively. Next, the model errors are tested for randomness (Lilliefors test), temporal autocorrelation (correlogram, all model scales), and spatial autocorrelation (correlogram, only models at the hillslope scale).

Table 5.2. Aggregation from plot to response unit. For WW (winter wheat), plots coincide with hillslopes, and for Gr (grass) the hillslope coincides with response unit.

Observation code	Plot code	Hillslope code	Response unit code
Gr.u	1	1	1
Gr.d	2	1	1
CST.u	3	2	2
CST.d	4	2	2
CVT.u	5	3	2
CVT.d	6	3	2
WW.n	7	4	2
WW.s	8	5	2
YM.u	9	6	2
YM.d	10	6	2
OO.u	11	7	3
OO.d	12	7	3
NO.u	13	8	3
NO.d	14	8	3

5.6 Model evaluation

The non-parametric water balance model is evaluated not only through cross validation and residual analysis but also by comparing its performance to that an AR(1) model as well as the conceptual water balance model, SWAP (Van Dam, 2000; Kroes and Van Dam, 2003). The AR (1) model has the following form.

$$S_{j,k} = a_j S_{j,k-1} + P_k \tag{5.8}$$

Where a_j is a model coefficient that is constant for the simulation period, but different per spatial unit. The parameterisation of SWAP and its calibration for the Catsop catchment is explained in Chapter 6.

We use the first half of the available data for every observation location (all observations before 5 February) for calibration (SWAP and AR(1) model) and deriving the non-parametric functions *f(..)* (GAMs, eq. 5.5). The second part of the data (all data after 5 February) is used for validation. Model predictions and the observations of the validation data are compared using the RMSE statistic. For a discussion on the relevance of the RMSE statistic and the relation between RMSE and other error measures see Chapter 6, section 6.3.5.

5.7 Results

5.7.1 Soil moisture variation and general results

The distribution of soil moisture per observation point is shown in Figure 5.4. The figure shows that there are large differences between observation points, even when looking at seasonally aggregated values. Especially the downslope locations (new orchard, grass and conservation tillage) are characterised by high soil moisture contents. Also the differences between old orchard (upslope) and new orchard fit into this pattern (see also Figure 5.1). Furthermore it is interesting to note that with increasing average soil moisture, variation increases (see the width of the 75 and 95 percentiles in relation to the mean soil moisture content), while there is not a pronounced skewness in the distributions. Relations between soil moisture mean and variance have been investigated for other catchments as well (see Figure 2 in Teuling and Troch, 2005), but relationships seem to be case dependent.

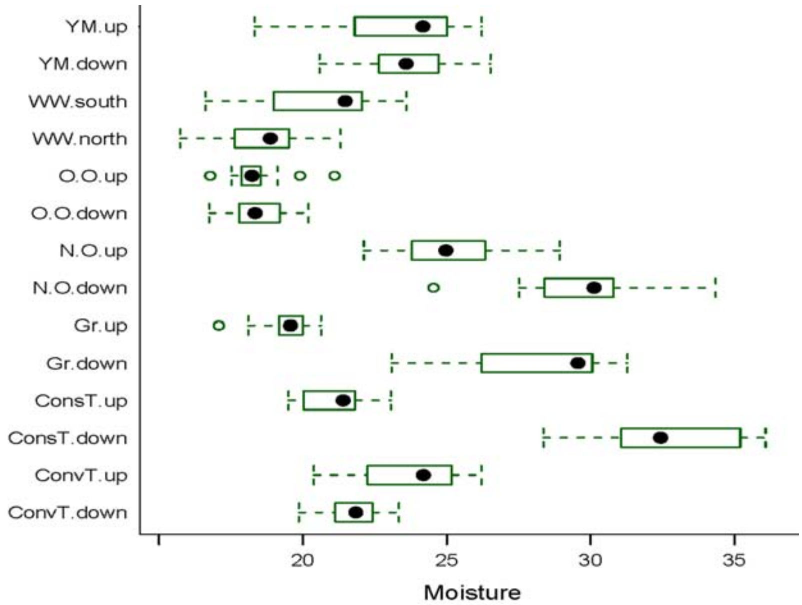

Figure 5.4. Box and whisker plot of soil moisture distribution per observation point.

5.7.2 Explanatory variables at different scales

The modelling procedure did result in significant models (only variables significant at $p < 0.05$ were included). A somewhat un-expected result was that all best performing models did contain non-parametric functions for the various water balance components that were not apparently wrong (on the basis of qualitative reasoning). In all but one case model errors were normally distributed (the one exception was a model at the catchment scale with weekly time steps, assuming a Poisson error), and only in two cases (models at the monthly time scale) the model errors had a temporal correlation. Spatially correlated model errors were not encountered. On the basis of this result it was decided to consider only the best performing models based on normal errors.

An example of model output is shown in Figure 5.5. Here the predictions for the upslope and downslope grassland plots are shown at monthly, bi-weekly and weekly scales (along with precipitation and reference evapotranspiration). For the upslope grassland plot the model operating at the monthly scale, is illustrated in detail in Figure 5.6.

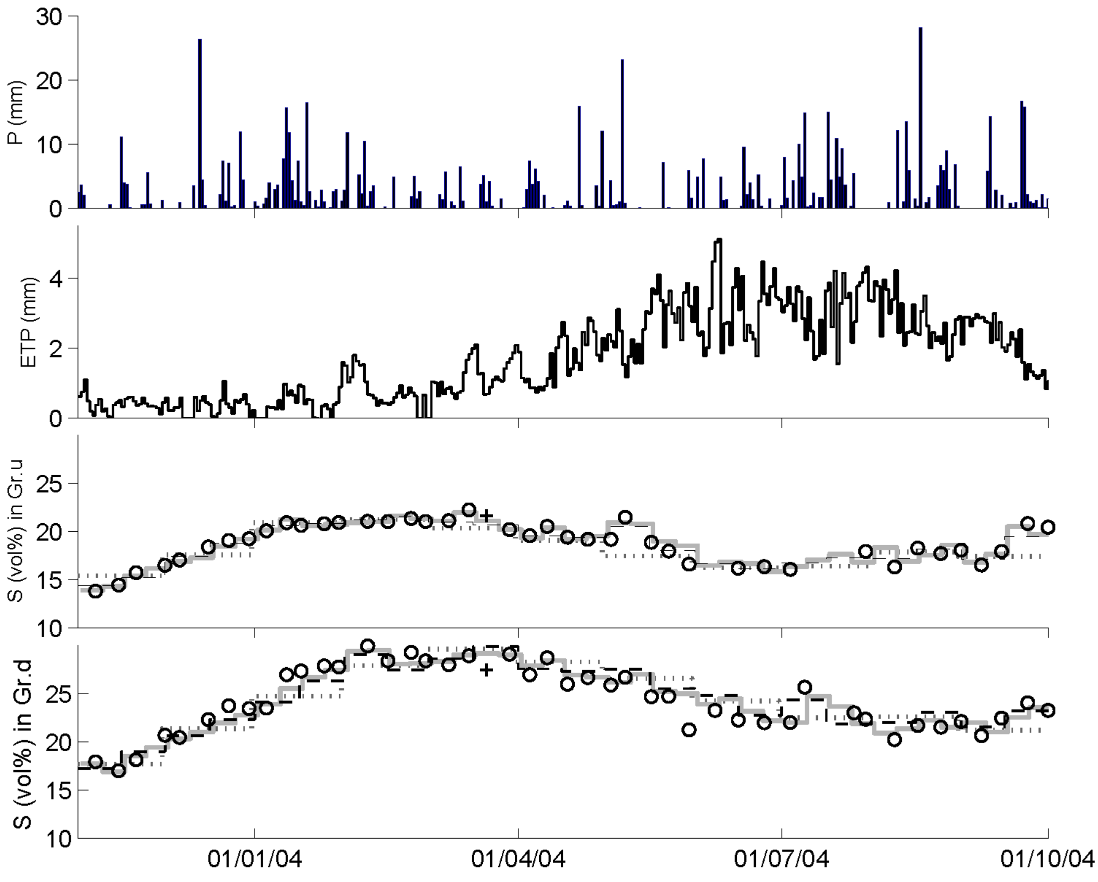

Figure 5.5. Example of prediction with GAM for the two grassland plots. The upper axis gives precipitation, the second gives reference evapotranspiration, the third axis from the top gives soil moisture of the upslope grassland plot (Gr.u), and the lowest axis gives soil moisture of the downslope grassland plot (Gr.d). The circles indicate observations that were used to derive the model, and the plus indicates the observation which is used for cross-validation. The solid line gives the weekly predictions, the dashed line the bi-weekly predictions and the dotted line the monthly predictions.

Figure 5.6 shows how effective precipitation declines above a threshold precipitation of 15 mm/h, but only in the case of a tilled soil (for an untilled soil the relation between observed precipitation and effective precipitation is nearly linear). Next, lateral inflow is shown to be a function of both precipitation and the wetness coefficient. Outflow is a function of the wetness coefficient only. The reference evapotranspiration is the main determinant for evapotranspiration and upstream area is the main determinant for drainage. The relations shown in Figure 5.6 relate to the lower five rows in Table 5.3 (2nd column). Table 5.3 shows, for all scales, the explanatory variables of the models with the smallest predictive error. Especially at the catchment and response unit scales, sometimes no significant relation was found for the drainage component (shown with a '-' in Table 5.3). With more detailed temporal scales, (bi-weekly and weekly), soil moisture becomes a suitable explanatory variable, whereas at monthly scales precipitation and evapotranspiration are more important. With finer spatial scale, the number of explanatory variables is increasing mainly with topographic variables (wetness coefficient, upslope area and topographic index). Especially for lateral outlfow as well as drainage there is a marked shift between the hillslope and plot scales.

Table 5.3. Selected explanatory variables for GAMs and model error for different spatio-temporal model scales. The model error is highlighted in bold. The explanatory variables are abbreviated as follows: S = soil moisture, ST = soil type, SL = slope, UL = upslope length, UA = upslope area, TI = topographic index, WC = wetness coefficient, CC = crop cover, TL = tillage, P = precipitation, E = Penman-Monteith reference evapotranspiration. The subscript *u* refers to the upslope unit.

Spatial scale		**Temporal scale**		
	water balance component	**month**	**two weeks**	**week**
Catchment		**0.014**	**0.012**	**0.012**
	EP	P	P	P
	LO	S	S	S
	ET	E	E, S	E, S
	D	-	-	-
Response unit		**0.015**	**0.011**	**0.007**
	EP	P	P, TL	P, TL
	LO	P,CC	P	P
	ET	E	E, S	E, S
	D	-	-	S
Hillslope		**0.013**	**0.006**	**0.007**
	EP	P, TL	P, S	P, S
	LO	WC	P,WC	S, WC
	ET	E, CC	E, CC	S, CC
	D	P	S	S
Plot		**0.016**	**0.012**	**0.006**
	EP	P, TL	P, S	P, S
	LI	P, WC	S_u, TI_u	S_u, TI_u
	LO	WC	UA	TI
	ET	E	E, CC	E, S
	D	UA	S, UA	S, TI

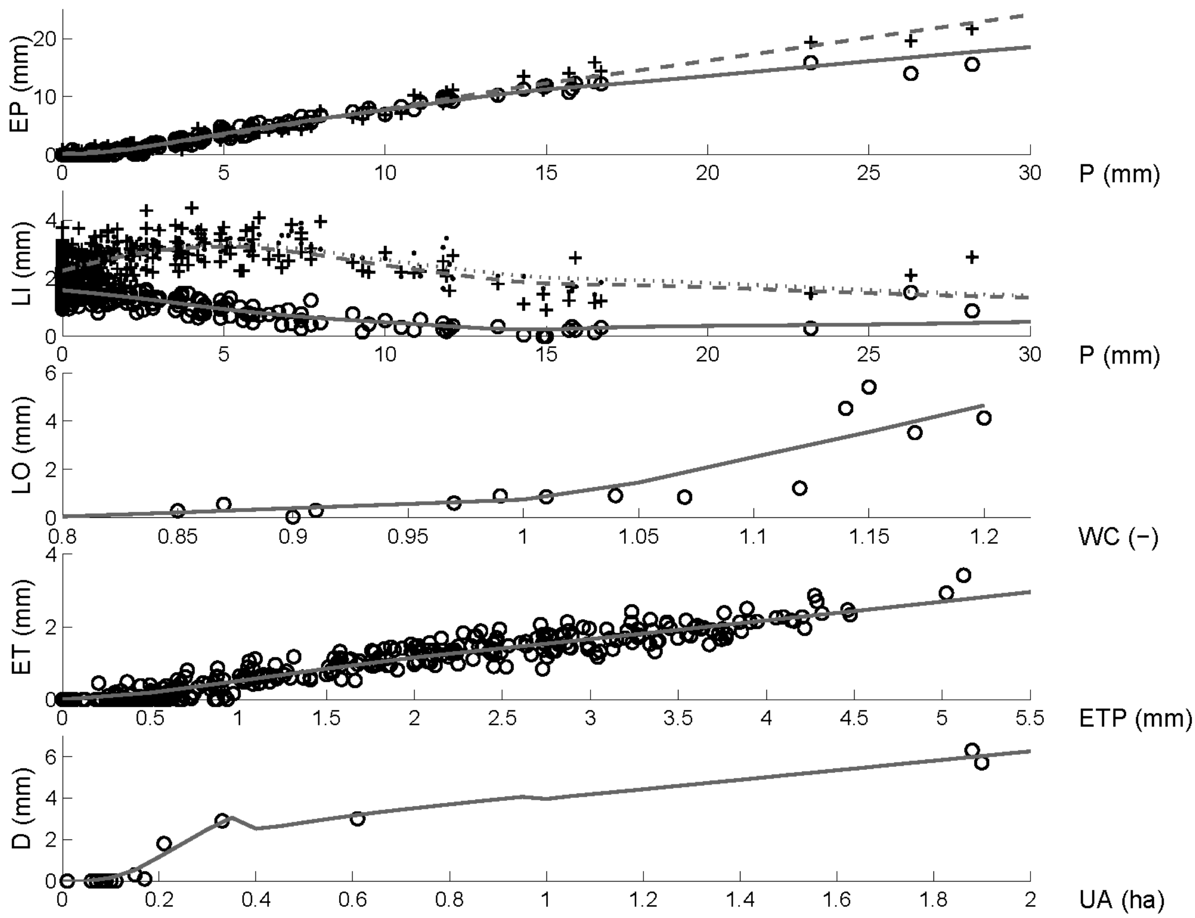

Figure 5.6. Example non-parametric functions of water balance components in the GAM for the upslope grassland plot, at the monthly time scale. The relations shown in this figure relate to the lower five rows in Table 5.3 (2nd column). In the upper axis effective precipitation is a function of observed precipitation and tillage (*EP = f(P,TI)*). The solid line refers to a tilled soil, and the dashed to an untilled soil. In the second axis from the top lateral inflow from upslope depends on both observed precipitation and the wetness coefficient (*LI = f(P,WC)*). This function is not shown fully in three dimensions, but rather with a two-dimensional graph with the relation *LI=f(P)* at three different values for WC: 0.86 (solid line), 1.0 (dashed line), and 1.2 (dotted line). For the grassland plot, the value of 0.86 is relevant. The two arrows (in the third and fifth axis) point at the WC and UA values for the grassland plot.

As stated in the section 5.4 non-linearity of the water balance terms was observed with an index relating a linear fit with the fit by the corresponding loess model for a water balance term (where fit is in both cases expressed in RMSE, see eq. 5.7). The results of this analysis are shown in Figure 5.7. It appears that the non-linearity increases with scale.

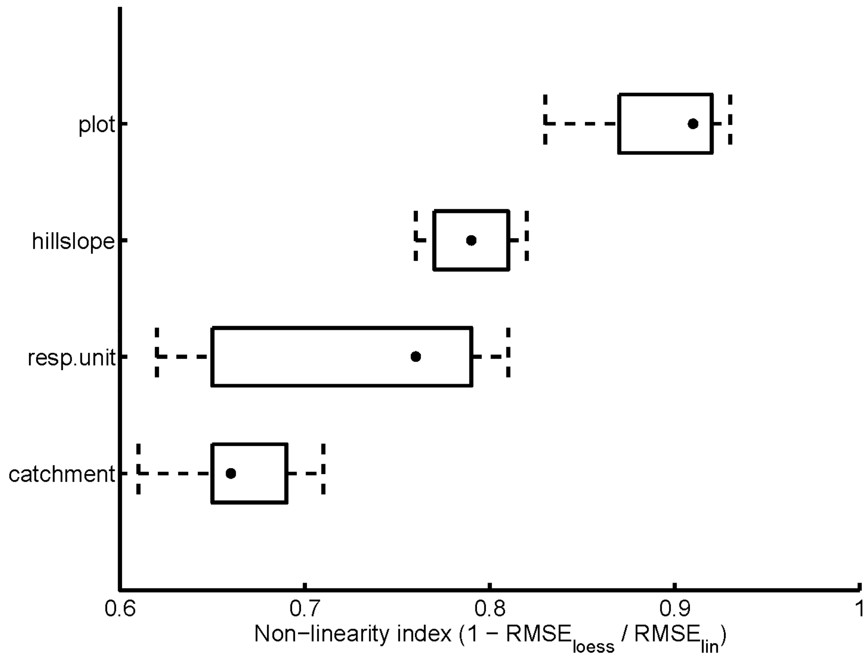

Figure 5.7. Non-linearity of the water balance terms, as a function of scale.

5.7.3 Comparing the generalized additive water balance model with an AR(1) model and SWAP

At all scales we see that the RMSE for the GAMs is smaller than for SWAP, which is in turn smaller than AR(1) (see Table 5.4). While this pattern is quite consistent, the differences are not big. Note that RMSE for the GAM in Table 5.4 is not entirely comparable to that in Table 5.3. In Table 5.3 it is based on cross validation, and in Table 5.4 on a split data set.

At the response unit and hillslope scales the pattern of RMSE variation over units/hillslopes is also quite consistent (especially when comparing the GAMs with SWAP). Arguably, RMSE of predicted soil moisture is a very limited measure for a water balance model (see also the discussion in section 6.3.5). But also detailed visual checks on the output from the three models lead to the conclusion that results for soil moisture are not dramatically different. The only outstanding structural error is that the AR(1) model appears to systematically underpredict extreme wetness and overpredict dry periods (see Figure 5.8). For the partitioning between actual evaporation and drainage there are however considerable differences between the GAM models and SWAP. Figure 5.9 illustrates these differences for the water balance over the entire study period. On average the GAMs underpredict actual evapotranspiration by 13% and drainage by 4%, both in comparison to SWAP. In the GAMs these terms are compensated by a lateral outflow term, which is not present in SWAP.

Table 5.4. Comparison of prediction error (RMSE) of GAM, SWAP and AR(1) model, all applied to the same calibration/validation data.

		RMSE	
Spatial scale	GAM	SWAP	AR(1)
Catchment	0.011	0.012	0.012
Response unit			
Arable	0.006	0.006	0.008
Grass	0.009	0.011	0.010
Orchard	0.011	0.012	0.012
Hillslope			
grass	0.008	0.015	0.017
winter wheat (two slopes averaged)	0.010	0.017	0.017
conservation tillage	0.005	0.009	0.012
conventional tillage	0.006	0.007	0.009
yellow mustard	0.007	0.009	0.015
new orchard	0.009	0.011	0.014
old orchard	0.010	0.014	0.014

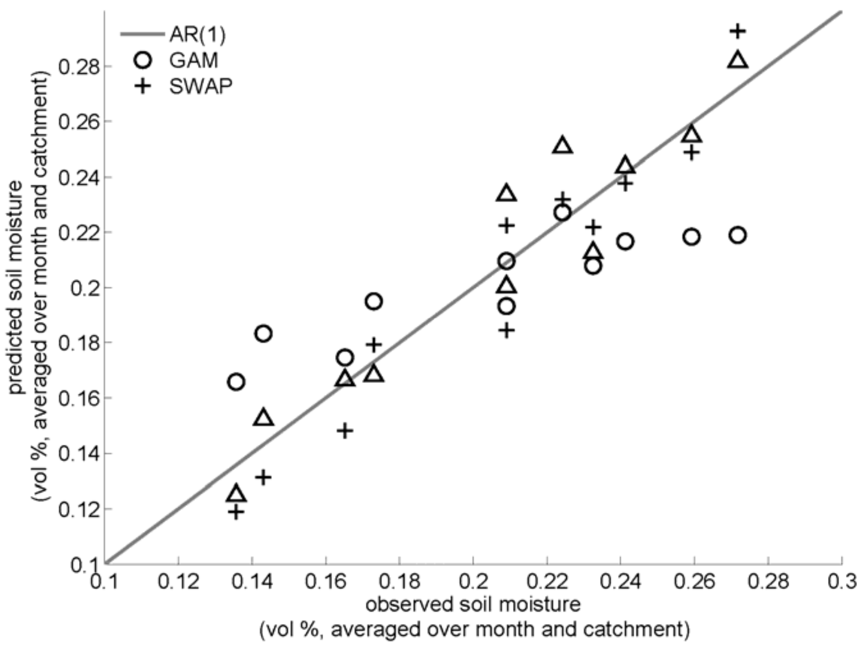

Figure 5.8. Model residuals for monthly averaged data. The GAM and SWAP predictions do not show a clear trend, but the AR model overpredicts at low soil moisture and overpredicts at high soil moisture values.

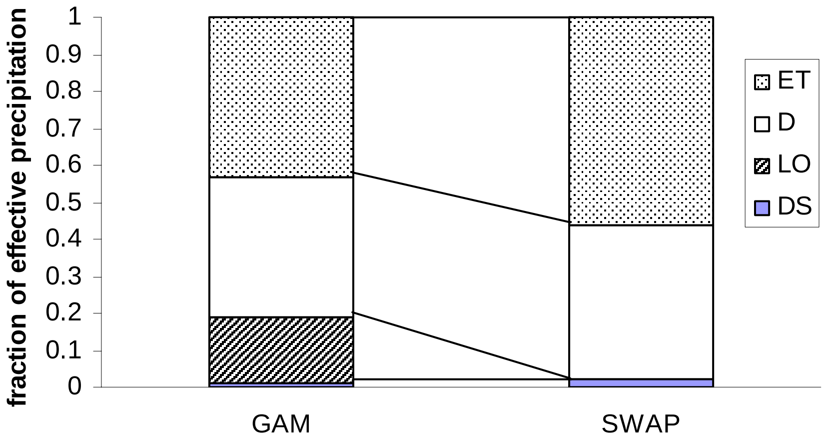

Figure 5.9. Visual display of the partitioning of the water balance terms, aggregated over the total study period, where DS means the difference in water storage, LO means lateral outflow, D means drainage and ET actual evapotranspiration; all terms integrated over the entire research period (see eq. 5.5).

5.8 Discussion and conclusions

The relation between soil moisture and topography (mainly slope gradient, aspect, relative elevation, and shape of slope profile) has been investigated frequently (Reid, 1973; Burt and Butcher, 1985; Carve and Gascuel-Odux, 1997; Famiglietti et al. 1998; Western et al. 1999; Moore et al. 1988; Qiu et al., 2001; Svetlitchnyi et al., 2003; Pellenq et al., 2003). Also the effect of land use often has been studied (Fu et al., 2000; Hawley et al., 1983; Qiu et al., 2001; Mahe et al., 2005). Findings in these studies differ due to locally different situations (e.g. climate, geology, human influence; see Qiu et al., 2001). We believe, on the basis of the results from this study, that different conclusions can also be reached when focussing at different spatial or temporal scales. When parameterising our water balance model at coarse temporal scales, we find e.g. that mainly rainfall and potential evapotranspiration are dominant factors, together with crop cover. At finer temporal scales soil moisture becomes more important (rendering precipitation less influential). Soil moisture acts as a non-linear filter on the rainfall input. Apparently this process is too fast to be visible at a monthly scale, but at bi-weekly and weekly scales it is (see Table 5.3, columns two - four). Land use is influential at all scales (Table 5.3), but especially at response unit and hillslope scales. The sharp differences between the hillslope and plot scales are remarkable. At the hillslope scale, the wetness coefficient and crop cover are the most effective terrain and land use variables, whereas at the plot scale it are upslope area and the topographic index (compare hillslope with plot in Table 5.3).

Overall, the shape of the response functions for the water balance components (such as shown in Figure 5.6) could be explained qualitatively. In addition, the residuals of the

GAMs were not correlated over time (tested for all scales) and were also not spatially correlated (tested for the models at the plot scale). With finer scales the non-linearity of the water balance components increases (Figure 5.7). This is an aspect which has been often mentioned in the hydrologic literature. It is generally believed that most processes lead to highly non-linear responses at point scales, and that responses become more linear at coarser due scales to spatio-temporal averaging (Blöschl and Sivapalan, 1995). However there is theoretical evidence for this property in hydrological systems, little direct empirical evidence of this property exists (especially at the intermediate scales of hillslope and response unit). Our results provide this evidence.

After meeting these minimal requirements for a useful model, the results from the GAM were compared with a (simpler) AR(1) model and a (more complex) physically based water balance model. This comparison leads to the conclusion that, measured by RMSE, the GAM performs slightly better than both other models (see Table 5.4). Apart from a structural difference between the AR(1) model and the other models, there appeared to be few differences for soil moisture. The AR(1) model appeared to structurally underpredict extreme wetness and overpredict dry periods, and the partitioning between the various loss terms appeared to be different between the GAMs and SWAP. In the GAMs a lateral outflow term was consistently present, whereas such a term is absent in the SWAP model (which models a 1D column). This leads to lower estimates of both actual evapotranspiration and drainage by the GAMs in comparison to SWAP. The presence of a significant lateral outflow term together with the observation that topographic variables are important at the hillslope and plot scale leads to the conclusion that lateral flow processes are important in Catsop. This result corresponds with the results by Michiels et al. (1989) but is in conflict with the conclusion from Ritsema et al. (1996) that lateral flow processes play a minor role in Catsop. Part of this difference is in the definition of the term lateral flow. Ritsema et al. (1996) consider only flow that is observed within the root zone of a hillslope (see also Jackson 1992). In this study it is all the water that leaves a spatial unit as discharge. Another explanation can be that Ritsema et al. (1996) collected (very detailed) data for a single slope in the catchment, whereas in this study various slopes were observed simultaneously.

This study addresses the issue of hydrological model identification at different scales. It is an old (and returning) subject of research (e.g. Klemes, 1983; Beven, 1995, Blöschl and Sivapalan, 1995). This study contributes with a new approach to identify dominant mechanics at different scales: a hierarchical generalized additive model. Generalized additive models are valuable research tools that are, in contrast to other non-parametric modeling techniques like neural networks (e.g. Jiang and Cotton, 2004) and self-organising maps (Schütze et al. 2005), hardly used for hydrologic applications. Yet, as this study demonstrates, the technique appears to be quite elegant, in particular for water balance models. GAMs can be calibrated fast, which allows the evaluation of many candidate models, and the response-curve of individual water balance components can be assessed visually and tested statistically (using all the techniques available for GLMs). With this study we would like to emphasize not the results for our research catchment, but rather the possibility to apply GAMs for finding appropriate parameterisations at a given scale. The result can be used as a starting point for building conceptual models of the entire water balance, or only a single component. An example of analysing a single water balance component within an identified GAM model would be to replace one component with a given parametric function, and subsequently evaluating whether the resulting model would perform equally well (or better) as its nonparametric counterpart. An example of a suitable formulation of drainage to a deeper layer can e.g. be taken from eq. 14 of Laio et al. (2001) and an example of a parametric replacement for the evapotranspiration function can be found in eq. 3 of Teuling and Troch (2005). Young (1998) and Wilby et al. (2003) have demonstrated that also other non-parametric techniques (viz. autoregressive TVP models and neural network models) can be used to evaluate hydrological model concepts.

For the Catsop catchment we can confirm that water balance models are scale dependent, meaning that when defining a model at a different spatio-temporal resolution an entirely different process description is required. Of course this situation is partially due to our limited set of observations (with RS-observations scale dependency might have been less), but therewith not less valid in any practical situation. Although the idea of scale dependent models has been hypothesized a while ago by Beven (1995), surprisingly little empirical evidence to either confirm or reject this hypothesis has been reported until now. This is probably due to the fact that most models have a parametric basis, for which it is laborous to specify a large number of different candidate models. On the other hand most data-based models (such as neural networks or complex autoregressive models) are entirely geared towards prediction and do not provide a method to single out individual water balance components. In relation to soil moisture prediction some work has been done to derive field-averaged values from point observations, using scaling theory (e.g. Warrick et al., 1977; Russo and Bresler, 1980; Rodriguez-Iturbe et al., 1995; Western and Blöschl, 1999). Scaling theories have however only been applied to relatively homogeneous fields with limited relief and human influence, and within a limited spatio-temporal range.

While GAMs are in principle suitable for water balance modelling, as stated previously, several practical difficulties need attention. The first is the risk for overparameterisation. GAMs always need (like any non-parametric model) a calibration-validation cycle to check whether the model that is found can be generalised. In this study this was implemented via a leave-one-out cross validation scheme. Next, GAMs are not always stable, hence one needs to check the stability of a solution through a sensitivity analysis, and often apply some form of regularization (Hansen, 1998). A very straightforward regularization scheme was applied in this study, first deriving coarse-scale models and then using these to constrain the fine-scale models (i.e. a hierarchical modelling approach). Apart from being easy to apply, it is unclear to us whether a hierarchical modelling approach offers any advantages over other regularization schemes like Tikhonov regularization or TSVD (Hansen, 1998). A potential source of problems are artefacts that result from the limited information content of the observations, relative to the number of water balance components that are being specified. In our study this results in the property that the same set of explanatory variables can only be used for one water balance component (it can be seen in Table 5.3 that this is the case in our study). If one water balance component (e.g. Effective Precipitation) is identified as being influenced by observed precipitation, another component (e.g. Lateral Outflow) will not be identified as being influenced by precipitation alone. While from a statistical perspective this is exactly what one desires, from a physical viewpoint it makes no sense because it is well possible that two independent processes rely on the same explanatory variable. This situation can only be resolved by additional observations (on individual water balance components). An additional observable that is available for our study area catchment discharge. With discharge it is e.g. possible to set the sum of lateral outflow (over all spatial units) equal to observed catchment discharge. If the model concept suits the system under study, this additional data should result in lower soil moisture prediction errors. A failure to achieve this does however not automatically lead to a rejection of the model. In that case there are many possible explanations that each has to be investigated. The question how and under which conditions catchment discharge leads to enhanced soil moisture predictions is subject of future study.

The possibility of GAMs to evaluate range of model structures relatively easy also opens new possibilities to re-think the concept of information content of observations in relation to the model complexity (Jakeman et al. 1993). For non-parametric model like GAMs one can express model complexity in terms of the number of required explanatory variables (provided that the resulting model is tested in some cross-validation scheme). Through the observation of longer records or additional state variables one can measure both changes in model performance and model complexity. The point where model performance does not increase is the complexity that is warranted.

Chapter 6

Adequacy of a 1D unsaturated zone model to describe the soil moisture dynamics from point to catchment scale

Vahedberdi Sheikh and Emiel van Loon
Submitted to: Vadose Zone Journal

6 Adequacy of a 1D unsaturated zone model to describe the soil moisture dynamics from point to catchment scale

Abstract

The utility of an unsaturated zone soil moisture model is not only its ability to describe the soil moisture dynamics at a given point, but also the possibility to generalize the results to larger areas. In this study we investigate the predictive performance of a 1D unsaturated zone soil moisture model when applied at point, field, response unit, and catchment scales, using detailed field observations from a 0.42 km^2 catchment in the Netherlands. Our main question is how model parameterisation and model performance can be compared across these scales. We consider two different calibration-validation schemes and three performance statistics. In all cases we apply the same Levenberg-Marquardt optimisation scheme. Differences between calibration-validation schemes (interpolation versus extrapolation) are surprisingly small. Using one particular model parameterisation across the various aggregation levels, the optimal Mualem-Van Genuchten parameters for a coarser aggregation level can be derived from an underlying level by simple arithmetic averaging. The different performance indices (root mean squared error, index of agreement, and the Nash-Sutcliffe coefficient) are highly variable between observation locations and for different aggregation levels. Overall, the indices are more favourable at higher aggregation levels, and in correspondence with errors reported in comparable studies. We did not succeed in deriving a meta-model to scale model performance indices with aggregation level. Multi-scale calibration studies will therefore remain useful to compare results from unsaturated zone models at different aggregation levels.

Keywords: soil moisture, unsaturated zone, parameter optimization, aggregation, effective parameters, Mualem-Van Genuchten, SWAP

6.1 Introduction

Soil moisture content in the top one to two meters of the earth’s surface controls the success of agriculture, and regulates partitioning of precipitation into surface runoff, evapotranspiration and drainage into deeper ground water storage. Therefore it is considered a key parameter in meteorological or hydrological studies (Walker, 1999). In spite of its importance it is not monitored regularly. Because it is highly variable both spatially and temporally it is not cost effective to measure soil moisture routinely using conventional methods. One possibility to cover spatial variability of soil moisture over large areas is the application of remote sensing techniques. However, the availability of satellite images at a low temporal frequency and at a relatively coarse spatial resolution (while only covering a very shallow surface layer), still limits their applicability. The efforts to enhance satellite sensors and extract better information are ongoing. Such efforts greatly benefit from well-designed in-situ soil moisture measurements, especially to calculate accurate spatially averaged estimates (Walker, 1999; Western &Grayson, 1998). Dynamical unsaturated zone models are generally believed to be appropriate tools to obtain such averages (Giacomelli et al., 1995; Teuling and Troch, 2005) while statistical interpolation techniques, when used in isolation, are only of limited value for soil moisture monitoring (e.g. Western & Grayson, 1998; Western et al., 2004). During the past few decades, a wealth of experimental studies have been done on infiltration and water movement in soil profiles (Scotter et al. 1982; Devaurs & Gifford, 1984; De Roo & Riezbos, 1992; Bagarello & Iovino, 2003). These results promoted a considerable progress in the conceptual understanding and mathematical description of water flow and solute transport processes in the unsaturated zone. This is illustrated by the variety of analytical (Ahuja et al., 1981; Hurley and Pantelis, 1985; Stagnitti et al., 1992; and Selim, 1987) and numerical (Beven, 1981; Rogers and Selim, 1989; Jackson, 1992; Simunek et al., 1992) models that have been developed. Nearly all of the currently available water flow and solute transport simulation models (e.g. SWAP, SWMS-2D, WAVES, HYDRUS) are based on the numerical solution of the Richards equation with different schemes. Models of this type were shown to be useful tools for extrapolating information from a limited number of field experiments to different soil, crop, land management, and climatic conditions (e.g. Yu et al., 2000). Apart from obvious omissions from these models (e.g. effects of temperature, freezing, or macropore flow), also more intricate problems of scale remain (Klemes, 1983; Blöschl and Sivapalan, 1995). It has also been outlined in several studies that a Richards equation model is not an appropriate parameterisation at every resolution (Downer et al., 2004; van Dam & Feddes, 2000). Yet, the questions remain at which scales exactly it does provide a suitable model, and how model performance should be evaluated in this context. The latter question comprises the choice of a calibration-validation scheme as well as a performance criterion. This study is meant to help in answering these questions. After explaining in detail the method used to calibrate a Richards equation model we evaluate two validation schemes and subsequently show and discuss the various statistics and aggregation levels to measure its performance.

6.2 Materials and methods

6.2.1 Study area

The data used in this study originate from the Catsop catchment. The catchment is situated in the hilly loess region of South Limburg in the Netherlands (50º 95´N, 5º 78´E; Figure 6.1). It has an area of 0.42 km^2, and is almost entirely used for agricultural purposes. Elevation ranges from 79 to 112 m.a.s.l, and the terrain is undulating with gently to moderately sloping topography. About 86 % of the slopes have a gradient of less than or around 10 % and 3.5 % of the slopes are steeper than 15 %. The catchment has a dominant flow direction to the west, the direction of the river Meuse. During major storms 3-30 % of the total rainfall reaches the catchment outlet (De Roo 1993). The soils of the catchment have been formed on aeolian deposits (Ice-age period 0.01 – 0.2 Ma) and are typical of the scatter loess areas in northwestern Europe. Depth of these deposits in the Catsop catchment exceeds 5 meters.

Within this small catchment four land use types were distinguished: Arable (79.5 %), Orchard (7.9 %), Grassland (11.8 %), and Infrastructure (0.8 %). Figure 6.2 presents the land use pattern of the Catsop catchment during the winter season of 2003-2004.

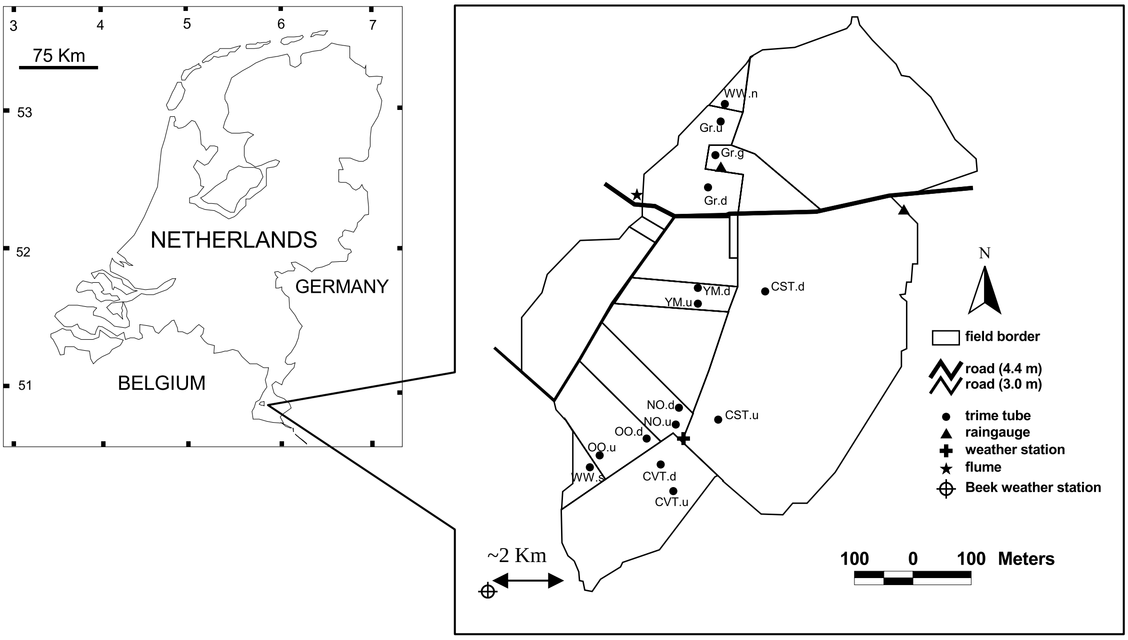

Figure 6.1. Geographical position of study area and location of the measurements (for abbreviations, see Table 6.1).

Arable land is cultivated mainly with winter wheat, spring barley, sugar beet, potato, and yellow mustard. Yellow mustard is a second crop, functioning as an erosion prevention measure. It is planted after harvesting the cereals at the end of the summer, and later in the season chopped into small pieces and spread on land surface as green manure and protection cover. Grasslands are utilized in two ways. One field is grazed by cows from April till October (less than 0.5 cows per ha) and the other fields are harvested by machinery. During the last 5 years the area of orchards increased from nil to about 8 %. The only available infrastructure within the catchment are a few tarred roads and one ditch near to the outlet which runs parallel to the main road (shown in Figure 6.1). Table 6.1 lists some of the properties of each land use. The climate is temperate humid, with a mean annual precipitation of ca. 740 mm. Precipitation occurs mainly as rainfall and is evenly distributed over the whole year. However the rainfall pattern in winter and summer is different. Summer events are shorter and more intensive while winter events are on average longer and less intensive.

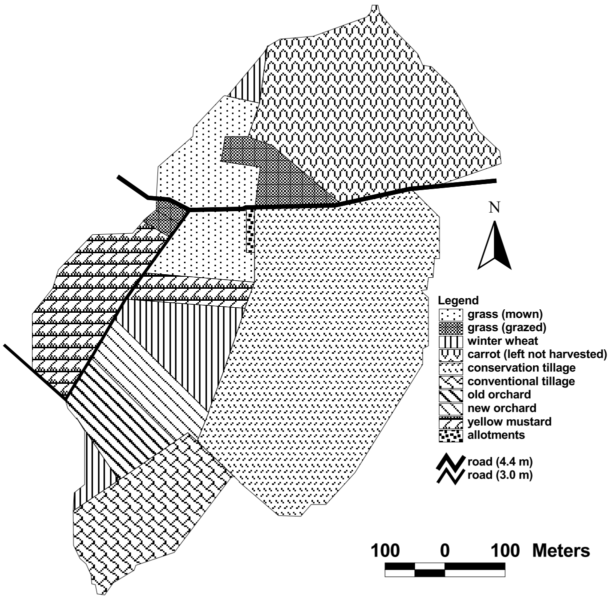

Figure 6.2. Land use in the Catsop catchment during the winter season of 2003-2004.

Table 6.1. General information of the measurement locations.

Tube	Land use	Soil[1]	Slope (%)	Uplength[2] (m)	Uparea[3] (ha)	Nr[4]
Gr.d	grass	Ld6h	14.1	78.3	0.1	47
Gr.u	grass (mown)	Ld6h	9.2	54.1	0.06	44
Gr.g	grass(grazed)	Ld6h	6.7	14.1	0.02	45
WW.n	winter wheat	BLb6	3.9	5.0	0.01	36
WW.s	winter wheat	BLb6	4.3	147.3	0.21	37
CST.d	conservation tillage	cBLb6	5.4	160.7	0.61	16
CST.u	conservation tillage	cBLb6	8.7	122.4	0.15	21
CVT.d	conventional tillage	cBLb6	4.1	60.0	0.07	14
CVT.u	conventional tillage	cBLb6	7.0	84.1	0.1	19
YM.d	yellow mustard	cBLb6	4.8	360.0	1.9	21
YM.u	yellow mustard	cBLb6	5.0	340.0	1.88	21
NO.d	orchard (2 years old)	cBLb6	7.1	224.1	0.33	21
NO.u	orchard (2 years old)	cBLb6	6.1	70.0	0.08	21
OO.d	orchard (5 years old)	Ld6c	7.7	162.4	0.17	16
OO.u	orchard (5 years old)	Ld6c	5.7	78.3	0.09	16

[1] Dutch classification according to Stolte et al. (1994)
[2] Distance between divide and the tube along hillslope
[3] Catchment area of the tube
[4] Number of measurement times for each tube

6.2.2 Data collection

Soil moisture was monitored in 15 tubes of 1 meter depth with a Time Domain Reflectometry system (*Trime-FM*) once every week for the period of November 2003 – September 2004. Measurements were taken over 5 depths intervals: 0 – 20, 20 – 40, 40 – 60, 60 – 80, and 80 – 100 cm from the surface downward. The measurement technique integrates soil moisture content over the entire 20-cm layer. Due to large errors in the measurements of the layer 80 – 100 cm its values were not used in this study. The locations of these tubes and other measurement equipments are shown in Figure 6.1. The topographic characteristics of each observation location are given in Table 6.1. For each land use type and management practice at least two tubes were installed. Two tipping bucket rain gauges and one small standalone weather station were installed as well. All observed meteorological variables did agree well with the observations at the Beek weather station (50 55'N, 5 47'E), at a distance of less than 2 km from the study area. The evapotranspiration rate has been calculated with the Penman-Monteith equation using daily meteorological data of the Beek station. Discharge was measured at the catchment outlet using a partial flume with a capacity of 950 l/s and a stilling well with a vertical float recorder. This station was initially installed by Wageningen University in 1987. Later the waterboard “Roer en Overmaas” has taken over the responsibility of this station. It has been used sporadically during the last two decades. For the purpose of this study discharge measurements were collected at 10 minute intervals during the period November 2003 – September 2004. Although the discharge observations may be relevant to questions about (multi-scale) unsaturated zone soil moisture modelling, these data were not used in this study (see the last part of the discussion and conclusions section).

6.2.3 Modeling

The Soil-Water-Atmosphere-Plant (SWAP) model was used to describe soil water movement in the unsaturated zone of our study catchment. SWAP is the successor of the agro-hydrological model SWATRE (Feddes et al., 1978; Kroes & van Dam, 2003). It assumes that the main flow process occurs in the vertical direction only (hence it is a one dimensional model) and considers soil moisture movement in close interaction with crop growth. SWAP can simulate crop growth either with a simple or a detailed crop growth model. In the simple crop growth model (used in this study) the measured leaf area index, crop height and rooting depth are prescribed as a function of crop development stage, which is either controlled by a temperature sum or linear in time. The simple module does not simulate the effect of water and salt stress. The detailed crop growth model comprises an implementation of WOFOST (Hijmans et al., 1994). This detailed model does include the effect of water and salt stress on crop growth. The following section describes in brief the soil water flow process in SWAP. For more detailed information the reader is referred to Kroes and van Dam (2003) and van Dam (2000).

6.2.4 Soil water flow

Transient soil water flow is simulated by the well known Richards equation.

$$C(h)\frac{\partial h}{\partial t}=\frac{\partial}{\partial z}\left[K(h)\left(\frac{\partial h}{\partial z}+1\right)\right]-S_a(z) \tag{6.1}$$

Where $C=d\Theta/dh$ is the soil water capacity [L^{-1}], h is the soil water pressure head [L], K is the hydraulic conductivity [LT^{-1}], S_a is the root water uptake rate [T^{-1}], and z is the vertical coordinate [L] (positive upward).

SWAP solves equation (6.1) numerically using an implicit finite difference scheme as described by Van Dam and Feddes (2000). The numerical solution of equation 6.1 is subject to specified initial and boundary conditions and soil hydraulic functions, which relate Θ, h and K. the Mualem-Van Genuchten equations (Mualem 1976; Van Genuchten, 1980) is implemented to relate Θ, h and K.

$$\theta(h)=\theta_{res}+\frac{\theta_{sat}-\theta_{res}}{\left[1+|\alpha h|^{n}\right]^{\frac{n-1}{n}}} \tag{6.2}$$

$$K(\theta)=K_{sat}S_e^{\lambda}\left[1-\left(1-S_e^{n/n-1}\right)^{\frac{n-1}{n}}\right]^2 \tag{6.3}$$

Where Θ_{res} is the residual water content [$L^3\ L^{-3}$], Θ_{sat} is the saturated water content [$L^3\ L^{-3}$], S_e is the relative saturation [-], α [L^{-1}] and n [-] are empirical shape factors, K_{sat} is the saturated hydraulic conductivity [LT^{-1}], and λ [-] is an empirical coefficient.

The upper boundary conditions are controlled by the rates of potential evapotranspiration, irrigation, precipitation and interception. Potential evapotranspiration (ET_p) is estimated by the Penman-Monteith equation, using daily weather data of solar radiation, air humidity, wind speed, and air temperature as well as crop characteristics such as minimum resistance, reflectance (albedo) and crop height (Allen et al., 1998).

When soil surface is partly covered by crop, ET_p is partitioned into soil evaporation rate E_a [LT^{-1}] and potential transpiration rate T_p [LT^{-1}]. This partitioning is achieved through the leaf area index LAI [$L^2\ L^{-2}$] or soil cover S_c [-] as a function of crop development stages (Goudriaan, 1997; Belmans et al., 1983).

$$E_p=ET_p e^{-K_{gr}LAI} \tag{6.4}$$

$$E_p = (1 - S_c) ET_p \tag{6.5}$$

$$T_p = \left(1 - \frac{P_i}{ET_{po}}\right) ET_p - E_p \qquad \text{with} \quad T_p \geq 0 \tag{6.6}$$

Where ET_{po} is the potential evapotranspiration rate of the wet crop as calculated with the Penman-Monteith equation neglecting crop aerodynamic resistance, κ_{gr} is the extinction coefficient for global solar radiation (0.39 for common crops), and P_i is the interception rate [L] which is estimated with the Von Hoyningen-Hüne (1981) formula:

$$P_i = aLAI\left(1 - \frac{1}{1 + \frac{bP_{gross}}{aLAI}}\right) \tag{6.7}$$

Where P_{gross} is gross precipitation [L], a is an empirical coefficient [L] and b is the soil cover fraction (≈ $LAI/3$) [-]. Generally for ordinary crops it is assumed that a = 0.25.

Under wet soil conditions, actual soil evaporation E [LT $^{-1}$] is governed by the atmospheric demand, and equals E_p. When soil becomes drier the actual evaporation decreases to a rate which is quantified with Darcy's law as:

$$E_{\max} = K_{1/2}\left(\frac{h_{atm} - h_1 - z_1}{z_1}\right) \tag{6.8}$$

Where $K_{1/2}$ is the average hydraulic conductivity [LT $^{-1}$] between the soil surface and the first node, h_{atm} is the soil water pressure head [L] in equilibrium with the air relative humidity, h_1 is the soil water pressure head [L] of the first node, and z_1 is the soil depth [L] at the first node.

SWAP also has an option to choose the empirical evaporation functions of Black (1969) or Boesten and Stroosnijder (1986) to avoid the serious limitations of the E_{max} model given in equation 6.8. In this study eq. 6.8 has been used. It is still not clear to which extent the soil hydraulic functions, that usually represent a top layer of a few decimeters, are valid for the top few centimeters of a soil. Because the top few centimeters of soil is subject to splashing rain, dry crust formation, root extension and various cultivation practices (Van Dam, 2000). SWAP will determine E_a by taking the minimum value of E_p, E_{max} or else actual evaporation rate calculated based on the empirical functions.

The lower boundary condition is defined by the fluxes at the bottom of soil profile. Since ground water level at the catchment is deeper than two meters for all the measurement locations, we applied the free drainage condition to calculate the bottom flux q_{bot} [LT $^{-1}$]:

$$q_{bot} = -K(h)\left(\frac{\partial h}{\partial t} + 1\right) = -K(h)(0+1) = -K(h) \tag{6.9}$$

6.2.5 Parameter Estimation and model validation

Generally speaking, models of soil water flow are very sensitive to soil hydraulic characteristics as parameterized via the soil hydraulic retention θ(h) and hydraulic conductivity $K(\theta)$ functions (Van Dam, 2000; Mertens et al., 2005). In SWAP, the Mualem-Van Genuchten equations (Eq. 6.2 and 6.3) are used to describe the soil hydraulic functions. In total, there are six parameters (θ_{res}, θ_{sat}, α, n, λ, K_{sat}) in these equations (the parameter m is calulated by 1-1/n). Of these parameters θ_{sat} and K_{sat} have a clear physical meaning and can in theory be measured directly. However, due to practical difficulties in the measurement of K_{sat} its value is usually derived through calibration. We have divided the profile into three layers: 0-20 cm, 20-40 cm, and 40-80 cm (from the soil surface downwards). This division was made based partially on our field observations, and partially on the basis of previous studies to soil properties in the Catsop catchment (Stolte et al., 1994). During augering to install TRIME access tubes, at most of the augering locations a compacted layer was present at a depth of between 15 and 50 cm in the soil profile. Also the penetrometer resistance survey with an electronic penetrologger confirmed the presence of this compacted layer throughout the catchment. Stolte et al. (1994) noticed a considerably lower hydraulic conductivity in the 20-40 cm layer. The θ_{res} is usually assigned a value near to zero. In our study it was given a fixed value of 0.01 for all three layers. The empirical shape parameter λ was derived from the literature (Ritsema et al., 1986), in our study a value of 0 was used for the top two soil layers and -1.17 for the third layer. Both θ_{res} and λ show low sensitivities in relation to soil water flow (van Dam 2000; Singh 2005). The α and n are shape parameters that can be estimated by fitting measured water retention data or be derived via calibration of a flow model to observed water content and pressure head data. We have chosen to derive α and n via calibration. In summary, there are three uncertain parameters per soil layer that have to be derived by calibration: α, n, and K_{sat} (9 parameters in total). For our system this large number of parameters leads to an ill-posed inverse problem (Kool and Parker, 1988). Thus we decided to fix 3 out of 9 parameters. We followed two strategies to decrease the number of parameters to be optimized. The first was a preliminary optimization procedure with 9 parameters in order to find less sensitive soil hydraulic parameters, and subsequently continued optimization with 6 parameters. The second strategy was to optimize with different combinations of two out of three parameters (α, n, and K_{sat}) for each soil layer. The initial values for the 9 parameters were taken from Ritsema et al. (1996) and Stolte et al. (1994). Parameters values for second and third layers were taken from Ritsema et al. (1996). They have given the Mualem-Van Genuchten parameters on the basis of soil profile description. Parameters of the first layer have been extracted from Stolte et al.(1994).

For calibration we used the PEST calibration software (Doherty, 2002). PEST is model-independent optimization software which requires the user to provide a communication link between the specified model and PEST. We used a communication link that is schematically shown in Figure 6.3.

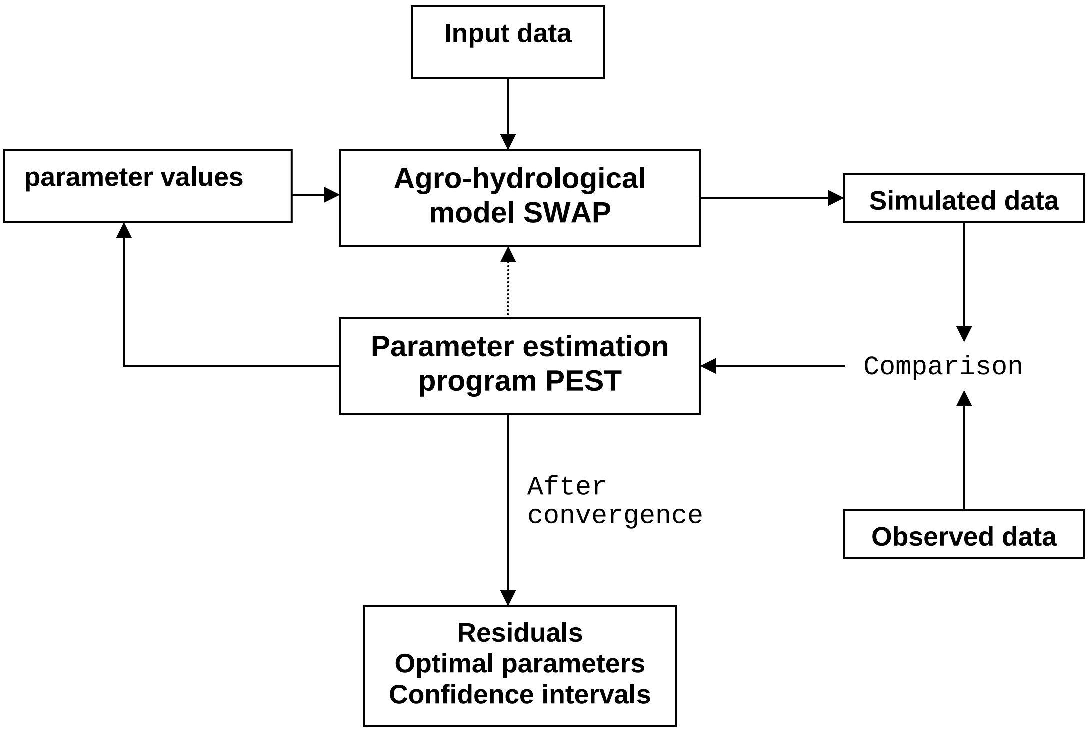

Figure 6.3. Communication between SWAP and PEST during parameter calibration (*source: Singh, 2005*).

PEST uses the Levenberg-Marquardt algorithm to find an optimal parameter set which minimizes the differences between model results and observations, using the following objective function Φ(b):

$$\Phi(b) = \sum_{j=1}^{m}\left[\sum_{i=1}^{n_j}\left(\frac{y_j^*(t_i) - y_j(b,t_i)}{w_j}\right)^2\right] \tag{6.10}$$

Where b is the vector with fitting parameters $y_j^*(t_i)$ denotes the observation of type j at time t_i, $y_j(b,t_i)$ is the corresponding model prediction, and w_j is the weighting factor. In case of random observation errors only, according to maximum likelihood the weighting factor w_j should be equal to the standard deviation of the observation error of observation type j. Since we have only one observation type in our optimization process the objective function does decrease to equation 6.11:

$$\Phi(b) = \sum_{i=1}^{N} \left[\theta_{obs}(t_i) - \theta_{sim}(b,t_i)\right]^2 \tag{6.11}$$

Where $\theta_{obs}(t_i)$ is the observed soil moisture content at time t_i, N is the number of observations, and $\theta_{sim}(b,t_i)$ is the simulated values of soil moisture using an array with parameter values *b* at time t_i. In comparing the observed with simulated soil moisture values, the observations for the 0-20 and 20-40 layers match the layers used the model. The observations for the 40-60 and 60-80 layers were averaged to match the 40-80 cm layer in the model.

Another parameter to measure model performance that we considered along with Φ (but not used in the optimization) is the correlation coefficient between observed an predicted values (R). This is calculated by

$$R = \frac{\sum_{i=1}^{N} \left[\left(\theta_{obs}(t_i) - \overline{\theta_{obs}}\right) - \left(\theta_{sim}(t_i) - \overline{\theta_{sim}}\right)\right]}{\sum_{i=1}^{N} \left(\theta_{obs}(t_i) - \overline{\theta_{obs}}\right)^2 . \sum_{i=1}^{N} \left(\theta_{sim}(t_i) - \overline{\theta_{sim}}\right)^2} \tag{6.12}$$

Where $\overline{\theta_{obs}}$ and $\overline{\theta_{sim}}$ are mean values of observed and simulated soil moisture contents, respectively. The correlation coefficient is more frequently reported in calibration studies than Φ, hence the inclusion of this parameter allows a better comparison of our results with other studies.

To evaluate performance of the model and uniqueness of optimized parameters set we used two calibration – validation schemes. In the first scheme we used the first part of the available data for every tube (all observations before 5 February) for calibration and the second part of the data (all data after 5 February) for validation. This calibration scheme is similar to that applied by Singh (2005). In the second scheme we chose every other one observation as a calibration set and the remaining ones as a validation set. It is generally believed that the fist is a more appropriate test for a model which leads to higher prediction errors for the validation set (McCuen and Snyder, 1986). Given that all model states occur more or less random in time (at least at a monthly time-scale), the first represents an extrapolation scheme, whereas the second is an interpolation scheme. We will label the two schemes as 'extrapolation' and 'interpolation'. For both calibration-validation schemes the initial parameter values were randomly chosen from a hypercube around the prior parameter set to evaluate whether the results were unique.

6.2.6 Evaluation of simulation quality

There are different criteria for evaluation of a model performance. A review of some recent the soil moisture simulation literature (Hymer et al., 2000; Mapfumo et al., 2004; Wegehenkel, 2005) indicates that three criteria have been used most frequently. These are the root mean squared error (RMSE), the index of agreement (IA) (Willmott, 1981), and the Nash-Sutcliffe (NS) coefficient (Nash and Sutcliffe, 1970). However for evaluation of SWAP results, usually the RMSE has been used (Singh, 2005; Crescimanno and Garofalo, 2005). In this paper all these criteria are evaluated. The equations for the evaluation criteria are as follows.

$$EF_{NS} = \left(\frac{\sum_{i=1}^{N} (\theta_{obs} - \bar{\theta}_{obs})^2 - \sum_{i=1}^{N} (\theta_{sim} - \theta_{obs})^2}{\sum_{i=1}^{N} (\theta_{obs} - \bar{\theta}_{obs})^2} \right) \tag{6.13}$$

$$EF_{IA} = 1 - \frac{\sum_{i=1}^{N} (\theta_{sim} - \theta_{obs})^2}{\sum_{i=1}^{N} \left[\left| \theta_{sim} - \bar{\theta}_{sim} \right| + \left| \theta_{obs} - \bar{\theta}_{obs} \right| \right]^2} \tag{6.14}$$

$$RMSE = \sqrt{\frac{\sum_{i=1}^{N} (\theta_{sim} - \theta_{obs})^2}{N}} \tag{6.15}$$

Where $\bar{\theta}_{sim}$ and $\bar{\theta}_{obs}$ are the mean values of the simulated and measured values, respectively. The range of IA is between 0 and 1, and the closer it is to 1, the better is the fit between measured and simulated model outputs.

6.2.7 The relation between level of aggregation and model performance

After evaluation of the model performance for each individual tube (coded as AggL0). The performance of the model was evaluated at three different aggregation levels. In the first aggregation level (AggL1) the tubes located in each field were put in the same group. There were at most two tubes in each field. For the second aggregation level (AggL2) the tubes with the same land use were put in one group. We assumed three different land use types: *Cropland*, *Grassland* and *Orchard*. At the third aggregation level (AggL3) all 15 tubes were put in one group. Values were aggregated separately for each layer. At the aggregate levels 1, 2, and 3, the layer-specific values used for the model calibration are the average values of the point measurements within each aggregation level. Thus, the model calibration to each aggregate level mimics the calibration to increasingly larger measurement scales. The depth-specific average across an aggregation level is a substitute for larger scale measurements, e.g., remote sensing data with a resolution equal to the larger, aggregated level.

6.3 Results

6.3.1 General

The many calibration-validation runs that were made in this study led to a large number of time series of predicted versus observed soil moisture. Typical results are shown in Figures 6.4 to 6.7. Figure 6.4 shows results for the unaggregated data (only the values for the upper soil layer of the four tubes in the orchards are shown). Figure 6.5 shows the predictions per field along (AggL1) with the unaggregated observations. Figure 6.6 shows the predictions per land-use (orchard in this case), and Figure 6.7 shows the predictions for the entire catchment. In this case the extrapolation scheme was applied (i.e. the period till 5 February was used for calibration and the remaining period was used for validation). As expected, the model error is slightly smaller in the calibration period then in the validation period. Also, the model error increases with aggregation level. The graphs clearly indicate that it will be very hard if not impossible to relate predictions at aggregation levels AggL2 and AggL3 to point observations. Figures 6.4 to 6.7 are merely used as an illustration of the results and the complexity of the multivariate output (different time instants, different soil layers, different aggregation levels). The full complexity is not shown because several land uses and other soil layers are omitted.

6.3.2 Calibration and parameter uniqueness

As stated in the method section, two strategies were evaluated to decrease the number of parameters for optimization. Both strategies showed that optimization with α and n for each soil layer gives the best results. For the first strategy the least sensitive parameter in at least one of the soil layers was saturated hydraulic conductivity (K_{sat}) in 70 % of the cases. Our initial hypothesis was that this low sensitivity of SWAP to K_{sat} could be attributed to the use of daily mean rainfall intensity as an input to the model. However, a test with rainfall data at a fine resolution led to the same (low) sensitivities for K_{sat}, and hence we found no supporting evidence for this hypothesis. Also De Roo et al. (1996) investigated the sensitivity to $K(\theta)$ for the Catsop catchment (using the Lisem model) and also noted the relatively low sensitivities of model output to K_{sat} (a 60 % model change due to 20 % of K_{sat}).

In the second strategy the objective function (Φ, equation 6.10) was minimized for the calibration period, while only changing combinations of two parameters. The optimization process with the combination of α and K_{sat} for each soil layer did lead to the worst result. These two parameters also appeared to be very strongly correlated. Probably an approach using scale factors (which are related to the hydraulic parameters) as in Rockhold et al. (1996) and Zhang et al. (2004) would have led to better results. With our present calibration schemes the best results were obtained for the combination of α and *n*. The results for the combination of *n* and K_{sat} were for most of the tubes comparable with the results of combining α and *n*. But the standard deviation of K_{sat} was generally much higher than that of α. Also, the relative sensitivity of K_{sat} was lower. Therefore we calibrated six parameters: α1, *n*1 (the first layer),α2, *n*2 (the second layer), α3 and *n*3 (the third layer). The values of K_{sat} were obtained from Ritsema et al. (1996) and Stolte et al. (1994). When calibrating with these six parameters, up to 20% uncorrelated Gaussian noise to the initial parameter values (by random selection within a hypercube) did always lead to the same optimal parameter sets. Adding a 5% uncorrelated Gaussian noise to the soil moisture observations and the rainfall data did lead to only minor changes in the parameter values. Hence our choice to represent the optimal parameter sets as a unique set rather than a parameter range seems to be justified. Apparently the information content of the observations in different soil layers, together with the objective function (eq. 6.11) lead to a unique optimum. Notwithstanding this result we do consider the optimal parameter sets as a realization from a joint probability distribution rather than some fixed value. The reason why we nonetheless represent the parameter sets as unique values in this study is to limit the complexity of our analysis.

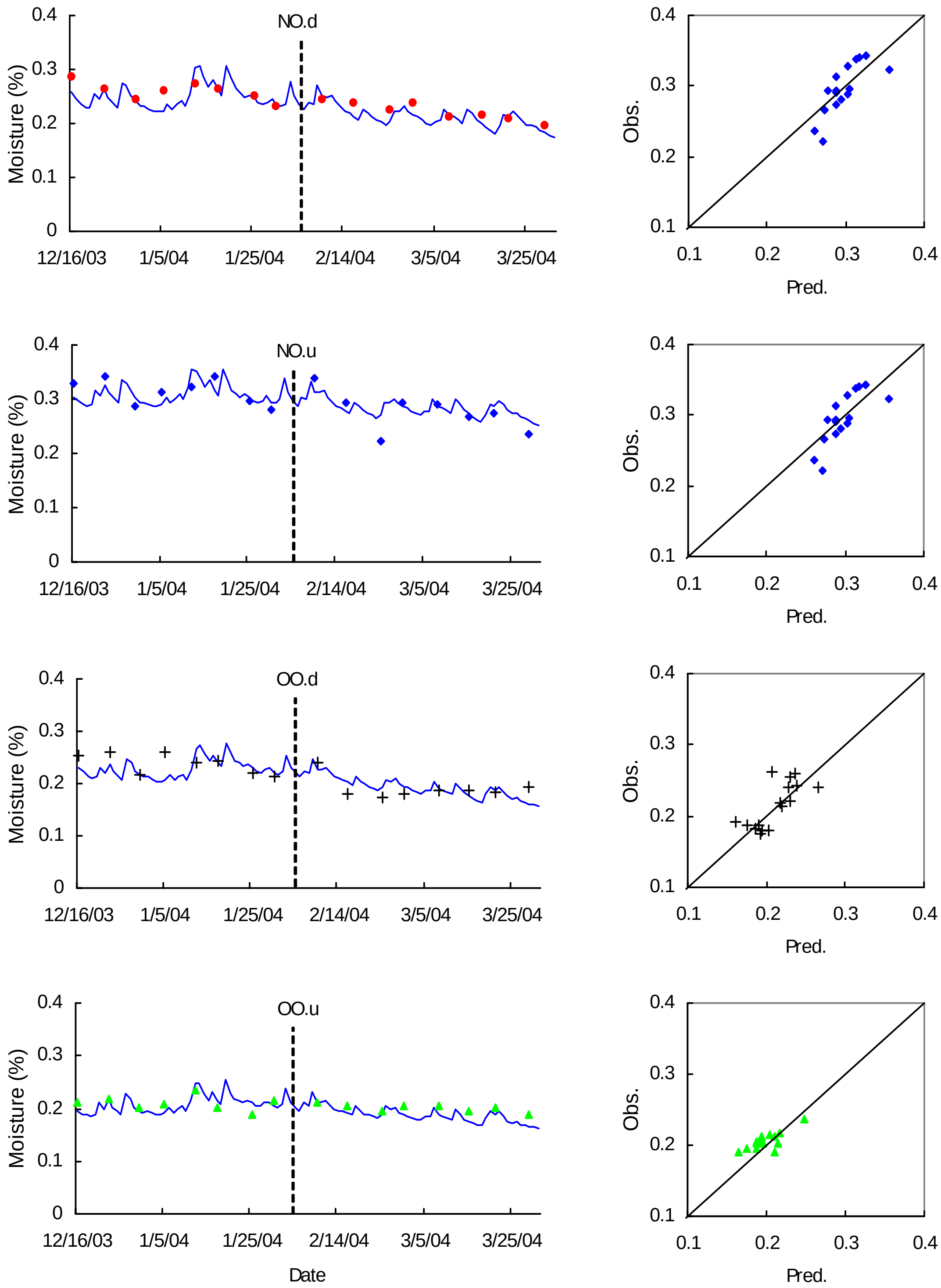

Figure 4. Comparison of observed and predicted soil moisture in the top layer (0 – 20 cm) for tubes within orchards for unaggregated observations and predictions (AggL0). The graphs in the left column show time series of observations (symbols) and predictions (lines). The vertical line in each time series separates calibration (left side) and validation (right side) period. The graphs in the right column show a scatter graph of observation versus predictions.

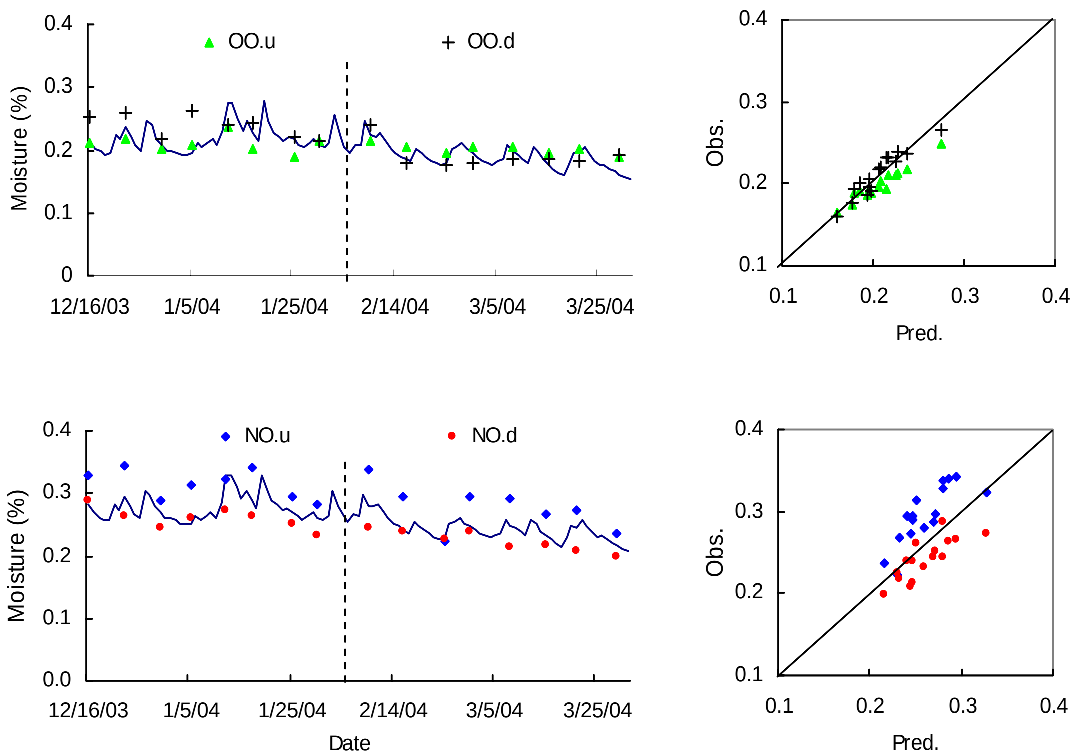

Figure 6.5. Comparison of observed and predicted soil moisture in the top layer (0 – 20 cm). Observations are unaggregated and predictions are for AggL1. For further explanation see caption of Figure 6.4.

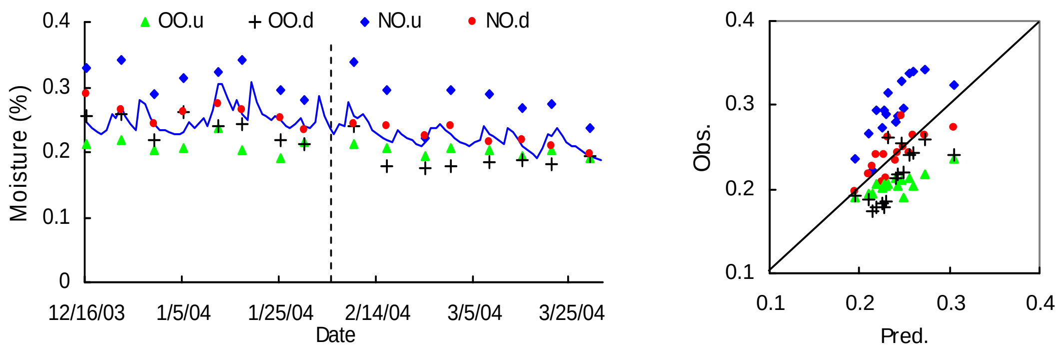

Figure 6.6. Comparison of observed and predicted soil moisture in the top layer (0 – 20 cm). Observations are unaggregated and predictions are for AggL2. For further explanation see caption of Figure 6.4.

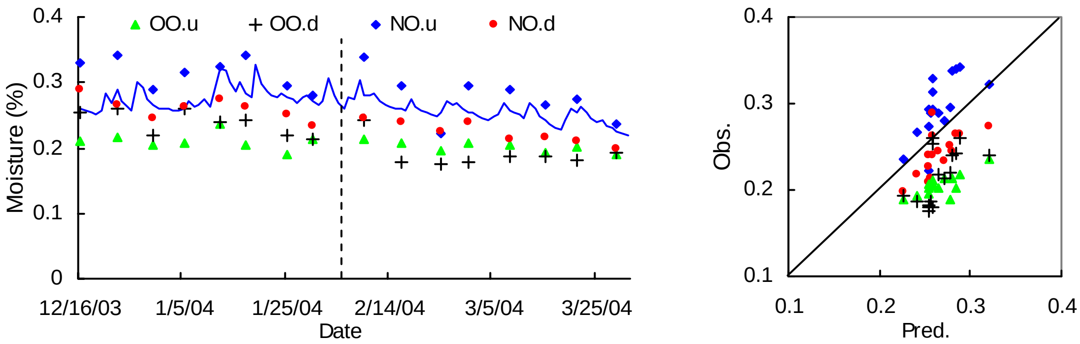

Figure 6.7. Comparison of observed and predicted soil moisture in the top layer (0 – 20 cm). Observations are unaggregated and predictions are for AggL3. For further explanation see caption of Figure 6.4.

6.3.3 The effect of different validation schemes

The rationale for evaluating two different validation schemes (viz. extrapolation and interpolation) was to answer the question to what degree a validation scheme influences model performance. The two schemes chosen in this study are in fact the most extreme examples for extrapolation and interpolation. We therefore do expect that the results generalize to intermediate cases. Both schemes used the same initial conditions, parameter values and optimization routine. The resulting parameter sets and performance statistics are indeed different for the two schemes (see Tables 6.2 and 6.3). In the interpolation scheme, Φ and R are more similar between calibration and validation than in the extrapolation scheme.

In fact, for interpolation there is no significant difference in Φ and R between calibration and validation (evaluated with a paired T-test), whereas for extrapolation there is a significant difference ($p<0.05$). Also the parameter values across the soil layers did show a more regular pattern for interpolation than for extrapolation. However, the model performance for the extrapolation scheme (considering validation Φ and R) is somewhat better than for interpolation (significant at the 0.05 level, according to a paired T-test). The almost equal performance for calibration – validation via interpolation or extrapolation is somewhat counter-intuitive. It is generally assumed that interpolation should lead to higher model performance than extrapolation, especially in a situation where some boundary conditions (like temperature and rainfall pattern in our system) and system states (hydraulic properties of the top layers) change considerably over the time scale of a few months (see Ritsema et al., 1996). Our explanation for this result in our study is that the observation frequency for the interpolation scheme (observation times more than ten days apart) is too low to capture the essential dynamics of a dry-down cycle. With higher observation-frequencies we would expect better performance indices for the interpolation scheme than the extrapolation scheme.

Table 6.2. Soil hydraulic parameter values (ϴsat, α, n, λ, Ksat, see eqs. 6.2 and 6.3) after optimization according to the extrapolation calibration-validation procedure. Φ is the optimization criterion to be minimized (eq. 6.10 and 6.11), R is the correlation coefficient between observed and predicted soil moisture (eq. 6.12).

							calibration		validation	
Tube	**Layer**	**Θ_{sat}**	**α**	***n***	**λ**	**K_{sat}**	**Φ**	**R**	**Φ**	**R**
CST.d	1 2 3	0.414 0.392 0.402	0.0024 0.0034 0.0010	1.438 1.860 1.245	0 0 -1.17	2.533 0.585 11.44	0.0351	0.800	0.0193	0.904
CST.u	1 2 3	0.414 0.392 0.402	0.0047 0.0213 0.0044	1.874 1.317 1.861	0 0 -1.17	2.533 0.585 11.44	0.0170	0.964	0.0207	0.963
CVT.d	1 2 3	0.435 0.392 0.402	0.0019 0.0081 0.0011	2.755 1.317 1.929	0 0 -1.17	2.533 0.585 11.44	0.0069	0.988	0.0185	0.954
CVT.u	1 2 3	0.435 0.392 0.402	0.0010 0.0010 0.0089	1.349 1.329 1.943	0 0 -1.17	2.533 0.585 11.44	0.0273	0.958	0.0301	0.944
Gr.d	1 2 3	0.420 0.392 0.402	0.0011 0.0018 0.0010	1.327 1.752 1.343	0 0 -1.17	0.944 0.955 11.44	0.0635	0.818	0.0652	0.795
Gr.u	1 2 3	0.420 0.392 0.402	0.0135 0.0010 0.0016	1.476 1.505 1.867	0 0 -1.17	0.944 0.955 11.44	0.0364	0.909	0.0845	0.802
Gr.g	1 2 3	0.420 0.392 0.402	0.0204 0.0010 0.0021	1.348 1.628 1.297	0 0 -1.17	0.050 0.955 11.44	0.0302	0.838	0.0403	0.658
NO.d	1 2 3	0.350 0.392 0.402	0.0046 0.0032 0.0011	1.341 1.556 1.295	0 0 -1.17	9.74 0.955 11.44	0.0426	0.678	0.0383	0.754
NO.u	1 2 3	0.350 0.392 0.402	0.0010 0.0139 0.0039	2.950 1.612 1.507	0 0 -1.17	9.74 0.955 11.44	0.0111	0.874	0.0177	0.765
OO.d	1 2 3	0.350 0.392 0.402	0.0051 0.0028 0.0066	1.922 2.720 1.990	0 0 -1.17	9.74 0.955 11.44	0.0124	0.837	0.0122	0.750
OO.u	1 2 3	0.350 0.392 0.402	0.0019 0.0010 0.0011	1.383 1.886 1.963	0 0 -1.17	9.74 0.955 11.44	0.0080	0.749	0.0203	0.727
WW.n	1 2 3	0.365 0.392 0.402	0.0012 0.0010 0.0010	1.560 1.424 1.833	0 0 -1.17	1.00 0.585 11.44	0.0348	0.858	0.0594	0.841
WW.s	1 2 3	0.365 0.392 0.402	0.0037 0.0010 0.0010	1.612 1.374 1.886	0 0 -1.17	1.00 0.585 11.44	0.0371	0.741	0.1200	0.640
YM.d	1 2 3	0.360 0.392 0.402	0.0017 0.0032 0.0056	1.511 1.779 1.684	0 0 -1.17	3.010 0.955 11.44	0.0171	0.830	0.0151	0.838
YM.u	1 2 3	0.360 0.392 0.402	0.0024 0.0013 0.0022	1.055 1.795 1.491	0 0 -1.17	3.010 0.955 11.44	0.0208	0.810	0.0317	0.849

Table 6.3. Soil hydraulic parameter values (Θ_{sat}, α, *n*, λ, K_{sat}, see eqs. 6.2 and 6.3) after optimization according to the interpolation calibration-validation procedure. Φ is the optimization criterion to be minimized (eq. 6.10 and 6.11), R is the correlation coefficient between observed and predicted soil moisture (eq. 6.12)

							calibration		validation	
Tube	**Layer**	**Θ_{sat}**	**α**	***n***	**λ**	**K_{sat}**	**Φ**	**R**	**Φ**	**R**
CST.d	1	0.414	0.0034	1.718	0	2.533	0.0321	0.780	0.0366	0.814
	2	0.392	0.0039	1.650	0	0.585				
	3	0.402	0.0010	1.265	-1.17	11.44				
CST.u	1	0.414	0.0079	1.476	0	2.533	0.0184	0.954	0.0302	0.923
	2	0.392	0.0076	1.329	0	0.585				
	3	0.402	0.0036	1.992	-1.17	11.44				
CVT.d	1	0.435	0.0010	2.755	0	2.533	0.0343	0.921	0.0329	0.920
	2	0.392	0.0051	1.329	0	0.585				
	3	0.402	0.0010	1.958	-1.17	11.44				
CVT.u	1	0.435	0.0015	1.354	0	2.533	0.0191	0.974	0.0331	0.942
	2	0.392	0.0010	1.292	0	0.585				
	3	0.402	0.0120	2.030	-1.17	11.44				
Gr.d	1	0.420	0.0028	1.415	0	0.944	0.1030	0.685	0.1030	0.681
	2	0.392	0.0027	1.729	0	0.955				
	3	0.402	0.0010	1.409	-1.17	11.44				
Gr.u	1	0.420	0.0040	1.397	0	0.944	0.0777	0.745	0.0561	0.821
	2	0.392	0.0010	1.663	0	0.955				
	3	0.402	0.0017	1.865	-1.17	11.44				
Gr.g	1	0.420	0.0254	1.352	0	0.050	0.0480	0.727	0.0713	0.658
	2	0.392	0.0011	1.627	0	0.955				
	3	0.402	0.0017	1.304	-1.17	11.44				
NO.d	1	0.350	0.0061	1.495	0	9.74	0.0492	0.668	0.0551	0.621
	2	0.392	0.0082	1.558	0	0.955				
	3	0.402	0.0021	1.339	-1.17	11.44				
NO.u	1	0.350	0.0043	1.230	0	9.74	0.0193	0.785	0.0291	0.598
	2	0.392	0.0105	1.600	0	0.955				
	3	0.402	0.0029	1.572	-1.17	11.44				
OO.d	1	0.350	0.0047	1.465	0	9.74	0.0241	0.671	0.0208	0.626
	2	0.392	0.0012	1.813	0	0.955				
	3	0.402	0.0017	1.966	-1.17	11.44				
OO.u	1	0.350	0.0052	1.704	0	9.74	0.0148	0.590	0.0101	0.650
	2	0.392	0.0027	1.499	0	0.955				
	3	0.402	0.0017	1.966	-1.17	11.44				
WW.n	1	0.365	0.0012	1.803	0	1.00	0.0740	0.667	0.0808	0.670
	2	0.392	0.0010	1.489	0	0.585				
	3	0.402	0.0010	2.012	-1.17	11.44				
WW.s	1	0.365	0.0031	1.805	0	1.00	0.0558	0.665	0.0527	0.687
	2	0.392	0.0012	1.516	0	0.585				
	3	0.402	0.0011	1.989	-1.17	11.44				
YM.d	1	0.360	0.0012	1.488	0	3.010	0.0189	0.819	0.0254	0.757
	2	0.392	0.0029	1.657	0	0.955				
	3	0.402	0.0044	1.713	-1.17	11.44				
YM.u	1	0.360	0.0010	1.448	0	3.010	0.0224	0.882	0.0242	0.845
	2	0.392	0.0058	1.659	0	0.955				
	3	0.402	0.0077	1.573	-1.17	11.44				

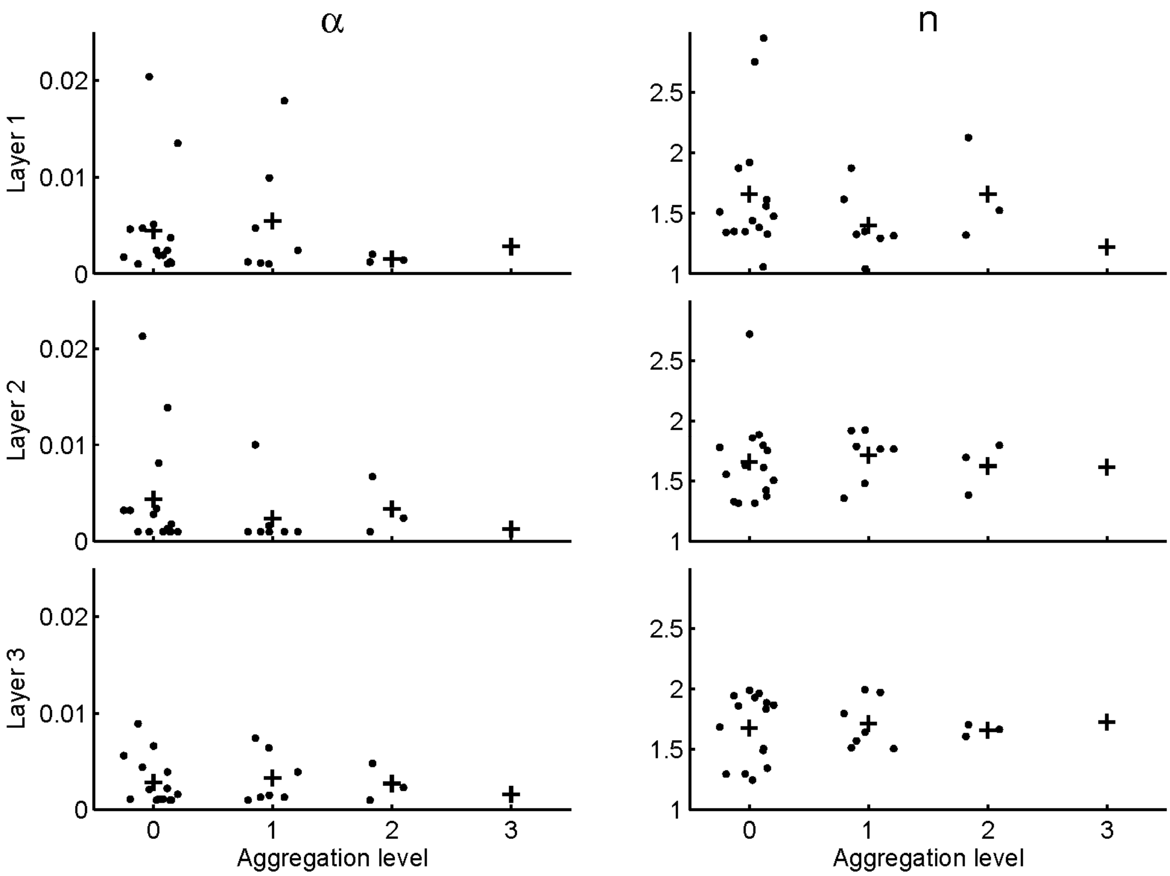

Figure 6.8. The values of Mualem-Van Genuchten parameters α and n per layer for different aggregation levels. Each dot is a parameter value for a particular land-unit, each + represents the mean of the parameter values per aggregation level. The dots are jittered per aggregation level to distinguish the individual parameter values. The parameter values for aggregation level 0 correspond with the values in Table 6.2.

6.3.4 Parameter values across scales

Very little structure is seen in the parameter values when moving from point to catchment scales. When moving from lower to higher aggregation levels, the parameter values change in a more or less random fashion, whereby the ordering over layers is not related between aggregation levels. The change of parameter values across scales is shown in Figure 6.8. The difference between parameter values from a lower to a higher aggregation level is in all cases insignificant (tested with pairwise Mann-Whitney U tests). Stated differently: the mean parameter values obtained at a lower aggregation level were in all cases quite close to the values obtained at a higher aggregation level. This result is similar to that in studies by Pachepsky and Rawls (1999) and Zhu and Mohanty (2002).

6.3.5 Relations between the different performance indices

Our study confirms that using only one index to evaluate model performance does not give a comprehensive view (Willmott, 1981; Legates and McCabe, 1999; McCuen and Snyder, 1986; Krause et al. 2005). This is illustrated by the apparent absence of a relation between *R* and Φ (see Tables 6.2 and 6.3) as well as EF_{IA}, EF_{NS}, and RMSE (Table 6.4 and Figure 6.9). In Table 6.4 and Figure 6.9 the statistics for each layer, the mean over four layers, and the mean over four layers and all observation times are given per observation location. Especially the Nash-Sutcliffe coefficient does sometimes deviate from the other statistics (see f.i. the indices for land use *OO.u and CVT.u* in Table 6.4). Considering the three evaluation criteria together, it is quite difficult to judge about the performance of the SWAP model for individual layers. However, with respect to the EF_{IA} values alone, the model gives consistently better results for the first layer. We attribute this to the fact that in deeper soil layers there are larger influences from lateral flows than in the top layer (while SWAP is a 1D model that does ignore any lateral flows). When considering soil layers separately, EF_{IA} and EF_{NS} are somewhat related, whereas RMSE is unrelated to the other two statistics. Strikingly, the relation between EF_{IA} and EF_{NS} becomes much stronger upon averaging, whereas a relation with RMSE remains absent (see Figure 6.9). We did not find any information about relations between performance indices under influence of aggregation level in the hydrological literature. Considering all three evaluation criteria, the quality of the model predictions would not be satisfactory when considering the separate layers, in 73 % of the cases either the EF_{IA} or the EF_{NS} coefficient is less than 0.50. However, when considering the averaged data, model predictions would be judged as sufficient. Apparently the evaluation criteria are only meaningful at a specific scale. When considering the RMSE alone it seems to agree well with the results of previous studies. The SWAP study by Singh (2005) reported an RMSE that varied between 0.016 and 0.033 for different layers till 3 m down. Crescimanno and Garofalo (2005), using Mualem-Van Genuchten equations (Mualem, 1976; Van Genuchten, 1980) reported RMSE ranges of 0.037 – 0.101 and 0.035 – 0.078 at soil depths of 30 and 45 cm, respectively. Mertens et al. (2005), using soil moisture measurements at 25 locations at three different depths (at the surface, at 30 and 60 cm depth) on an 80 by 20 m hillslope, reported RMSE values ranging from 0.041 to 0.089 when applying the MIKE-SHE model. Heathman et al. (2003), comparing the simulation results of the RZWQM model with soil moisture data from different depths up to 60 cm, found that RMSE ranges from 0.016 to 0.097. In a validation study of the THESEUS model in Germany, Wegehenkel (2005) obtained RMSE ranges of 0.030 – 0.043, 0.028 – 0.030, and 0.026 – 0.049 for layer 1 (0 – 30 cm), layer 2 (30 – 60 cm), and layer 3 (60 – 90 cm), respectively. While the current study resulted in RMSE ranges of 0.015 – 0.045, 0.016 – 0.040, 0.012 – 0.050 and 0.011 – 0.051 for layers 1 (0 – 20 cm), 2 (20 – 40 cm), 3 (40 – 60 cm) and 4 (60 – 80 cm) respectively.

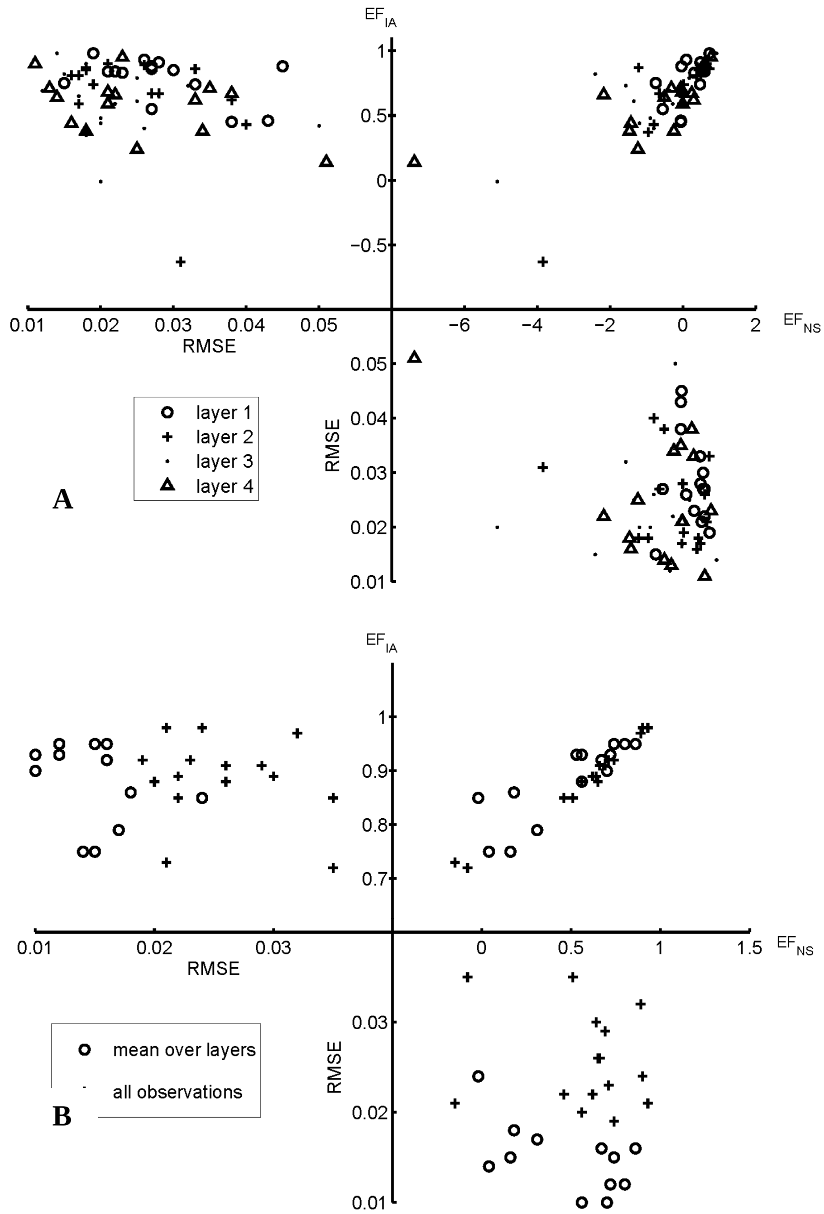

Figure 6.9. Relation between RMSE, EF_{IA} and EF_{NS} in the form of three 2D projections (a graphical representation of Table 6.4) for the separate soil layers (upper axis, A); and for two different averages over soil layers (lower axis, B). One outlier (OO.u) is omitted from B for display purposes.

6.3.6 The relation between level of aggregation and model performance

After evaluation of the model performance for each individual tube (AggL0), it was repeated at three different aggregation levels. In the first aggregation level (AggL1) the tubes located in each field were put in the same group. There were at maximum two tubes in each field. For the second aggregation level (AggL2) the tubes with the same land use were put in one group. We assumed three different land use types: *Cropland, Grassland,* and *Orchard*.

Table 6.4. The values of several error criteria of soil moisture prediction (RMSE, EF_{IA} and EF_{NS}, see eq. 6.13 – 6.15) per measurement location and layer, using the extrapolation calibration-validation scheme. Although our model distinguishes three layers, we distinguish four layers when considering the error criteria because there are separate observations for layer 3 (40 – 60 cm) and 4 (60 – 80 cm).

	Layer 1			Layer 2			Layer 3			Layer 4			Mean of layers†			All observations‡		
Tube	**RMSE**	**EF_{IA}**	**EF_{NS}**	**RMSE**	**EF_{IA}**	**EF_{NS}**	**RMSE**	**EF_{IA}**	**EF_{NS}**	**RMSE**	**EF_{IA}**	**EF_{NS}**	**RMSE**	**EF_{IA}**	**EF_{NS}**	**RMSE**	**EF_{IA}**	**EF_{NS}**
CST.d	0.026	0.93	0.09	0.028	0.67	-0.01	0.028	0.65	-0.08	0.034	0.038	-0.25	0.012	0.93	0.72	0.029	0.91	0.69
CST.u	0.038	0.45	-0.06	0.018	0.87	-1.22	0.020	0.48	-0.90	0.013	0.71	-0.32	0.008	0.93	0.53	0.024	0.98	0.90
CVT.d	0.033	0.74	0.47	0.017	0.59	-0.03	0.012	0.69	-0.36	0.016	0.44	-1.43	0.008	0.88	0.56	0.021	0.98	0.93
CVT.u	0.045	0.88	-0.04	0.038	0.62	-0.52	0.015	0.82	-2.41	0.018	0.38	-1.47	0.010	0.93	0.56	0.032	0.97	0.89
Gr.d	0.028	0.91	0.48	0.027	0.67	-0.65	0.025	0.79	0.17	0.038	0.67	0.24	0.012	0.95	0.80	0.030	0.89	0.64
Gr.u	0.030	0.85	0.55	0.040	0.43	-0.80	0.025	0.61	-1.35	0.022	0.66	-2.18	0.018	0.86	0.18	0.023	0.92	0.71
Gr.g	0.023	0.83	0.31	0.018	0.37	-0.96	0.026	0.40	-0.80	0.021	0.68	-0.03	0.015	0.75	0.16	0.022	0.85	0.46
NO.d	0.019	0.98	0.73	0.033	0.86	0.72	0.050	0.42	-0.21	0.033	0.62	0.29	0.016	0.95	0.86	0.035	0.85	0.51
NO.u	0.022	0.84	0.59	0.017	0.81	0.48	0.017	0.65	-0.01	0.021	0.59	-0.01	0.010	0.90	0.70	0.019	0.92	0.74
OO.d	0.021	0.84	0.51	0.018	0.85	0.42	0.014	0.98	0.92	0.023	0.95	0.77	0.015	0.95	0.74	0.020	0.88	0.56
OO.u	0.015	0.75	-0.75	0.031	-0.63	-3.85	0.020	-0.01	-5.10	0.014	0.64	-0.51	0.018	0.07	-6.75	0.021	0.73	-0.15
WW.n	0.027	0.86	0.55	0.021	0.90	0.65	0.018	0.90	0.38	0.035	0.71	-0.06	0.016	0.92	0.67	0.026	0.91	0.66
WW.s	0.027	0.88	0.59	0.026	0.89	0.60	0.032	0.73	-1.57	0.051	0.14	-7.38	0.024	0.85	-0.02	0.035	0.72	-0.08
YM.d	0.027	0.55	-0.56	0.016	0.81	0.38	0.020	0.44	-1.20	0.025	0.24	-1.24	0.014	0.75	0.04	0.022	0.89	0.62
YM.u	0.043	0.46	-0.06	0.019	0.74	0.02	0.022	0.59	-0.28	0.011	0.90	0.60	0.017	0.79	0.31	0.026	0.88	0.65

†Average of four layers was used as the mean moisture content for each tube. ‡ Each observation within a profile (four for each measurement date) is used as a unique observation for the profile and compared with the counterpart simulated value.

In the third aggregation level (AggL3) all tubes were put in one group. For every group, the observed soil moisture content of each layer is the average of the corresponding layer of the included tubes in the group. For the comparison across different aggregation levels we use only RMSE as a performance measure (EF_{NS} and EF_{IA} did show a behavior similar to RMSE for aggregation).

Like the optimization process for individual tubes, the initial values of the parameters per aggregation level were obtained from literature according to soil type and land management practices. Since the tubes in each group of AggL1 have the same soil type and land management practices the initial values of the parameters were in this case the same as optimization process with individual tubes. In AggL2 both the soil type and land management practices were different only for the tubes included in the *Cropland* group. For this group, the optimization process started with the initial parameter values which had been used for the tube CST.u at AggL1 because its parameter values were intermediate all other tubes in this group. Evapotranspiration differences between crop types did not play a role since the study period data covers the winter (transpiration is negligible and evaporation is the same for all tubes in this group).

In AggL3 the contemporary measured soil moisture content of all tubes for each layer were averaged and used as observation values. Initial values of the parameters were obtained by averaging the initial values of the parameters for each individual tube. For calculating the evapotranspiration rate in this aggregation level, grass was used a representative land use type. The results of the different aggregation levels are presented in Tables 6.5 and 6.6. Table 6.5 shows the RMSE of the simulation results when they are compared to the aggregated soil moisture values for each group. Table 6.6 presents the RMSE values of the simulated moisture content for each group when compared to the measured ones of each individual tube in the related group. As expected, the RMSE values for each group (on the basis of the average of observed soil moisture for each group) are lower than the RMSE values for each individual tube (see also Figures 6.4 to 6.7). The ranges of RMSE values for the three layers were 0.009-0.037, 0.006-0.025, and 0.009-0.025 ($cm^3.cm^{-3}$) for AggL1, AggL2, and AggL3 respectively. These results are quite comparable with those found in other studies. For instance Crow et al. (2005) found that RMSE of spatially averaged predicted soil moisture content decreased from 0.043 to 0.032 ($cm^3.cm^{-3}$) when compared to spatially averaged measured soil moisture content of field and regional scale, respectively (measuring and modeling soil moisture in the 0-6 cm surface layer). On the other hand, when comparing measured soil moisture of each individual tube with the simulated soil moisture of the pertinent group at different aggregation levels indicates that by increasing the aggregation level the RMSE increases too (Table 6.6). The ranges of the RMSE for all layers are 0.011 – 0.051, 0.015 – 0.12, 0.018 – 0.174, and 0.015 – 0.181 (cm^3 cm^{-3}) for AggL0, AggL1, AggL2, and AggL3, respectively.

Table 6.5. The RMSE of soil moisture predictions at different aggregation levels and per layer, using the extrapolation calibration-validation scheme. The measured values are averaged before calculating the RMSE.
.

Agg. group	Agg. level	Layer1	Layer2	Layer3	Layer4	Mean
Conservation tillage	AggL1	0.027	0.019	0.016	0.016	0.009
Conventional tillage	AggL1	0.037	0.020	0.015	0.019	0.007
Grass	AggL1	0.025	0.029	0.016	0.027	0.015
New orchard	AggL1	0.017	0.019	0.026	0.021	0.011
Old orchard	AggL1	0.017	0.018	0.016	0.017	0.014
Yellow mustard	AggL1	0.026	0.016	0.021	0.031	0.012
Winter wheat	AggL1	0.030	0.020	0.017	0.018	0.017
Cropland	AggL2	0.025	0.008	0.010	0.016	0.006
Grassland	AggL2	0.025	0.020	0.015	0.019	0.011
Orchard	AggL2	0.015	0.017	0.014	0.022	0.012
Catchment	AggL3	0.016	0.009	0.014	0.025	0.012

The degree of change in the RMSE is not equal for all soil layers. Layers 1 and 4 show relatively large changes in the RMSE values. Layer 2 shows the least changes. We think that high changes in the first layer are related to land use type and land management practices while the high changes in the fourth layer are related to the effect of the topography. To illustrate this last point, the RMSE values of the *CST.d* and *CST.u* tubes for AggL1 and AggL0 can be compared compared with the RMSE of the *YM.d* and *YM.u* tubes. Topography of *CST.d* and *CST.u* (which have the same land use and land management practices) differs a lot while for the *YM.d* and *YM.u* it is comparable (see Table 6.1). Table 6.1 shows that of *CST.d* is located in downstream part of a long hilslope and its catchment area (Uparea) is 4 times larger than *CST.u*. This might provoke the higher values of soil moisture content in the deeper layers of downhill tubes due to likely effects of lateral flow or re-infiltration of surface runoff I downstream areas. We think this explains that the RMSE values of *CST.d* and *CST.u* (especially for layer 3 and 4) are quite high for AggL1 in comparison to AggL0, while for *YM.d* and *YM.u* the RSME values are comparable. Beyond these qualitative considerations we were unable to relate RMSE (nor IE_{NS} or IE_{IA}) to its value at a lower (or higher) aggregation level and other explanatory variables with regression techniques. The explanatory variables used were those listed in Table 6.1 (land use, soil, slope steepness, upslope length, upslope area) and Table 6.2 (Θ_{sat} , α, n, λ, K_{sat} - all per layer as well as averaged over the three soil layers; calibration Φ, calibration R, validation Φ, and validation R). Both generalized linear regression (Mcullagh and Nelder, 1989) as well as generalized additive models (Hastie and Tibshirani, 1990) were used, while evaluating all combinations of the explanatory variables up to four dimensions.

Table 6.6. The RMSE of soil moisture predictions at different aggregation levels per layer using the extrapolation calibration-validation scheme. To calculate RMSE, the point scale measurements are used.

	AggL0 †				AggL1				AggL2				AggL3			
Tube	**layer 1**	**layer 2**	**layer 3**	**layer 4**	**layer 1**	**layer 2**	**layer 3**	**layer 4**	**layer 1**	**layer 2**	**layer 3**	**layer 4**	**layer 1**	**layer 2**	**layer 3**	**layer 4**
CST.d	0.026	0.028	0.028	0.034	0.043	0.046	0.074	0.120	0.077	0.036	0.0127	0.174	0.023	0.053	0.136	0.181
CST.u	0.039	0.015	0.020	0.013	0.052	0.025	0.085	0.095	0.031	0.034	0.037	0.046	0.089	0.017	0.027	0.34
CVT.d	0.033	0.017	0.012	0.016	0.049	0.066	0.017	0.022	0.035	0.052	0.047	0.046	0.090	0.035	0.037	0.036
CVT.u	0.045	0.038	0.015	0.018	0.042	0.052	0.016	0.019	0.051	0.065	0.050	0.053	0.121	0.082	0.040	0.043
Gr.d	0.028	0.027	0.025	0.038	0.031	0.031	0.055	0.110	0.026	0.022	0.061	0.100	0.039	0.024	0.067	0.126
Gr.u	0.030	0.040	0.026	0.021	0.028	0.041	0.052	0.058	0.032	0.047	0.044	0.050	0.037	0.020	0.043	0.049
Gr.g	0.023	0.018	0.026	0.021	0.041	0.047	0.045	0.033	0.035	0.038	0.037	0.024	0.055	0.064	0.035	0.024
NO.d	0.019	0.033	0.050	0.033	0.026	0.042	0.035	0.061	0.018	0.059	0.079	0.133	0.030	0.050	0.101	0.156
NO.u	0.022	0.017	0.017	0.021	0.040	0.024	0.036	0.040	0.061	0.019	0.046	0.044	0.039	0.018	0.068	0.066
OO.d	0.021	0.018	0.014	0.023	0.025	0.025	0.015	0.023	0.033	0.018	0.056	0.059	0.057	0.024	0.034	0.038
OO.u	0.015	0.031	0.020	0.014	0.019	0.023	0.020	0.014	0.038	0.032	0.054	0.056	0.062	0.035	0.033	0.033
WW.n	0.028	0.021	0.018	0.035	0.050	0.024	0.026	0.042	0.122	0.032	0.064	0.044	0.047	0.015	0.050	0.033
WW.s	0.027	0.026	0.032	0.051	0.043	0.021	0.024	0.036	0.145	0.036	0.065	0.051	0.065	0.025	0.052	0.039
YM.d	0.027	0.016	0.020	0.025	0.023	0.026	0.021	0.024	0.075	0.020	0.025	0.023	0.033	0.024	0.018	0.034
YM.u	0.040	0.022	0.030	0.017	0.045	0.022	0.023	0.015	0.076	0.035	0.021	0.021	0.061	0.025	0.030	0.027

†AggL0 stands for “no aggregation”, in this case simulation has been done for each tube separately.

6.4 Discussion and Conclusions

In the hydrologic literature, 1D Richards models are applied at all levels of aggregation that are encountered in this study, i.e. point scale (Mertens et al. 2005), field scale (Feddes et al. 1978; Ritsema et al. 1996), and more inhomogeneous response units (Heathman et al. 2003; Crow, 2005) . With these studies at various scales but a similar system conceptualization in mind, the question presents itself, why is it (still) so hard to compare results between these studies at different aggregation levels. To contribute in answering this intriguing question we have investigated model parameterisation and performance for a research catchment at various levels of aggregation.

In spite of the theoretical impossibility to derive effective parameters for the non-linear Richards equation by simple aggregation or disaggregation procedures (Kim and Stricker, 1986), many studies have ignored this fact and investigated the derivation of Mualem-Van Genuchten parameters by both aggregation and disaggregation (see e.g. Pachepsky and Rawls 1999; Zhu et al. 2006). These approaches have been stimulated by the availability of parametric and non-parametric pedotransfer functions, which in most cases do not explicitly refer to an aggregation level for their application (e.g. Wösten et al. 1988; Pachepsky et al. 1996, Schaap et al. 1998). Our study does not assume any relation between parameter values at different levels of aggregation. However, the results do show that a simple averaging procedure would have worked for our study. The values for the Mualem-Van Genuchten parameters α and n at higher aggregation levels are very close to the arithmetic mean of these parameters at lower aggregation levels (K_s is omitted from this analysis because it was constrained at an early stage in the calibration procedure), see Figure 6.8. These results are in line with the recommendations by Zhu and Mohanty (2002). The approach in our study also differs in a few ways from the aforementioned 'effective parameter' studies. In the first place our study lacks any geostatistical component, whereas most effective parameter studies do consider spatially correlated fields of soil properties. Using this information about spatial heterogeneous soils 'effective parameter' studies normally focus on matching the steady-state vertical flow, whereas our study does not match an integrated flux but rather a set of distributed soil moisture observations. Finally, as stated previously, effective parameter studies assume some kind of analytical or statistical relation between soil hydraulic parameters at different levels of aggregation. On the basis of this distribution, effective values for hydraulic parameters are directly derived at another aggregation level, i.e. without recalibrating a model. In our study these hydraulic parameters are derived by calibration at each distinct aggregation level. Overall, we think our approach and the effective parameter approach are rather complementary in terms of analytic techniques, and hydrologic assumptions. Our study suggests that both approaches may in fact lead to similar conclusions or even similar effective parameter values. Such a comparative study has to our knowledge not been made and could add valuable insights to the current understanding of unsaturated zone hydrology.

Evaluation of model performance at multiple scales is rare. Our study shows, however, that studies of this type are in fact required to enable the inter-comparison between results from studies at different aggregation levels. Some frequently used performance measures (RMSE, Nash-Sutcliffe coefficient and Index of Agreement) do show a dependence on aggregation level, albeit a dependence that we were not able to fully explain or characterize in a simple manner. With higher aggregation levels the prediction error becomes smaller, but not in an equal manner for the various indices. Hence, the relation between the various indices changes with aggregation level.

Usually, the validation scheme as well as the parameter calibration procedure is also quite distinct between different modeling studies. This also complicates a comparison of results from different studies. To investigate the relative importance of these factors we varied the validation scheme (i.e. interpolation versus extrapolation) and the parameter optimization scheme (i.e. the procedure to select the subset of parameters to calibrate). The results lead to the conclusion that both the validation and the parameter optimization scheme do not significantly influence the results of model parameter values and performance at different aggregation levels. Overall, our study shows that different Mualem-Van Genuchten parameters are required when modeling at different scales, stressing what has already been concluded by others (Reynolds, 1974; Crow et al., 2005). However, it should be mentioned that nearly all studies focused, until now, only on the effects of aggregating soil moisture in the surface layer of limited depth (0 – 6 cm). The way in which the Mualem-Van Genuchten parameters change will depends very much on both observation and site characteristics.

The use of discharge data in addition to distributed soil moisture observations is an extension of the current study that deserves further investigation. In our framework, an additional integrative observation like discharge acts as a regularizing constant across aggregation levels. In the research catchment of this study discharge was measured only at one location. Hence the discharge record to be matched is the same for each aggregation level, and parameter values would therefore become more similar between aggregation levels. A more extensive data set with discharge observations at various locations in the stream network could lead to a more complex behaviour.

Chapter 7

A simple model to predict soil moisture: Bridging Event And Continuous Hydrological modelling (BEACH)

Vahedberdi Sheikh, Saskia Visser, Leo Stroosnijder
To be submitted to: Hydrological Processes

7 A simple model to predict soil moisture: Bridging Event And Continuous Hydrological modelling (BEACH)

Abstract
This paper introduces a simple two-layer soil water balance model developed to **B**ridge **E**vent **A**nd **C**ontinuous **H**ydrological (BEACH) modelling. BEACH is a spatially distributed daily basis hydrological model formulated to predict the initial condition of soil moisture for event- based soil erosion and rainfall–runoff models. The latter models usually require the spatially distributed values of antecedent soil moisture content and other input parameters at the onset of an event. BEACH uses daily meteorological records, soil physical properties, basic crop characteristics and topographical data. The basic processes incorporated in the model are precipitation, infiltration, transpiration, evaporation, lateral flow, vertical flow and plant growth. The principal advantage of this model lies in its ability to provide timely information on the spatially distributed soil moisture content over a given area without the need for repeated field visits. The application of this model to the CATSOP experimental catchment showed that it has the capability to estimate soil moisture content with acceptable accuracy. The root mean squared error of the predicted soil moisture content for 6 monitored locations within the catchment ranged from 0.011 to 0.065 cm^3 cm^{-3}. The predicted daily discharge at the outlet of the study area agreed well with the observed data. The coefficient of determination and Nash–Sutcliffe efficiency of the predicted discharge were 0.824 and 0.786, respectively. BEACH has been developed within freely available GIS and programming language, PCRaster. It is a useful teaching tool for learning about distributed water balance modelling and land use scenario analysis.

***Keywords*:** BEACH, soil moisture, event-based model, continuous model, PCRaster.

7.1 Introduction

The soil moisture content of the root zone is a key variable that controls nearly all the hydrological processes occurring at or near the land surface. It regulates the partitioning of precipitation into infiltration, runoff, storage in the root zone and percolation into deeper ground water storage. Soil moisture also influences evapotranspiration and water availability to plants and thus affects the success of agriculture. Therefore it is considered to be an important parameter in land surface hydrology models, climate models and general circulation models at a variety of scales. However, due to its high spatial and temporal variability, soil moisture is not monitored continuously like precipitation and discharge (Georgakakkos, 1996). Generally speaking, soil moisture is measured at two extreme scales (Mohanty et al., 2000). It is either observed at a scale of square centimetres (point scale) with in situ measurement methods (e.g. gravimetric, TDR, etc.) or it is observed at a scale of square metres (pixel size) with the use of remote sensing techniques. Neither the in situ techniques nor the remote-sensing techniques provide observations at the appropriate resolution or sampling interval and are prone to large measurement errors (Walker, 1999; Evett et al., 2002). For these reasons, during the last 30 years there have been various studies that have attempted to develop a method to estimate the soil moisture content over a range of scales.

In general, the methods for estimation of spatially distributed moisture content are classified into three main groups: (i) extrapolation approaches; (ii) simulation models in open loops; and (iii) data assimilation and integration of remote sensing observations and computational modelling.

In the first group, areal average of soil moisture is estimated by extrapolating point measurements across the landscape, either with geostatistical techniques (Western & Grayson, 1998; Wang et al., 2001;Western et al., 2004) or using wetness indices based on terrain information (e.g. Beven and Kirkby, 1979; O'Loughlin, 1986; Svetlitchnyi et al., 2003; Teuling and Troch, 2005). In practice, both methods are difficult to apply. Due to the small correlation length of soil moisture variability, the application of geostatistical methods requires a large number of soil moisture observations for medium- to large-scale catchments. The usefulness of the wetness indices is limited by the restrictive assumptions underlying their derivation (Grayson and Western, 1998). Moreover, the inclusion of these functions increases the complexity of the hydrological simulations (Engman and Rogowski 1974), which may not be justifiable for a given marginal improvement in catchment prediction.

Another method of estimating spatially distributed soil moisture that falls within the first group is the application of "time stability" (Vachaud et al., 1985). According to this concept, particular sites in the field always display the mean behaviour while others always represent extreme values (Teuling et al., 2006).

The second group includes Soil–Vegetation–Atmosphere Transfer (SVAT) models, Land Surface Model (LSM) and unsaturated zone models, which usually require the solution of a form of the Richards equation (Moran et al., 2004). Most of these models solve the Richards equation in 1-D vertical direction and regionalisation is carried out based on land use, or soil, or topography, or two or three of these combined. (Renschler et al., 2001). In a review study, Moran et al. (2004) reported that simulation models are generally of limited practical use because of the difficulties of specifying parameters and the initial and boundary conditions.

The third group, a fairly new method for estimating a spatially distributed soil moisture profile, comprises the integration of remote sensing observations and hydrological modelling using data assimilation. For an excellent overview of this approach, see Heathman et al., (2003) and Moran et al., (2004). In this method, the profile soil moisture content is linked to the surface soil moisture content in order to combine the advantages of spatial predictability of the remote sensing data with the continuous and depth-wise predictability of the in situ measurement tools and 1-D hydrological modelling (Kostov and Jackson, 1993; Entekhabi et al., 1994; Georgakakos, 1996; Hymer et al., 2000; Heathman et al., 2003). However, the remotely sensed soil moisture data is prone to errors introduced by soil type, landscape roughness and vegetation cover (Houser et al, 1998). Also, there is a mismatch in scale between the in situ measurements and the areal estimates from remote sensing (Grayson and Western, 1998). Remote sensing data yields the average value of the soil moisture content at the scale of a footprint that is larger than the scale of variability of soil moisture (Western and Blöschl, 1999; Heathman et al., 2003; Western et al., 2004).

Despite the above-mentioned problems related to the measurement and prediction of the spatial and temporal distribution of soil moisture, the initial soil moisture is an important input parameter in many event-based surface runoff generation and soil erosion models. In addition, distributed physically based models such as ANSWERS, EUROSEM, KINEROS2 and LISEM have proven to be most sensitive to the initial soil moisture (De Roo, 1993; De Roo et al., 1996; Folly et al, 1999; Hantush and Kalin, 2005).

Users of physically based, event-scale models are in need of a tool that provides detailed information on the spatial distribution of soil moisture at the onset of an event. The BEACH (Bridging Event And Continuous Hydrological modelling) model is such a tool. In this paper, the development and application of the BEACH model are presented.

7.2 Model formulation

BEACH is a simple conceptual soil moisture routing model developed as a tool to provide spatial distribution of soil moisture content at the onset of a rainfall event, which will be simulated with a detailed physically based event-scale surface runoff generation and soil erosion model. The model has been written within a public domain GIS and environmental programming language, PCRaster (http://pcraster.geo.uu.nl). PCRaster is a dynamic modelling system for the construction of iterative spatio-temporal environmental models. PCRaster as a GIS provides an efficient environment for the storage, manipulation and visualisation of inputs and outputs. Furthermore, being a high-level programming language, PCRaster facilitates a clear understanding of model structure as a sequence of commands and with potential for modification for different conditions.

BEACH is a grid-based model that predicts the daily moisture content of the root zone in two layers for each cell, with daily precipitation as the main forcing variable. The basic processes incorporated in the model are precipitation, infiltration, transpiration, evaporation, lateral flow, vertical flow and plant growth. The water balance for each cell *i* is calculated as follows:

$$D\frac{d\theta_i}{dt} = P_i - R_i + \Delta LF_i - Ea_i - Ta_i - DP_i \tag{7.1}$$

where D is root zone depth (m), θ is soil moisture content (m^3 m^{-3}), dt is the model time-step (day), P is precipitation (m), R is surface runoff (m), ΔLF is the difference between the lateral inflow into the cell and the lateral outflow out of the cell (m), Ea is the actual evaporation (m), T_a is actual transpiration (m), and *DP* is the leakage or deep percolation (m). Figure 7.1 is a schematic representation of the soil water balance in a grid cell.

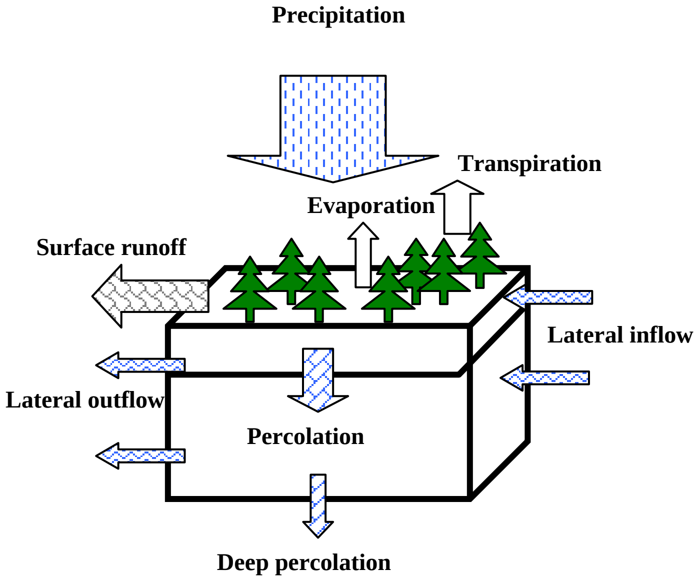

Figure 7.1. Schematisation of input and output fluxes in a single grid cell

The basic processes occurring within the surface layer and bottom layer are slightly different. For instance, infiltration, surface runoff generation, and evaporation from the soil surface are limited to the surface layer only. Percolation out of the surface layer is regarded as infiltration to the bottom layer.

7.2.1 Runoff and infiltration

For estimation of infiltration and surface runoff, the user can choose either a simple bucket model (BEACH-Bucket) or the widely known SCS curve number (BEACH-CN) method. The bucket model assumes that infiltration proceeds until the uptake capacity of the surface layer (0–0.20 m) has been reached as a result of precipitation. Infiltration for each cell *i* is calculated as:

$$I = \min\left[P, (\theta_{s1} - \theta_1) D_1\right] \tag{7.2}$$

where *I* is infiltration *(m)*, θ_{s1} is the saturated soil moisture content ($m^3\ m^{-3}$), θ_1 is the actual soil moisture content of the surface layer ($m^3\ m^{-3}$), and D_1 is the surface layer thickness (m).

Runoff occurs when daily precipitation exceeds the surface layer uptake capacity and is calculated for each cell *i* as:

$$R = P - I \qquad \text{if} \qquad P > I \tag{7.3}$$

When using the CN method, runoff occurs when the initial abstraction capacity of the surface layer is exceeded by precipitation. The infiltration for each cell *i* is calculated as:

$$I = P - R \tag{7.4}$$

$$R = \frac{(P - 0.2S)^2}{P + 0.8S} \tag{7.5}$$

$$S = 0.254\left(\frac{100}{CN} - 1\right) \tag{7.6}$$

where S is the retention parameter (m) and CN is the SCS curve number. Usually the curve number for the average moisture content (CN_2) per land use type and hydrological soil group is derived from tabulated values proposed by the Soil Conservation Service Engineering Division (1986). To adjust the CN values for other soil moisture conditions we followed the methodology applied in the SWAT model (Neitsch et al., 2002).

7.2.2 Lateral flow or interflow

When the soil moisture content exceeds the field capacity in a specific cell *i*, the soil water is redistributed according to the relationship proposed by Manfreda et al. (2005):

$$\Delta LF_k = \left(\frac{W_k \sum_{j=1}^{N(t)} \max[c_{j,k}(s_{j,k} - s_{fc,j,k}),0]}{\sum_{j=1}^{N(t)} W_{j,k}} \right) - \max[c_k(s_k - s_{fc,k}),0] \tag{7.7}$$

where ΔLF is the difference between subsurface lateral inflow and outflow for cell *i*, $W_j = \ln(a/\tan\beta)$ (a is the drainage area per unit contour length and $\tan\beta$ is the local slope in the direction of steepest descent) is the wetness index at cell *j* (index *j* is used for cells located upstream of cell *i*), *N(t)* is the number of cells that exceed the field capacity in the areas draining to the cell *i*, s is amount of soil water (m), s_{fc} is the amount of soil water at field capacity (m), and *k* indicates the soil layer, *c* is the shallow subsurface flow coefficient, which appears to remain fairly constant around 0.25 (d^{-1}) for a time scale of one day (Manfreda et al., 2005).

The wetness index (*W*) was introduced by Kirkby (1975) to describe the spatial variation of soil moisture, reflecting the tendency of water to accumulate in regions with a large drainage area and a relatively low local slope. It is assumed that interflow occurs between the same layers of adjacent cells. In other words, subsurface flow out of the surface layer in a cell enters the surface layer of the downstream neighbouring cell. Also it is assumed that all subsurface flow from an upstream cell enters only one downstream cell in the steepest direction.

7.2.3 Deep percolation

To simulate the drainage inside and the percolation out of a soil layer for each cell *i*, we used the method applied in the BUDGET model (Raes, 2002).

$$DP_k = D_k \tau_k (\theta_{s,k} - \theta_{fc,k}) \frac{e^{\theta_k - \theta_{fc,k}} - 1}{e^{\theta_{s,k} - \theta_{fc,k}} - 1} \tag{7.8}$$

Where DP is percolation to the deeper layer (m), θ is actual soil moisture content ($m^3\ m^{-3}$), θ_s is soil moisture content at saturation ($m^3\ m^{-3}$), θ_{fc} is soil moisture content at field capacity ($m^3\ m^{-3}$) and τ is a dimensionless drainage characteristic that is closely related to the saturated hydraulic conductivity (K_{sat}) as follows:

$$\tau = 0.0866 e^{0.8063 \log_{10}(K_{sat})} \qquad 0 < \tau \le 1 \tag{7.9}$$

where K_{sat} is the saturated hydraulic conductivity in mm d^{-1}.

7.2.4 Evapotranspiration

Evapotranspiration is a major component of the water balance in the root zone soil profile. It consists of two parts: evaporation from the soil surface and transpiration by plants. In many agroclimatical and water balance studies they are considered as a single variable, while in other situations, separation of evaporation and transpiration will give a better understanding of the relevant processes under consideration (Stroosnijder, 1987). In the current study they have been estimated separately using the simplified version of the Penman–Monteith (FAO56) approach (Allen et al., 1998). FAO56 calculates a reference evapotranspiration rate (ET_o) for a hypothetical grass cover with an assumed height of 0.12 m, a surface resistance of 70 s m^{-1} and an albedo of 0.23. To calculate the potential evapotranspiration rate for other surfaces, the ET_o is multiplied by a coefficient (K_c) that is crop-specific.

$$ET_p = K_c ET_o \tag{7.10}$$

where ET_p is the crop evapotranspiration under standard condition, and K_c is the crop factor that integrates the effects of characteristics that distinguish a typical field crop from the hypothetical reference surface. K_c combines the effect of soil evaporation and crop transpiration. When the evaporation and transpiration are considered separately, the K_c is split into two separate coefficients, one for crop transpiration (K_{cb}) and one for soil evaporation (K_e) as follows:

$$K_c = K_{cb} + K_e \tag{7.11}$$

In the standard condition, actual evapotranspiration (ET_a) is equal to ET_p. When soil moisture supply is limited, the actual rate of evapotranspiration (ET_a) is less than ET_p. In this study the evapotranspiration was split into two components: (i) root water uptake and (ii) evaporation from bare surface.

The extraction of soil water in the root zone by a plant is governed by the atmospheric demand and the supply of water in the soil. When moisture supply is sufficient, transpiration will occur at a potential rate (T_p) equal to the atmospheric demand. For the calculation of T_p we follow Allen et al. (1998):

$$T_p = K_c \, fET_o \tag{7.12}$$

$$f = 1 - e^{-\mu . LAI} \tag{7.13}$$

where LAI is the leaf area index, f is the proportion of soil covered by vegetation, μ is the light use efficiency parameter depending on land use: 0.35 for grass, 0.45 for crops, 0.5–0.77 for trees (Larcher, 1975).

The maximum transpiration rate within each soil layer depends on the water uptake capacity of the roots in that layer. The water uptake capacity of each layer depends on the root extension within the layer and is calculated as follows (Prasad, 1988):

$$T_{p,k} = 2\left(1 - \frac{RD_{k,0.5}}{RD}\right)\left(\frac{RD_k}{RD}\right)T_p \tag{7.14}$$

where $T_{p,k}$ is the maximum daily uptake of water from soil layer k (mm), RD_k is the extension of roots within the soil layer k (m), $RD_{k,0.5}$ equals the soil depth in the middle of root extension in the soil layer k (m), and RD is the total rooting depth (m).

When soil water supply in a layer is insufficient to meet the atmospheric demand, the root water uptake will be reduced and the actual transpiration rate (T_a) becomes less than T_p in that layer:

$$T_a = K_s T_p \tag{7.15}$$

$$K_s = \max\left[0, \min\left(1, \frac{\theta_t - \theta_{wp}}{\theta_c - \theta_{wp}}\right)\right] \tag{7.16}$$

$$\theta_c = \theta_{wp} + (1 - p)(\theta_{fc} - \theta_{wp}) \tag{7.17}$$

$$p = p_{tab} + 0.04(5 - ET_p) \tag{7.18}$$

where K_s is a reduction parameter [0–1] which depends on available soil water content, θ_c is the critical soil moisture content that defines the transition between unstressed and stressed transpiration rate, *p* represents the fraction of total available soil water that can be depleted from the root zone before moisture stress occurs, p_{tab} is the depletion factor for $ET_p \approx 5$ mm d^{-1} which is derived from a reference table (Table no. 22) in Allen et al. (1998).

The evaporation from the soil surface is limited to the bare surfaces. The amount of evaporation underneath the plant cover is assumed to be negligible. The evaporation rate from the soil surface is governed by the atmospheric demand and the supply of water in the soil evaporation layer (~ 0.15 m). When the soil water supply is sufficient, evaporation occurs at its potential rate (E_p) which is controlled by the atmospheric demand. Generally speaking, evaporation from the exposed soil surface (*1-f*) is assumed to take place in two stages: an energy limiting stage and moisture supply limiting stage (Ritchie, 1972; Boesten & Stroosnijder, 1986; Stroosnijder, 1987; Allen et al., 1998). In the first stage, evaporation occurs at the potential rate (E_p). In the second stage, the evaporation decreases in proportion to the available soil water content.

For the calculation of evaporation from soil surface we follow Allen et al. (1998):

$$E_p = K_e ET_o \tag{7.19}$$

$$K_e = K_{c\max} - K_{cb} \tag{7.20}$$

$$K_{c\max} = \max\left[\left\{1.2 + \left[0.04(u_2 - 2) - 0.004(RH_{\min} - 45)\right]\left(\frac{h}{3}\right)^{0.3}\right\}, \left\{K_{cb} + 0.05\right\}\right] \tag{7.21}$$

$$E_a = K_r E_p \tag{7.22}$$

$$K_r = \frac{\theta_t - \theta_{dr}}{\theta_{fc} - \theta_{dr}} \tag{7.23}$$

where K_e is the soil evaporation coefficient, $K_{c\max}$ represents an upper limit to the evaporation and transpiration from any cropped surface and ranges from about 1.05 to 1.30, *u* is wind speed at the height of 2 m (m s^{-1}), RH_{min} is air relative humidity (%), *h* is the mean maximum plant height during the period of calculation, E_a is the actual evaporation from soil surface (mm d^{-1}), K_r is a dimensionless evaporation reduction coefficient dependent on the topsoil water content, θ_t is actual soil moisture content (m^3 m^{-3}), and θ_{dr} is the moisture content of air-dry soil (m^3 m^{-3}). The moisture content of air-dry soil is estimated as one-third of the soil moisture content at wilting point (Allen et al., 1998).

7.2.5 Crop growth parameters

Crop height and root growth are required to estimate the maximum transpiration rate according to FAO56 (Allen et al., 1998). For crops, it is assumed that height increases at a constant rate from emergence to the end of vegetative stage when the crop attains its final height. This assumption is acceptable, since the transpiration rate is relatively insensitive to small uncertainties in the value used for crop height (Allen et al., 1998). Root growth is assumed to proceed at a constant rate from emergence to the end of the vegetative stage. Therefore a linear relationship can sufficiently approximate the root growth.

For simulation of the Leaf Area Index (LAI), the method applied in the DAICROS model is used (Verdoodt et al., 2004). In that model, four different leaf growth stages have been distinguished during their development: 1) fast linear growth stage, 2) reduced linear growth stage, 3) zero growth stage, and 4) exponential decay stage (Figure 7.2).

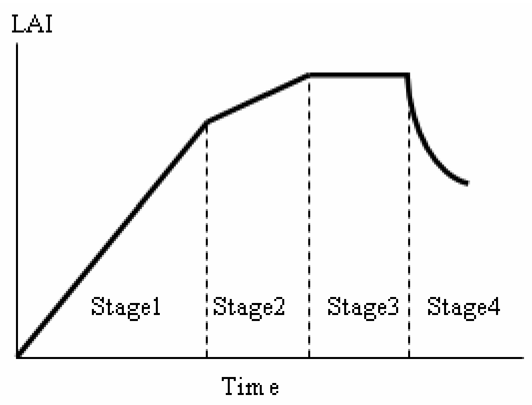

Figure 7.2. Schematised course of leaf area index rate (after Verdoodt et al. 2004).

The first stage, which extends from emergence to the end of the crop development stage, is referred to as the period of fast linear growth. In this stage the LAI (m^2 m^{-2}) increases at a constant rate and is calculated as follow:

$$LAI_t = LAI_{t-1} + \frac{LAI_{\max}}{L_{fg}} \tag{7.24}$$

where LAI_t and LAI_{t-1} represent the leaf area index on day t and on the previous day, respectively. L_{fg} is the length of the first stage in days; $LAI_{\max}$ is the maximum possible LAI at the end of development stage. The value of $LAI_{\max}$ is available from the literature (Sys et al., 1993).

From the beginning to halfway through the reproduction stage is referred to as the reduced, linear growth stage (stage 2). During this stage, leaf development continues at a constant, but reduced rate as follows:

$$LAI_t = LAI_{t-1} + \frac{LAI_{full} - LAI_{\max}}{L_{hm}} \tag{7.25}$$

where L_{hm} is the half of the duration of the mid-season crop growth stage and LAI_{full} is the leaf area at full canopy development. Since relevant data on LAI_{full} are not always available it is assumed to be $LAI_{\max} + 0.5$.

From halfway to the end of reproduction stage is referred to as the zero growth stage (stage 3). During this stage, leaf growth stops and all assimilates are used for the development of flowers and seeds, and consequently, the *LAI* keeps its value at full canopy development.

$$LAI_t = LAI_{full} \tag{7.26}$$

The period from the beginning of the late season until the end of the late season is referred to as the exponential decay stage. During stage 4, which coincides with the maturation stage, the leaf area index decreases exponentially due to leaf senescence. Penning de Vries and van Laar (1982) estimated the relative leaf death rate during this stage at 3 % per day:

$$LAI_t = LAI_{t-1} - 0.03 LAI_{t-1} \tag{7.27}$$

7.2.6 Overview of input data

The input data required to run BEACH can be classified into four main groups: (i) climate, (ii) soil physical properties, (iii) land use, and (iv) topography. Apart from the saturated hydraulic conductivity there is no other difficult-to-measure input parameter. An overview of all necessary input data to run the BEACH model is given in Table 7.1. The climate data includes the daily values of reference evapotranspiration, minimum relative humidity, wind speed and precipitation. The minimum relative humidity and wind speed are required for further adjustment of the potential evapotranspiration calculated with the FAO 56 approach.

All the relevant topographical information is derived from a digital elevation model (DEM). The soil map of a study area can be obtained from relevant databases or prepared by field survey. The soil input data for each map unit can be measured in the laboratory using soil samples taken from the study area. Due to the difficulty of measuring the saturated hydraulic conductivity (K_{sat}) there might be a large uncertainty in the measured values of K_{sat}, however, it will not translate into a remarkable uncertainty in the results of BEACH. This is because BEACH is not sensitive to K_{sat}, which is only used for estimating the drainage coefficient (τ). When K_{sat} data are not available, the user can specify a value for τ ranging between 0 and 1, based on soil texture. It is suggested to use large values for τ for coarse-textured soils and smaller values for fine-textured soils (Raes, 2002). Land use data comprises the land use map and crop specific information that can be obtained from the literature or field surveys. Most of the required crop-specific information is available in tablular format in Allen et al. (1998).

Table 7.1. Input requirements of the BEACH model.

Type	Data resolution	Input variables and parameters	Unit	Source
Climate				
	daily	reference evapotranspiration (ET_o)	m	weather station
	daily	minmum relative humididty (RH_{min})	%	weather station
	daily	wind speed (U_2)	m s^{-1}	weather station
	daily	precipitation (P)	m	weather station
Topography				
	constant	slope map	m m^{-1}	DEM
	constant	local drainage direction (LDD) map	-	DEM
	constant	wetness index (W)	-	DEM
Soil				
	constant	soil map	-	database, field survey
	for each layer	layer depth (D)	m	user specified
	constant	soil evaporation depth (D_e)	m	user specified
	for each layer	subsurface flow coefficient (c)	d^{-1}	user specified
	for each layer	drainage coefficient (τ)	-	user specified
	for each layer	soil moisture at saturation (θ_{sat})	m^3 m^{-3}	field measurement
	for each layer	soil moisture at field capacity (θ_{fc})	m^3 m^{-3}	measurement
	for each layer	soil moisture at wilting point (θ_{wp})	m^3 m^{-3}	measurement
	for each layer	saturated hydraulic conductivity (K_{sat})	m d^{-1}	measurement
Land use				
	seasonally	land use map	-	field survey, cadastral maps
	constant	maximum leaf area index (LAI_{max})	m^2 m^{-2}	literature, measurement
	constant	maximum crop height (H_{max})	m	literature (FAO56)
	constant	maximum root depth (RD_{max})	m	literature (FAO56)
	constant	light use efficiency (μ)	-	literature
	constant	sowing and harvesting dates	-	local information
	constant	growth stages	-	literature (FAO56)
	constant	basal crop coefficient (Kcb)	-	literature (FAO56)
	constant	water stress sensitivity (p)	-	literature (FAO56)

Each climate input variable should be provided as separate time series. All the land use and soil input parameters can be filled in a main matrix table. This table is linked to the land use map and the soil map through a lookup function. Recorded land use changes per field should be provided as time series in another table. Using a lookup function, the land use map is updated continuously according to the table of land use time series.

7.3 Application of BEACH

7.3.1 Site description

We have applied the BEACH model to the *Catsop* catchment in South Limburg, the Netherlands (50º 95´N, 5º 78´E; Figure 7.3), which has an area of 0.42 km^2 and is located approximately 2 km north of Maastricht–Aachen international airport. This typical agricultural catchment is in the loess district of the Netherlands (De Bakker, 1979). The loess district is characterised by an undulating topography and deep aeolian deposits of the late-Weichsel ice age. These deposits blanket older formations of Tertiary sand deposits and Quaternary deposits of the “West-Meuse” river. The weak aggregate stability of loess soils favours crust formation and reduces infiltration. During major events in the catchment 3–30 % of the total rainfall reaches the catchment outlet (De Roo, 1993). The altitude of the catchment ranges from 79 m at the outlet to 112 m above mean sea level. The climate of the study area is temperate humid, and annual precipitation is about 740 mm, which is evenly distributed throughout the year. On average, the summer events are short and rather intensive while the winter events last longer and are less intensive. Four main land use types can be distinguished within the catchment: Arable (80 %), Orchard (8 %), Grassland (12 %), and Infrastructure (1 %). Arable land is mainly cultivated with cereals such as winter wheat and barley, or root crops such as sugar beet and potato.

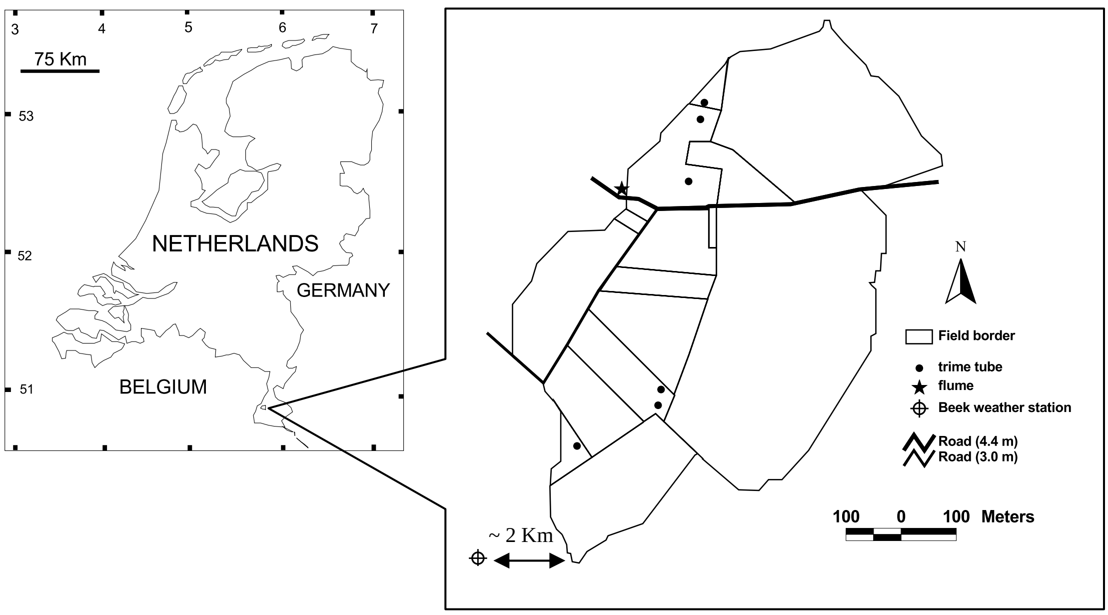

Figure 7.3. Geographical location of the study area and the location of measurement units.

7.3.2 Data collection and estimation of input parameters

Daily records from the Beek station were used for climate inputs. The station is one of the 10 main weather stations in the Netherlands supervised by the KNMI Royal Netherlands Meteorological Institute. It is a synoptic weather station located less than 2 km south of the study area, near the Maastricht–Aachen international airport.. The reference evapotranspiration was calculated with the Penman-Monteith equation. Figure 7.4 displays the time series of daily precipitation and reference evapotranspiration at the Beek station during 2004.

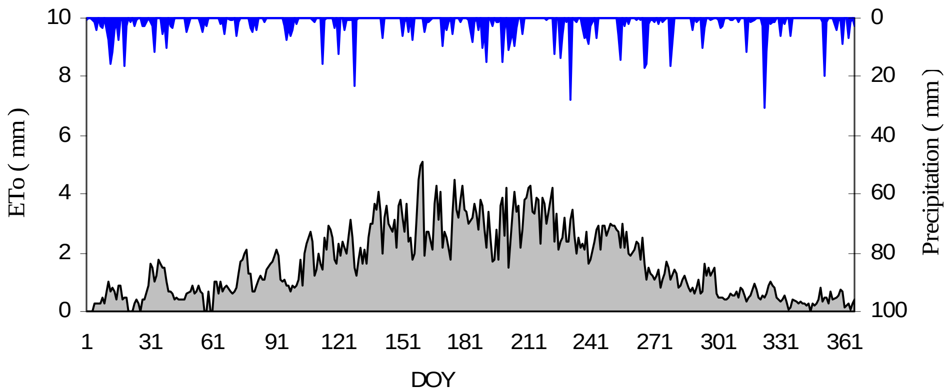

Figure 7.4. Time series of daily reference evapotranspiration and precipitation in 2004 at the Beek weather station.

Topographical information was derived from an available 5 m resolution Digital Elevation Model (DEM) of the study area. Based on the DEM, the catchment boundary, slope map, Local Drainage Direction (LDD) and wetness index maps were prepared within PCRaster. Figure 7.5 shows the slope map, LDD map, and the wetness index map of the Catsop catchment.

Field borders and the geographical position of the measurement equipment were obtained by field survey and using a hand-held GPS with horizontal accuracy of 5 m. The crop rotation information and specific land use practices in each field were recorded during field surveys in 2004 and 2005. The crop-specific input data were obtained from the literature (e.g. Allen et al., 1998) and were adjusted for the local conditions. For the sake of simplicity we assumed a constant plant height for orchards (3 m). Figure 7.6 shows the land use map of the study area in 2004.

Since the whole catchment area is covered with loess soils, it was assumed that differences in soil hydraulic properties are mainly induced by land use type. Soil moisture content at saturation, field capacity, and wilting point were obtained in the laboratory from soil samples taken in the field. Undisturbed soil samples were taken with thin-walled stainless steel cylindrical tube samplers of a known volume of 100 cm^3. Data on saturated hydraulic conductivity data were obtained from previous studies on the area (Ritsema et al., 1996 and Stolte et al., 1994). Table 7.2 presents the values of input parameters for each land use type and soil layer at the locations of soil moisture observations.

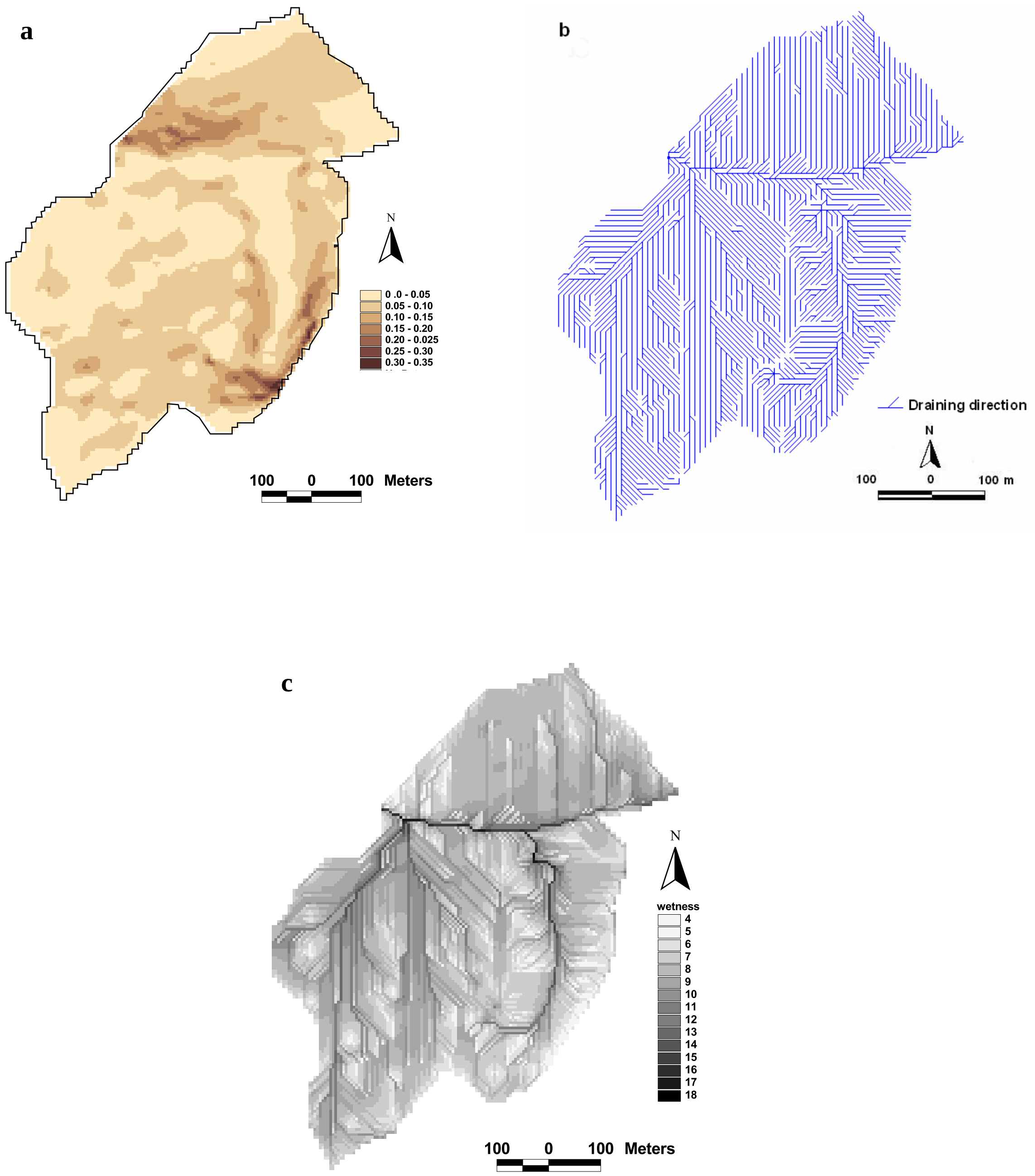

Figure 7.5. Topography-driven input maps for the Catsop catchment in South Limburg, the Netherlands. a) Slope map, b) Local Drainage Direction map, and c) Wetness index map.

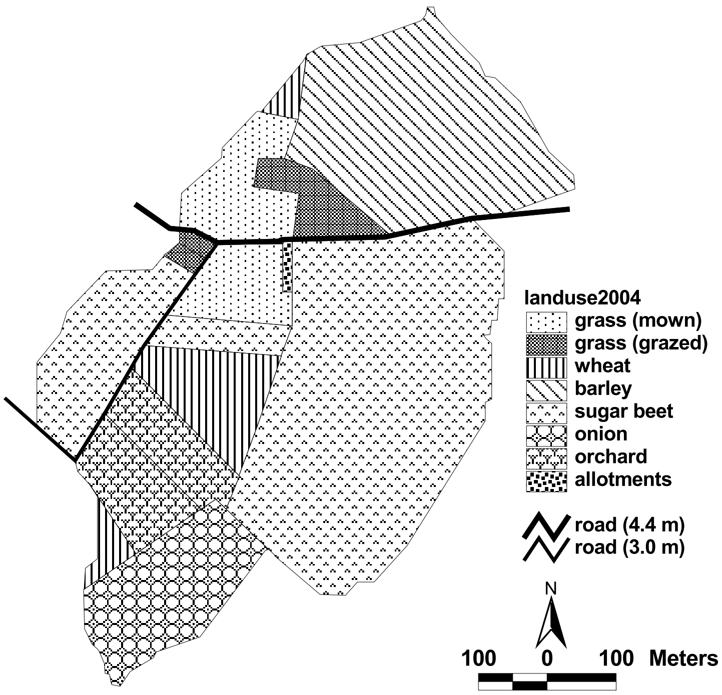

Figure 7.6. Land use map in the Catsop catchment, the Netherlands during 2004.

Table 7.2. Values of input variables and parameters.

Input	Unit	Grass	Wheat	Orchard
$\theta_{sat\ 1}$	$m^3\ m^{-3}$	0.42	0.36	0.36
$\theta_{sat\ 2}$	$m^3\ m^{-3}$	0.40	0.40	0.40
$\theta_{fc\ 1}$	$m^3\ m^{-3}$	0.26	0.23	0.22
$\theta_{fc\ 2}$	$m^3\ m^{-3}$	0.22	0.20	0.25
$\theta_{wp\ 1}$	$m^3\ m^{-3}$	0.13	0.13	0.13
$\theta_{wp\ 2}$	$m^3\ m^{-3}$	0.13	0.13	0.13
$K_{sat\ 1}$	$m\ d^{-1}$	0.01	0.01	0.03
$K_{sat\ 2}$	$m\ d^{-1}$	0.03	0.03	0.03
c	d^{-1}	0.25	0.25	0.25
D_e	m	0.15	0.15	0.15
LAI_{max}	$m^2\ m^{-2}$	2.50	3.00	4.50
H_{max}	m	0.40	1.00	3.00
RD_{max}	m	0.50	0.90	1.20
μ	-	0.40	0.45	0.30
Kcb_{ini}	-	0.40	0.25	0.50
Kcb_{mid}	-	0.90	1.10	0.95
Kcb_{end}	-	0.70	0.25	0.75
p	-	0.55	0.55	0.50
CN_2	-	60	76	74

7.3.3 Model evaluation

For the evaluation of the model we compared the simulated soil moisture content and total discharge at the outlet with their measured counterparts in the Catsop catchment. Soil moisture observations from 6 locations were used: 2 locations in croplands, 2 in grasslands, and 2 in orchards. The soil moisture content at these locations was monitored from November 2003 to October 2004 with a portable Time Domain Reflectometry (TDR) tool called *Trime-FM* that operates in a fibreglass access tube. The Trime-FM gives averaged soil moisture content over a layer of 18 cm. Therefore we measured soil moisture content in 5 layers (every 20 cm) down to 100 cm depth. Any air gaps between the access tube and surrounding soil will result in large observation errors, especially during the first few weeks after installation. We therefore excluded the first 5 weeks of observations at each location from the analysis.

Since BEACH is a two-layer (top layer and sub-layer) model, we used the first layer (0–20 cm) observations for the evaluation of the simulation results for the top layer and the average of observations in the next 3 layers (20–80 cm) for the evaluation of the simulated sub-layer moisture content. The observations from the 5th layer were excluded from the analysis because during monitoring we observed that some water had accumulated at the bottom of some tubes. We assumed that this water had accumulated either because of leakage at the bottom of tubes or condensation of vapour inside the tubes.

Discharge at the outlet of the catchment was monitored using a partial flume with a capacity of 950 l s^{-1}. Water height at the flume was recorded at 5-minute intervals on a data logger. The measured values of total daily discharge at the outlet provide a good criterion for integrated evaluation of the model.

A comparison of observed and simulated results for calibration and validation periods would be the ideal method to demonstrate a model's adequacy. However, the available data set comprised only one year of soil moisture observations of acceptable quality. This hindered the validation of the BEACH model based on a separate observed data set. Another way to validate the accuracy of a model is to see how the results compare with other acceptable models (Frankenberger et al., 1999). Therefore the model was calibrated using the available dataset, and then model performance was compared with the performance of the BUDGET model (Raes, 2002). BUDGET is a 1D soil water balance model composed of a set of submodels describing the various processes involved in water extraction by plant roots and water movement in the soil profile at the field level. This model runs with a constant time-step of one day.

The correspondence between simulated and observed soil moisture content was analysed using the Index of Agreement (IA), correlation coefficient (R), Mean Error (ME) and Root Mean Squared Error (RMSE) using the following equations:

$$EF_{IA} = 1 - \frac{\sum_{i=1}^{N} (\theta_{sim} - \theta_{obs})^2}{\sum_{i=1}^{N} \left[\left| \theta_{sim} - \overline{\theta}_{sim} \right| + \left| \theta_{obs} - \overline{\theta}_{obs} \right| \right]^2} \tag{7.28}$$

$$R = \frac{\sum_{i=1}^{N} \left(\theta_{obs} - \overline{\theta}_{obs} \right) \sum_{i=1}^{N} \left(\theta_{sim} - \overline{\theta}_{sim} \right)}{\sqrt{\sum_{i=1}^{N} \left(\theta_{obs} - \overline{\theta}_{obs} \right)^2 \sum_{i=1}^{N} \left(\theta_{sim} - \overline{\theta}_{sim} \right)^2}} \tag{7.29}$$

$$ME = \frac{\sum_{i=1}^{N} (\theta_{sim} - \theta_{obs})}{N} \tag{7.30}$$

$$RMSE = \sqrt{\frac{\sum_{i=1}^{N} (\theta_{sim} - \theta_{obs})^2}{N}} \tag{7.31}$$

where $\overline{\theta}_{sim}$ and $\overline{\theta}_{obs}$ are the daily mean values of the simulated and measured soil moisture content, respectively. The range of IA is between 0 and 1, and the closer it is to 1, the better is the fit between measured and simulated model outputs. R varies from +1 or -1 when the simulated and observed variables are a perfect match, to zero when there is no fit at all. Whereas IA and R are dimensionless criteria, ME and RMSE have the same dimension as the observations. A negative value of ME represents the model underestimation and a positive value indicates overestimation. The RMSE is the most widely used criterion used to evaluate soil moisture prediction.

7.4 Results and discussion

7.4.1 Soil moisture

Hydrographs at the outlet of catchments are widely used as the evaluation measure for hydrological models; however, they provide ambiguous information about the detailed hydrology within catchments (Frankenberger, 1999). On the other hand, soil moisture is a state variable that can be used as the most suitable alternative measure for the spatial evaluation of distributed hydrological models.

The time series of the simulated soil moisture content at 6 locations (2 locations per land use type) were used for the spatial evaluation of the model. Figures 7.7 and 7.8 show the time series of simulated and observed soil moisture content in the surface layer (0–20 cm) and the second layer (20–80 cm), respectively.

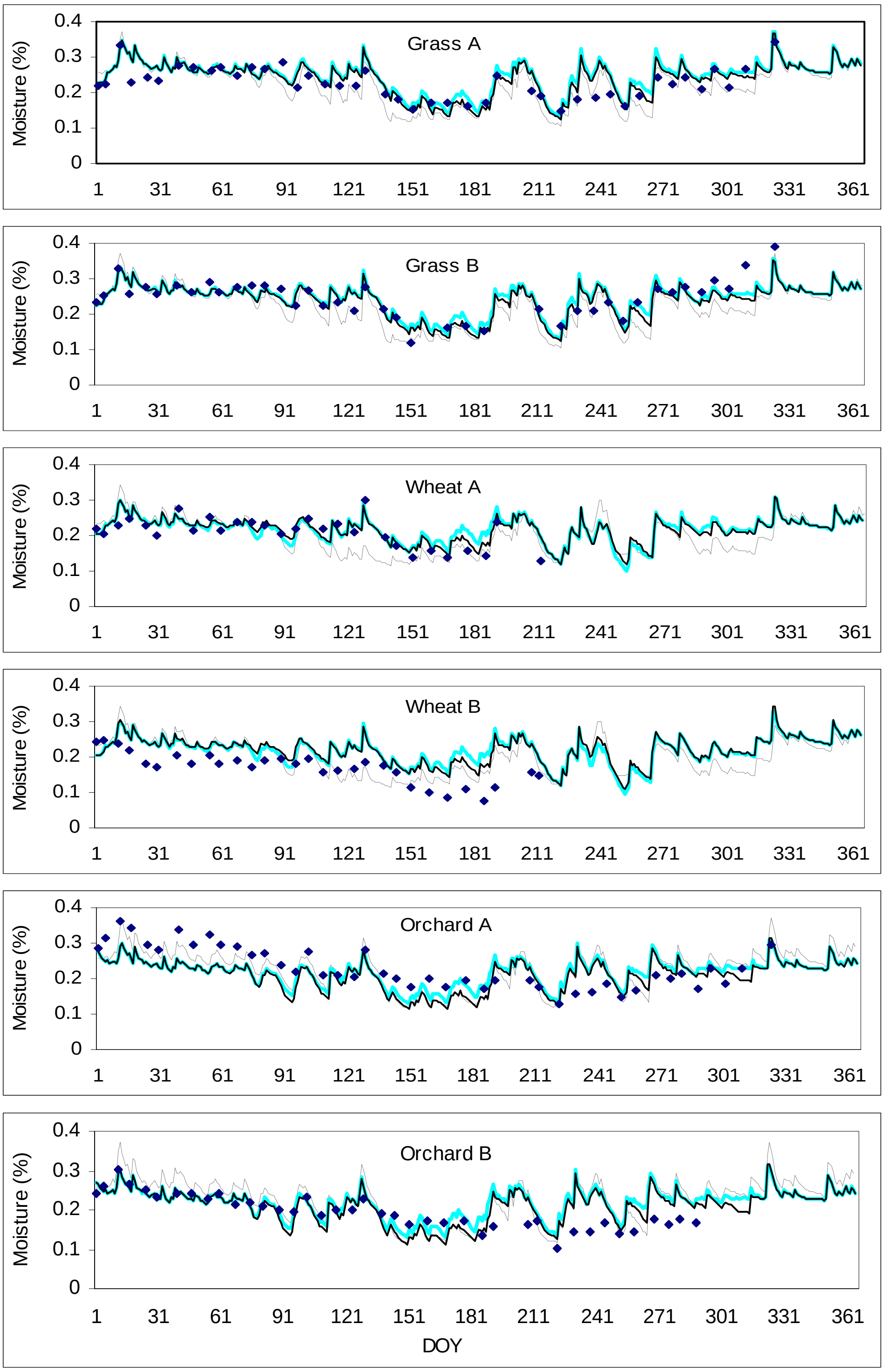

Figure 7.7. Time series of observed versus simulated values of soil moisture content in the first layer, at three different land uses during the year 2004. Dots show the observations, the thick line represents predictions by BEACH-CN, the thin black line and the thin grey line represent predictions by BEACH-Bucket and the BUDGET, respectively.

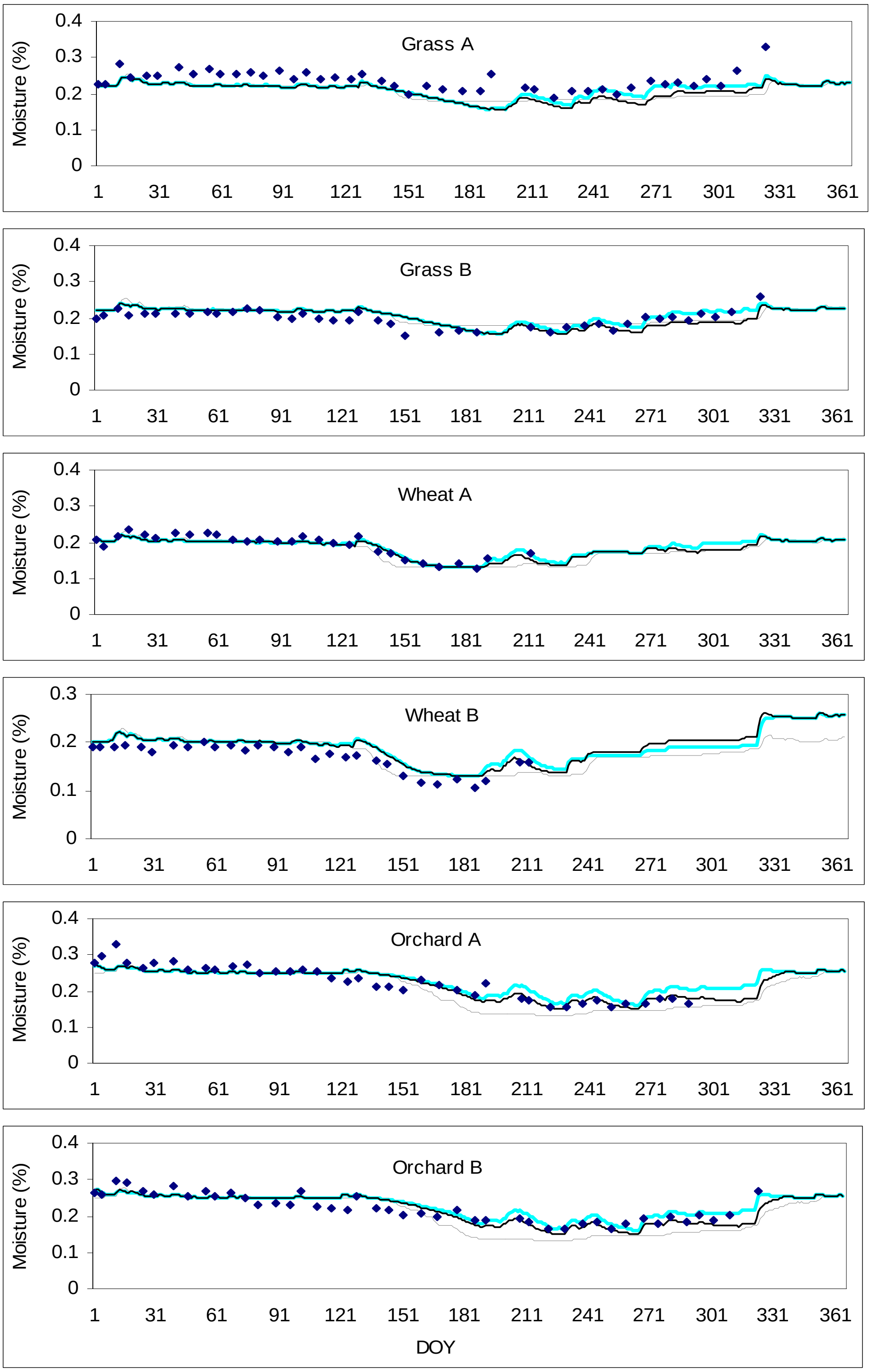

Figure 7.8. Time series of observed versus simulated values of soil moisture content in the second layer at three different land uses during the year 2004. Dots show the observations, the thick line represents predictions by BEACH-CN, the thin black line and the thin grey line represent predictions by BEACH-Bucket and the BUDGET, respectively.

As expected, all models showed abrupt temporal variations of soil moisture content in the surface layer in response to the daily variation of climate variables. The variation of soil moisture content in the second layer is gentle and seasonal. Moreover, there are some sporadic variations in the soil moisture content of the second layer which correspond to large precipitation events (Figure 7.8).

Table 7.3 summarises the statistical parameters comparing the predicted and observed values of soil moisture content per location and soil layer. Generally speaking, all the evaluation statistics show that all models performed better for the second layer (Table 7.3). In grasslands the values for the index of agreement and the correlation coefficient are higher for the first layer.

The ranges of RMSE of simulated soil moisture content in the first layer are 0.026–0.065, 0.023–0.061, and 0.032–0.051 m^3 m^{-3} for BEACH-CN, BEACH-Bucket, and BUDGET, respectively. For the second layer they were 0.011–0.032, 0.012–0.031, and 0.014–0.035 m^3 m^{-3}, respectively. These values agree well with the range of results reported in previous investigations. For instance, the SWAP study by Sheikh and Van Loon (2006) on the same study area and observation data set resulted in RMSE ranges of 0.015–0.045, 0.016–0.040, 0.012–0.050, and 0.011–0.051 m^3 m^{-3} for layers 1(0–20 cm), 2(20–40 cm), 3(40–60 cm) and 4(60–80 cm) respectively. Mertens et al. (2005), using soil moisture measurements at 25 locations at three different depths (at the surface, and at 30 and 60 cm) on an 80 by 20 m hill slope, reported RMSE values ranging from 0.041 to 0.089 when applying the MIKE-SHE model. Heathman et al. (2003), comparing the simulation results of the RZWQM model with soil moisture data from different depths up to 60 cm, found that RMSE ranges from 0.016 to 0.097. In a validation study of the THESEUS model in Germany, Wegehenkel (2005) obtained RMSE ranges of 0.030–0.043, 0.028–0.030, and 0.026–0.049 for layer 1 (0–30 cm), layer 2 (30–60 cm), and layer 3 (60–90 cm), respectively. All these studies used the numerical solutions of the Richards equation. Furthermore most of these results were obtained after an extensive parameter optimisation routine. Herbst et al. (2005) compared the results of four flow and transport models (MARTHE, TRACE, ANSWERS and MACRO) of different complexities and concepts with the observations from five lysimeters. The ranges of RMSE of soil moisture predictions at 25 and 85 cm depth were 0.025–0.057 and 0.026–0.037 m^3 m^{-3}, respectively. In addition, they obtained an IA of 0.90 or higher for all the models investigated. The values of IA we obtained are less than 0.90 in most cases (Table 7.3). The better values of performance criteria in the study by Herbst et al. (2005) might be related to the good quality observation data. They measured soil moisture content with a neutron probe.

In our study the poorest results were obtained for the first layer of *Wheat* B location. This is clearly due to the errors in the observations at this location. When the soil around the access tubes was dug out at the end of monitoring period we found that at this location there was a significant gap between the TRIME access tube and the soil around it. The presence of a small air space between access tube and surrounding soil induces a considerable deviation in the soil moisture measurements (IMKO Micromodultechnik GmbH., 2001; see also discussion in section 3.7.2 of this thesis).

Table 7.3. Statistical parameters comparing the observed values of soil moisture content with the values simulated by the BEACH and BUDGET models

Tube	No. Obs.	Model	ME	RMSE	IA	R
		First layer (0 – 20 cm)				
Grass A	44	BEACH – CN	0.021	0.033	0.995	0.884
		BEACH - BU	0.010	0.030	0.898	0.843
		BUDGET	-0.006	0.032	0.902	0.867
Grass B	39	BEACH – CN	-0.001	0.026	0.924	865
		BEACH - BU	-0.008	0.023	0.939	0.900
		BUDGET	-0.024	0.038	0.860	0.815
Wheat A	30	BEACH – CN	0.009	0.030	0.802	0.721
		BEACH - BU	0.005	0.023	0.891	0.812
		BUDGET	-0.011	0.045	0.731	0.591
Wheat B	28	BEACH – CN	0.050	0.065	0.153	0.463
		BEACH - BU	0.047	0.061	0.365	0.583
		BUDGET	0.031	0.051	0.696	0.681
Orchard A	39	BEACH – CN	0.020	0.050	0.686	0.559
		BEACH - BU	0.011	0.046	0.774	0.625
		BUDGET	0.026	0.051	0.764	0.731
Orchard B	43	BEACH – CN	-0.013	0.040	0.706	0.568
		BEACH - BU	-0.023	0.041	0.730	0.640
		BUDGET	-0.006	0.045	0.853	0.673
		Second layer (20 – 80 cm)				
Grass A	44	BEACH – CN	-0.025	0.032	0.995	0.671
		BEACH - BU	-0.027	0.031	0.550	0.829
		BUDGET	-0.030	0.033	0.349	0.740
Grass B	39	BEACH – CN	0.011	0.017	0.840	0.837
		BEACH - BU	0.004	0.018	0.828	0.711
		BUDGET	0.008	0.019	0.757	0.660
Wheat A	30	BEACH – CN	-0.005	0.011	0.960	0.949
		BEACH - BU	-0.006	0.012	0.958	0.947
		BUDGET	-0.010	0.014	0.949	0.950
Wheat B	28	BEACH – CN	0.018	0.020	0.866	0.957
		BEACH - BU	0.016	0.019	0.890	0.953
		BUDGET	0.011	0.018	0.917	0.918
Orchard A	39	BEACH – CN	0.004	0.022	0.900	0.880
		BEACH - BU	-0.003	0.019	0.940	0.891
		BUDGET	-0.016	0.031	0.897	0.871
Orchard B	43	BEACH – CN	0.006	0.019	0.927	0.890
		BEACH - BU	-0.002	0.017	0.941	0.892
		BUDGET	-0.015	0.035	0.876	0.879

A comparison of the measured and simulated values of soil moisture content at this location shows that in all the models applied, the measured values are always less than the simulated values. The large and positive (>0.03 $m^3.m^{-3}$) values of mean error (ME) for the simulation results at this location (Table 7.3) should not be regarded as overestimation by the models. Comparing the results of BUDGET and two options of the BEACH model indicates that the BEACH-Bucket gives the best prediction of soil moisture content for both soil layers. However, for most of the soil moisture monitoring locations, the difference between BEACH-CN and BEACH-BUCKET is not so large.

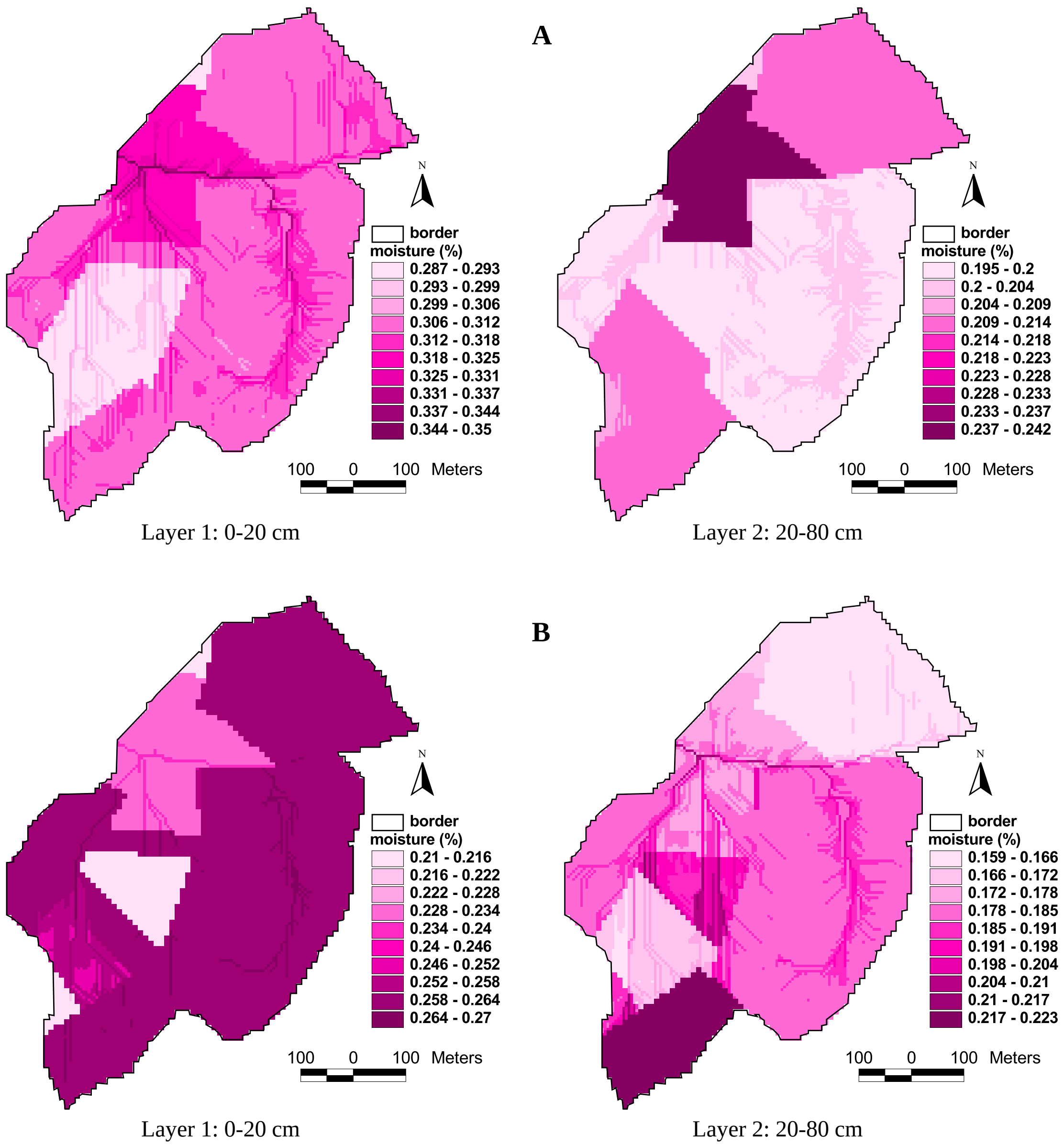

Figure 7.9. Spatial distribution of predicted soil moisture content (%) in two layers in the Catsop catchment, the Netherlands on two dates: A) 12-01-2004, B) 27-10-2004.

Given that the simple BEACH model is as adequate as the other models (BUDGET in this chapter and SWAP in Chapter 6), its ability to produce spatially distributed soil moisture data is a big advantage. Figure 7.9 shows the spatially distributed soil moisture maps of the study area for two dates (12-01-2004 and 27-10-2004) per soil layer. On 12-01-2004 there was about 15 mm rainfall; therefore BEACH shows high variation of soil moisture content in the first layer. Visual comparison of this map with the wetness index map (Figure 7.5 c) indicates that the soil moisture distribution on this date shows a good relation with the wetness index. The impact of the land use is also visible in the predicted soil moisture map (Figure 7.9). Whereas on 27-10-2004 there was no rainfall, there had been a rainfall event of more than 10 mm some 6 days earlier (21-10-2004). Therefore BEACH gave a higher variation of soil moisture content in the second layer.

Although the effects of topography and lateral flow are taken into account in the BEACH model, it is still not possible to reproduce the observed spatial variation of soil moisture content accurately. According to the observations, the soil moisture content of the second layer for two monitoring locations within the grassland is very different: it is assumed this is attributable to the topography. Their soil moisture content in the first layer is similar because this soil moisture content is mostly influenced by land use type. *Grass A* is located in the downstream section of a hill slope, while *Grass B* is located in the upstream part of the hill slope. Therefore the values of soil moisture content measured in the second layer of *Grass A* are always higher than the *Grass B* (Figure 7.10).

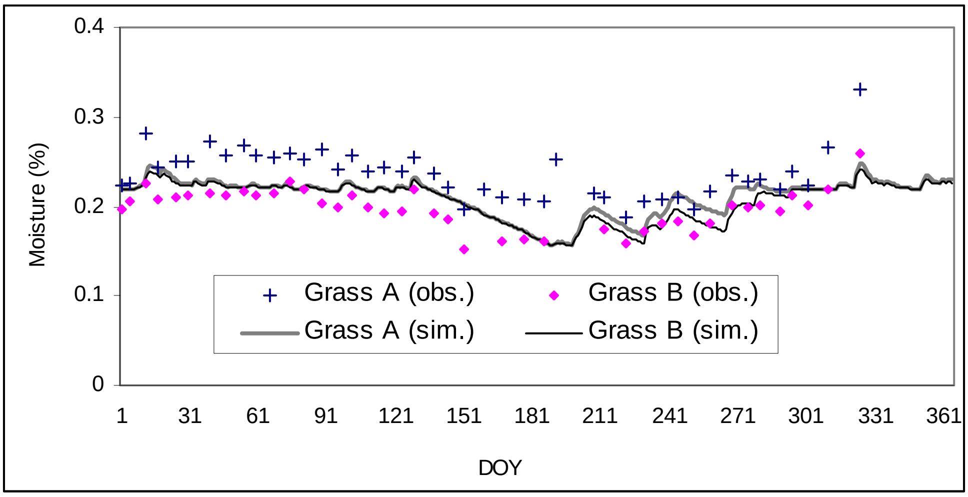

Figure 7.10. Simulated and observed soil moisture content in the second layer of two locations in the grasslands, in the Catsop catchment, the Netherlands. Note that for most of the simulation period the simulated values of Grass A and Grass B are similar. They differ from day 210 to day 300.

The BEACH model gives slightly higher estimates of the second layer soil moisture content for *Grass A*, but the estimates are very different from the observed values. The inability of BEACH to represent the soil moisture differences between *Grass A* and *Grass B* is related either to inefficiency of the implemented lateral subsurface flow equation or to deficiency of surface runoff routing and re-infiltration processes. In the BEACH model, it is assumed that lateral flow occurs only when the soil moisture content exceeds the field capacity, whereas it might occur at lower moisture content levels too.

7.4.2 Surface runoff

Although the primary objective of the BEACH model is to predict soil moisture, the predicted values of discharge at the outlet of the catchment can also be used in the overall assessment of model performance. As mentioned earlier in the model formulation section (section 2), infiltration and runoff generation processes can be simulated with either the bucket approach (BEACH-Bucket) or the CN approach (BEACH-CN).

Table 7.4. Observed and predicted values of total discharge at the Catsop outlet.

DOY	Precipitation (mm)	$Q_{observed}$ (m^3)	$Q_{BEACH-CN}$ (m^3)	$Q_{BEACH-Bucket}$ (m^3)
11	7.7	0	0.5	0
12	15.7	406.7	423.4	0
13	11.8	390.2	337.6	0.8
16	7.4	0	4.7	0
19	16.5	157.5	389.6	0
33	11.8	164.2	33.7	0
39	10.5	0	12.2	0
113	15.9	7.9	0.2	0
128	23.2	174.2	113.4	0
191	14.9	14.9	1.6	0
199	15.0	89.5	13.1	0
202	10.9	14.9	1.1	0
204	9.3	0	1.3	0
231	28.2	471.5	506.5	0
255	14.3	148.5	0	0
266	16.7	11.4	3.2	0
267	15.8	11.1	100.9	0
279	16.5	150.2	51.1	0
323	30.4	672.8	937.2	1384
324	11.8	234.1	242.4	423.9
352	20.0	431.1	220.5	0
360	8.7	239.2	0.2	0

Table 7.4 summarises the measured and simulated values of daily total discharge at the outlet of the study area for application of both options of the BEACH model. While the results of BEACH-CN correspond well with the observed values of total discharge, BEACH-Bucket predicts the total discharge poorly: it predicts discharge at the outlet of the catchment for only two days during the simulation period. Twelve discharge events with magnitudes of more than 100 m^3 were recorded during 2004 and for 9 (75 percent) of them BEACH-CN also simulated discharge at the outlet of the Catsop catchment (Figure 7.11).

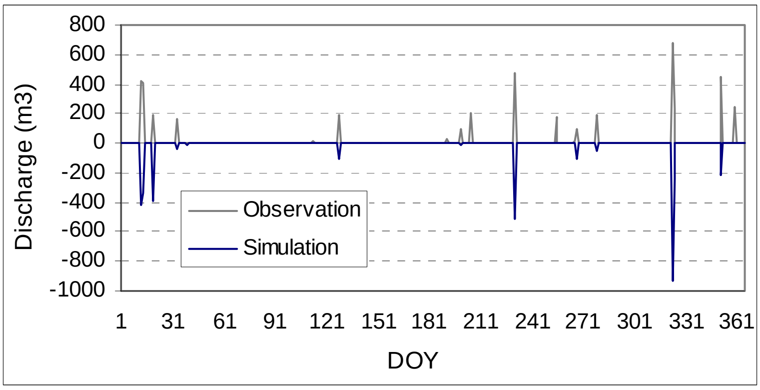

Figure 7.11. Observed (positive) vs. values of total discharge simulated (Negative) with the BEACH-CN model in the Catsop catchment, South Limburg, the Netherlands.

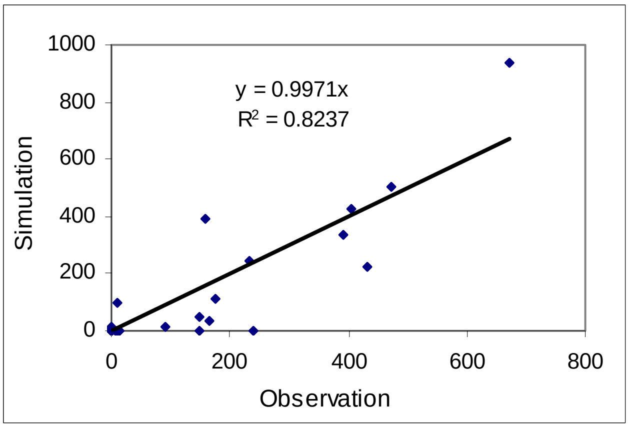

Figure 7.12. Simulated (BEACH-CN) versus observed values of total discharge (m^3) of the Catsop catchment, South Limburg, the Netherlands.

In Figure 7.11 the simulated values of total discharge have been inverted (negative values) in order to avoid overlap of observed and simulated discharge and to facilitate visual comparison. BEACH-Bucket predicted 1384 and 424 m^3 total discharge for days 323 and 324, respectively (Table 7.4).

On day 323, the total discharge was highest both for the observations and for BEACH-CN: respectively 673 and 937 m^3. The coefficient of determination (R^2) and Nash–Sutcliffe efficiency of daily discharge predicted by the BEACH-CN are 0.824 (Figure 7.12) and 0.786, respectively. These results are similar to those reported by Frankenberger et al. (1999). Using the Soil Moisture Routing (SMR) model for a small catchment (170 ha) they obtained a coefficient of determination and Nash–Sutcliffe efficiency of respectively 0.73 and 0.64 for daily streamflow. SMR is also a spatially distributed conceptual model that has been developed for shallow soils over impermeable or less permeable bedrock. Since BUDGET is a point-scale 1D model, it gives only the depth of surface runoff generation at each simulation point, without any possibility for routing and integrating the generated surface runoff to the outlet. To run the BUDGET model, the same values of input parameters as in the BEACH model were used. BUDGET predicts high surface runoff generation for all land use types (left-hand side of Figure 7.13). Both options of BEACH predict negligible surface runoff generation for grassland, orchard, and wheat (right-hand side of Figure 7.13).

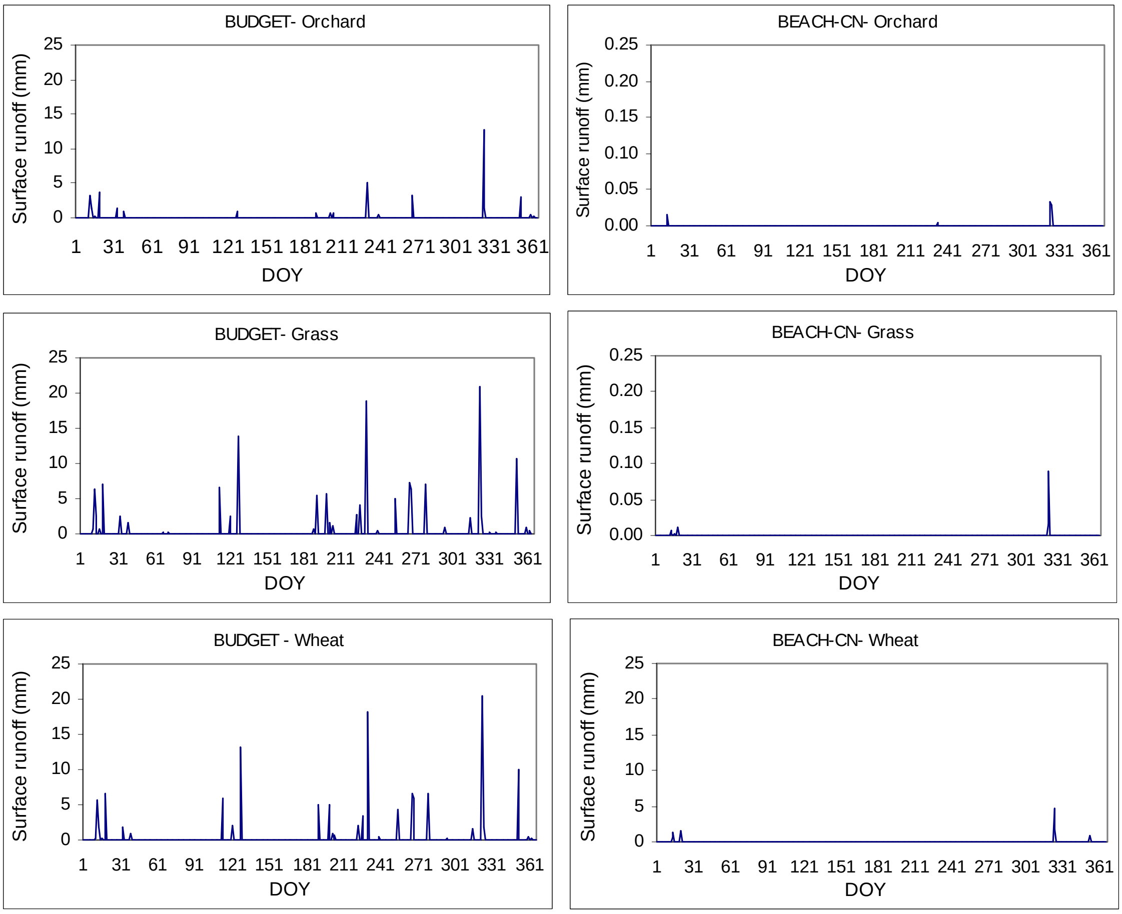

Figure 7.13. Comparison of surface runoff predicted by the BUDGET and BEACH-CN models, for three different land use types in the Catsop catchment, South Limburg, the Netherlands.

Although both the BEACH-CN and BUDGET model implement the CN approach for infiltration and surface runoff generation processes, BUDGET predicts higher values of surface runoff for most days with considerable precipitation rate, even for days on which no runoff was observed at the catchment outlet. This is so because in the BUDGET model the CN_2 is calculated on the basis of the given physical soil parameters (e.g. saturated hydraulic conductivity), whereas in BEACH-CN values of CN_2 are entered as user-specified input parameters. Since the values of saturated hydraulic conductivity were small in the Catsop area, the BUDGET model calculated high values of CN_2 for all land use types and consequently high values of surface runoff generation were estimated.

Saturated hydraulic conductivity has great spatial variability and is difficult to measure accurately. Therefore measured values are usually prone to large uncertainties and in most hydrological models the optimum value is obtained by a parameter optimisation procedure. Being aware of these problems, when BEACH was being developed it was decided to use a user-specified and standalone value of CN_2 without relating it to the saturated hydraulic conductivity.

BEACH integrates the surface runoff from across the catchment to the outlet and the daily discharge is assumed to be the sum of surface runoff generated anywhere in the catchment. The small size of the study area and the large time scale of the BEACH model prevent the surface runoff routing and calculation of the re-infiltration along the routing direction. Therefore, the model can only be expected to give reliable results on the occurrence of runoff and not on the exact volume of discharge.

7.5 Conclusion

The results of the application of the BEACH model to a small catchment in South Limburg in the Netherlands showed that it has an acceptable capability to provide the spatially distributed initial soil moisture content of the root zone profile which is necessary for event-based surface runoff generation and soil erosion models. Our results have demonstrated that different methods of calculating the infiltration and surface runoff generation do indeed produce a high variation in the simulation results of different models. For instance, using the simple bucket concept in the BEACH-Bucket did not generate surface runoff for most of the days with appreciable precipitation (>10 mm d^{-1}). Using the SCS CN method resulted in a time series of daily discharge which agreed well with its measured counterpart. However, the soil moisture prediction with BEACH-CN is less accurate than the one with BEACH-Bucket.

A comparison of different model evaluation criteria indicated that in general, when one criterion showed good performance of the model, the other criteria did too. However, there were notable exceptions. For instance, the RMSE of simulated values of soil moisture in the second layer of *Grass A* is the same magnitude for all models, while their *IA* differs significantly. Generally speaking, the values of RMSE agreed well with the results of previous studies (Frankenberger et al., 1999; Heathman et al., 2003; Wegehenkel, 2005;

Sheikh & Van Loon, 2006). But whereas most of those studies used the physically based Richards equation with an extensive parameter optimisation at a point scale, the BEACH model assembles simple equations and in a spatially distributed manner.

Since the BEACH model has been developed in the PCRaster environment, its results can easily be linked to the detailed soil erosion models such as LISEM and EUROSEM. LISEM is completely integrated in PCRaster and the EUROSEM code has also been translated into the PCRaster code (Visser et al., 2005; Van Dijk and Karssenberg, 2000). As outlined in Chapter 4 of this thesis these models are sensitive to initial soil moisture content and require its information in a spatially distributed format. In a further study, the coupling of these models to BEACH should be investigated. These issues require further attention in future studies.

BEACH can be used as a useful computer-based training package for teaching distributed water balance modelling and land use scenario analysis. The code is written as easily understandable sequences of commands.

Chapter 8

Synthesis

8 Synthesis

8.1 Introduction

The root zone soil moisture content is an insignificant component of the global water budget in magnitude but is very important in controlling the magnitude (or share) of other components such as evapotranspiration, surface runoff generation and aquifer recharge. It is widely considered as an important variable in many environmental studies such as hydrology, agrohydrology, meteorology, climate change, and soil erosion and non-point source pollution. Therefore accurate information on soil moisture content over a study area is crucial for water resources management, flood forecasting, drought forecasting, soil erosion control studies of global climate change. Regional soil moisture information is usually obtained either by monitoring or by modelling. Despite increasing advances in both observation technology and modelling techniques, the provision of soil moisture information at the right spatial and temporal resolution is not yet practical. This problem is mostly due to the high spatial and temporal variability of soil moisture content.

Initial soil moisture content has been shown to be the most sensitive input parameter for most (if not all) event-based hydrological models (Chapter 4 and references therein). LISEM is a typical spatially distributed event-based hydrology and soil erosion model. At the start of a simulation it requires spatially distributed values of initial soil moisture content. Given the difficulties and limitations associated with obtaining observations close before a rainfall event and at the right spatial resolution, the question arose of how to provide the spatially distributed values of initial soil moisture content over a study area in order to obtain reliable simulation results with the LISEM model. That was the main research question addressed by this PhD research. More specifically, an answer was sought for the following subsidiary research questions:

1. How sensitive is the discharge or overland flow predicted with the LISEM model to initial soil moisture content at different depths of root zone profile?

2. What is the relationship between the soil moisture content of the root zone, topography, land use and land management practices in a small-scale catchment?

3. How adequate is a one-dimensional unsaturated zone model for describing the soil moisture dynamics at the catchment scale?

4. How can the requirement for large amounts of data at the beginning of each new event be avoided by using a buddy model that links events?

5. How can qualitative observations in the form of visible and near infrared photography be used to reduce parameter uncertainty and therewith also the reliability of LISEM predictions?

The field data from the experimental catchment of Catsop (0.42 km^2) in South Limburg, the Netherlands were used when investigating these research questions in detail.

Chapters 4 to 7 addressed the first four questions separately. The last question remained unanswered, as the planned approach had to be abandoned due to the failure of equipment. Chapter 3 described in detail the methods and equipment used for data collection, and the advantages, disadvantages, successes and failures. In the current chapter, the findings presented in the previous chapters will be integrated into a more general synthesis in order to highlight the achievements of this research and also to identify future research needs. As noted in the general outline of the thesis (Chapter 1), first the soil moisture measurement procedures and problems are discussed. In section 8.3, the results of investigation on the influence of errors in measured or predicted values of soil moisture content on the surface runoff simulation by the LISEM model will be given. Then the relation between soil moisture content and terrain and land use factors for the Catsop catchment are briefly described. In section 8.5, soil moisture modelling procedures, advantages and disadvantages of different soil moisture models, and the application of various types of models to the study area will be discussed. In the final section the major conclusions of this thesis and recommendations for future studies are presented.

8.2 Soil moisture monitoring

There have been steady improvements in soil moisture measurement methods during the last 60 years; however, the introduction and advances of electromagnetic (EM) methods during the past 20 years are considered to be a revolutionary step in soil moisture monitoring. Currently there are different techniques of soil moisture measurement based on EM methodology, but most of them not operational at this time (Topp, 2003). Exceptionally, Time Domain Reflectometry (TDR) as an operational EM technique has been used extensively in many soil water balance studies and model calibration and evaluation (Chapter 6 and references therein). Most previous studies have reported considerable errors in the measured values of soil moisture content due to factors such as waveguide shape, length of cables, air gaps, disturbance of soil samples, soil temperature and soil density.

Generally speaking, soil moisture monitoring methods are classified into two main groups: in situ and remote sensing measurements. While most of the currently available in situ measurements tools can potentially provide continuous estimates of soil moisture values at a point scale over entire soil profile, remote sensing gives intermittent snapshots of spatially distributed soil moisture information at the footprint scale over a limited and variable soil depth (between 2 and 20 cm). Both in situ and remotely sensed soil moisture data are prone to large errors. The sole standard and direct method of soil moisture measurement is the thermogravimetric method. This method is time-consuming and destructive to the sampled soil, thus cannot be used for iterative measurement at a fixed location. It is mostly used as a reference method for the calibration of other methods. The Soil Moisture Neutron Probe (SMNP), developed more than 50 years ago, is a longstanding, well-established method for measuring soil moisture in deeper layers (> 30 cm). It has been one of the most accurate methods to date. However, regulations concerning the use of radioactive sources and impossibility for automated and unattended data acquisition have limited its usefulness. The newer methods which apply electromagnetic (EM) allow data logging and unattended measurement of soil moisture content, but with limited precision and accuracy and relatively small support (Chapter 3).

The three different devices applying the TDR technique used in this study resulted in considerable errors. The Theta Probe which is suitable for surface layer (5 cm) soil moisture measurement resulted in smaller errors than the TRIME-FM which is used in access tubes for profile moisture measurements. The disparity between the results of these two devices is largely related to the effects of an air gap between the waveguides and surrounding soil. With the Theta Probe, the thin cylindrical (diameter = 1.5 mm) waveguides are inserted directly into the ground, so there is close contact between them and the soil. However, in case of TRIME-FM the presence of air gaps (due to deviations during augering) between the access tubes and surrounding soil induced large errors in measurements. The effect of an air gap is intensified by the small measurement volume of TRIME-FM (the effective penetration depth of measurement field is up to 100 mm into the soil) and the high sensitivity in the immediate vicinity of the access tube. It appeared to be impossible to avoid air gaps between the access tube and surrounding soil. In addition, in this study one of the most recent soil moisture monitoring devices, e-SENSE, (see Chapter 3) was used. In this system, intelligent sensors are installed in the field and connected to a modem or a central computer station. In this study, six sensors were installed in the field and connected to 3 modems which relayed the measured data as SMS codes to the internet database (www.longcat.nl). Though these sensors failed to function in the first year (2004) of study they showed promising results the next year. This system requires a further evaluation study in the field. If it proves to give reliable soil moisture data, then more insightful information on soil moisture dynamics and their temporal variation can be obtained.

8.3 Impacts of soil moisture uncertainty on surface runoff simulation

Although the root zone soil moisture content controls most (if not all) of the hydrological processes occurring at or near the land surface, its influence on infiltration and surface runoff generation processes has been studied most thoroughly. The reason for this is that soil erosion and inundation (especially the former) are the most tangible on-site and off-site problems induced by infiltration and surface runoff generation processes. As a result of this research focus, many simulation models have been developed to simulate these processes. Apart from being convenient vehicles to summarise and test scientific knowledge, simulation models provide important tools for scenario analysis and decision-making for appropriate soil and water resources management. In addition, simulation models and their results are useful tools for researchers to communicate with stakeholders (e.g. policy makers at several levels and land owners, water companies, environmental agencies). To be reliable tools, the uncertainty of these models should be limited to an acceptable range. To limit the uncertainty of a model, the sources of uncertainty and their magnitude should be known; sensitivity analysis is the correct measure for acquiring this knowledge.

The LImburg Soil Erosion Model (LISEM) is a typical event-based simulation model, designed for the purposes described previously. It is a hydrology and soil erosion model, originally developed to investigate the impacts of different soil and water conservation measures in South Limburg, the Netherlands. Its application has been further expanded to other areas of the world as a tool in soil erosion assessment and modelling. Therefore a sensitivity analysis of the model will provide useful information about the collection of appropriate input data and also the reliability of the simulation results. A literature review revealed that two previous studies have investigated the sensitivity of the LISEM model (De Roo et al., 1996; and Jetten et al., 1998). In these studies the saturated hydraulic conductivity (Ksat) was found to be the most influential parameter for almost all processes. Initial soil moisture was not included in the study by Jetten et al. (1998); the study by De Roo et al. (1996) ranked it as one of the less important parameters (although they used pressure head for calibrating the LISEM model in their study). Both of these studies applied an OAT (One factor-At-a-Time) type of sensitivity analysis, which overlooks interactions and non-linear effects. On the other hand, the literature review indicated that initial soil moisture content is the most sensitive parameter for most other similar models (Chapter 4). Furthermore, previous studies have only studied the impact of initial soil moisture content in the surface layer. Therefore in Chapter 4 a broad sensitivity analysis of the LISEM model to initial soil moisture content in two soil layers, considering seven topsoil/soil depth configurations (5/95, 10/90,15/85,20/80,25/75,30/70, and 40/60 cm), two rainfall events and two infiltration models (Green–Ampt and Richards) was carried out. The soil moisture in each layer was varied from 0.05 to 0.40 $cm^3\ cm^{-3}$ in intervals of 0.05 $cm^3\ cm^{-3}$. The results showed that the sensitivity of predicted discharge to the initial soil moisture condition depends highly on the infiltration model, the event properties, topsoil/subsoil depth configuration and the initial condition itself. In other words, there are interaction effects between these factors. Among the factors considered, the most pronounced was the effect of different infiltration models. For the Richards model the relation between discharge and initial soil moisture was highly nonlinear and with pronounced interaction effects of other variables, but for the Green–Ampt model the relation was much more linear. In Chapter 4 it was concluded that topsoil depth has a major influence on the discharge calculated by the Richards model, whereas it rarely affects discharge calculated by the Green–Ampt model. The initial condition of soil moisture in the second layer hardly influences the calculated discharge when the topsoil is thicker than

30 cm. It was also concluded that the initial soil moisture has a large influence on discharge prediction, particularly when a rainfall event is less intensive and surface runoff constitutes only a small fraction of the precipitation. In general, changes of approximately 0.05 $cm^3\ cm^{-3}$ in the initial condition of surface layer soil moisture in the case of a less intensive rainfall event resulted in changes of -25 to +50 percent in the discharge calculated by the Green–Ampt model, depending on topsoil/subsoil depth configuration and initial condition of the second layer. In the case of the Richards model the change varied from -100 to +100 percent.

8.4 Impacts of land use and terrain factors on soil moisture

It is well known that spatial heterogeneity in topography and soil, and spatio-temporal variation in vegetation and weather result in highly variable soil moisture content at various scales. This knowledge has been gained by frequent studies in the past investigating the relation between soil moisture and topography as well as the relation between soil moisture and land use. Chapter 5 has cited some of these studies. A careful review of these studies, however, indicates that the particular relations vary significantly between the studies. Obviously some of these differences are induced by differences in the local conditions (e.g. climate, geology, human influence, etc.) of the areas studied, but they also seem to be attributable to differences in the spatial and temporal scale of studies. Therefore in Chapter 5 it was attempted to define the most important factors controlling the soil moisture dynamics within the Catsop catchment when the spatial and temporal scales of the study vary.

The Catsop catchment has an undulating topography, heterogeneous land use and contains deep, well-drained soils with a high retention capacity. Under these conditions it is unclear whether soil moisture patterns (both laterally and vertically) arise due to topography or land use effects. A Generalised Additive Model (GAM) was employed to find the relationship between various influencing factors and soil moisture at various spatial (catchment, response unit, hill slope and plot) and temporal (monthly, two-weekly, and weekly) scales. The results showed that the importance of land use variables varies with temporal resolution. At a coarse resolution, land use is unimportant, whereas at finer temporal resolutions it becomes more relevant. Land use is equally important over all spatial resolutions. The influence of topography is most pronounced at the plot scale. At the hill slope scale, the wetness coefficient and crop cover are the most effective terrain and land use variables, whereas at the plot scale, the upslope area and the topographical index are important. In general, the results of this study showed that the impacts of terrain and land use factors on soil moisture distribution are scale-dependent and that separate models should be identified for different scales.

8.5 Soil moisture modelling

As mentioned in the section 8.3 and Chapter 4 of this thesis, the LISEM model shows a high sensitivity to profile-averaged moisture content, especially within the top 30 cm. On the other hand, currently there is no observation method that can provide soil moisture measurements at the appropriate spatial and temporal resolution, especially when soil moisture information on deeper layers is required. Therefore soil moisture modelling is usually used as an alternative method to generate soil moisture data.

During the past few decades the many experimental studies on infiltration and water movement in soil profiles have resulted in considerable progress in the conceptual understanding and mathematical description of soil water dynamics within the unsaturated zone. This progress has resulted in the development of various soil water dynamic models with different levels of complexity, process description, data requirement and scale of applicability. In general, existing models in hydrology are distinguished into three types, namely 1) empirical models (data-based models); 2) conceptual models; and 3) physically-based models. Each type has its advantages and disadvantages. Empirical models are purely data-based and often spatially lumped at the catchment scale. Conceptual models are often semi-distributed and based on the representation of a catchment as a series of internal storages linked through fluxes. Physically based models are based on conservation laws (mostly mass, but occasionally momentum and energy as well) and also on the solution of partial differential equations; hence these models are by definition spatially distributed. In the current PhD study a wide variety of models with different bases and complexities was used. At least one soil water balance model from each type of model was applied and evaluated with the data measured in the experimental catchment of Catsop.

8.5.1 Empirical models

Empirical models are based on the analysis of observations and are therefore stochastic in nature. They usually require less input data and computational time than the conceptual and physically based models. They use available time-series of input and output variables to derive both the model structure and the corresponding parameter values. These models are often criticised for ignoring the prior knowledge about the flow processes, heterogeneity in inputs, and non-linearity in the catchment system. However, the insufficient knowledge about integral flow processes that occur within the catchment and the lack of appropriate spatially distributed input data favour the development and application of these models. Empirical models are frequently used in preference to more complex models, as they can be used in situations with limited data and input parameters, because they are usually spatially lumped and treat the catchment as a single unit. Apart from having a proven use for prediction, empirical models provide a useful tool for model identification, particularly in the first step of the modelling procedure.

Recent examples of empirical modelling techniques in soil moisture dynamics are the application of Artificial Neural Networks (ANN, Jiang and Cotton, 2004), self-organising maps (Schütze et al., 2005), and Data-Based Mechanistic models (DBM, Young, 1998). DBM models are not absolutely empirical models; the modelling procedure starts with data analysis but the physical knowledge is used *a posteriori*. Generalised Additive Models (GAM) are other data-based models that have been used as valuable research tools in biological modelling since the early 1990s, but they have rarely been applied for hydrological modelling. In Chapter 5 a hierarchical Generalised Additive Model (GAM) was used for water balance modelling in the Catsop catchment. The GAM applied in Chapter 5 defines the water balance as sum of non-parametric non-linear components. Each water balance component is parameterised as a function of topographical variables, land use variables, weather variables, or antecedent soil moisture. The application of a GAM for the Catsop catchment at various spatio-temporal scales showed that it can be used as an efficient tool for identifying dominant processes over a range of scales. Though it facilitates a straightforward sensitivity analysis to evaluate e.g. the importance of bio-physical factors, relative to forcing or state variables, no such analysis was done in this thesis. Identifying these dominant processes makes it easier to build suitable conceptual models for predicting soil moisture at different scales of interest. The evaluation of profile soil moisture predictions with the GAM at various scales indicated that it gives a comparable or even better result than a simple autoregressive model with a time lag of one day (AR1) and the physically based Soil–Water–Atmosphere–Plant (SWAP) model.

8.5.2 Physically-based models

Physically-based models are based on the solution of fundamental physical equations describing the processes within a real world situation. In theory, it is assumed that the parameter values in these models can be obtained from measurements as long as the models are used at the appropriate scale. In hydrology, following the proposition of the blueprint for physically based, computer simulation models in hydrology by Freeze and Harlan (1969), a wide variety of physically based models have been developed. Nearly all the currently available physically-based water flow models apply the Richards equation, which is a combination of standard equations of conservation of mass and momentum. Most of the dynamic unsaturated zone models solve the Richards equation in a 1D vertical direction at point scale and under specific assumptions and boundary conditions (Chapter 6). In practice, these models are implemented at larger units, up to the catchment scale by discretising the catchment into small grid cells and specifying a parameter set per grid cell (Merritt et al., 2003). Since the Richards equation is a continuous equation, the veracity of scaling up parameters from point to grid is questionable (Beven, 1989). The lack of enough data and their large computational demand make these models it difficult to apply in a fully distributed manner. Generally speaking, the physically based models are applied at a much larger scale than the parameters' measurement scale. Therefore effective parameter values are estimated by regionalisation based on land use, soil, and topographical characteristics or a combination of these, and then adjusted by calibration. This leads to loss of physical significance, as well as problems of overparameterisation and equifinality (Beven, 1993; Savenije, 2001). A review of the hydrological literature revealed that 1D Richards-based models are applied at all levels of aggregation (i.e. from point scale to hydrological response units), though it is theoretically impossible to derive effective parameters for the non-linear Richards equation by simple aggregation or disaggregation procedures (Kim and Stricker, 1986). Many studies have ignored this fact and investigated the derivation of Mualem–Van Genuchten parameters by both aggregation and disaggregation (see e.g. Pachepsky and Rawls 1999; Zhu et al. 2006).

In light of the above, in Chapter 6 of this thesis the question was raised of how model parameterisation and model performance can be compared across different scales. To answer this question the parameterisation and predictive performance of SWAP model were investigated when applied at point, field, response unit and catchment scale. Detailed field observations from the experimental catchment of Catsop were used in this investigation. Two different calibration validation schemes (interpolation versus extrapolation) and three performance statistics (root mean squared error (RMSE), Index of Agreement (EF_{IA}), and the Nash–Sutcliffe coefficient (EF_{NS})) were studied. In all cases, the same Levenberg–Marquardt optimisation scheme was applied. Predictions by SWAP appeared to be highly sensitive to the shape parameters (α and n) of the Mualem–Van Genuchten equations. For this reason, the values of the shape parameters for each layer (0–20, 20–40, and 40–80 cm) of soil profile were optimised, while the other parameters were constrained at fixed values. Contrary to expectations, a calibration-validation scheme based on interpolation led to worse performance than a scheme based on extrapolation. It was concluded that the low observation frequency (intervals of approximately two weeks) in the interpolation scheme was the most likely explanation for overlooking the essential dynamics of the soil moisture dry-down cycle. When one particular model parameterisation was used across the various aggregation levels, the optimal values for the Mualem–Van Genuchten parameters α and n at higher aggregation levels were very close to the arithmetical means of these parameters at lower levels of aggregation. These results confirm that in practice, parameters at a coarser aggregation level can be derived from an underlying level by simple arithmetical averaging. The different performance indices were highly variable between observation locations and for different aggregation levels. Overall, the indices were more favourable at higher aggregation levels, and corresponded with errors reported in comparable studies. Comparing the measured soil moisture content in each individual tube with the simulated soil moisture of the pertinent group at different aggregation levels suggested that when the aggregation level was increased, RMSE increased too. Comparing different performance indices showed that there was no clear relation between these indices. The Nash–Sutcliffe coefficient in particular sometimes deviated from the other indices. When soil layers were considered individually, EF_{IA} and EF_{NS} were somewhat related, whereas RMSE was unrelated to the other two indices. However, the relation between EF_{IA} and EF_{NS} become much stronger upon averaging, whereas a relation with RMSE remained absent. The more favourable values of performance indices and the stronger correlation of EF_{IA} and EF_{NS} at higher levels of aggregation corresponded with the favourable results of lumped models, which were usually evaluated with data on discharge at the outlet of catchments.

Considering the three indices together, the performance of the SWAP model for each separate layer was not satisfactory. However, when averaging over the soil layers, the model predictions were judged as sufficient. Considering RMSE alone, the results were comparable with similar studies in the literature.

8.5.3 Conceptual models

Conceptual models, which lie somewhere between empirical models and physically based models, are based on a conceptualisation of a real world watershed as a system of storage elements. In contrast to the empirical models, in conceptual models the model structure is specified *a priori* e.g. the number of stores (states) and fluxes, and the parametric description of the flux–state relations. However, in contrast to physical models, conceptual models include only a general description of the catchment processes, without specifying details of process interactions. Like empirical models, the parameter values for conceptual models are obtained through calibration against observed data such as outlet discharge.

Due to the difficulties in application of physically based models as well as the lack of physical significance of empirical models, conceptual models are the models most frequently developed and applied by hydrologists. Currently, there is a wide variety of conceptual models, which differ from each other in terms of the mathematical representation of the component processes, spatial and temporal scale of application, number of parameters and input data required. Most of the conceptual hydrological models have been developed in a spatially lumped manner. However, the emergence and refinement of remote sensing products have made available spatially distributed terrain and land use data. These data have stimulated the development of conceptual models that are spatially distributed or semi-distributed in nature (e.g. SMR model (Frankenberger et al., 1999) and DREAM model (Manfreda et al., 2005)). The best known example of this model type is TOPMODEL (Beven et al., 1995). Parameters in this type of model, however, lack physical meaning and cannot be measured in the field. Therefore parameter values are usually optimised using the observed discharge data at the catchment outlet, which leads to the problems associated with parameter identification and equifinality, similar to the problems with physically based models (Beven, 1993; Zhang and Savenije, 2005). These problems can be minimised by reducing the number of parameters to be estimated through calibration (Wheater et al., 1993) or by calibrating the parameters through spatially distributed data such as soil moisture content (Chapter 7).

In general, simpler models are believed to have fewer problems with model identification than more complex models (Merritt et al., 2003). In Chapter 7 of this thesis, two simple conceptual models were applied to the Catsop catchment. The first model was a 1D soil water balance model named BUDGET. BUDGET is composed of a set of validated subroutines describing the various processes involved in water extraction by plants and water movement in the soil profile (Raes, 2002). The other model, BEACH, was developed during the current PhD study (Chapter 7). BEACH is a spatially distributed simple soil water balance, which is implemented in the PCRaster GIS. It operates on time-steps of a day, using daily meteorological records, soil physical properties, basic crop characteristics and topographical data. The basic processes incorporated in the model are precipitation, infiltration, transpiration, evaporation, lateral flow, vertical flow and plant growth. The main motivation for the development of this model was the need for distributed event-based surface runoff and soil erosion models (e.g. LISEM and EUROSEM) for spatially distributed information on antecedent soil moisture content.

The application of the BEACH model to the Catsop catchment showed that it is able to estimate spatially distributed values of soil moisture content. The root mean squared error of the predicted soil moisture content for 6 monitored locations within the catchment ranged from 0.011 to 0.065 $cm^3\ cm^{-3}$. The predicted daily discharge at the outlet of the study area also agreed well with the observed data. The coefficient of determination and Nash–Sutcliffe efficiency of the predicted discharge were 0.80 and 0.77, respectively. The soil moisture values BUDGET predicted were comparable to those predicted by the BEACH model.

8.6 Conclusion and recommendations for soil moisture monitoring and modelling

Soil moisture content exhibits a high spatio-temporal variation over a study area and is one of the most sensitive and critical parameters for most event-based hydrological and soil erosion models (Chapter 4). This study focused on putting new observation technology into operation (Chapter 3) and on modelling techniques (Chapters 5, 6 and 7) to obtain soil moisture information at a resolution fine enough for event-based hydrology and soil erosion models. It appeared that despite the advances in monitoring and modelling techniques, there are still large uncertainties associated with soil moisture information at the correct spatial and temporal resolution. In the following paragraphs the major conclusions of this thesis and some ideas for future research are presented.

At present there is no observation method that can prove its value at the correct spatial and temporal resolution, especially when the soil moisture information is required over a study area and in a deeper layer of the soil profile (Chapter 6). Therefore, inevitably, the way to obtain the spatial (horizontal and vertical) and temporal distribution of soil moisture over a study area is to apply hydrological models and data assimilation techniques.

In general, soil moisture measurements in deeper layers are prone to larger errors. In the case of TRIME-FM this is mostly due to the small measurement volume by TRIME-FM and to air gaps between access tube and surrounding soil which are generated by deviation during augering or heterogeneities in the soil profile. To reduce the measurement errors, it is recommended to increase the measurement volume of TRIME-FM by increasing the effective depth of EM wave penetration and enlarging the contact area of the sensors (waveguide aluminium plates).

A simple sensitivity analysis method such as OAT is not sufficient for a nonlinear complex model such as LISEM, which has a large number of input variables and parameters that probably have interaction effects (Chapter 4). Complex models with many input factors should be subjected to more elaborate sensitivity analysis schemes. The results of this analysis should then be interpreted with multiple regression techniques (including GLM and GAM).

The impacts of land use and terrain factors on the spatio-temporal distribution of soil moisture content are scale-dependent. In other words, the most influential factors at a specific spatio-temporal scale might not be relevant at another scale. For instance, land use variables are not important for soil moisture modelling at large temporal scales (monthly or seasonally), or topography is only influential for soil moisture modelling at plot and hill slope scale. Therefore it is recommended that the model identification for different scales should be carried out separately. Furthermore, the validation of a model developed for a specific scale should be taken as a validation for model application at a different scale. In addition, scale differences should be taken into account when comparing model results reported in different studies.

The performance evaluation of the various soil moisture models in this study showed that in spite of large differences in the complexity and structure of the models, the simulation quality was similar. This is partly due to the large errors in the observed hydrological data used for model evaluation. These errors are often so large that they overshadow any differences resulting from the differing capabilities of various models. For instance, in the current study, the errors in soil moisture observation were remarkably large (Chapter 3).

We did not succeed in deriving a meta-model to scale model performance indices with aggregation level. Multi-scale calibration studies will therefore remain useful for comparing the results from unsaturated zone models at different levels of aggregation (Chapter 6). However, such a meta-model would be extremely useful; this topic deserves much more attention than the little research that has been done so far.

Despite the possibility of giving a physical description of soil water flux (and other relevant processes like evapotranspiration), physically based dynamic unsaturated zone models have limited use in practice for catchment scale studies, because it is very difficult to accurately specify all model input parameters, initial and boundary conditions without an extensive optimisation process. When spatial variability is considered, it even becomes more difficult (or impossible) to obtain a unique optimal parameter set. For studies at the catchment scale, it is therefore more useful to investigate ways to connect physically based models with conceptual models (which have better prospects for practical use) than to design physically based models of ever-increasing complexity.

References

Acs, F. 1994. A coupled soil-vegetation scheme: description, parameters, validation, and sensitivity studies. *Journal of Applied Meteorology, **33**: 268 – 284.*

Ahuja, L.R., Lehman, O.R. 1981. A theoretical analysis of interflow of water through surface soil horizons with implications for movement of chemicals in field runoff. *Water Resources Research, **17**: 1091 – 1105.*

Akinremi, O.O., McGinn, S.M., Barr, A.G. 1995. Simulation of soil moisture and other components of the hydrological cycle using a water budget approach. *Canadian Journal of Soil Science, **75**: 133 – 142.*

Allen, R.G., Pereira, L.S., Raes, D., Smith, M. 1998. Crop evapotranspiration. Guidelines for computing crop water requirements. Irrigation and Drainage Paper 56, FAO, Rome, Italy, 300p.

Bagarello, V., Iovino, M. 2003. Field testing parameter sensitivity of the two-term infiltration equation using differentiated linearization. *Vadose Zone Journal **2**: 358 – 367.*

Belmans, C., Wesseling, J.G., Feddes, R.A. 1983. Simulation of the water balance of a cropped soil: SWATRE. *Journal of Hydrology, **63**: 271 – 286.*

Beven, K.J. 1981. Kinematic subsurface stormflow. *Water Resources Research, **17**: 1419 – 1424.*

Beven, K.J. 1989. Changing ideas in hydrology – the case of physically based models. *Journal of Hydrology*, ***105:*** *157 – 172.*

Beven, K.J. 1993. Prophecy, reality and uncertainty in distributed hydrological modeling. *Advances in Water Resources,* ***16:*** *41 – 51.*

Beven, K.J. 1995. Linking parameters across scales: Subgrid parameterizations and scale dependent hydrological models. In: J. D. Kalma and M. Sivapalan (Editors), Scale Issues in Hydrological Modelling. Wiley, Chichester, UK. 263 – 281.

Beven, K.J., Kirkby, M.J. 1979. A physically-based variable contributing area model of basin hydrology. *Hydrological Science Bulletin, **24**: 43 – 69.*

Beven, K.J., Lamb, R., Quinn, P., Romanowicz, R., Freer, J. 1995. TOPMODEL, In: Singh, V.P. (Editor), Computer models of watershed hydrology. Water Resources Publications, USA, 627 – 668.

Binley, A., Elgy, J., Beven, K. 1989. A physically based model of heterogeneous hillslopes. 1. Runoff production. *Water Resources Research, **25**: 1219 – 1226.*

Black, T.A., Gardner, W.R., Thurtell, G.W. 1969. The prediction of evaporation, drainage, and soil water storage for a bare soil. *Soil Sciences Society of American Journal, **33**: 655 – 660.*

Blöschl, G., Sivapalan, M. 1995. Scale issues in hydrological modeling: a review. *Hydrological Processes, **9**: 251 – 290.*

Boesten, J.J.T.I., Stroosnijder, L.1986. Simple model for daily evaporation from fallow tilled under spring conditions in a temperate climate. *Netherlands Journal of Agricultural Science,* ***34****: 75 – 90* (downloadpdf).

Bronstert, A., Bardossy, A. 1999. The role of spatial variability of soil moisture for modeling surface runoff generation at the small catchment scale. *Hydrology and Earth System Sciences,* ***3****: 505 – 516.*

Burt, T.P., Butcher, D.P. 1985. Topographic controls of soil moisture distributions. *Journal of Hydrology,* ***36:*** *469 – 486.*

Chen, F., Mitchell, K., Schaake, J., Xue, Y., Pan, H.L., Koren, V., Duan, Q.Y., Ek, M., Betts, A. 1996. Modelling of land surface evaporation by four schemes and comparison with FIFE observations. *Journal of Geophysical Research,* ***101(D3)****: 7251 – 7268.*

Chen, X., Hu, Q. 2004. Groundwater influences on soil moisture and surface evaporation. *Journal of Hydrology,* ***297****: 285 – 300.*

Chen, Z., Govindaraju, R.S., Kavvas, M.L. 1994. Spatial averaging of unsaturated flow equations under infiltration conditions over areally heterogeneous fields 2. Numerical simulations, *Water Resources Research,* ***30****: 535–548.*

Cleveland, W.S. 1979. Robust Locally Weighted Regression and Smoothing Scatterplots. *Journal of the American Statistical Association,* ***74:*** *829 – 836.*

Coles, N., Sivapalan, M., Larsen, J., Linnet, P., Fahrner, C. 1997. Modelling runoff generation of small agricultural catchments: Can real world runoff response be captured? *Hydrological Processes,* ***11****: 111 – 136.*

Crave, A.,Gascuel-Odux, C. 1997. The influence of topography on the time and space distribution of soil surface water content. *Hydrological Processes,* ***11:*** *203 – 210.*

Crescimanno, G., Garofalo, P. 2005. Application and evaluation of the SWAP model for simulating water and solute transport in a cracking clay soil. *Soil Sciences Society of American Journal,* ***27****: 1943 – 1953.*

Cressie, N. 1991. Statistics for Spatial Data. Wiley, New York.

Crow, W.T., Ryu, D., Famiglietti, J.S. 2005. Upscaling of field-scale soil moisture measurements using distributed land surface modeling. *Advances in Water Resources,* ***28****: 1 – 14.*

Damoiseaux, J.H., Rosing, H. 1993. Toelichting bij de herziene kaartbladen 59 Peer en 60 West en Oost-Sittard. DLO-Staring Centrum, Wageningen, the Netherlands.

De Bakker, H. 1979. Major soils and soil regions in the Netherlands. Center for Agricultural Publishing and Documentation, Wageningen. Junk & Pudoc publishers, the Hague, the Netherlands.

De Bakker, H., Schelling, J. 1976. System van bodemclassificatie voor Nederland, de hogere niveaus (with 30 pages summary: A system of soil classification for the Netherlands, the higher levels). Pudoc, Wageningen.

De Gier, N. 2004. Changes in landscape and land use that influence water erosion, in Zuid Limburg, the Netherlands. MSc thesis, Erosion, Soil and Water Conservation group, Wageningen University and Research Centre.

De Roo, A.P.J. 1993. Modelling surface runoff and soil erosion in catchments using geographical information systems. Validity and applicability of the "ANSWERS" model in two catchments in the loess area of South Limburg (The Netherlands) and one in Devon (UK). Ph.D thesis. Utrecht University: Utrecht, the Netherlands.

De Roo, A.P.J., Jetten, V.G. 1999. Calibrating and validating the LISEM model for two data sets from the Netherlands and South Africa. *Catena, **37**: 477 – 493.*

De Roo, A.P.J., Offermans R.J.E., Cremers, N.H.D.T. 1996. LISEM: A single event physically-based hydrologic and soil erosion model for drainage Basins. II: sensitivity analysis, validation and application. *Hydrological Processes, **10**: 1118 – 1127.*

De Roo, A.P.J., Riezbos, H.Th. 1992. Infiltration experiment on loess soils and their implications for modeling surface runoff and soil erosion. *Catena, **19**: 221 – 239.*

De Roo, A.P.J., Wesseling, C.G., Jetten, V.G, Ritsema, C.J. 1995. LISEM: Limburg Soil Erosion Model. A User Guide, Version 3.1. Department of Physical Geography, Utrecht University: Utrecht, the Netherlands.

De Roo, A.P.J., Wesseling, C.G., Ritsema, C.J. 1996a. LISEM: a single event physically-based hydrologic and soil erosion model for drainage basins. I: Theory input and output. *Hydrological Processes, **10:** 1107 – 1117.*

Devaurs, M., Gifford, G.F. 1984. Variability of infiltration within large runoff plots on rangelands. *Journal of Range Management, **37(6)**: 523 – 528.*

Diemont, W.H. Van de Westeringh, W. 1978. Graften in Zuid-Limburg: groen of kaal, levend of verwijnend. Tijdschrift Kon. Ned. Heidemij.

Doherty, J. 2002. PEST: Model-Independent Parameter Estimation. Watermark Numerical Computing.

Downer, C.W., Ogden, F.L. 2004. Appropriate vertical discretization of Richards'equation for two-dimensional watershed-scale modeling. *Hydrological Processes, **18**: 1 – 22.*

Dunin, F.X., Aston, A.R. 1981. Spatial variability in the water balance of an experimental catchment. *Australian Journal of Soil Research, **19**: 113 – 120.*

Engman, E.T., Rogowski, A.S. 1974. A partial area model for storm flow synthesis. *Water Resources Research, **10**: 464 – 472.*

Entekhabi, D., Eagleson, P.S. 1989. Land surface hydrology parameterization for atmospheric general circulation models including subgrid spatial variability. *Journal of Climate*, ***2**: 816 – 831.*

Entekhabi, D., Nakamura, H., Njoku, E.G. 1994. Solving the inverse problem for soil moisture and temperature profiles by sequential assimilation of multifrequency remotely sensed observations. *IEEE Transaction of Geosciences and Remote Sensing, **32**: 438 – 448.*

Evett, S., Laurent, J.P., Cepuder, P., Hignett, C. 2002. Neutron scattering, capacitance, and TDR soil water content measurements compared on four continents. 17th WCSS, Symposium No.59, Paper No. 1021, 14 – 21 August 2002, Thailand.

Evett, S., Ruthardt, B., Kottkamp, S., Howell, T., Schneider, A., Tolk, J. 2002. Accuracy and precision of soil water measurements by neutron, capacitance, and TDR methods. 17th WCSS, Symposium No.59, Paper No. 318, 14 – 21 August 2002, Thailand.

Famiglietti, J.S., Rudnicki, J.W., Rodell, M. 1998. Variability in surface moisture content along a hillslope transect: Rattlesnake Hill, Texas. *Journal of Hydrology*, ***210**: 259 – 281.*

Feddes, R.A., Kowalik, P.J., Zarandy, H. 1978. Simulation of field water use and crop yield. Simulation Monographs, Pudoc, Wageningen, the Netherlands, 189p.

Folly, A., Quinton, J.N., Smith, R.E. 1999. Evaluation of the EUROSEM model using data from the Catsop watershed, the Netherlands. *Catena, **37**: 507 – 519.*

Frankenberger, J.R., Brooks, E.S., Walter, M.T., Walter, M.F., Steenhuis, T.S. 1999. A GIS-based variable source area hydrology model. *Hydrological Processes, **13**: 805 – 822.*

Freeze, R.A., Harlan, R.L. 1969. Blueprint for a physically-based digitally-simulated hydrologic response model. *Journal of Hydrology, **9:** 237 – 258.*

Gamerman, D., Moreira, A.R.B, Rue, H. 2003. Space-varying regression models: specifications and simulation. *Computational Statistics & Data Analysis*, ***42:** 513 – 533.*

Georgakakkos, K.P. (Editor.). 1996. Soil moisture theories and observations. Special issue of *Journal of Hydrology, Vol.184, 152pp.*

Giacomelli, A., Bacchiega, U., Troch, P.A., Mancini, M. 1995. Evaluation of surface soil moisture by means of SAR remote sensing techniques and conceptual modelling. *Journal of Hydrology*, ***166**: 445 – 459.*

Goudriaan, J. 1977. Crop meteorology: a simulation study. Simulation Monographs, Pudoc, Wageningen, the Netherlands.

Grayson, R.B., Blöschl, G., Moore, I.D. 1995. Distributed parameter hydrologic modelling using vector elevation data: THALES and TAPES-C. In: Singh, V.P. (Editor), Computer models of watershed hydrology. Water Resources Publications: Highlands Ranch, Colorado.

Grayson, R.B., Western, A.W. 1998. Towards areal estimation of soil water content from point measurements: time and space stability of mean response. *Journal of Hydrology, **207**: 68 – 82.*

Groeneveld, D.A., Daniels, P.J.M. 1985. Korstvorming, doorlaatbaarheid en infiltratiecapaciteit bij lossbodems in Zuid-Limburg. MSc thesis, Department of Physical Geography, University of Utrecht.

Guisan, A., Edwards, J., Thomas, C., Hastie, T. 2002. Generalized linear and generalized additive models in studies of species distributions: setting the scene. *Ecological Modelling, **157:** 89 – 100.*

Hansen, P.C. 1998. Rank-Deficient and Discrete Ill-Posed Problems: Numerical Aspects of Linear Inversion. SIAM, Philadelphia, USA.

Hantush, M.M., Kalin, L. 2005. Uncertainty and sensitivity analysis of runoff and sediment yield in a small agricultural watershed with KINEROS2. *Hydrological Science Journal*, ***50(6)****: 1151 – 1171.*

Hastie, T.J., Tibshirani, R. 1990. *Generalized additive models*. London: Chapman and Hall.

Hastie, T.J. 1991. Generalized additive models. Chapter 7 of Statistical Models in S, J. M. Chambers and T. J. Hastie (editors), Wadsworth & Brooks/Cole.

Hastie, T., Tibshirani, R. 1990. Generalized additive models, Chapman & Hall.

Hawley, M.E., Jackson, T.J., McCuen, R.H. 1983. Surface soil moisture variation on small agricultural watersheds. *Journal of Hydrology,* ***62****: 179 – 200.*

Heathman, G.C., Starks, P.J., Ahuja, L.R., Jackson, T.J. 2003. Assimilation of surface soil moisture to estimate profile soil water balance content. *Journal of Hydrology,* ***279****: 1 – 17.*

Herbst, M., Fialkiewicz, W., Chen, T., Putz, T., Thiery, D., Mouvet, C., Vachaud, G., Vereecken, H. 2005. Intercomparison of flow and transport models applied to vertical drainage in cropped lysimeters. *Vadose Zone Journal,* ***4****: 240 – 254.*

Hessel, R. 2002. Modeling soil erosion in a small catchment on the Chinese Loess Plateau. PhD thesis. Utrecht University, the Netherlands, 317p.

Hijmans, R.J., Guiking-Lens, I.M., Van Diepen, C.A. 1994. User’s guide for the WOFOST 6.0 crop growth simulation model. Technical Document 12, Alterra Green World Research, Wageningen, 144p.

Hillel, D. 1998. Environmental Soil Physics. Academic Press, London, 771p.

Houser, P.R, Shuttleworth, W. J., Famiglietti, J.S., Gupta, H.V., Syed, K.H., Goodrich, D.C. 1998. Integration of soil moisture remote sensing and hydrologic modeling using data assimilation. *Water Resources Research,* ***34(12)****: 3405 – 3420.*

Hsu, S.M., Ni, C.F., Hung, P.F. 2002. Assessment of Three Infiltration Formulas based on Model Fitting on Richards Equation. *Journal of Hydrologic Engineering,* ***7****: 373 – 379.*

Huisman, J.A, Sperl, C., Bouten, W., Verstraten, J.M. 2001. Soil water content measurements at different scales: accuracy of time domain reflectometry and ground-penetrating radar. *Journal of Hydrology,* ***245****: 48 – 58.*

Hupet, F., Vanclooster, M. 2002. Interseasonal dynamics of soil moisture variability within a small agricultural maize cropped field. *Journal of Hydrology,* ***261****: 86 – 101.*

Hurley, D.G., Pantelis, G. 1985. Unsaturated and saturated flow through a thin porous layer on hillslope. *Water Resources Research,* ***21****: 821 – 824.*

Hymer, D.C., Moran, M.S., Keefer, T.O. 2000. Soil water evaluation using a hydrologic model and calibrated sensor network. *Soil Sciences Society of American Journal,* ***64****: 319 – 326.*

IMKO Micromodultechnik GmbH. 2001. TRIME-FM user manual. 22p.

Jackson, C.R. 1992. Hillslope infiltration and lateral downslope unsaturated flow. *Water Resources Research,* ***28****: 2533 – 2539.*

Jakeman, A.J., Hornberger, G.M. 1993. How much complexity is warranted in a rainfall-runoff model? *Water Resources Research*, ***29:*** *2637 – 2649.*

Jetten, V., De Roo, A.P.J., Guėrif, J. 1998. Sensitivity of the model LISEM to variables related to agriculture, In: J. Boardman, D. Favis-Mortlock (Editors), Modelling Soil Erosion by Water. *NATO ASI Series I.,* ***55****: 89 – 127.*

Jetten, V.G. 2002. LISEM User's Manual, windows version 2.X. Utrecht University, the Netherlands, 64p.

Jetten, V.G., De Roo, A.P.J., Favis-Mortlock, D. 1999. Evaluation of field-scale and catchment-scale soil erosion models. *Catena*, ***37****: 521 – 541*.

Jiang, H., Cotton, W.R. 2004. Soil moisture estimation using an artificial neural network: a feasibility study. *Canadian Journal of Remote Sensing*, ***30:*** *827–839.*

Kim, C.P., Stricker, J.N.M.1996. Influence of spatially variable soil hydraulic properties and rainfall intensity on the water budget. *Water Resources Research*, ***32****: 1699–1712.*

Kirkby, M.J. 1975. Hydrograph modeling strategies. In: R.F. Peel, M.D. Chisholm, and P. Haggett (Editors), Progress in Physical and Human Geography. Heinemann, London, 69 – 90.

Kleijnen, J.P.C. 2005. An overview of the design and analysis of simulation experiments for sensitivity analysis. *European Journal of Operational Research*, ***164****: 287-300.*

Klemes, V. 1983. Conceptualization and scale in hydrology. *Journal of Hydrology,* **65**:1 – 23

Koninklijk Nederlands Meteorologisch Instituut. Daily weather data. (http://www.knmi.nl/klimatologie)

Kool, J.B., Parker, J.C. 1988. Analysis of the inverse problem for transient unsaturated flow. *Water Resources Research*, ***24****: 817 – 830.*

Koster, R.D., Milly, P.C.D. 1997. The interplay between transpiration and runoff formulation in land surface schemes used with atmospheric models. *Journal of Climate*, ***10****: 1578 – 1591*.

Kostov, K.G., Jackson, T.J. 1993. Estimating profile soil moisture from surface layer measurements- a review. *SPIE,* ***1941****: 125 – 136.*

Krause, P., Boyle, D.P., Bäse, F. 2005. Comparison of different efficiency criteria for hydrological model assessment. *Advances in Geosciences*, ***5****: 89 – 97.*

Kroes, J.G., Van Dam, J.C. 2003. Reference manual SWAP. Version 3.0.3. Alterra, Green World Research, Wageningen. Report No.773.

Laio, F., Poporato, A., Ridolfi, L., Rodriguez-Iturbe, I. 2001. Plants in water-controlled ecosystems: active role in hydrologic processes and response to water stress II. Probabilistic soil moisture dynamics, *Advances in Water Resources*, ***24****: 707 – 723.*

Larcher, W. 1975. Physiological Plant Ecology. Springer Verlag, New York.

Legates, D. R., McCabe Jr, G.J. 1999. Evaluating the use of 'goodness-of-fit' measures in hydrologic and hydroclimatic model validation, *Water Resources Research*, ***35****: 233 – 241*.

Luisman, H. 2005. The creation and validation of a DEM from amateur aerial photographs. MSc thesis, Erosion, Soil and Water Conservation group, Wageningen University and Research Centre.

Lyon, S.W., Walter, M.T., Gérard-Marchant, P., Steenhuis, T.S. 2004. Using a topographic index to distribute variable source area runoff predicted with the SCS curve-number equation. *Hydrological Processes,* ***18:*** *2757 – 2 771*

Mahe, G., Paturel, J., Servat, E., Conway, D., Dezetter, A. 2005. The impact of land use changes on soil water holding capacity and river flow modeling in the Nakambe River, Burkina-Faso. *Journal of Hydrology,* ***300:*** *33 – 43.*

Manfreda, S., Fiorentino, M., Iacobellis, V. 2005. DREAM: a distributed model for runoff, evapotranspiration, and antecedent soil moisture simulation. *Advances in Geosciences,* ***2****: 31 – 39.*

Mapfumo, E., Chanasyk, D.S., Willms, W.D. 2004. Simulating daily soil water under foothills fescue grazing with the soil and water assessment tool model (Alberta, Canada). *Hydrological Processes,* ***18****: 2787 – 2800.*

Margulis, S.A., McLaughlin, D., Entekhabi, D., Dunne, S. 1997. Land data assimilation and estimation of soil moisture using measurements from the Southern Great Plains 1997 Field Experiment. *Water Resources Research,* ***38(10)****: 1299, doi:10.1029/2001WR001114*

McCuen, R. H., Snyder, W.M. 1986. Hydrologic Modeling: Statistical Methods and Applications. Prentice-Hall, Englewood Cliffs, NJ. 568 p.

McCullagh, P., Nelder, J.A. 1989. Generalized linear models (2nd edition). London, Chapman and Hall.

Merritt, W.S., Letcher, R.A., Jakeman, A.J. 2003. A review of erosion and sediment transport models. *Environmental Modelling & Software,* ***18:*** *761 – 799.*

Mertens, J., Madsen, H., Kristensen, M., Jacques, D., Feyen, J. 2005. Sensistivity of soil parameters in unsaturated zone modeling and the relation between effective, laboratory and in situ estimate. *Hydrological Processes,* ***19****: 1611 – 1633.*

Merz, B., Plate, E.J. 1997. An analysis of the effects of spatial variability of soil and soil moisture on runoff. *Water Resources Research,* ***33****: 2909 – 2922.*

Mohanty, B.P., Skaggs, T.H., Famiglietti, J.S. 2000. Analysis and mapping of field-scale soil moisture variability using high-resolution, ground-based data during the Southern Great Plains 1997 (SGP97) Hydrology Experiment. *Water Resources Research,* ***36(4)****: 1023 – 1031.*

Moore, I.D., Burch, G.J., Mackenzie, D.H. 1988. Topographic effects on the distribution of surface soil water and the location of ephemeral gullies. *Transactions of the American Society of Agricultural Engineering,* ***31:*** *1098 – 1107.*

Moran, M.S., Peters-Lidard, C.D., Watts, J.M., McElroy, S. 2004. Estimating soil moisture at the watershed scale with satellite-based radar and land surface models. *Canadian Journal of Remote Sensing,* ***30(5)****: 805 – 826.*

Mualem, Y. 1976. A new model for predicting the hydraulic conductivity of unsaturated porous media. *Water Resources Research,* ***12****: 513 – 522.*

Nash, J.E., Sutcliffe, J.V. 1970. River flow forecasting through conceptual models, part 1- a discussion of principles. *Journal of Hydrology,* ***10****: 282 – 290.*

Neitsch, S.L., Arnold, J.G., Kiniry, J.R., Williams, J.R., King, K.W. 2002. Soil and Water Assessment Tool theoretical documentation. Version 2000. Texas Water Resources Institute, College Station, Texas, TWRI report, TR-191.

O'Loughlin, E.M. 1986. Prediction of surface saturation zones in natural catchments by topographic analysis. *Water Resources Research,* ***22****: 794 – 804.*

Pachepsky, Ya.A., Rawls, W.J. 1999. Accuracy and reliability of pedotransfer functions as affected by grouping soils. *Soil Sciences Society of American Journal,* ***63****: 1748–1757.*

Pachepsky, Ya.A., Timlin, D., Varallyay, G. 1996. Artificial neural networks to estimate soil water retention from easily measurable data. *Soil Sciences Society of American Journal,* ***60****: 727–733*

Pellenq, J., Kalma, J., Boulet, G., Saulnier, G.M., Wooldridge, S., Kerr, Y., Boulet, G., Chehbouni, A. 2003. A disaggregation scheme for soil moisture based on topography and soil depth. *Journal of Hydrology,* ***276:*** *12 – 27.*

Pening de Vries, F.W.T., van Laar, H.H. 1982. Simulation of growth processes and the model BACROS. In: F.W.T. Pening de Vries and H.H.van Laar (Editors), Simulation of plant growth and crop production. Simulation Monographs, Pudoc, Wageningen, The Netherlands. Pp. 114 – 135.

Philip, J.R. 1957. The theory of infiltration, 5. The influence of the initial moisture content. *Soil Science,* ***83****: 329 – 339.*

Prasad, R. 1988. A linear root water uptake model. *Journal of Hydrology,* ***99****: 297 – 306.*

Raes, D. 2002. BUDGET: a soil water and salt balance model. Reference manual. Version 5.0. Katholic University of Leuven. Belgium.

Reid, I. 1973. The influence of slope orientation upon the soil moisture regime, and its hydrogeomorphological significance. *Journal of Hydrology,* ***19:*** *309 – 321.*

Renschler, C.S., Cochrane, T., Harbor, J., Diekkruger, B. 2001. Regionalization methods for watershed management- Hydrology and soil erosion from point to regional scales. In: Stott et al., (Eds). Sustaining the global farm. Selected papers from 10^{th} international soil conservation organization meeting held May 24 – 29, 1999 at Purdue University and the USDA-ARS National Soil Erosion Research Laboratory.

Reynolds, S.G. 1974. A note on the relationship between size of area and soil moisture variability. *Journal of Hydrology,* ***22****: 71 – 76.*

Ritchie, J.T. 1972. A model for predicting evaporation from s row crop with incomplete cover. *Water Resources Research,* ***8****: 1204 – 1213.*

Ritsema, C.J., Oostindie, K., Stolte, J. 1996. Evaluation of vertical and lateral flow through agricultural loessial hillslopes using a two-dimensional computer simulation model. *Hydrological Processes,* ***10****: 1091 – 1105.*

Rockhold M.L., Rossi, R.E., Hills, R.G. 1996. Application of similar media scaling and conditional simulation for modeling water flow and tritium transport at the Las Cruces Trench Site. *Water Resources Research,* ***32:*** *595 – 609.*

Rodriguez-Iturbe, I., Vogel, G.K., Rigan, R., Entekhabi, D., Costelli, F., Rinaldo, A. 1995. On the spatial organization of soil moisture fields. *Geophysical Research Letters, 22: 257–276.*

Rogers, J.S., Selim, H.M. 1989. Water flow through layered anisotropic bedded soil with subsurface drains. *Soil Sciences Society of American Journal,* ***53****: 18 – 24.*

Russo, D., Bresler, E. 1980. Scaling soil hydraulic properties of a heterogeneous field. *Soil Sci. Soc. Am. J.* ***44:*** *681–702.*

Saltelli, A., Chan, K., Scott, E.M. 2000. Sensitivity analysis. Wiley series in probability and statistics, John Wiley & Sons, Chichester, England.

Saltelli, A., Tarantola, S., Campolongo, F., Ratto, M. 2004. Sensitivity Analysis in Practice: A Guide to Assessing Scientific Models. John Wiley & Sons: Chichester, England.

Saris, F.J.A. 1984. Lijnvormige landschapselementen, belangrijke onderdelen van een ecologische infrastructuur. *Landschap,* ***1****: 91 – 108.*

Savenije, H.H.G. 2001. Equifinality, a blessing in disguise? *Hydrological Processes,* ***15:*** *2835 – 2838.*

Schaap, M.G., Leij, F.L., Van Genuchten, M.Th. 1998. Neural network analysis for hierarchical prediction of soil hydraulic properties. *Soil Sciences Society of American Journal,* ***62****: 847–855.*

Schmugge, T.J., Jackson, T.J., McKim, H.L. 1980. Survey of methods for soil moisture determination. *Water Resources Research,* ***33(7)****: 1585 – 1593.*

Schütze, N., Schmitz, G.H., Petersohn, U. 2005. Self-organizing maps with multiple input-output option for modeling the Richards equation and its inverse solution, *Water Resources Research,* ***41:*** *W03022. doi:10.1029/2004WR003630.*

Scotter, D. R., Clothier, B. E., Harper, E. R. 1982. Measuring saturated hydraulic conductivity and sorptivity using twin rings. *Australian Journal of Soil Research,* ***20****: 295 – 304.*

Selim, H.M. 1987. Water seepage through multilayered anisotropic hillside. *Soil Sciences Society of American Journal,* ***51****: 9 – 16.*

Shao, Y., Henderson-Sellers, A. 1996. Validation of soil moisture simulation in land surface parameterization schemes with HAPEX data. *Global Planet Change,* ***13****: 11 – 46.*

Sheikh, V., Van Loon, E.E. 2006. Adequacy of a 1D unsaturated zone model to describe the soil moisture dynamics from point to catchment scale. Vadoze Zone Journal (in review).

Silberstein, R.P., Sivapalan, M., Wyllie, A. 1999. On the validation of coupled water and energy balance model at small catchment scales. *Journal of Hydrology,* ***220****: 149 – 168.*

Simunek, J., Vogel, T., Van Genuchten, M. Th. 1992. The SWMS_2D code for simulating water flow and solute transport in two dimensional variably saturated media, version 1.1. Research Report 126. U.S. Salinity Laboratory, Riverside, California. 169 p.

Singh, R. 2005. Water productivity analysis from field to regional scale. Integration of crop and soil modellings, remote sensing and geographical information. Ph.D thesis. Wageningen University, Wageningen, the Netherlands.

Soil Conservation Service Engineering Division. 1986. Urban hydrology for small watersheds. U.S. Department of Agriculture, Technical Release 55.

Soil Survey Staff. 2003. Keys to Soil Taxonomy (9th edition). USDA_NRCS, Washington DC, USA.

Stagnitti, F., Parlange, J. Y., Steenhuis, T.S., Parlange, M.B., Rose, C.W. 1992. A mathematical model of hillslope and watershed drainage. *Water Resources Research, **28**: 2111 – 2122.*

Starks, P.J., Heathman, G.C., Jackson, T.J., Cosh, M.H. 2006. Temporal stability of soil moisture profile. *Journal of Hydrology, **324:** 400 – 411*

Stolte, J. 1997. Determination of the saturated hydraulic conductivity using the constant head method. In: Stolte, J. (ed). Manual for soil physical measurements. Technical Document 37, DLO Winand Staring Centre, Wageningen, the Netherlands, Pp. 27 – 32.

Stolte, J., Ritsema, C.J., Veerman, G.J., Hamminga, W. 1994. Bodemfysische schematisatie van drie stroomgebieden in Zuid-Limburg op basis van een erosiegevoeligheidsanalyse. DLO-Staring centrum, Wageningen, the Netherlands.

Stolte, J., Ritsema, C.J., Veerman, G.J., Hamminga, W. 1996. Establishing temporally and spatially variable soil hydraulic data for use in a runoff simulation in loess region of the Netherlands. *Hydrological Processes, **10**: 1027 – 1034.*

Stroosnijder, L. 1987. Soil evaporation: test of a practical approach under semi-arid conditions. *Netherlands Journal of Agricultural Science, **35**: 417 – 426* (download.pdf)

Stroosnijder, L., Hoogmoed, W.B. 1984. Crust Formation on sandy soils in the Sahel; II. Tillage and its effects on the water balance. *Soil & tillage Research, **4**: 321 – 337.*

Svetlitchnyi, A. A., Plotnitskiy, S.V., Stepovaya, O.Y. 2003. Spatial distribution of soil moisture content within catchments and its modeling on the basis of topographic data. *Journal of Hydrology, **277**: 50 – 60.*

Sys, c., Van Ranst, E., Debaveye, J., Beernaert, F. 1993. Land evaluation. Part III: crop requirements. Agic. Publ. 7. General Administration for Dev. Coop., Brussels, Belgium.

Teuling, A.J., Uijlenhoet, R., Troch, P.A. 2005. On bimodality in warm season soil moisture observations. *Geophysical Research Letters, **32:** L13402, doi:10.1029/2005GL023223*

Teuling, A. J., Troch, P. A. 2005. Improved understanding of soil moisture variability dynamics. *Geophysical Research Letters, **32:** L05404, doi:10.1029/2004GL021935*

Teuling, A.J., Uijlenhoet, R., Hupet, F., van Loon, E.E., Troch, P.A. 2006. Estimating spatial mean root-zone soil moisture from Point-scale observation. *Hydrology and Earth System Sciences. Discussion, **3**: 1447–1485*

The ASCE Task Committee on Application of Artificial Neural Networks in Hydrology. 2000a. Artificial Neural Networks in Hydrology I: Preliminary Concepts. *Journal of Hydrologic Engineering, **5:** 115 – 123.*

The ASCE Task Committee on Application of Artificial Neural Networks in Hydrology. 2000b. Artificial Neural Networks in Hydrology II: Hydrologic Applications. *Journal of Hydrologic Engineering, **5:** 124 – 137.*

Tokar, A.S., Markus, M. 2000. Precipitation-runoff modeling using artificial neural networks and conceptual models. *Journal of Hydrologic Engineering, **5:** 156 – 161*

Topp, G.C., Davis, J.L., Annan, A.P. 1980. Electromagnetic determination of soil water content: measurements in coaxial transmission lines. *Water Resources Research, **16(3)**: 574 – 582.*

Troch, P.A., Mancini, M., Paniconi, C., Wood, E.F. 1993. Evaluation of a distributed catchment scale water balance model. *Water Resources Research, **29**: 1805 – 1817.*

Vachaud, G., De Silans Passerat, A., Balabanis, P., Vauclin, M. 1985. Temporal stability of spatially measured soil water probability density function. *Journal of Soil Sciences. Society of America, **49**: 822 – 827.*

Van Dam, J.C. 2000. Field-scale water flow and solute transport. SWAP model concepts, parameter estimation and case studies. Ph.D thesis. Wageningen University, Wageningen, the Netherlands.

Van Dam, J.C., Feddes, R.A. 2000. Numerical simulation of infiltration, evaporation and shallow ground water levels with Richards' equation. Simulation of field-scale water flow and bromide transport in a cracked clay soil. *Journal of Hydrology, **233**: 72 – 85.*

Van Deursen, W.P.A., Wesseling, C.G. 1992. The PCRaster package: Department of Physical Geography, Utrecht University. http://www.pcraster.nl.

Van Genuchten, M.Th. 1980. A closed form equation for predicting the hydraulic conductivity of unsaturated soils. *Soil Sciences Society of American Journal, **44**: 892 – 898.*

Van Griensven, A., Meixner, T., Grunwald, S., Bishop, T., Diluzio, M., Srinivasan, R. 2006. A global sensitivity analysis tool for the parameters of multi-variable catchment models. *Journal of Hydrology, **324**: 10 – 23.*

Van Loon, E.E., Troch, P.A. 2002. Tikhonov regularization as a tool for assimilating soil moisture data in distributed hydrological models. *Hydrological Processes, **16**: 531 – 556.*

Veihe, A., Quinton, J. 2000. Sensitivity analysis of EUROSEM using Monte Carlo simulation I: hydrological, soil and vegetation parameters. *Hydrological Processes, **14**: 915 – 926.*

Venables, W.N., Ripley, B.D. 2002. Modern Applied Statistics with S. New York: Springer.

Verdoodt, A., Van Ranst, E., Ye, L. 2004. Modeling daily simulation of potential dry matter production of annual field crops in tropical environments. *Agronomy Journal,* ***96****: 1739 – 1753.*

Von Hoyningen-Huene, J.V. 1981. Die interzeption des Niedeschlags in landwirtschaftlichen Pflanzenbeständen. Arbeitsbericht Deutscher Verband für Wasserwirtschaft und Kulturbau, DVWK, Braunschweig, 63p.

Walker, J.P. 1999. Estimating soil moisture profile dynamics from near-surface soil moisture measurements and standard meteorological data. Ph.D thesis. The University of Newcastle: New South Wales, Australia.

Walker, J.P., Willgoose, G.R., Kalma, J.D. 2004. In situ measurement of soil moisture: a comparison of techniques. *Journal of Hydrology,* ***293****: 85 – 99.*

Wang, J., Fu, B., Qiu, Y., Chen, L., Wang, Z. 2001. Geostatistical analysis of soil moisture variability on Da Nangou catchment of the loess plateau, China. *Environmental Geology,* ***41****: 113 – 120.*

Warrick, A.W., Mullen, G.J., Nielsen, D.R. 1977. Scaling field measured soil hydraulic properties using similar media concept. *Water Resources Research,* ***13:*** *355–362.*

Wegehenkel, M. 2005. Validation of a soil water balance model using soil water content and pressure head data. *Hydrological Processes,* ***19****: 1139 – 1164.*

Western, A.W., Grayson, R.B., Blöschl, G., Willgoose, G.R., McMahon, T.A. 1999. Observed spatial organization of soil moisture and its relation to terrain indices. *Water Resources Research,* ***35(3):*** *797 – 810.*

Western, A., Blöschl, G. 1999. On the spatial scaling of soil moisture. *Journal of Hydrology,* ***217****: 203 – 224.*

Western, A., Grayson, R. 1998. The Tarrawarra data set: soil moisture patterns, soil characteristics, and hydrological flux measurements. *Water Resources Research,* ***34(10)****: 2765 – 2768.*

Western, A., Zhou, S.L., Grayson, R.B., MacMahon, T.A., Blöschl, G., Wilson, D. 2004. Spatial correlation of soil moisture in small catchments and its relationship to dominant spatial hydrological processes. *Journal of Hydrology,* ***286****: 113 – 134.*

Wheater, H.S., Jakeman, A.J., Beven, K.J. 1993. progress and directions in rainfall-runoff modelling. In: Jakeman, A.J., Bech, M.b., McAleer, M.J. (Editors), Modelling Chhange in Environmental Sciences. John Wiley and Sons, Chichester, Pp. 101 – 132.

Wilby, R.L., Abrahart, R.J., Dawson, C.W. 2003. Detection of conceptual model rainfall–runoff processes inside an artificial neural network. *Hydrological Sciences Journal,* ***48:*** *163 – 182. doi:10.1623/hysj.48.2.163.44699*

Wilkening, H.A. 1981. Sensitivity of rainfall excess to antecedent soil moisture and soil hydraulic properties. MSc. Thesis, University of Maryland, College Park, Md. (unpublished).

Willmot, C. J. 1981. On the validation of models, *Physical Geography,* ***2****: 184–194.*

Wood, E.F., Lettenmaier, D.P., Zatarian, V.G. 1992. A land surface hydrology parameterization with subgrid variability for general circulation models. *Journal of Geophysical Research, **97**: 2717 – 2728.*

Wooldridge, S., Kalma, J., Kuczera, G. 2001. Parameterisation of a simple semi-distributed model for assessing the impact of land-use on hydrologic response. *Journal of Hydrology, **254:** 16 – 32.*

Wooldridge, S., Kalma, J. 2001. Regional-scale hydrological modeling using multiple-parameter landscape zones and a quasi-distributed water balance model. *Hydrology and Earth System Sciences, **5:** 59 – 74.*

Wösten, J.H.M., Van Genuchten, M.Th. 1988. Using texture and other soil properties to predict the unsaturated soil hydraulic functions. *Sciences Society of American Journal, **52**: 1762–1770.*

Young, P. 1998. Data-based mechanistic modelling of environmental, ecological, economic and engineering systems. *Environmental Modelling and Software*, ***13:** 105–122.*

Yu, Z., Gburek, W.J., Schwartz,F.W. 2000. Evaluating the spatial distribution of water balance in a small watershed, Pennsylvaina. *Hydrological Processes, **14**: 941 – 956.*

Zegelin, S. 1996. Soil Moisure Measurement, Field Measurement Techniques in Hydrology-Workshop Notes, Corpus Christi College, Clayton, Pp. C1-C22.

Zehe, E., Becker, R., Bardossy, A., Plate, E. 2005. Uncertainty of simulated catchment runoff response in the presence of threshold processes: Role of initial soil moisture and precipitation, *Journal of Hydrology, **315**: 183 – 202.*

Zhang, Z.F., Ward, A.L., Gee, G.W. 2004. A combined parameter scaling and inverse technique to upscale the unsaturated hydraulic parameters for heterogeneous soils. *Water Resources Research, **40(8)**, W08306, doi:10.1029/2003WR002925.*

Zhang, G.P., Savenije, H.H. 2005. Rainfall-runoff modelling in a catchment with a complex groundwater flow system: application of the Representative Elementary Watershed (REW) approach. *Hydrology and Earth System Sciences, **9:** 243 – 261.*

Zhu, J., Mohanty, B. P., Das, N. N. 2006. On the Effective Averaging Schemes of Hydraulic Properties at the Landscape Scale. *Vadose Zone Journal, **5**: 308 – 316.*

Zhu, J., Mohanty, B.P. 2002. Spatial averaging of van Genuchten hydraulic parameters for steady-state flow in heterogeneous soils; a numerical study**.** *Vadose Zone Journal, **1:** 261 – 272.*

Summary

This thesis, entitled “Soil Moisture Prediction: Bridging Event and Continuous Runoff Modelling”, covers aspects of soil moisture monitoring and modelling. The general objective was to investigate the possibility of providing spatially distributed soil moisture data for event-based hydrological models close before a rainfall event. The thesis comprises 8 chapters.

Chapter 1: General introduction

This chapter discusses the importance of soil moisture for different fields of study and application, and explains the difficulties encountered in measuring and modelling soil moisture. The main objectives and research questions for this PhD study are defined. The main objectives are: 1) to understand the relation between topography, land use and soil moisture content, 2) to determine the sensitivity of the LISEM model to the initial condition of soil moisture, 3) to evaluate the adequacy of the SWAP model in predicting profile soil moisture content when upscaled from point to catchment scale, and 4) to develop a simple spatially distributed conceptual model to predict the soil moisture content of the root zone. Finally, the content and structure of the thesis are presented.

Chapter 2: Study area

This chapter describes the eco-physical characteristics of the study area in detail. The study site, known as “Catsop”, is a small (0.42 km^2 in area) experimental catchment in south Limburg, the Netherlands. It is a typical agricultural catchment with deep loess soils and undulating topography. The altitudinal range is from 79 to 112 m.a.s.l. The climate is temperate humid with annual precipitation of 740 mm. During major storms 3–30 % of the rainfall reaches the catchment outlet.

Chapter 3: Data collection and methods

This chapter gives an overview of data collection procedures and methodology followed in this thesis. Data were collected to enable the parameterisation, calibration and evaluation of the hydrological models used in the research. The data were particularly targeted at obtaining information on forcing variables and model state variables, but were also used to derive initial estimates of several model parameters. Some parameters were obtained in a spatially distributed form and others were measured in lumped form at the catchment scale. Soil properties and land use data were gathered in a spatially distributed way. Soil moisture was monitored at point scale with different tools, all applying the Time Domain Reflectometry (TDR) technique. Profile soil moisture was monitored during several seasons at 15 locations

distributed over the catchment. Surface hydrology and weather variables were monitored both spatially distributed and also integrated at the catchment scale. However, only integrated values were used in model validation. The meteorological data used were from Beek weather station, a standard synoptic station at the international airport of Aachen–Maastricht. This station is less than 2 km from the catchment. Discharge was measured at the catchment outlet, using a partial flume with a capacity of 950 l s^{-1} and with a stilling well in a safely reservoir with a vertical float recorder.

Chapter 4: Sensitivity of catchment discharge to initial soil moisture

The LImburg Soil Erosion Model (LISEM) was used to investigate the sensitivity of catchment discharge to the initial condition of profile soil moisture content. The influence of initial soil moisture content in two soil layers was considered in relation to layer depths, event properties and two infiltration models. Using the terrain data from the Catsop research catchment and two different rainfall events, the sensitivity of discharge is investigated for a range of pre-event soil moisture contents (0.05 to 0.40 cm^3 cm^{-3}) in two layers for a two-layer Green–Ampt model and a Richards infiltration model. The sensitivity of the predicted discharge to the initial condition of soil moisture appears to depend on many factors: the infiltration model, the event properties, topsoil/soil depth configuration and the initial soil moisture content itself. There are interaction effects between all these factors. However, the effect of the different infiltration models is most pronounced. With the Green-Ampt model, discharge is less sensitive to the moisture content of both topsoil and underlying soil by comparison to the Richards model. Moreover, the response is much more linear. With the Richards model, the correlation between discharge and initial soil moisture varies greatly with changing rainfall intensity and topsoil/soil depth configurations. For changes of approximately 0.05 cm^3 cm^{-3} to the initial soil moisture content of the surface layer, the Green–Ampt model shows -25 to +50 percent changes in discharge depending on topsoil / soil depth and the initial condition of the second layer. For the Richards model, discharge varies from -100 to more than +100 percent.

Chapter 5: Understanding the relation between topography, land use and soil moisture in a small rural catchment in the Dutch Loess area

This chapter deals with the relationship between topography, land use, and topsoil moisture storage. A Generalised Additive Model (GAM) was employed to find relationships between the various factors influencing soil moisture. GAM defines a water balance as a sum of non-linear components. The model framework is hierarchical: the analysis starts at the coarsest spatial and temporal resolution (here catchment and monthly resolution). The water balance components at these resolutions act as constraints when identifying models at finer spatial (response unit, hillslope and plot) and temporal (weekly and daily) resolutions. It turns out that the importance of land-use variables varies considerably with temporal resolution. At coarse resolutions, land use is unimportant, whereas at finer temporal resolutions it becomes more relevant. Land use is equally important over all spatial resolutions, whereas topography is only relevant at the plot scale. Evapotranspiration and drainage to deeper layers are found to depend mainly on land use. Lateral transport is weakly dependent on topography. All the water balance components become increasingly non-linear at finer scales. While the model does not assume any structural relationships (it is entirely data-based), it leads to prediction errors that are similar to those obtained with a Richards-based water balance model (SWAP) when applied at the same resolution. This case study shows that the hierarchical model framework tested provides an elegant way to summarise and structure hydrological observations at different scales. It enables the identification of dominant processes over a range of scales and also facilitates a straightforward sensitivity analysis to evaluate e.g. the importance of bio-physical factors, relative to forcing or state variables.

Chapter 6: Adequacy of a 1D unsaturated zone model to describe the soil moisture dynamics from point to catchment scale

This chapter evaluates the predictive performance of the SWAP model to simulate the root zone soil moisture content when applied at point, field, response unit and catchment scales. Though it can be argued that the SWAP is a 1-D unsaturated zone developed for point scale, the hydrological literature indicates that 1-D unsaturated zone models are also applied at other scales of interest by means of regionalisation. The main question addressed here is how model parameterisation and model performance can be compared across different scales. Two different calibration/validation schemes and three performance statistics were used in this study. In all cases, the same Levenberg–Marquardt optimisation scheme was applied. It was found that the differences between calibration/validation schemes (interpolation versus extrapolation) are surprisingly small. Using one particular model parameterisation across the various aggregation levels, the optimal Mualem–Van Genuchten parameters for a coarser aggregation level can be derived from an underlying level by simple arithmetical averaging. Different performance indices (root mean squared error, index of agreement, and the Nash–Sutcliffe coefficient) are highly variable between observation locations and for different levels of aggregation. Overall, the indices are more favourable at higher aggregation levels and are in agreement with errors reported in comparable studies.

Chapter 7: A simple model to predict soil moisture: Bridging Event And Continuous Hydrological modelling (BEACH).

This chapter presents the development and application of the BEACH model. BEACH is a spatially distributed hydrological model that operates at time steps of one day. It has been formulated to predict the initial condition of soil moisture for event-based soil erosion and rainfall runoff models. BEACH uses daily meteorological records, physical soil properties, basic crop characteristics and topographical data. The basic processes incorporated in the model are precipitation, infiltration, transpiration, evaporation, lateral flow, vertical flow and plant growth. The principal use of this model is to provide timely information on the spatially distributed soil moisture content over a study area without the need for repeated field visits. The application of this model in the Catsop catchment showed that it is capable of estimating soil moisture content reasonably accurately. The root mean squared error of the predicted soil moisture content for 6 locations within the catchment ranged from 0.011 to 0.065 $cm^3\ cm^{-3}$. The predicted daily discharge at the outlet of the study area agreed well with the observed data. The coefficient of determination and Nash–Sutcliffe efficiency of the predicted discharge were 0.824 and 0.786, respectively. BEACH has been developed within a freely available GIS and programming language, PCRaster. It is a useful teaching tool for learning about distributed water balance modelling and land use scenario analysis.

Chapter 8: Synthesis

This chapter integrates the most important results and conclusions from the preceding chapters. The achievement or failure of each of the main objectives and answers to the questions posed in Chapter 1 are briefly discussed. After the main research questions have been briefly introduced and restated, the soil moisture measurement campaign during this research is discussed. Thereafter, the themes corresponding to the main research questions are elaborated. Finally, the main conclusions and recommendations for future study are presented.

Samenvatting

Dit proefschrift 'Het voorspellen van bodemvocht: van gedetailleerde hydrologische modellen naar continue hydrologische modellen', gaat over meet- en modeleer-aspecten van bodemvocht. Het algemene doel van de studie was om de mogelijkheden te onderzoeken voor het aanleveren van ruimtelijk verdeelde bodemvochtgegevens ten behoeve van gedetailleerde hydrologische modellen. Het proefschrift omvat acht hoofdstukken.

Hoofdstuk 1: algemene introductie

In hoofdstuk 1 wordt het belang van bodemvocht metingen voor verschillende wetenschappen en toepassingen besproken. Tevens wordt ingegaan op problemen die optreden bij het meten en modelleren van bodemvocht. De doelstellingen van het promotieonderzoek worden behandeld: 1) Het begrijpen van de relatie tussen topografie, landgebruik en het bodemvochtgehalte, 2) Het bepalen van de gevoeligheid van het LISEM model voor de vochttoestand van de bodem vlak voor een regenbui, 3) Het evalueren van het SWAP model voor het voorspellen van bodemvochtprofielen wanneer er schaalvergroting van punt naar stroomgebied wordt toegepast en 4) het ontwikkelen van een eenvoudig ruimtelijk gedistribueerd conceptueel model voor bodemvochtvoorspellingen in de wortelzone. Het hoofdstuk sluit af met een overzicht van de inhoud en de structuur van het proefschrift.

Hoofdstuk 2: het onderzoeksgebied

Hoofstuk 2 beschrijft in detail de ecologische en fysische kenmerken van het onderzoeksgebied. Het onderzoeksgebied, Catsop, is een stroomgebied van 0.42 km^2 in Zuid-Limburg, waar al sinds lange tijd verschillende experimentele onderzoeken plaatsvinden. Het stroomgebied heeft een voor de regio karakteristiek agrarisch landgebruik, een licht hellende topografie en diepe löss bodems. Het stroomgebied ligt op 79 – 112 m boven NAP. Het heersende klimaat is gematigd en vochtig met een jaarlijkse neerslag van 740 mm. Tijdens grote regenbuien verlaat 3 – 30 % van de neerslag het stroomgebied als opervlakte afvoer.

Hoofstuk 3: het verzamelen van data en gebruikte methoden

Hoofstuk 3 geeft een overzicht van de procedures die zijn gevolgd bij het verzamelen van de gegevens en de toegepaste methoden. Het doel van de gegevensverzameling was parametrisatie, ijking en evaluatie van de gebruikte hydrologische modellen. In eerste instantie dienen de gegevens voor het verkrijgen van informatie over randvoorwaarden, model invoer en toestandsvariabelen, maar daarnaast zijn de gegevens ook gebruikt om de initiële waarden van de verschillende modelparameters te schatten. De gegevens voor de parameters werden verkregen in zowel ruimtelijk verdeelde metingen als door middel van één

geïntegreerde meting op stroomgebiedniveau: bodem en landgebruikkenmerken werden ruimtelijk verspreid verzameld, het bodemvocht werd door puntsmetingen gemeten (met verschillende TDR-gebaseerde meetinstrumenten), bodemvochtprofielen werden geobserveerd gedurende een aantal seizoenen op 15 locaties verspreid in het stroomgebied. Meteorologsiche gegevens en ook gegevens over de oppervlakte hydrologie werden zowel ruimtelijk verspreid als geïntegreerd bepaald. In het model werden slechts de geïntegreerde waarden gebruikt. De meteorologische gegevens zijn afkomstig van het weerstation in Beek, een standaard overzichtsgevend weerstation op het internationale vliegveld van Aken-Maastricht. Het weerstation ligt op minder dan 2 km afstand van het Catsop stroomgebied. Oppervlakte afstroming werd gemeten door middel van een meetgoot met een capaciteit van 950 l s^{-1} en met een woelbak in een veiligheidsreservoir. In het reservoir bevindt zicht een verticale drijver ter bepaling van de waterhoogte. De meetgoot is geplaatst op het uitstroompunt van het stroomgebied.

Hoofdstuk 4: gevoeligheid van stroomgebiedafvoer voor de initiële bodemvochttoestand

Om de gevoeligheid van de stroomgebiedafvoer voor de initiële bodemvochttoestand te onderzoeken is gebruik gemaakt van het LImburg Soil Erosion Model (LISEM). De invloed van het bodemvocht in twee bodemlagen werd beschouwd in relatie tot de diepte van de lagen, de eigenschappen van de regenbui en twee infiltratiemodellen. De gevoeligheid van de afstroming is voor een reeks van initiële bodemvochtcondities (0.05 – 0.40 cm^3 cm^3) in twee lagen onderzocht voor zowel het Green-Ampt als het Richards infiltratiemodel. De terreinkenmerken van het stroomgebied en twee verschillende regenbuien zijn hierbij in beschouwing genomen. De gevoeligheid van de voorspelde afstroming voor de initiële bodemvochtconditie hangt af van vele factoren: het infiltratiemodel, de eigenschappen van de regenbui, de toplaag/bodemdiepte verhouding en de initiële bodemvochttoestand. Het effect van de infiltratiemodellen is echter het meest opvallend. Het Green-Ampt model is, in vergelijking met het Richards-model, minder gevoelig voor de bodemvochttoestand van zowel de toplaag als de onderliggende bodem. De reactie van het Green-Ampt model is meer lineair. Bij het Richards model varieert de correlatie tussen afstroming en initieel bodemvochtgehalte bij variatie van de regenintensiteit en de toplaag/bodemdiepte verhouding. Veranderingen van 0.05 cm^3 cm^{-3} in het bodemvochtgehalte van de toplaag resulteren bij het Green-Ampt model in -25 tot +50% verandering in de stroomgebiedafvoer, afhankelijk van de toplaag/bodemdiepte en de initiële bodemvochtconditie van de tweede bodemlaag. Bij het Richards model is deze verandering -100 tot meer dan +100 %.

Hoofdstuk 5: de relatie tussen topografie, landgebruik en bodemvocht in een klein landelijk stroomgebied in het Nederlandse lössgebied

Hoofstuk 5 gaat over de relatie tussen topografie, landgebruik en bodemvochtgehalte van de wortelzone. Een Generalized Additive Model (GAM) is toegepast om de relatie te vinden tussen de verschillende factoren die van invloed zijn op het bodemvocht. In GAM wordt de waterbalans gedefinieerd als de som van niet-lineaire componenten. Het modelraamwerk is hiërarchisch: de analyse begint op de grove ruimtelijke en temporele resolutie (in dit onderzoek stroomgebiedschaal en maandelijkse perioden). De waterbalanscomponenten die bij deze resoluties worden verkregen gelden vervolgens als beperkende factoren bij het definiëren van modellen bij fijner gedefinieerde ruimtelijke (sub-stroomgebied, helling en veldniveau) en temporele (week en dag) resoluties. Het blijkt dat afhankelijk van de temporele resolutie, de invloed van landgebruikvariabelen in belangrijke mate varieert. Bij grof gedefinieerde resoluties zijn de landgebruikvariabelen belangrijk, terwijl deze bij de fijne resoluties minder relevant blijken. Landgebruik is evenredig belangrijk bij alle niveaus van ruimtelijke resolutie, terwijl topografie alleen van belang is bij het plotniveau. Evapotranspiratie en drainage naar de diepe ondergrond blijken voornamelijk afhankelijk te zijn van de landgebruikvariabelen. Laterale afstroming is licht afhankelijk van de topografie. Alle waterbalansfactoren worden in toenemende mate niet-lineair bij een fijner wordende resolutie. Alhoewel GAM volledig data gestuurd is, en dus geen enkele structurele relatie veronderstelt, zijn de voorspellingsfouten van GAM, bij gelijke resoluties, vergelijkbaar met die van een Richards-waterbalansmodel (SWAP). De studie laat zien dat het geteste hiërarchische modelraamwerk een elegante aanpak is om hydrologische observaties te structuren en samen te vatten. Het model maakt het mogelijk om dominante processen op verschillende schaalniveaus te definiëren. Ook vergemakkelijkt het model een duidelijke gevoeligheidsanalyse waarmee b.v. het belang van biofysische factoren afhankelijk van model invoer en toestandsvariabelen kan worden geëvalueerd.

Hoofdstuk 6: geschiktheid van een 1D onverzadigde zone model voor het beschrijven van de bodemvochtdynamiek van puntschaal naar stroomgebiedschaal

In dit hoofdstuk wordt het voorspellende kracht van het SWAP model geëvalueerd, voor het stimuleren van het bodemvocht gehalte in de wortelzone op punt-, veld-, landgebruikseenheid- en stroomgebiedschaal. Hoewel SWAP ontwikkeld is voor het punt schaalniveau, blijkt uit de literatuur dat 1D onverzadigde zone modellen door middel van regionalisatie ook toegepast kunnen worden op andere schaalniveaus. De belangrijkste vraag die hier wordt behandeld is hoe parametrisatie en modelgedrag op verschillende schaalniveaus kunnen worden vergeleken. In deze studie zijn twee soorten validatieschema's en drie verschillende prestatiestatistieken toegepast. In alle gevallen is dezelfde Levenberg-Marquardt optimalsiatie gebruikt. De gevonden verschillen tussen de validatieschema's (interpolatie vs. extrapolatie) zijn opvallend klein. Met gebruikmaking van één specifieke modelparametrisatie voor de verschillende aggregatieniveau's, kunnen de optimale Mualem-Van Genuchten parameters voor grovere aggregatieniveaus worden afgeleid van een onderliggende niveau door een simpel rekenkundig gemiddelde. Verschillende prestatiestatistieken, zoals de vierkantswortel van de gemiddelde kwadraatsom (RMSE), index van overeenkomst en de Nash-Sutcliffe coëfficiënt, zijn zeer variabel over de verschillende meetlocaties en aggregatieniveaus. Algemeen kan worden gesteld dat de indicatoren gunstiger zijn bij hogere aggregatieniveaus en overeen komen met afwijkingen die in vergelijkbare studies zijn gevonden.

Hoofdstuk 7: een eenvoudig buddy model voor het voorspellen van bodemvocht: van gedetailleerde hydrologische modellen naar continue hydrologische modellen (BEACH)

In hoofdstuk 7 wordt de ontwikkeling en toepassing van het BEACH model beschreven. BEACH is een ruimtelijk verdeeld hydrologisch model dat werkt met een tijdsfrequentie van één dag. Het model dient om de initiële vochttoestand van de wortelzone te voorspellen voor het gebruik in gedetailleerde bodemerosie- en regenvalafstromingsmodellen. BEACH gebruikt dagelijkse weersgegevens, fysische bodemeigenschappen, algemene gewaskenmerken en topgrafische data. De processen die in het model zijn ingebouwd omvatten neerslag, infiltratie, transpiratie, evapotranspiratie, evaporatie, laterale afstroming, verticale stroming en plantengroei. Het belangrijkste gebruiksdoel van het model is het beschikbaar maken van in tijd en ruimte verdeelde bodemvochtgegevens voor een studiegebied, om zo herhaaldelijk bezoek aan het gebied overbodig te maken. Door toepassing van het model in het Catsop stroomgebied werd aangetoond dat het model in staat is om redelijk nauwkeurig bodemvochtschattingen te leveren. De RMSE van de voorspelde bodemvochtwaarden over 6 locaties in het stroomgebied varieerde van 0.011 tot 0.065 cm^3 cm^3. De voorspelde dagelijkse afvoer uit het stroomgebied kwam goed overeen met de gevonden waarden. De index van overeenkomst en Nash-Sutcliffe coëfficiënt van de voorspelde afstroming waren respectievelijk 0.824 en 0.786. BEACH is ontwikkeld in een freeware GIS en programmeertaal, PCRaster. Het is een geschikt hulpmiddel om inzicht te krijgen in waterbalansmodellering en landgebruiks-analyse.

Hoofdstuk 8: synthese

In dit laatste hoofstuk worden de belangrijkste resultaten en conclusies van de voorgaande hoofdstukken geïntegreerd. De onderzoeksvragen die in hoofdstuk 1 zijn gesteld worden al dan niet succesvol beantwoord. Nadat de belangrijkste onderzoeksvraag kort herhaald wordt, volgt een discussie van de bodemvocht meetcampagne. Hierna worden de thema's die gerelateerd zijn aan de onderzoeksvraag uitvoerig besproken. Tenslotte worden de belangrijkste conclusies en aanbevelingen gepresenteerd.

خلاصه

این رساله تحت عنوان " پیش بینی رطوبت خاک: عامل پیوند دهنده مدل سازی رواناب بصورت پیوسته در زمان و مدل سازی سیلاب های موقتی" جنبه های متفاوت مدل سازی و پیش بینی رطوبت خاک را بررسی می کند. هدف اصلی این رساله، ررسی امکان تهیه نقشه پراکنش مکانی (spatial distribution) رطوبت خاک درست قبل از شروع رگبار میباشد که برای مدل سازی سیلابهای زودگذر حاصل از رگبارها حائز اهمییت می باشد. این رساله شامل هشت فصل می باشد.

فصل اول: مقدمه

در این فصل اهمییت رطوبت خاک در زمینه های مختلف مطالعاتی و کاربردی بررسی شده و مشکلات موجود در اندازه گیری و مدل سازی رطوبت خاک توضیح داده می شوند. همچنین اهداف اصلی و پرسش های تحقیقاتی مطرح شده در این تحقیق تعیین و تعریف می شوند. اهداف اصلی عبارتند از: 1- درک روابط موجود بین توپوگرافی و کاربری اراضی ورطوبت خاک 2- تعیین حساسیت مدل LISEM به شرایط پیشین رطوبت خاک 3- ارزیابی قابلیت مدل SWAP جهت تخمین پروفیل رطوبتی خاک در مقیاس های مختلف مکانی 4- توسعه یک مدل تفهیمی ساده جهت تخمین توزیع مکانی رطوبت خاک در منطقه توسعه ریشه.
در انتهای این فصل مطالب و ساختار رساله حاضر ارائه می گردد.

فصل دوم: منطقه مورد مطالعه

در این فصل خصوصیات اکوفیزیکی منطقه مورد مطالعه بطور مفصل توصیف می گردند. منطقه مورد مطالعه، حوضه آبخیز Catsop می باشد که یک حوضه آبخیز آزمایشی کوچک در استان SOUTH LIMBURG در جنوب هلند میباشد. Catsop یک حوضه آبخیز تیپیک با کاربری اراضی کشاورزی، خاکهای عمیق لسی و توپوگرافی تپه ماهوری می باشد. ارتفاع هیپسومتریک حوضه بین 79 تا 112 متر از سطح دریا متغیر میباشد. اقلیم منطقه مرطوب معتدل با میانگین باران سالانه 740 میلیمتر میباشد. حدود 3 الی 30 درصد رگبارها بصورت رواناب سطحی از نقطه خروجی حوضه خارج می شود.

فصل سوم: جمع آوری آمار و اطلاعات وروش تحقیق

این فصل بطور اجمال روش های جمع آوری داده ها و روش تحقیق این رساله را بررسی می کند. هدف از جمع آوری داده ها، بهینه سازی پارامتر ها وکالیبره کردن و ارزیابی مدلهایی میباشد که در این تحقیق استفاده گردیده اند. خصوصاً این داده ها جهت تعیین آمار و اطلاعات متغیرهای ورودی و متغیرهای سیستم به کار می روند. همچنین این داده ها برای تخمین شرایط اولیه پارامترهای متعدد مدلها استفاده میشوند. مقادیر بعضی از پارامترها بصورت توزیع مکانی در سطح

حوضه (spatial distribution) و بعضی دیگر بصورت یکپارچه (lumped) برای کل حوضه آبخیز برآورد شدند. داده های خصوصیات فیزیکی خاک و کاربری اراضی بصورت توزیع مکانی جمع آوری شدند. داده های رطوبت خاک بوسیله دستگاههای مختلف در مقیاس نقطه برای بعضی نقاط مشخص در سطح حوضه اندازه گیری شدند. تمام این دستگاهها از تکنیک TDR برای اندازه گیری رطوبت خاک استفاده می کنند. پروفیل رطوبت خاک در 15 نقطه برای چندین فصل متوالی اندازه گیری شد. متغیرهای هیدرولوژی و هواشناسی، هم بصورت توزیع مکانی وهم بصورت یکپارچه اندازه گیری شدند. هر چند برای امتحان درستی (validation) مدلها فقط داده های یکپارچه استفاده شدند. داده های هواشناسی از ایستگاه سینوپتیک Beek واقع در مجاورت فرودگاه بین المللی Aachen-Maastricht اتخاذ گردیدند. فاصله این ایستگاه تا حوضه آبخیز Catsop کمتر از 2 کیلومتر می باشد. دبی خروجی در نقطه خروجی حوضه توسط یک پارشال فلوم با ظرفیت انتقال آب 950 لیتر درثانیه اندازه گیری شد.

فصل چهارم: حساسیت دبی خروجی حوضه به رطوبت پیشین خاک

مدل LISEM جهت بررسی حساسیت دبی خروجی حوضه نسبت به تغییرات شرایط پیشین پروفیل رطوبتی خاک استفاده گردید. تأ ثیر شرایط پیشین رطوبت خاک در لایه های سطحی و زیرین خاک بهمراه تأ ثیر عمق لایه ها، خصوصیات رگبار و نوع مدل نفوذپذیری مورد بررسی قرار گرفت. با استفاده از داده های زمینی (terrain) حوضه آبخیز Catsop و دو رگبار متفاوت، حساسیت دبی حوضه به تغییرات شرایط پیشین رطوبت خاک در لایه های خاک برای مدلهای نفوذپذیری گرین- امپت دو لایه (two layers Green-Ampt) و ریچارد (Richards) بررسی شد. بنظر می رسد که حساسیت دبی حوضه نسبت به تغییرات شرایط پیشین رطوبت خاک به عوامل دیگری از جمله نوع مدل نفوذپذیری، خصوصیات رگبار، نسبت عمق لایه سطحی به لایه زیرین و همچنین خود مقدار رطوبت پیشین خاک بستگی دارد. در حقیقت بین این عوامل اثر متقابل (interaction effect) وجود دارد. اگرچه، تأ ثیر نوع مدل نفوذپذیری بسیار قابل ملاحظه می باشد. برای مدل گرین- امپت دو لایه دبی حوضه حساسیت کمتری به تغییرات رطوبت پیشین خاک در هر دو لایه نشان می دهد و تغییرات دبی به حالت خطی نزدیک می باشد. برای مدل ریچارد همبستگی دبی حوضه و شرایط پیشین رطوبت خاک با تغییر شدت بارندگی و نسبت عمق لایه سطحی به لایه زیرین شدیداً تغییر می کند. بسته به نسبت عمق لایه سطحی به لایه زیرین و مقدار رطوبت لایه زیرین، $0.05\ cm^3\ cm^{-3}$ تغییر در شرایط پیشین رطوبت خاک لایه سطحی باعث 25- الی 50+ درصد تغییر در دبی محاسبه شده بوسیله مدل گرین- امپت دو لایه می گردد. در صورتیکه برای مدل ریچارد بین 100- الی 100+ تغییر می کند.

فصل پنجم: ارتباط بین توپوگرافی، کاربری اراضی و رطوبت خاک دریک حوضه آبخیز کوچک در منطقه لسی هلند

در این فصل رابطه بین توپوگرافی، کاربری اراضی وذخیره رطوبت لایه رویین خاک مورد بررسی قرار میگیرد. به منظور یافتن روابط بین فاکتورهای موثر در وضعیت رطوبت خاک، نوعی مدل GAM (Generalized Additive Model) مورد استفاده قرار گرفت. مدل GAM بیلان آبی را بصورت مجموعه ای از اجزاء (روابط) غیر خطی در نظر می گیرد. ساختار مدل بصورت سلسله مراتبی (hierarchical) می باشد بطوریکه تجزیه و تحلیل از بالاترین مقیاس

زمانی و مکانی شروع می شود. در این مطالعه بالاترین مقیاس زمانی "ماه" و بالاترین مقیاس مکانی "حوضه آبخیز" می باشد. مقادیر محاسبه شده مولفه های بیلان آبی در مقیاس های بالاتر بعنوان معیاری جهت محدود کردن دامنه تغییرات این مولفه ها در مقیاس های پایین تر استفاده می شوند. بنظر میرسد که با تغییر مقیاس زمان، اهمیت متغیرهای مربوط به کاربری اراضی بصورت قابل ملاحظه ای تغییر می کند بطوریکه در مقیاس های بزرگتر این متغیرها تأ ثیر چندانی ندارند ولی در مقیاس های گوچکتر اهمیت آنها افزایش می یابد. نوع کاربری اراضی برای تمام مقیاس های مکانی اهمیت یکسانی دارد در صورتیکه تأ ثیر توپوگرافی فقط در مقیاس های مکانی کوچکتر ظهور پیدا می کند. تبخیر و تعرق و زهکشی به لایه های عمیق تر عمدتا با تغییرکاربری اراضی تغییر می کنند. جریانهای جانبی رابطه ضعیفی با توپوگرافی نشان می دهند. با کوچکتر شدن مقیاس، تمام مولفه های بیلان آبی بطور فزاینده ای غیر خطی می شوند. هر چند که هیچ گونه پیش فرضی در مورد ساختار مدل انجام نگرفت مقدار خطا در نتایج مدل GAM قابل مقایسه با خطای مدل های بیلان آب بر پایه معادله ریچارد (بطور مثال SWAP) می باشد. این مطالعه نشان داد که کاربرد مدلهای سلسله مراتبی روش جالبی جهت تعیین ساختار داده های مشاهداتی در هیدرولوژی می باشد. کاربرد GAM تعیین و تعریف فرآیندهای غالب را در مقیاس های متفاوت امکانپذیر می سازد. همچنین روش واضحی را جهت آنالیز حساسیت و ارزیابی اهمیت فاکتورهای بیوفیزیکی نسبت به متغیرهای ورودی و متغیرهای سیستم فراهم می کند.

فصل ششم: کارائی مدل یک بعدی (1D) منطقه غیراشباع جهت شبیه سازی دینامیک رطوبت خاک برای مقیاس های مکانی متفاوت (از نقطه تا حوضه آبخیز)

این فصل قابلیت مدل SWAP را برای شبیه سازی رطوبت در منطقه توسعه ریشه برای زمانیکه مقیاس مکانی بطور تدریجی از " نقطه" به " حوضه آبخیز" افزایش می یابد مورد بررسی قرار میدهد. هر چند که مدل SWAP یک مدل یک بعدی بوده و برای مقیاس " نقطه " طراحی شده است اما مرور منابع معتبر در هیدوراوژی نشان می دهد که مدلهای یک بعدی با استفاده از تکنیک تعمیم (upscaling) برای دیگر مقیاسها نیز به وفور بکار رفته اند. حال سوال اصلی این است که مقادیر پارامتر ها و قابلیت این مدلها برای مقیاسهای مختلف چگونه تغییر می کند. در این مطالعه دو روش متفاوت بهینه سازی – امتحان درستی (calibration – validation) و سه معیارارزیابی مورد استفاده قرار گرفتند. برای تمام موارد روش بهینه سازی Levenberg – Marquardtاستفاده گردید. نتایج نشان داد که تفاوت بین روشهای مختلف بهینه سازی – امتحان درستی ناچیز میباشد. در صورت استفاده از یک روش ثابت بهینه سازی پارامترها (Parameterization) برای مقیاس های مختلف، بنظر میرسد که مقادیر بهینه پارامترهای ون گنوختن (van Genuchten) برای مقیاسهای بزرگتر نزدیک به مقادیر متوسط این پارامترها در مقیاس های کوچکتر می باشد. مقادیر معیارهای مختلف (RMSE, Nash-Sutcliffe, and Index of Agreement) برای نقاط مختلف داخل حوضه و همچنین برای مقیاسهای مختلف کاملا متفاوت می باشد. بطور کلی برای مقیاس های بزرگتر مقادیر معیارها بهتر بوده و همخوانی خوبی با نتایج مطالعات مشابه قبلی دارند.

فصل هفتم: مدلی ساده جهت پیش بینی رطوبت خاک: عامل پیوند دهنده مدل سازی رواناب رگبارها و مدل سازی پیوسته

در این فصل توسعه و کاربرد عملی مدل BEACH ارائه می گردد. BEACH یک مدل هیدرولوژی بصورت توزیع مکانی (spatially distributed) با گامهای زمانی یک روزه می باشد. مدل BEACH جهت پیش بینی شرایط پیشین رطوبت خاک برای کاربرد در مدلهای فرسایش خاک و سیلابهای موقتی طراحی شده است. داده های مورد نیاز مدل شامل داده های روزانه هواشناسی، خصوصیات فیزیکی خاک، خصوصیات پایه گیاه و داده های توپوگرافی می باشند. بارندگی، نفوذپذیری، تبخیروتعرق، جریان های جانبی، زهکشی و رشد گیاه فرآیندهای اساسی می باشند که توسط این مدل شبیه سازی می شوند. کاربرد عمده این مدل فراهم نمودن داده های بموقع توزیع مکانی رطوبت خاک در سطح منطقه مورد مطالعه بدون بازدیدهای مکرر صحرائی می باشد. کاربرد مدل BEACH در حوضه آبخیز Catsop نشان دادکه این مدل با دقت قابل قبولی رطوبت خاک را پیش بینی می کند. میانگین مجذور مربعات انحراف مقادیر پیش بینی شده رطوبت خاک برای 6 نقطه در درون حوضه بین 0.011 الی 0.065 $cm^3\ cm^{-3}$ متغیر می باشد. دبی برآورد شده بطور قابل قبولی با مقادیر مشاهداتی همخوانی داشت. ضریب همبستگی و ضریب Nash – Sutcliffe برای دبی خروجی حوضه بترتیب 0.824 و 0.786 می باشد. مدل BEACH در محیط PCRaster توسعه داده شد. PCRaster یک محیط برنامه نویسی و GIS می باشد. BEACH می تواند بعنوان ابزاری جهت تدریس و آموزش مدل سازی بیلان هیدرولوژی بصورت توزیع مکانی و برای تجزیه و تحلیل سناریوهای مختلف کاربری اراضی بکار رود.

فصل هشتم: تلفیق

این فصل نتایج مهم بدست آمده در فصلهای قبلی را جمع بندی می کند. موفقیت و یا شکست هر یک از اهداف اصلی این تحقیق و همچنین پاسخ هر یک از پرسش های مطرح شده در فصل اول بطور خلاصه مورد بحث وبررسی قرار می دهد. سپس به عملیات صحرائی اندازه گیری رطوبت اشاره ای نموده و بدنبال آن موضوعات مربوط به هر یک از پرسش های اصلی این تحقیق را مورد بررسی قرار میدهد. نهایتا نتایج عمده این تحقیق و پیشنهادات برای مطالعات آینده ارائه می گردند.

Curriculum Vitae

Vahedberdi Sheikh was born on 24th April 1973 in the village Dashtak in North Khorasan, Iran. After finishing his primary school at his birth place, at the age of 12 years he continued his secondary education at the nearest (~100 km) city named Bojnord. In 1992 he was accepted at the Gorgan University of Agricultural Sciences & Natural Resources, Gorgan, Iran. There he obtained his B.Sc degree in the field of Rangeland and watershed management in 1996. In the same year he joined the Tehran University where he accomplished his M.Sc degree in 1998 in the field of Watershed management. The title of his master thesis was: "Estimating the instantaneous peak discharge of floods using the daily records of discharge in Iran's rivers". During 1998-2000 he fulfilled his compulsory military service. In 2001, under a temporary contract, he was appointed as a watershed management expert in the Agricultural Jihad Directorate of Bojnord. In 2002 he was awarded a full-time PhD scholarship by the Iranian Ministry of Science, Research, and Technology. In October 2002 Vahedberdi Sheikh joined the Erosion and Soil & Water Conservation Group of Wageningen University and Research Centre, the Netherlands. He initiated his research by focusing on on-site and off-site impacts of land use changes but later he shifted his research direction towards the soil moisture monitoring and modeling. Within his PhD study, he followed several brush up as well as postgraduate courses. After his PhD, he will start his new job as a lecturer in the Gorgan University of Agricultural Science & Natural Resources, Gorgan, Iran.

Vahedberdi can be contacted via: v.sheikh@yahoo.com.

PE&RC PhD Education Statement Form

With the educational activities listed below the PhD candidate has complied with the educational requirements set by the C.T. de Wit Graduate School for Production Ecology and Resource Conservation (PE&RC) which comprises of a minimum total of 22 credits (= 32 ECTS = 22 weeks of activities)

Review of Literature (3 credits)

- Impact of land use change studies (2002/2003)
- Soil moisture measurement and modelling (2003)

Writing of Project Proposal (4 credits)

- Impact of land use changes and on-site soil and water conservation measures on field and catchment-scale water balances (2003)

Post-Graduate Courses (5 credits)

- Wind and water erosion: modelling and measurement (2003)
- Uncertainty modelling and analysis (2004)
- GIS applications in land resources and land use studies (2004)

Deficiency, Refresh, Brush-up and General Courses (9 credits)

- Scientific writing (2002)
- English fluency (2003)
- Processes and models in erosion and soil land water conservation (2003)
- Introduction to geo-information science
- Basic statistics

PhD Discussion Groups (3 credits)

- Statistics, maths and modelling in production ecology and resource conservation (2005-2006)
- Seminar series ESW: Advances in land and water management (2004-2006)

PE&RC Annual Meetings, Seminars and Introduction Days (1 credit)

- PE&RC Introduction day (2003)
- Scientific publishing: an introductory workshop for PhD students and young authors (2005)
- PE&RC annual meeting: "The truth of science"(2005)

International Symposia, Workshops and Conferences (2 credits)

- Uncertainties in the "monitoring-conceptualisation-modelling" sequence of catchment research", Luxembourg (2006)
- 3rd International conference on water resources in Mediterranean Basin, Tripoli, Lebanon (2006)

Laboratory Training and Working Visits (1 credit)

- Soil and water measurement techniques (2002/2005)